Design, synthesis and property of π -conjugated polymers with optical and magnetic functionalities

Design, synthesis and property of π-conjugated polymers with optical and magnetic functionalities

Zhiyong Qin
Doctoral Program in Materials Science

Submitted to the Graduate School of
Pure and Applied Sciences
in Partial Fulfillment of the Requirements
for the Degree of Doctor of Philosophy in
Engineering

at the
University of Tsukuba

CONTENTS

Chapter 1

Introduction of π–conjugated polymers

1.1 Introduction

The conducting polymer researches were began nearly half a century ago, when films of polyacetylene were found to exhibit profound increases in electrical conductivity when exposed to halogen vapor [1]. The "doped" polyacetylene can conduct electricity changed the way that polymer was viewed by Alan Heeger, Alan MacDiarmid, and Hideki Shirakawa. The de-localized electrons may move around the whole system and become the charge carriers to make them conductive [2]. If electrons are removed from the backbone resulting in cations or added to the backbone resulting in anions, this polymer can be transformed into a conducting form. Anions and cations act as charge carriers, which hopping from one site to another under the influence of an electrical field and increasing conductivity [3]. These groundbreaking works have a great impact on the development of new conjugated polymers for organic electronics. The conjugated polymers present several main structure types shown in the Scheme 1. More recently, these materials have been the development of organic semiconductors and their broad applications in photonics and electronics. They are promising in terms of their versatility of functionalization, thin film flexibility, electronic properties, ease of processing, low cost, and so on. Many research groups particularly are exciting to explore the synthesis of conjugated polymers with tunable energy levels, optical bandgaps, desired electronic and magnetic properties [4-7]. Therefore, the aim of the research of conjugated polymers is to highlight some important factors in the synthesis, characterisation and applications of functionalized polymers. Functional groups are introduced to polymers and obtained functionalize polymers, have become very useful now.

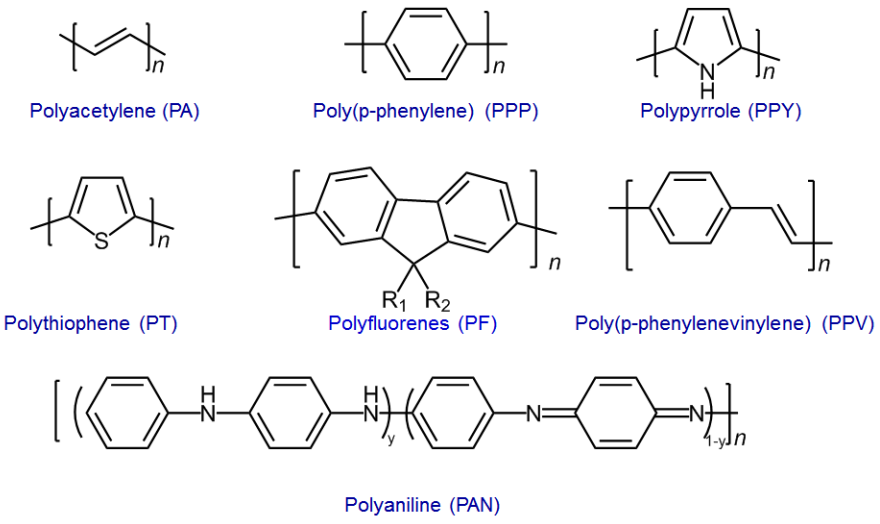

Scheme 1. 1. The commonly structures of main conjugated polymers

1.2. Types of conjugated polymers

At present, the conjugated polymers are divided by structure of main chain into three classes (Table 1. 1.), which are as follows: First, the polymers of aromatic cycles as main chain and their copolymers are the main class of conjugated polymers. For example, poly(fluorene)s, polyphenylenes, polypyrenes, polyazulenes, polynaphthalenes, poly(pyrrole)s, poly(thiophene)s and so on. Second, the polymers of double bonds as main chain and its derivatives have emerged as the doped conductive polymers. For example, poly(acetylene)s. Third, The polymers of aromatic cycles and double bonds as main chain are the frequently used class of conjugated polymers. For example, Poly(p-phenylene vinylene) and polyanilines. Today, these polymers are playing a more and more important role in our daily life. However, the synthesis of conjugated polymers with high quality is often a challenge for chemists. Therefore, much interest has been concentrated on developing synthesis methods of conjugated polymers.

Table 1. 1. Types of conjugated polymers (according to structure of main chain) and synthesis method.

Main types	Conjugated polymers	Synthesis methods
Aromatic rings as main chain	PPP, PT, PPY, PF	Suzuki method, Stille method, Yamamoto method and so on
Alternant single and double bonds	PA	Addition polymerization
Aromatic rings and alternant single and double bonds as main chain	PPV, PAN	Heck method, McMurry method, Wessling method, Gilch method, Vanderzande method, Knoevenagel method, Witting-Horner method and so on

PPP, PPY, PPV, PPP, PF, PT PAN were shown in Scheme 1.

1.3. Several common synthesis methods of conjugated polymers

Polymerization is a process of reacting monomer molecules together in a chemical reaction to form polymer chains or three-dimensional networks. [8] The polymerization of conjugated polymers can be classified into two major categories: electrochemical polymerization and chemical polymerization. Electrochemical polymerization is a solution containing monomers and an electrolyte produces a conductive polymer film on the anode. [9] Electrochemical polymerization is convenient, since the polymer does not need to be isolated and purified. But electropolymerisation can result in poorly adherent or inhomogeneous polymer coatings, and the quite positive potentials usually required. The chemical polymerization in aqueous solutions was studied as a function of a wide variety of synthesis parameters, such as pH, relative concentration of reactants, polymerization temperature and time, and so on. [10] Chemical synthesis offers two advantages compared with electrochemical synthesis of conjugated polymers. On the one hand, chemical synthsis has a greater selection of monomers. On the other hand, chemical synthsis has the ability to synthesize perfectly regioregular substituted polymers using the proper catalysts. Conjugated polymers are prepared by electrochemical polymerization and chemical polymerization in many reaction methods. For example, Stille coupling reaction,

Suzuki coupling reaction, Heck reaction, Heck-Sonogashira reaction, Gilch reaction, and so on (Table 1. 2). The several commonly synthesis methods of conjugated polymers as follow:

Table 1. 2. Reaction conditions of five common reaction for CPs and CPEs

Methods	Reaction Equations	Polymerization conditions [a]	Polymerization conditions [b]
Heck reaction	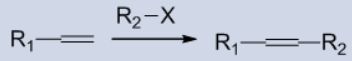	$Pd_2(PPh_3)_4$, $PbCl_2$, K_2CO_3 or NEt_3, Toluene, 100 °C	$Pd_2(PPh_3)_4$, $PbCl_2$, NEt_3, Toluene, 90 °C
Heck-Sonogashira reaction	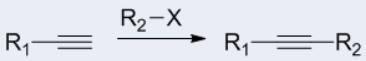	$Pd(PPh_3)_4$, CuI, DMF or toluene, Diethylamine, 90 °C	$Pd(PPh_3)_4$, CuI, DMF, Diethylamine, 70 °C
Stille reaction	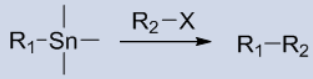	$Pd_2(PPh_3)_4$, DMF or toluene, 100 °C	
Gilch reaction	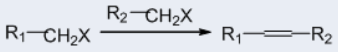	t-BuOK, THF	t-BuOK, t-BuOH, THF
Suzuki reaction	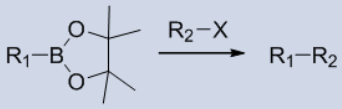	$Pd(PPh_3)_4$ THF/water or toluene/water, K_2CO_3, 100 °C	$Pd(0)/K_2CO_3$, DMF/water, 85 °C

a: Polymerization condition of conjugated polymer in chemical polymerization
b: Polymerization condition of conjugated polymer in electrochemical polymerization

(1) Stille coupling reaction.

Stille coupling reaction is known as one of the very useful carbon-carbon bond-forming reactions. It is versatile and selective method for formation of aryl-aryl bonds. Besides, it also has advantages to allow introduction of a wide range functional side chains in the polymer and tolerate a wide variety of functional groups so that tedious protection-deprotection reactions. The reaction has been shown to tolerate many functional groups, such as amines, aldehydes, esters, ethers, and nitro groups. The reaction yield is usually high, which is essential to obtain high molecular weight polymers. [11]

Stille coupling polymerization generally uses the cross-coupiling of organicmetallic ragents to catalyze the reaction of organotin reagents and organic halides. The polymeration was easily carried out the solvents of DMF/water, toluene/water or THF/water in presence of catalytic amount (about 5% mol) the palladium(0) under a nitrogen atmosphere. The reaction finished and the polymer was precipitated into acetone or methanol by which the tin compound was removed. Clearly, if there are properly choose monomers which are functionalized and should be able to prepare conjugated polymers. This synthsis method is a very powerful way to prepare processible functional conjugated polymers

However, these tin reagents tend to be highly toxic and stannane byproduct is often inseparable. In addition,

the methods for their synthesis are somewhat limiting. The methods for the alkylation of organomercurials are unfortunately limited almost solely to halides, [12-15] Organometallic partners in which the metal is boron or aluminum often are not conveniently synthesized, [16, 17] the structure of the organic portion can be limited by the methods of synthesis available. [18-20]

(2) Suzuki-Miyaura coupling reaction.

Synthsis of polymers by palladium-catalyzed Suzuki-Miyaura coupling reaction is similer to the Migita-Kosugi-Stille coupling method. These methods are tolerating a large number of functional groups. Different types of functional groups endow conjugated polymers with different properties and applications. Generally, Palladium-catalyzed Suzuki-Miyaura coupling of organoborons with aryl or vinyl halides is known as one of the most useful carbon-carbon bond-forming reactions. [21-29] It is an extremely versatile and selective method for the formation of aryl–aryl bonds and has the advantages of tolerating a wide range of functional groups, and its reagents have low toxicities and can be easily handled and manipulated under air. [30, 31] Consequently, recent years, much effort has been focused on the synthesis of the functionalized conjugated polymers using this method.

In the case of catalyst-transfer Suzuki-Miyaura coupling polymerization, the polymers could be obtained in a controlled manner. [32, 33] The polymerization of organic halides monomer with a Pd complex initiator was attempted under the nitrogen atmosphere conditions used for the polymerization of benzoate unit with aqueous Na_2CO_3 as a typical base to afforded polymer with a broad molecular weight distribution. [32] The functional polymers can be synthesized by successive catalyst-transfer Suzuki-Miyaura coupling polymerization.

However, the methods for their synthesis are limited almost solely to vinyl halides. On the other hand, the fact that steric hindrance between substituents of monomer blocks depresses progress of the polymerization. The molercular weight can be affect.

(3) Heck reaction.

Palladium-catalyzed Heck reaction has been well recognized as polweful method to the prepareation of substituted olefins. The palladium-catalyzed Heck reaction of halide compound with olefins is a standard carbon- carbon bond-forming reaction. [34] The halide compound is an aryl, benzyl or vinyl compound and olefins is often electron-deficient such as acrylate ester or an acrylonitrile. The treatment of olefins with halides in the presence of an organopalladium catalyst, which can be tetrakis(triphenylphosphine)palladium(0), palladium chloride or palladium(II) acetate. [35] The base is triethylamine, potassium carbonate or sodium acetate and the ligand is triphenylphosphine, PHOX or BINAP. [36,37]

(4) Gilch reaction.

Gilch polymerization is very simple and can normally result in polymers with high molecular weights, narrow polydispersity indices and high structural regularity. [38] At present, the synthsis of PPV (poly(p-phenylenevinylene)) mainly is by Gilch reaction. The reaction rate is very fast even at low temperatures result

in the lack of mechanistic knowledge and suffers from the fact that its mechanism is not yet fully understood. Control of chain length or chain length distribution, chain architecture and minimization of defect structures within the chains are therefore extremely difficult. [39, 40]

1.4. My design strategy of conjugated polymers.

Clearly, work in this field must begin with synthesis of the monomers or the polymers itself. The synhesis of products begins with some general remarks about synthetic routes to monomers and polymers. Design and synthesis of polymers are growing interest in polymer chemistry in exploiting molecular complexity as a tool to create precisely tuned materials with desired properties. In my work, I have design and synthesis four groups as follows:

1.4.1. Exploration for synthesis method of multi-functional products.

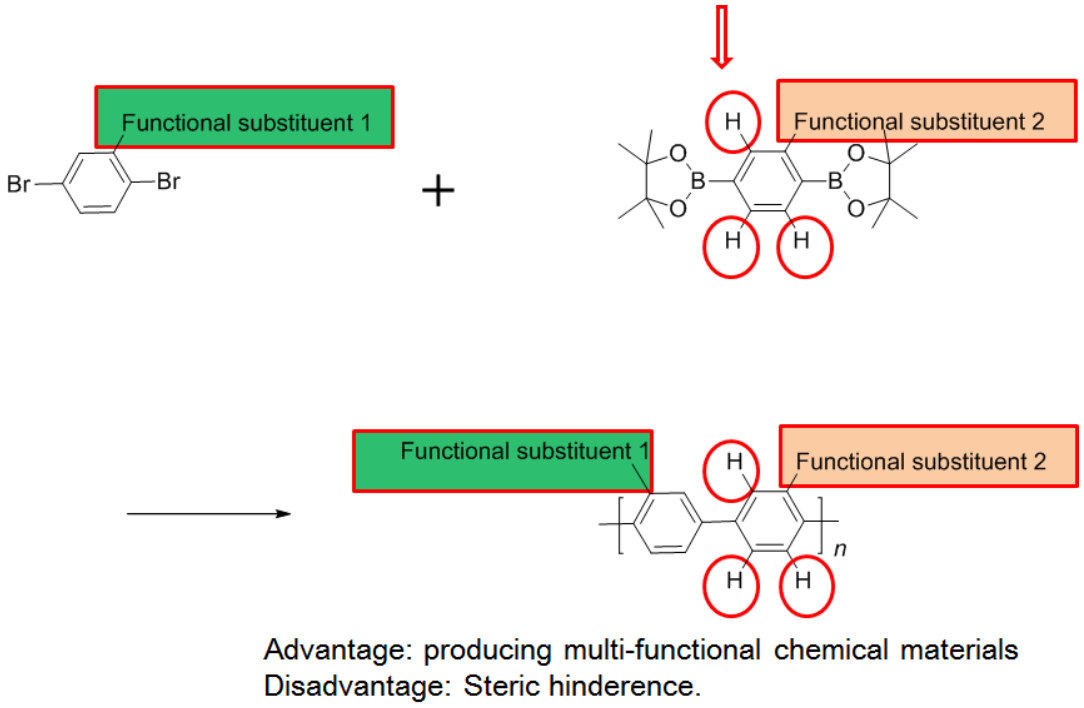

Figure 1. 1. Synthesis method of functional conjugated polymers

In this design strategy, I designed a series of π-conjugated materials with Miyaura-Suzuki coupling reaction. The aims are order to exploration of new type coupling and new functional products (Figure1. 1). The phenylene, thiophene and fluorene rings are employed as main chains. Flexible alkyl group, azobenzene, and optically active groups was introduced into conjugated polymer as side chains. The different functional groups were introduced into the conjugated main chain, which can get novel functional conjugated polymers from effect of functional substituents. [41, 42] Herein, the resultant polymers showed low-molecular weight, which may be due to the fact that steric hindrance between substituents of monomer blocks depresses progress of the polymerization. Therefore, the design and synthsis of polymers need to consider steric hindrance in Miyaura-

Suzuki type polycondensation. The effect of steric hindrance is disadvantage to the reaction progressing. This reaction can afford to produce polymers of multi-functionality, such as light isomerization and chiroptical activity and so on. In addtion, diborane compound to prepare the precursor allows no use of n-BuLi for preparation of precursor, expanding possibility of the Miyaura-Suzuki polycondensation reaction. Because n-BuLi with high activity needs to be used in the preparation of precursor of monomers compare with Miyaura-Suzuki coupling. For example, some groups (ester group and amino groups) limit the reaction to produce functional polymers by n-BuLi reacts. These are advantage in the method to synthesize functional polymers by Miyaura-Suzuki type reaction. The exploration experiment in this study indicates that the Suzuki-Miyaura coupling polymerization can produce π-conjugated skeleton, and this reaction allows producing multi-functional chemical materials.

1.4.2. Functional paramagnetic polymers having 2,6-di-tert-butylphenoxyl radicals.

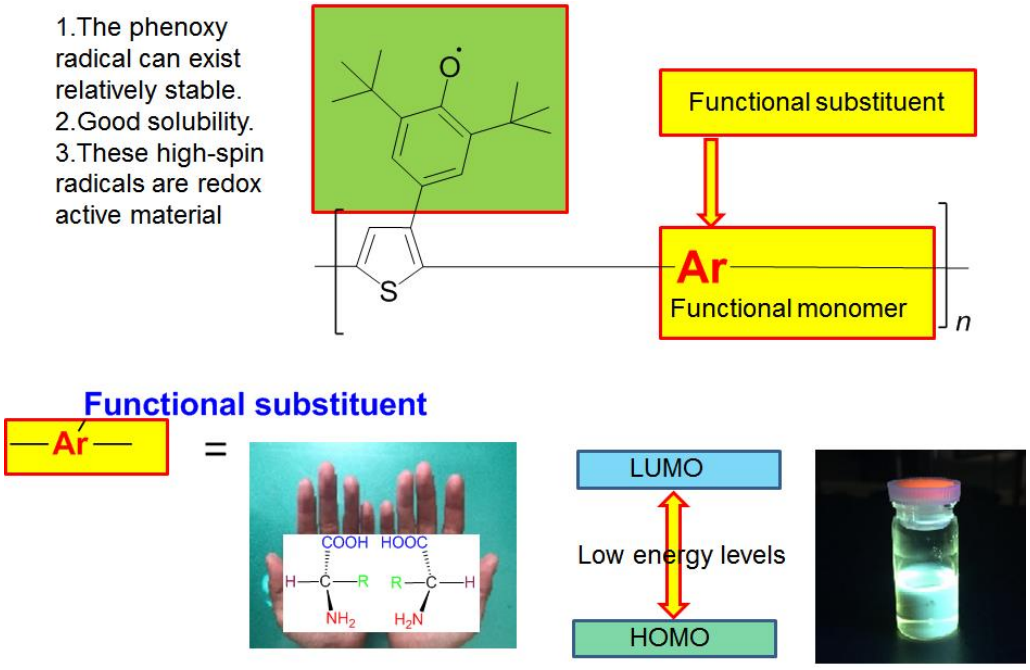

Figure 1. 2 The side chain of conjugated polymers functionalized

Some molecular radicals are stable, organic free radicals with a single unpaired (paramagnetic) electron, which are redox active material and undergo an electrochemical redox reaction between their neutral and oxidized forms. [43] The most widely studied family of stable radical polymers is based on 2,6-di-tert-butylphenoxyl radicals, which offer exceptional stability towards air. [44-49] The 2,6-di-tert-butylphenoxyl pendant radical groups are π-conjugated with the polymers backbone, the molecular connectivity can lead to the expectation of molecular-based and high-spin magnetism caused by intramolecular through bond spin ordering. The molecular connectivity can lead to the expectation of high-spin magnetic properties. [50] On the basis of these considerations, these polymers bring 2,6-di-tert-butylphenoxyl radical groups and functional groups were designed and synthesized by Stille and Suzuki method (Figure 1. 2). The structure polymers include chiral

alkyl chain and bornyl group, [51-53] which the chirality primarily results from ordered main chain of macromolecular helical conformations or helical arrangement of intermolecular. [54] Naphthalene molecules have been taken up as a subject matter of organic semiconductor researches. [55, 56] The polymers contain naphthalene molecules of organic semiconductor showing intense photoluminescence, which is due to π-electronic interaction of the molecular stacks. The low-energy electronic bands [57, 58] will be designed to introduce the conjugated main chain to get lower bandgap polymers. In addition, the structure of polymers including optical property's polyfluorine, [59, 60] generally, a derivative of fluorene, inherits many properties of fluorene and acts as a good construction block for light emitters via readily available functionalization. Up to now, these properties of polymers were few reported, as a newly emerging type of π-conjugated polymer, must be a significant research filed.

1.4.3. Low band gap isothianaphthene-based polymers bearing bornyl side groups

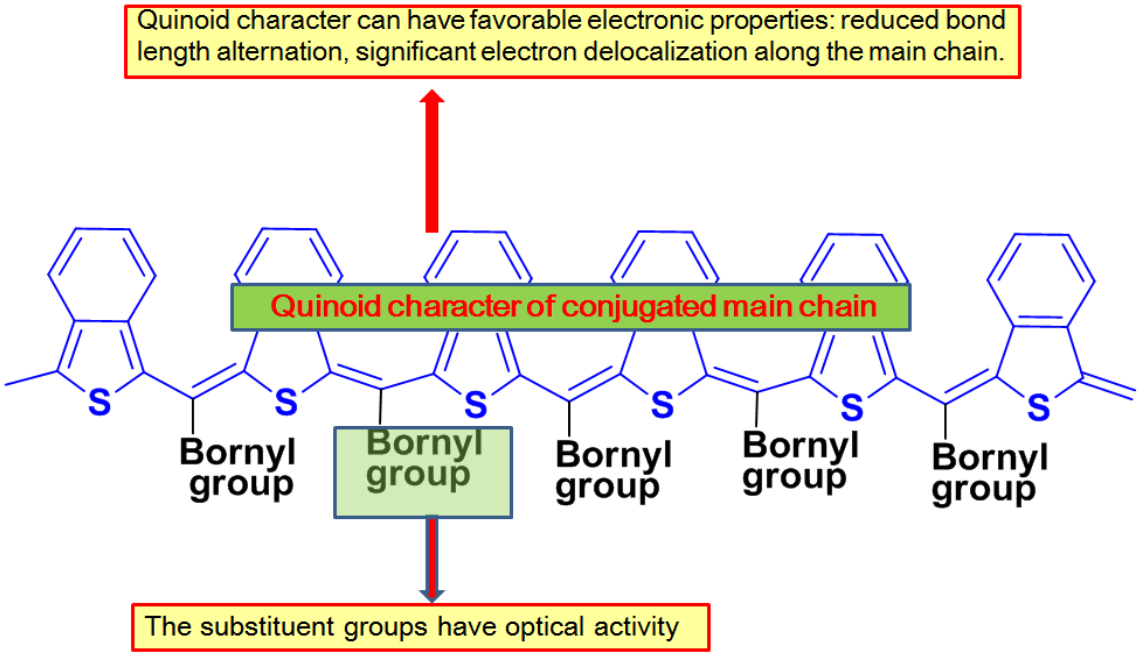

Figure 1. 3. Design strategy of the optically active low bandgap conjugated polymers.

In this design strategy, I want to design low band gap polymers. At present, there are four main ways to obtain low bandgap conjugated polymers as follows:

(1) Substituent modifications. The substituent groups can affect the coplanarity that can decrease the bandgap of conjugated polymers.

(2) Increasing quinoid character of conjugated main chain. Polymers with quinoidal character can have favorable electronic properties, including reduced bond length alternation, significant electron delocalization along the polymer backbone, so the quinoid character can decrease the bandgap to obtain low bandgap

conjugated polymers.

(3) Regular alternation of donors and acceptors. There are regular alternation of electron-donors and electron-acceptors in the conjugated main chain that form lower energy level to conjugated polymers.

(4) Ladder polymer. The structural deformation of single-double Localization is decreased in the ladder polymers, so alternating single-double is decreased to the main chain and decrease the bandgap to obtain low bandgap conjugated polymers. But the synthesis is difficultly, the method is few researches.

In this design strategy, I design the low bandgap conjugated polymers by method of (1) and (2) (Figure 1. 3). The substituent of bornyl group was introduced the conjugated main chain and increase the coplanarity of main chain to decease the energy level. The group as a chiral side chain was often introduced into the conjugated main chain. [61] The bornyl group has spherical with three chiral centers. The baulky group in the side chain can change the coplanarity of the main chain, [62] and should change main chain chirality in conjugated polymers. [63, 64] On the other hand, the conjugated backbones contain isothianaphthene structure.

Isothianaphthene (ITN) units are excellent candidates to investigate structural effects on energy gaps and optical properties of π-conjugated polymers [65-67]. If containing ITN units in the main chain, the polymers tend to have low bandgaps because their main chains favors quinoid resonance forms to preserve the benzene aromaticity at the expense of the thiophene aromaticity [68]. Poly(isothianaphthene) (PITN) [69, 70] with quinoidal character can have favorable electronic properties, a narrow band gap, significant electron delocalization along the polymer backbone and reducing bond length alternation [71, 72]. Although important progress has been designed the mechanistic aspects of its structure and made in the synthesis of PITN [73, 74], the subject of low bandgap polymers has until remained academic research [75, 76] rather than progressing into application to our life. This is due to the poor processability, insolubility, and infusibility of PITN. To provide solubility, stability, and physical properties of the PITN, alkyl chains have been introduced into the isothianaphthene-based polymers [77-79].

1.4.4. Synthesis of chiral inducers and polymers.

Three new chiral compounds were designed based on core of [1,1'-biphenyl]-4-yl benzoate. The liquid crystal (LC) electrolyte solution was prepared by adding it as a chiral inducer to LC of 4-Cyano-4'-hexylbiphenyl (6CB). Liquid crystal molecules form one-handed helical structure by the inducers of three rings, which induce one-handed helical aggregation of polymer backbone during the polymerization process in the LC. Therefore, a series of chiral polymer films were prepared by electrochemical polymerization by inducing (Figure 1. 4). The polymer thus obtained forms an intermolecular twisted structure, which the orientation is transcript of the electrolyte solution texture. Such a process would be expected to produce a fingerprint structure in the polymer. [80]

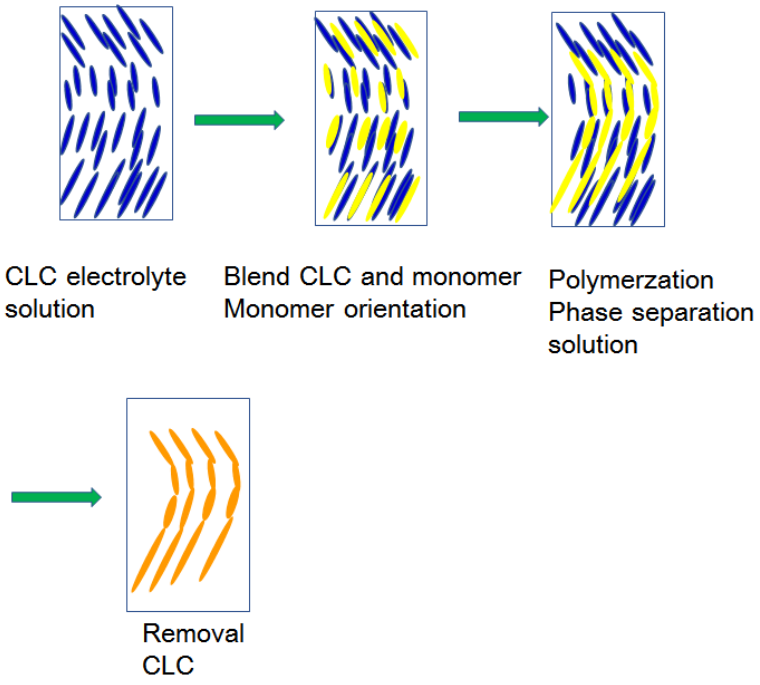

Figure 1. 4. Design strategy of electrochemical polymerization of carbazole in a cholesteric electrolyte solution

1.5. References

[1] Bredas JL, Chance RR, Silbey R. Comparative theoretical study of the doping conjugated polymers; Polarons in polyacetylene and polyparaphenylene. Physical Review B. 1982;26:5843-5854.

[2] Shirakawa H, Louis EJ, MacDiarmid AG, Chiang CK, Heeger AJ. Synthesis of electrically conducting organic polymers: halogen derivatives of polyacetylene, (CH)x. Journal of Chemical Society of Chemical Communication. 1977;474:578-580.

[3] Dou L, Liu YS, Hong ZR, Li G, Yang Y. Low-bandgap near-IR conjugated polymers/molecules for organic electronics. Chem. Rev. 2015;115:12633-12665.

[4] Sun SS, Dalton LR, Introduction to organic electronic and optoelectronic materials and devices; CRC Press: New York, 2008.

[5] Li G, Zhu R, Yang Y. Polymer solar cells. Nat. Photonics. 2012;6:153−161.

[6] Janssen RA, Nelson J. Factorsl limiting device efficiency in organic photovoltaics. Adv. Mater. 2013;25: 1847−1858.

[7] Zhao Y, Guo Y, Liu Y. 25th anniversary article: recent advances in n-type and ambipolar organic field-effect transistors. Adv. Mater. 2013;25.5372−5391.

[8] Kato M, Kamigaito M, Sawamoto M, Higashimura T. Polymerization of methyl methacrylate with the carbon tetrachloride/dichlorotris-(triphenylphosphine) ruthenium (II)/methylaluminum bis (2, 6-di-tert-butylphenoxide) Initiating system: possibility of living radical polymerization. Macromolecules. 1995;28:1721–1723.

[9] Satoh M, Kaneto K, Yoshino K. Dependences of electrical and mechanical properties of conducting

polypyrrole films on conditions of electrochemical polymerization in an aqueous medium. Synthetic Metals. 1986;14:289-296.

[10] Cao Y, Andreatta A, Heeger A J, Smith P. Influence of chemical polymerization conditions on the properties of polyaniline. Polymer. 1989;30:2305-2311.

[11] Stille JK. The palladium-catalyzed cross-coupling reactions of organotin reagents with organic electrophiles. Angew. Chem. Int. Ed. Engl. 1986; 25:508-524

[12] Wilkinson G, Stone FGA, Abel EW. Pergamon: Oxford, 1982;8:Chapter 57.

[13] Takai K, Oshima K, Nozaki H. For the palladium-catalyzed coupling of alanes with enol phosphates. Tetrahedron Lett. 1980;21:2531-2534.

[14] Heck RF. For some examples of the palladium-catalyzed coupling of vinyl halides. Chem. Res. 1979;12: 146-151.

[15] Wenkert E, Michelotti E L, Swindell CS. For the nickel-catalyzed coupling of Grignard reagents with methyl vinyl ethers. J. Am. Chem. Soc. 1979;101:22462247.

[16] Hayashi T, Katsura Y, Kamuda M. For the nickel-catalyzed coupling of Grignard reagents with silyl enol ethers. Tetrahedron Lett. 1980;21:3915-3918.

[17] Trost BM, Chan DMT. Palladium-mediated cycloaddition approach to cyclopentanoids. Introduction and initial studies. J. Am. Chem. Soc. 1983;105:2315-2325.

[18] Matsushita H, Negishi E. Palladium-catalyzed reactions of allylic electrophiles with organometallic reagents. A regioselective 1,4-elimination and a regio- and stereoselective reduction of allylic derivatives. J. Org. Chem. 1982;47:4161-4165.

[19] McMurry JE, Scott WJ. A new method of olefin synthesis. Coupling of lithium dialkylcuprates with enol triflates. Tetrahedron Lett. 1980;21:4313-4316.

[20] Kosugi M, Hagiwara I, Migita T. For an example of the palladium-catalyzed reaction of vinyl halides withorganostannanes. Chem. Letr. 1983;839-840.

[21] Miyaura N, Suzuki A. Palladium-Catalyzed Cross-Coupling Reactions of Organoboron Compounds. Chem. ReV. 1995;95:2457-2483.

[22] Suzuki A. Recent advances in the cross-coupling reactions of organoboron derivatives with organic electrophiles, 1995-1998. J. Organomet. Chem. 1999;576:147-168.

[23] Walker SD. A rationally designed universal catalyst for Suzuki–Miyaura coupling processes. Angew. Chem. Int. Edit. 2004;43:2201-2203.

[24] Stevens PD, Li G, Fan J, Yen M, Gao Y. Recycling of homogeneous Pd catalysts using superparamagnetic nanoparticles as novel soluble supports for Suzuki, Heck, and Sonogashira cross-coupling reactions. Chem. Commun. 2005;4435:4435-4437.

[25] Stanforth SP. Catalytic cross-coupling reactions in biaryl synthesis. Tetrahedron. 1998;54:263-303.

[26] Thompson LA, Ellman JA. Synthesis and applications of small molecule libraries. Chem. ReV. 1996;96:555-600.

[27] Matthew SC, Glasspoole BW, Eisenberger P, Crudden CM. Synthesis of enantiomerically enriched triarylmethanes by enantiospecific suzuki–miyaura cross-coupling reactions. J. Am. Chem. Soc. 2014;136:5828-5831.

[28] Hassan J, Sevignon M, Gozzi C, Schulz E, Lemaire M. Ligand-free palladium catalysis of the Suzuki reaction in water using microwave heating. Chem. ReV. 2002;102:1359-2976.
[29] Wolfe JP, Singer RA, Yang BH, Buchwald SL. Highly active palladium catalysts for Suzuki coupling reactions. J. Am. Chem. Soc. 1999;121:9550-9561.
[30] Miyaura N, Yanagi T, Suzuki A. The palladium-catalyzed cross-coupling reaction of phenylboronic acid with haloarenes in the presence of bases. Synth Commun. 1981;11:513-519.
[31] Miyaura N, Suzuki A. Palladium-catalyzed cross-coupling reactions of organoboron compounds. Chem Rev. 1995;95:2457-2483.
[32] Yokoyama A, Suzuki H, Kubota Y, Ohuchi K, Higashimura H, Yokozawa T. Chain-Growth Polymerization for the Synthesis of Polyfluorene via Suzuki-Miyaura Coupling Reaction from an Externally Added Initiator Unit. J. Am. Chem. Soc. 2007;129:7236–7237.
[33] Beryozkina T, Boyko K, Khanduyeva N, Senkovskyy V, Horecha M, Oertel U, Simon F, Stamm M, Kiriy A. Angew. Grafting of polyfluorene by surface-initiated Suzuki polycondensation. Chem. Int. Ed. 2009;48:2695–2698.
[34] Jackson DA. DNA: Template for an economic revolution. Sci. 1995, 758, 356-365.
[35] Clayden J, Greeves N, Warren S. Organic chemistry (Oxford University Press) 2000;1450–1466.
[36] Bettelheim A, White BA, Raybuck SA, Murray RW. Electrochemical polymerization of amino-, pyrrole-, and hydroxy-substituted tetraphenylporphyrins. Inorg. Chem. 1987;26:1009–1017.
[37] Cao Y, Andreattat A, Heegert AJ, Smitht P. Influence of chemical polymerization conditions on the properties of polyaniline. Polymer. 1989;30:2305-2311.
[38] Chen ZK, Lee NHS, Huang W, Xu YS, Cao Y. New phenyl-substituted PPV derivatives for polymer light-emitting diodes-synthesis, characterization and structure-property relationship study. Macromolecules. 2003;36:1009-1020.
[39] Hsieh BR, Antoniadis H, Bland DC, Feld WA, Chlorine precursor route (CPR) chemistry to poly (p-phenylene vinylene)-based light emitting diodes. Adv. Mater. 1995;7:36-38.
[40] Gilch HG, Wheelwright WL, J. Polym. Sci. Part A 1966;4:1337.
[41] Miyaura N, Suzuki A. Palladium-catalyzed cross-coupling reactions of organoboron compounds. Chem. Rev. 1995;95:2457-2483.
[42] He G, Kang L, Torres DW, Shynkaruk O, Ferguson M, McDonald R, Rivard E. The marriage of metallacycle transfer chemistry with suzuki-miyaura cross-coupling to give main group element-containing conjugated polymers, J. Am. Chem. Soc. 2013;135:5360-5363.
[44] Tomlinson EP, Hay ME, Boudouris BW. Radical polymers and their application to organic electronic devices. Macromolecules. 2014;47:6145-6158.
[45] Goto H, Koyanob T, Ikedab H, Yoshizakib R, Akagia K. Synthesis and magnetic properties of polydiphenylamine derivative bearing stable radical groups. Polymer. 2004;45:4559-4564.
[46] Inoue K, Hayamizu T, Iwamura H, Hashizume D, Ohashi Y. Assemblage and alignment of the spins of the organic trinitroxide radical with a quartet ground state by means of complexation with magnetic metal ions. A molecule-based magnet with three-dimensional structure and high T_C of 46 K. J. Am. Chem. Soc. 1996;118:1803-1804.

[47] Rostro L, Wong SH, Boudouris BW. Solid state electrical conductivity of radical polymers as a function of pendant group oxidation state. Macromolecules. 2014;47:3713-3719.
[48] Hyakutake T, Park JY, Yonekuta Y, Oyaizu K, Nishide H, Advincula R. Nanolithographic patterning via electrochemical oxidation of stablepoly(nitroxide radical)s to poly(oxoammonium salt)s. J. Mater. Chem. 2010;20:9616-9618.
[49] Wingate AJ, Boudouris BW. Recent advances in the syntheses of radical-containing macromolecules. J . Polym. Sci. Polym. Chem. 2016;54:1875-1894.
[50] Yoshioka N, Nishide H, Kaneko T, Yoshiki H, Tsuchida E. Poly[(p-ethynylphenyl)hydrogalvinoxy] and its polyradical derivative with high spin concentration. Macromolecules. 1992;25:3838-3842.
[51] Krieger PE, Landgrebe JA. Asymmetric induction in the addition of chiral carbalkoxycarbenoids to styrene. J. Org. Chem. 1978;43:4447-4452.
[52] Song J, Bi H, Xie X, Guo J, Wang X, Liu D. Natural borneol enhances geniposide ophthalmic absorption in rabbits. Int. J. Pharm. 2013;445:163-170.
[53] Al-Farhan KA, Warad I, Al-Resayes SI, Fouda MM, Ghazzali M. Synthesis, structural chemistry and antimicrobial activity of-(-)borneol derivative. Cent. Eur. J. Chem. 2010;8:1127-1133.
[54] Mohammad F, Calvert PD, Billingham NC. Thermal stability of electrochemically prepared polythiophene and polypyrrole. Bull. Mater. Sci. 1995;18:255-261.
[55] Huang X, Kim M, Suh H, Kim I. Hierarchically nanostructured carbon-supported manganese oxide for high-performance pseudo-capacitors. Korean J. Chem. Eng. 2016;33:2228-2234.
[56] Princea W, Edwards-Lajnef M, Aıtcinb PC. Interaction between ettringite and a polynaphthalene sulfonate superplasticizer in a cementitious paste. Cement Concrete Res. 2002;32:79-85.
[57] Long G, Wan X, Zhou J, Liu Y, Li Z, He U, Zhang M, Hou Y, Chen Y. Isothianaphthene-based conjugated polymers for organic photovoltaic cells. Macromol. Chem. Phys. 2012;213:1596-1603.
[58] Hoogmartens I, Adriaensens P, Vanderzande D, Gelan J. Low-bandgap conjugated polymers. A joint experimental and theoretical study of the structure of polyisothianaphthene. Macromolecules. 1992:25:7347-7356.
[59] Oh HS, He GS, Law WC, Baev A, Jee H, Liu X, Urbas A, Lee CW, Choi BL, Swihart MT, Prasad PN. Manipulating nanoscale interactions in a polymer nanocomposite for chiral control of linear and nonlinear optical functions. Adv. Mater. 2014;26:1607-1611.
[60] Xie N, Wang J, Guo Z, Chen G, Li Q. Fluorene/carbazole alternating copolymers tethered with polyhedral oligomeric silsesquioxanes: synthesis, characterization, and electroluminescent properties. Macromol. Chem. Phys. 2013;214:1710-1723.
[61] Matsumura A, Kawabata K, Goto H. Synthesis, properties, and doping behavior of optically active polythiophenes bearing a bornyl group, Macromol. Chem. Phys. 2015;216:931-938.
[62] Mohammad F, Calvert PD, Billingham NC. Thermal stability of electrochemically prepared polythiophene and polypyrrole. Bull. Mater. Sci. 1995;18: 255-261.
[63] Kawashima H, Goto H. Synthesis and properties of a chiroptically active oligomer from 3,4-ethylenedioxythiophene and (-)-myrtenal. Materials. 2011;4:1013-1022.
[64] Cremer LD, Verbiest T, Koeckelberghs G. Influence of the Substituent on the Chiroptical Properties of

Poly (thieno [3,2-b] thiophene)s. Macromolecules. 2008;41: 568-578.
[65] Kim JY, Qin Y, Stevens DM, Kalihari V, Hillmyer MA, Daniel-Frisbie C. High open-circuit voltage photovoltaic cells with a low bandgap copolymer of isothianaphthene, thiophene, and benzothiadiazole units. J. Phys. Chem. C. 2009;113: 21928-21936.
[66] Long GK, Wan XJ, Zhou JY, Liu YS, Li Z, He GR, Zhang MT, Hou YH, Chen YS, Isothianaphthene-based conjugated polymers for organic photovoltaic cells. Macromolecular. 2012;213:1596-1603.
[67] Ramar A, Saraswathi R. Synthesis and characterization of a novel poly(isothianaphthene)-C60 double-cable polymer. J Mater Sci: Mater Electron. 2016;27:852-861.
[68] Roncali J. Synthetic principles for bandgap control in linear π-conjugated systems. Chem. ReV. 1997;97:173-206.
[69] Meng H, Tucker D, Chaffins S, Chen Y, Helgeson R, Dunn B, Wudl F. An unusual electrochromic device based on a new low bandgap conjugated polymer. Chem. ReV. 2003;15:146-149.
[70] Vangeneugden DL, Vanderzande DJM, Salbeck J, Van Hal PA, Janssen RAJ, Hummelen JC, Brabec CJ, Shaheen SE, Sariciftci NS. Synthesis and characterization of a poly (1,3-dithienylisothianaphthene) derivative for bulk heterojunction photovoltaic cells. J. Phys. Chem. B. 2001;105:11106-11113.
[71] Mullekom HV, Vekemans J, Havinga EE, Meijer EW. Developments in the chemistry and band gap engineering of donor-acceptor substituted conjugated polymers. Mater. Sci. Eng., R. 2001;32:1-40.
[72] Cheng YJ, Yang SH, Hsu CS. Synthesis of conjugated polymers for organic solar cell applications. Chem. Rev. 2009;109:5868-5923.
[73] Hoogmartens I, Adriaensens P, Vanderzande D, Gelan J, Quattrocchi C, Lazzaroni R, Bredas JL. Low-bandgap conjugated polymers. A joint experimental and theoretical study of the structure of polyisothianaphthene. Macromolecules. 1992;25:7347-7356.
[74] Polec I, Henckens A, Goris L, Nicolas M, Loi MA, Adraensens PJ, Lutsen L, Manca JV, Vanderzande, D, Sariciftci NS. Convenient synthesis and polymerization of 5,6-disubstituted dithiophthalides toward soluble poly(isothianaphthene): An initial spectroscopic characterization of the resulting low-band-gap polymers. J Polym Sci Pol Chem. 2003;41:1034-1045.
[75] Kiebooms R, Hoogmartens I, Adriaensens P, Vanderzande D, Gelan J. Low-band-gap conjugated polymers. Improved model compounds for the structural analysis of poly (isothianaphthene). Macromolecules. 1995;28:4961-4969.
[76] Zerbi G, Magnoni MC, Hoogmartens I, Kiebooms R, Carleer R, Vanderzande D, Gelan J. On the quinoid structure of poly (isothianaphthene): A vibrational spectroscopic study. Adv. Mater. 1995;7:1027-1030.
[77] Meng H, Wudl F. A robust low band gap processable n-type conducting polymer based on poly (isothianaphthene). Macromolecules. 2001;34:1810-1816.
[78] Douglas JD, Griffini G, Holcombe TW, Young EP, Lee OP, Chen MS, Fréchet JMJ. Functionalized IsothianaphtheneMonomers That Promote QuinoidalCharacter in Donor-Acceptor Copolymers for Organic Photovoltaics. Macromolecules. 2012;45: 4069-4074.
[79] Umeyama T, Hirose K, Noda K, Matsushige K, Shishido T.; Hayashi, H, Matano Y, Ono N, Imahori H. Thermal conversion of precursor polymer to low bandgap conjugated polymer containing isothianaphthene dimer subunits. J. Phys. Chem. C. 2012;116:1256-1264.

[80] Kawabata K, Goto H. Periodic structure in a fluorene-based polymer prepared by electrochemical polymerization. Chem. Lett. 2009;38:706–707.

Chapter 2

Polycondensation for Synthesis of Multi-functional Products

2.1 Introduction

Conjugated polymers have attracted much attention among numerous scientists and engineers because of their applications for organic light emitting diodes (OLEDs) [1], photovoltaic cells (PVCs) [2], biological sensors [3, 4], organic thin film transistors (OTFTs) [5] and bio-electrochromic devices [6]. Furthermore, much interest has been concentrated on developing novel properties of conjugated polymers. Conjugated polymers have been functionalized that are known as one of the most useful way of high quality of conjugated polymers. Palladium-catalyzed Suzuki coupling reaction [7–10] is one of the most important methods. The benzoate units are excellent functional material and can carry functional groups to form conjugated polymers with aromatic derivatives, and then the conjugated polymers show novel chemical properties, such as apply to estrogenic drugs and preservative.

In this work, we synthesized a series of novel π-conjugated polymers having benzoate units in the main chains. As other one part of conjugated backbones, we employed phenylenes, thiophenes and fluorene rings with side chains (Scheme2. 1). Benzoate and different dibromo aromatic compounds can be not only be conjugated backbone but also be able to bear the building blocks of side groups, which might likely provide the polymer with the unexpected chemical properties. The dibromo aromatic compound with optically active groups was introduced conjugated polymer P1, which tend to form chiral higher order structures, for example, predominantly one-handed helices or chiral aggregates, due to the small mobility of the conjugated main chains [23, 24]. Herein, poly(benzophenylene), polybenzothiophene and polybenzofluorenes backbone were designed and the properties of different main chains were evaluated.

Their optical and electronic properties were examined by UV-vis absorption spectrometry and photoluminescence spectrometry. These results showed that the conjugated system was constructed through the benzoate unit having ester group, and it should be able to expand main-chain conjugations. The synthsis method was explored that benzoate unit of the functional groups and dibromo aromatic hydrocarbons of functional side chains linked to conjugated main-chain via Suzuki-Miyaura coupling reaction. Sometimes, The functional polymers are difficultly obtained by the method of *n*-BuLi, which reacts with ester group and amino groups. The method is limited to produce the desired products (Scheme 2. 2). However, the diborane compound to prepare the precursor allows no use of *n*-BuLi for preparation of precursor, the Miyaura-Suzuki polycondensation reaction is expanding possibility. The tentative synthetic method, which is related to produce π-conjugated skeleton and this reaction allows producing multi-functional chemical materials.

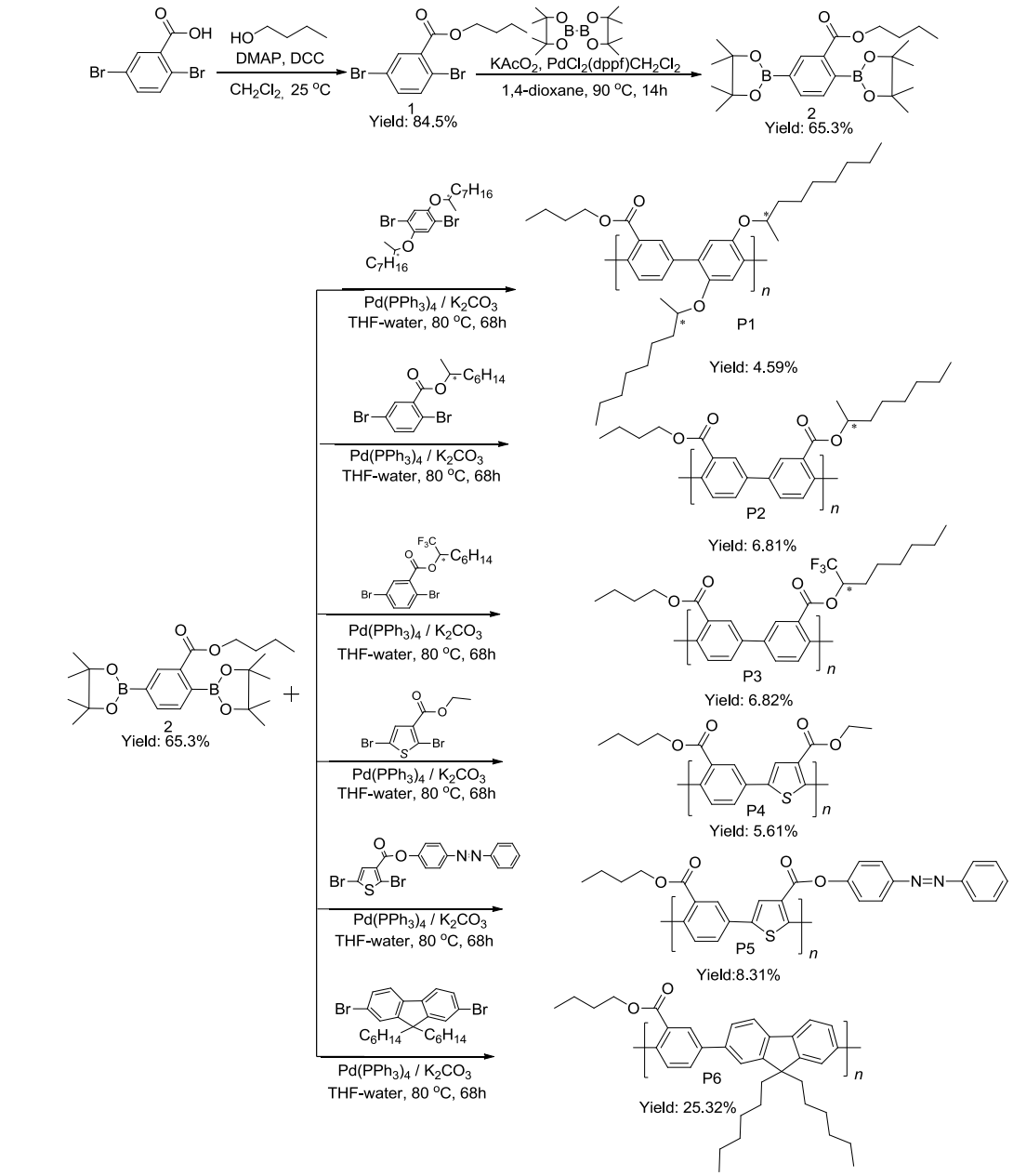

Scheme 2. 1. Synthesis of monomers and polycondensation

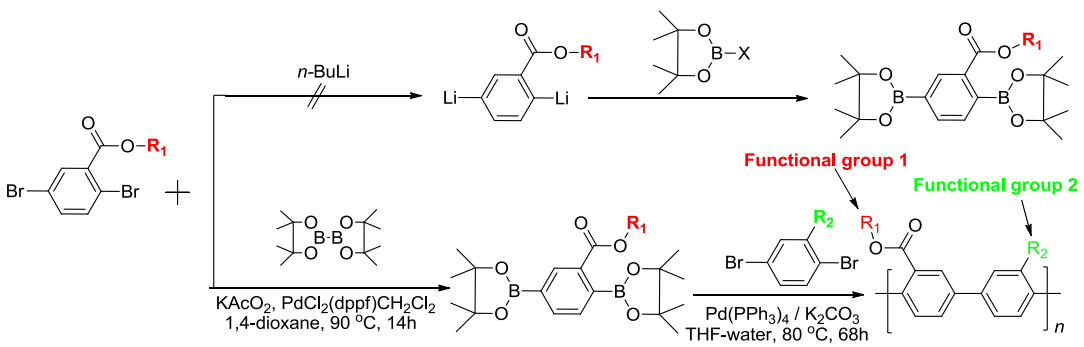

Scheme 2. 2. Synthesis of a precursor compound for Miyaura-Suzuki type polycondensation.

2.2 Experimental

2.2.1 Chemicals

Commercially available reagents were received from Nacalai Tesque (Japan), Sigma-Aldrich (Japan), Kanto Chemical (Japan) and Tokyo Chemical Industry (Japan) and used without further purification. Common organic solvents such as dichloromethane and tetrahydrofuran (THF) were distilled and handled in a moisture-free atmosphere. The purification of the newly synthesized compounds was performed by column chromatography on silica gel (Silica gel 60 N).

2.2.2 Techniques.

^{1}H NMR spectra of the compounds were recorded using JNM ECS 400 spectrometer (JEOL, Japan) with $CDCl_3$ as the deuterated solvent and tetramethylsilane (TMS) as the internal standard. Chemical shifts were given in parts permillion and coupling constant (*J*) in Hz. FT-IR absorption spectra were obtained with an FT/IR-300 spectrometer (Jasco) using a KBr method. UV-vis absorption spectra were recorded on a JASCO V-630 UV-vis optical absorption spectrometer. Circular dichroism (CD) spectra were measured with a J-720 (JASCO, Tokyo, Japan). Photoluminescence (PL) spectra of the polymers in chloroform were measured with F-4500 fluorescence spectrophotometer (HITACHI, Japan). Molecular weights of the polymers were determined by gel permeation chromatography (GPC) with MIXED-D HPLC column (Polymer Laboratories), PU-980 HPLC pump (Jasco) and MD-915 multiwavelength detector (Jasco), with tetrahydrofuran (THF) used as the solvent, with the instruments calibrated by polystyrene standard. Matrix-assisted laser desorption ionization time-of-flight mass spectroscopy (MALDI-TOF-MS) analysis was conducted using TOF/TOF 5800 (AB SCIEX, USA) with dithranol as a matrix.

2.2.3 Synthesis

Butyl 2,5-dibromobenzoate (1).

1-Butanol (1.20 g, 14.3 mmol), 2,5-dibromobenzoic acid (1.00 g, 3.50 mmol) and 4-dimethylaminopyridine (DMAP, 0.109 g, 0.89 mmol) were dissolved in 50 mL of dry dichloromethane in a 100 mL a two-necked round-bottom flask filled with nitrogen. N,N'-dicyclohexylcarbodiimide (DCC, 2.40 g, 11.8 mmol) in 50 mL of dichloromethane was added under stirring via a dropping funnel at 0–5 °C with an ice-water bath. The reaction mixture was stirred overnight. After filtering out the formed insoluble urea, the filtrate was concentrated by a rotary evaporator. The product was purified by a silica gel column using ethyl acetate/hexane (v/v = 1:20) as the eluent. The product is colorless oil. Yield: 84.5%. ^{1}H NMR (400MHz, $CDCl_3$, δ, ppm): 8.32 (s, 1H, Ar–*H*), 7.93–7.92 (d, 1H, J = 8, Ar–*H*), 7.48-7.46 (d, 1H, J = 8, Ar–*H*), 4.34-4.30 (t, 2H, J = 10.3, -O-C*H*$_2$(CH$_2$)$_2$CH$_3$), 1.81–1.72 (m, 2H, -OCH$_2$-C*H*$_2$CH$_2$CH$_3$), 1.63–1.51 (m, 2H, -OCH$_2$CH$_2$-C*H*$_2$CH$_3$), 0.99–0.97 (t, J = 11.2, 3H, -OCH$_2$(CH$_2$)$_2$-C*H*$_3$).

Butyl 2,5-bis(4,4,5,5-tetramethyl-1,3,2-dioxaborolan-2-yl)benzoate (2).

Potassium acetate ($KAcO_2$, 1.69 g, 17.2 mmol), [1,1′-bis(diphenylphosphino)ferrocene]dichloropalladium(II) complex with dichloromethane ($PdCl_2(dppf)CH_2Cl_2$, 0.0814 g, 0.10 mmol), bis(4,4,5,5-tetramethyl-[1,3] dioxolan-2-yl)borane (1.02 g, 4.31 mmol) and butyl 2,5-dibromobenzoate (1.00 g, 2.87 mmol) were added into

a three necked round bottom with 1,4-dioxane 20 mL under an argon stream. The mixture was heated to 90 °C with stirring for 16h. The reaction mixture was extracted with CH_2Cl_2 three times after cool to room temperature. The organic layer was washed with water and dried over with anhydrous $MgSO_4$. Evaporation of the solvents, the product was purified by a silica gel column using ethyl acetate/hexane (v/v = 1:20) as an eluent. The product is yellow solid. Yield: 65.3%. ^{1}H NMR (400MHz, $CDCl_3$, δ, ppm): 8.31 (s, 1H, Ar–*H*), 7.92–7.90 (d, 1H, J = 8, Ar–*H*), 7.49-7.47 (d, 1H, J = 8, Ar–*H*), 4.34-4.30 (t, 2H, J = 10.3 -O-C*H*$_2$(CH$_2$)$_2$CH$_3$), 1.81–1.72 (m, 2H, -OCH$_2$-C*H*$_2$CH$_2$CH$_3$), 1.63–1.51 (m, 2H, -OCH$_2$CH$_2$-C*H*$_2$CH$_3$), 1.41–1.33 (m, 24H, -CC-(C*H*$_3$)$_2$), 0.99–0.94 (t, 3H, J = 14.2 , -OCH$_2$(CH$_2$)$_2$-C*H*$_3$). *m*/*z* = 431.

P1.

Into a 10 mL three-necked, round-bottom flask containing potassium carbonate (K_2CO_3, 77.8 mg, 0.564 mmol), tetrakis(triphenylphosphine)palladium(0) ($Pd(PPh_3)_4$) (10.8 mg, 0.0093 mmol), compound M1 (100 mg, 0.188 mmol), monomer 2 (121 mg, 0.282 mmol) in 0.2 mL of water and 2 mL of THF were added under an argon stream. In an argon atmosphere, the mixture was heated to 80 °C with stirring around 68 h. The reaction mixture was extracted with CH_2Cl_2 after cooling to room temperature. The organic layer was washed two times with water and dried with over anhydrous $MgSO_4$. After the evaporation of the solvents, the crude product was diluted in 3 mL of chloroform. The solution was added dropwise to 100 mL of methanol with stirring. The precipitate was allowed to stand overnight and centrifugal separation to obtain 10 mg black solid. Y = 4.59%. ^{1}H NMR (400MHz, $CDCl_3$, *δ*, ppm): 8.26-6.87 (m, 5H), 4.38-4.04 (m, 4H), 1.82-1.07 (m, 34H), 0.91-0.77 (m, 9H).

P2.

P2 was synthesized using the same method as synthesis of P1, K_2CO_3 (109 mg, 0.795 mmol), tetrakis(triphenylphosphine)palladium(0) ($Pd(PPh_3)_4$) (15.3 mg, 0.0133 mmol), monomer 2 (171 mg, 0.398 mmol), compound M2 (100 mg, 0.265 mmol) in 0.2 mL of water and 2 mL of THF were raction. The final product, a brown solid polymer, was obtained after drying in vacuo, with a yield of 6.81%. ^{1}H NMR (400MHz, $CDCl_3$, *δ*, ppm): 8.38-7.32 (m, 6H), 4.22-4.03 (m, 3H), 1.92-1.06 (m, 17H), 0.93-0.76 (m, 6H).

P3.

P3 was synthesized using the same method as synthesis of P1, K_2CO_3 (96 mg, 0.696 mmol), tetrakis(triphenylphosphine)palladium(0) ($Pd(PPh_3)_4$) (13.4 mg, 0.0116 mmol), monomer 2 (149 mg, 0.348 mmol), compound M3 (100 mg, 0.232 mmol) in 0.2 mL of water and 2 mL of THF were reaction. The final product, a brown solid polymer, was obtained after drying in vacuo, with a yield of 6.82%. ^{1}H NMR (400MHz, $CDCl_3$, *δ*, ppm): 8.42-7.30 (m, 6H), 4.25-4.04 (m, 3H), 1.94-1.08 (m, 14H), 0.94-0.78 (m, 6H).

P4.

P4 was synthesized using the same method as synthesis of P1, tetrakis(triphenylphosphine)palladium(0) ($Pd(PPh_3)_4$) (18.5 mg, 0.0159 mmol), K_2CO_3 (132 mg, 0.958 mmol), monomer 2 (206 mg, 0.479 mmol), compound M4 (100 mg, 0.319 mmol) in 0.2 mL of water and 2 mL of THF were reaction. The final product,

a brown solid polymer, was obtained after drying in vacuo, with a yield of 5.61%. ^{1}H NMR (400MHz, $CDCl_3$, δ, ppm): 8.38-7.01 (m, 4H), 4.33-4.05 (m, 4H), 1.92-1.02 (m, 7H), 0.94-0.78 (t, 3H).

P5.

P5 was synthesized using the same method as synthesis of P1, K_2CO_3 (188 mg, 0.643 mmol), tetrakis(triphenylphosphine)palladium(0) ($Pd(PPh_3)_4$) (12.4 mg, 0.0107 mmol), monomer 2 (138 mg, 0.322 mmol), compound M5 (100 mg, 0.214 mmol) in 0.2 mL of water and 2 mL of THF were reaction. The final product, a brown solid polymer, was obtained after drying in vacuo, with a yield of 8.31%. ^{1}H NMR (400MHz, $CDCl_3$, δ, ppm): 8.32-6.96 (m, 13H), 4.42-4.01 (d, 2H), 1.96-1.06 (m, 4H), 1.05-0.78 (t, 3H).

P6.

P6 was synthesized using the same method as synthesis of P1, K_2CO_3 (21 mg, 0.152 mmol), tetrakis(triphenylphosphine)palladium(0) ($Pd(PPh_3)_4$) (2.9 mg, 0.0025 mmol), monomer 2 (32.8 mg, 0.0762 mmol), compound M6 (25 mg, 0.0508 mmol) in 0.2 mL of water and 2 mL of THF were raction. The final product, a brown solid polymer, was obtained after drying in vacuo, with a yield of 25.32%. ^{1}H NMR (400MHz, $CDCl_3$, δ, ppm): 8.32-6.96 (m, 9H), 4.16-3.98 (d, 2H), 2.12-0.91 (m, 24H), 0.89-0.58 (m, 9H).

2.3. Results and discussion.

Polycondensation results of P1-P6 are summarized in Table 2. 1. The results of Number average molecular weights (M_n) of the conjugated polymers evaluated with gel permeation chromatography (GPC) are corresponding to the result of MALDI-TOF-MS. However, degree of polymerization (DP) of polymer P1 to polymer P6 is small. This may be due to steric hindrance between the monomers in the reaction process and affect to yield polymer with high molecular weight.

Table 2. 1. GPC and MALDI-TOF-MS results for P1-P6.

Polymer	M_n[a] [g/mol]	M_w[a] [g/mol]	M_w/M_n	DP[b]	MS[c]
P1	2,300	5300	2.3	4	2,592
P2	2,400	3,600	1.5	4	2,447
P3	2,400	3,200	1.3	6	2,383
P4	1,500	2,200	1.5	5	1,206
P5	2,500	3,100	1.2	5	2,632
P6	2,200	2,700	1.2	4	2,769

[a]Estimated with GPC using THF as an eluent against polystyrene standard.

[b]Degree of polymerization (calculated by M_n/M, M: molecular weight of monomer repeat unit). [c]MALDI-TOF-MS measurements results of these polymers

2.3.1 Characterization

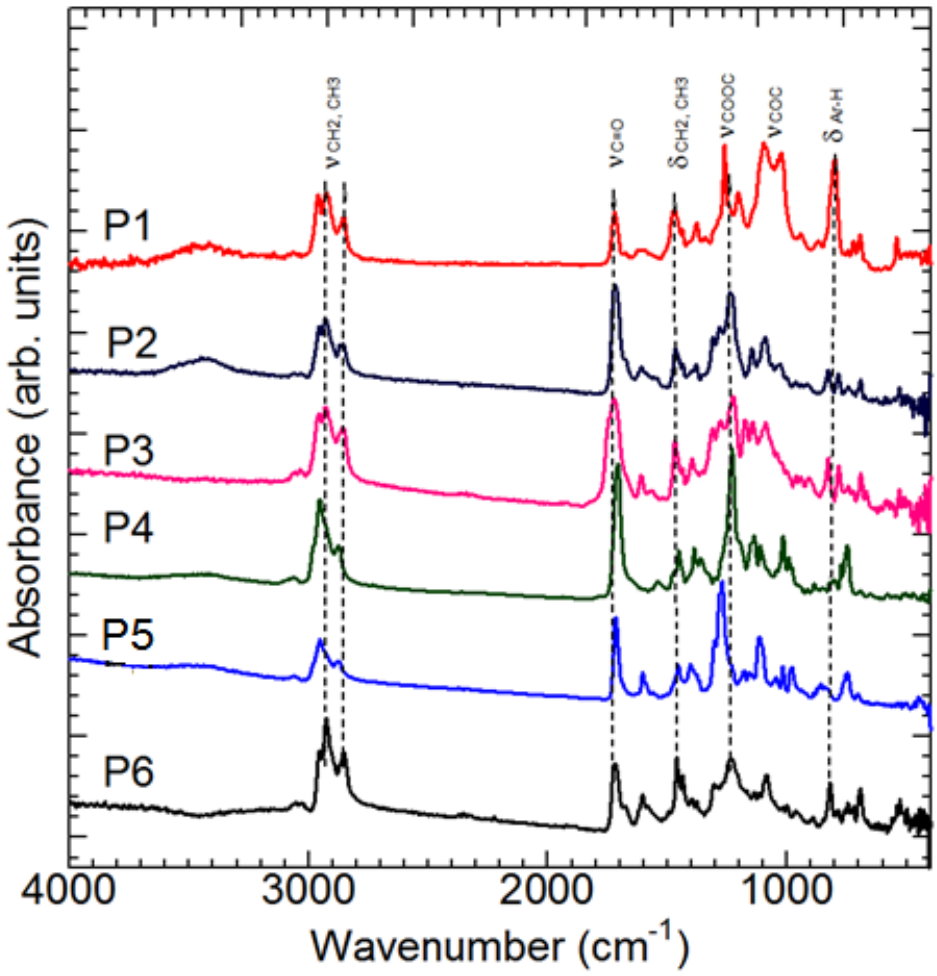

Figure 2. 1. IR spectra of P1, P2, P3, P4, P5, and P6.

IR spectroscopy of the polymers was characterized and shown in the Fingure2. 1. All of the polymers gave satisfactory analysis data corresponding to their expected molecular structures. The polymers show C=O stretching band at 1711 cm^{-1} attributed to ester groups in the side chain. A intense absorptions at 2851cm^{-1}-2982 cm^{-1} is attributed to C–H stretching of the long alkyl chain. The polymers also show an absorption band at 1248 cm^{-1} attributed to CO-O-C (ester) stretching in the benzoate units. Particularly, Ar-H and C-H out-of-plane vibration was observed at 830 cm^{-1} and 1476 cm^{-1}. On the other hand, P1 has an intense absorption band at 830 cm^{-1} due to *p*-substituents in benzene ring. P1 displays relatively intense absorption band at around 1089 cm^{-1} because of the C–O–C stretching of thire monomer units. These results indicate that the polymes were successfully polymerized by Suzuki coupling reaction.

The structures were verified by ^{1}H NMR spectroscopy as well. All the peaks of P1-P6 can be readily assigned to the resonances of appropriate protons. In here, P6 was as an example to verify and shown in Figure2. 2. The peaks resonate at 0.78–2.07 ppm are attributed to the protons in alkyl chains. It was noteworthy that the chemical shift at 4.09 ppm of the NMR spectra of the monomers benzoate unit was attributable to the chemical shift of the proton in COOC*H* group. NMR spectrum of polymer P6 along with that of benzoate unit was

clearly observed. Particularly, the protons of the aryl rings of P6 were observed around low magnetic field which intensity increases as the aryl unit concentration in the polymer backbone increases. The aromatic rings of the phenyl groups give signals in the same region as those of the aromatic rings of the fluorene groups. The region between 7.26 and 8.13 ppm gets more crowded with increased content of aromatic rings. This is easily noticed for P6, where the concentration of the aryl groups is higher.

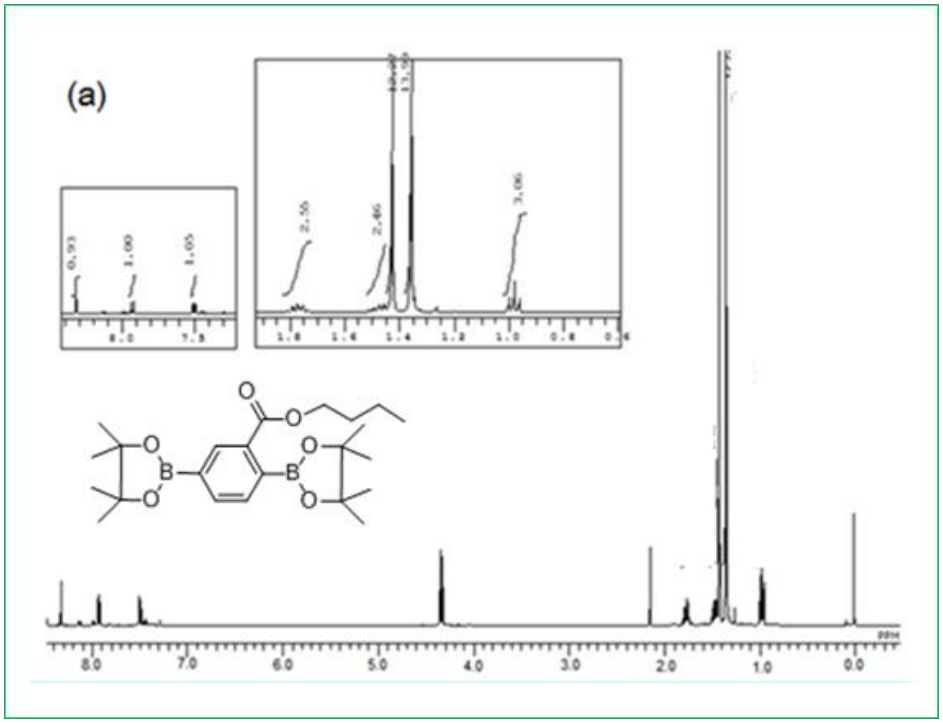

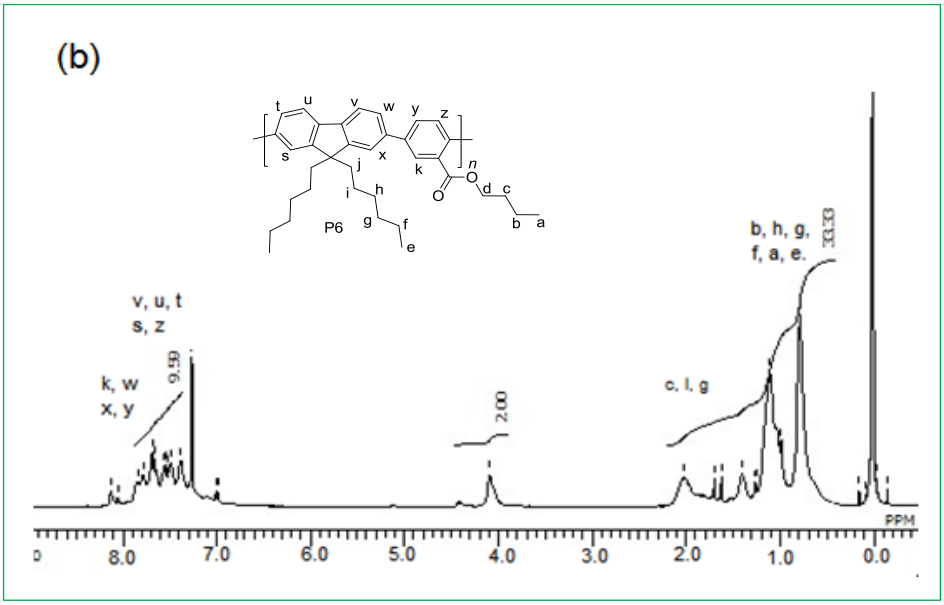

Figure 2. 2. ^{1}H NMR spectra of butyl 2,5-bis(4,4,5,5-tetramethyl-1,3,2-dioxaborolan-2-yl)-benzoate and P6 with deuterated chloroform as solvent.

2.3.2 Optical properties of polymers

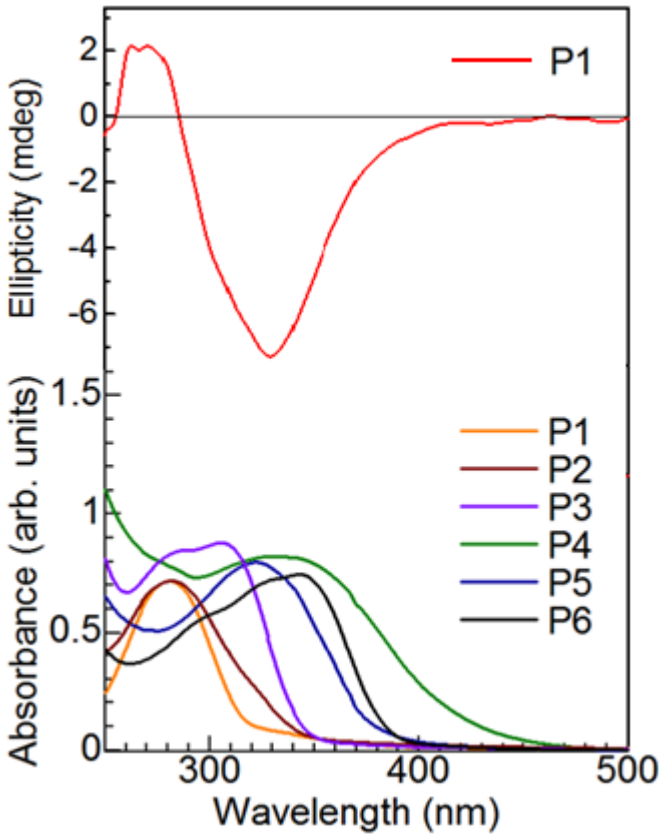

Figure 2. 3. Circular dichroism (CD) absorption spectrum and UV-vis absorption spectra of the polymers in THF solution.

The CD and UV-vis absorption spectra of the polymers are shown in Figure 2. 3. The polymer P1 shows a clear couplet with a negative Cotton effect at 324 nm and a positive one at 271 nm, which corresponds to a strong optical absorption band at around 280 nm, indicate that it formed helices of preferential helicity. But other polymers did not exhibit considerable CD signal. To all the polymers, was having strong, broad and structureless absorption peaks around 280-347 nm, corresponding to the intramolecular charge-transfer transition, which the lowest-energy band was largely of charge transfer character. It was this lowest-energy absorption band that was most sensitive to the main-chain structure. The polymers of poly(benzophenylene) type P1, P2, P3 have a maximum absorption at 280 nm, 281 nm and 311 nm. The polymers of polybenzothiophene type P4 and P5 were absorbed strongly at 338 and 319 nm. The strong absorption of polybenzofluorene type P6 was observed at 347 nm. Consequently, intramolecular charge-transfer (ICT) effects in the benzofluorene and benzothiophene were expected to be stronger than benzophenylene structure. The experimental observations from all the absorption spectra were in accord with this expectation.

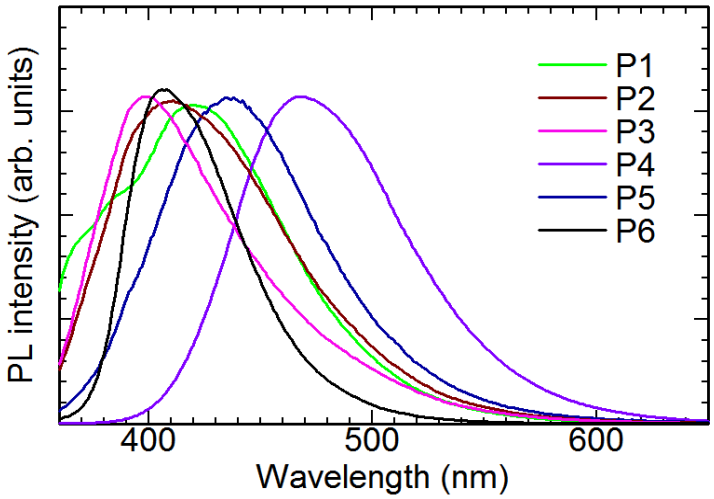

Figure 2. 4. Photoluminescence spectra of THF solutions of P1, P2, P3, P4, P5, and P6.

A polymer with light-emitting properties may find unique technological applications, so the fluorescence properties of all polymers are investigated, as shown in Figure 2. 4. When poly(benzophenylene) type P1, P2, P3 were photoexcited at 320 nm, they emit strong UV-vis light of at 421nm, 412 nm, 395 nm in THF, and polybenzothiophene type P4, P5 shown emission peaks at 471 nm, 443 nm. Polybenzothiophene type P6 show emission peaks at 408 nm. These stronger and broader single peaks indicate complete energy transfer. In solution, the predominant energy transfer is expected to be intramolecular due to the low concentration of the polymer chains. As the polymer chains get closer to each other intermolecular energy transfer becomes dominant. [11]

2.4. Conclusion and future prospect

A series of π-conjugated polymers having benzoate units with several conjugated backbones were synthesized by Suzuki-Miyaura coupling polymerization. The benzoate unit can carry functional groups to form conjugated polymers with aromatic derivatives and then the conjugated polymers show novel chemical properties. The exploration experiment in this study indicates that the Suzuki-Miyaura coupling polymerization can produce π-conjugated skeleton, and this reaction allows producing multi-functional chemical materials. The polymers were soluble in THF, CH_2Cl_2, $CHCl_3$ and DMF. CD and UV−vis spectroscopic analysis revealed that P1 formed chiral higher-order structures in THF, while P2 and P3 did not. But all conjugated polymers absorb in the longer wavelength region. In addition, structures of obtained conjugated polymers are fully characterized spectroscopically, demonstrating well-defined conjugated polymers have been prepared through Suzuki-Miyaura coupling polymerization method.

2.5. Acknowledgments

We would like to thanks Research Facility Center for Science and Technology, University of Tsukuba, and Glass workshop of University of Tsukuba.

2.6. References

[1] Mitschke U, Bäuerle P. The electroluminescence of organic materials. J. Mater. Chem. 2000;10:1471-1507.

[2] Brabec CJ, Sariciftci NS, Hummelen JC. Plastic solar cells. Adv. Funct. Mater. 2001;11:15-26.

[3] Zhu CL, Liu LB, Yang Q, Lv FT, Wang S. Water-soluble conjugated polymers for imaging, diagnosis, and therapy. Chem. Rev. 2012;112:4687–4735.

[4] Thomas SW, Joly GD, Swager TM. Chemical sensors based on amplifying fluorescent conjugated polymers. Chem. Rev. 2007;107:1339-1386.

[5] Roberts E, Sokolov AN, Bao Z. Material and device considerations for organic thin-film transistor sensors. J. Mater. Chem. 2009;19:3351-3363.

[6] Groenendaal L, Zotti G, Aubert PH, Waybright SM, Reynolds JR. Electrochemistry of Poly (3, 4-alkylenedioxythiophene) Derivatives. Adv. Mater. 2003;15:855-879.

[7] Yokozawa T, Kohno H, Ohta Y, Yokoyama A. Catalyst-Transfer Suzuki−Miyaura Coupling Polymerization for Precision Synthesis of Poly (p-phenylene). Macromolecules. 2010;43:7095–7100.

[8] Horie M, Majewski LA, Fearn MJ, Yu CY, Luo Y, Song A, Saunders BR, Turner ML. Cyclopentadithiophene based polymers—a comparison of optical, electrochemical and organic field-effect transistor characteristics. J. Mater. Chem. 2010;20:4347–4355.

[9] Liu Y, Chen X, Qin J, Yu G, Liu Y. New linear π-conjugated polymers via Suzuki coupling of (1Z, 3Z)-1,4-dibromo-1,4-diaryl-buta-1,3-diene with aromatic diborates: Synthesis and photophysical properties, Polymer. 2010;51:3730–3735.

[10] Zhang C, Trudell ML. Palladium-bisimidazol-2-ylidene complexes as catalysts for general and efficient Suzuki cross-coupling reactions of aryl chlorides with arylboronic acids. Tetrahedron Letters. 2000;41:595–598.

[11] Kimyonok A, Tekin E, Haykır G, Turksoy F. Synthesis, photophysical and electroluminescence properties of anthracene-based green-emitting conjugated polymers. J Lumin 2014;146:186-192.

2.7. Supporting Information

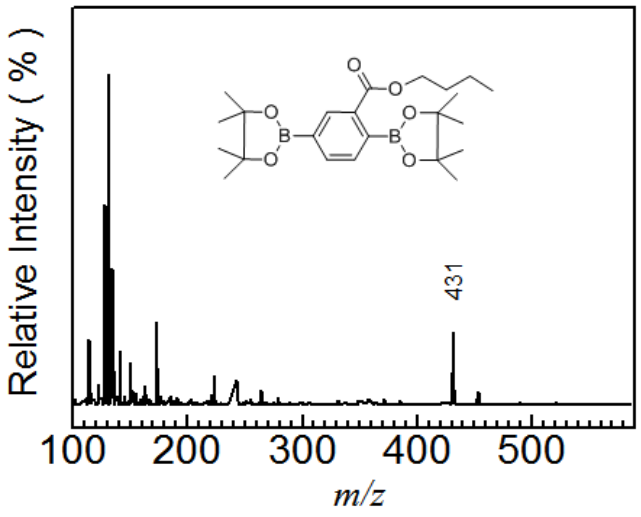

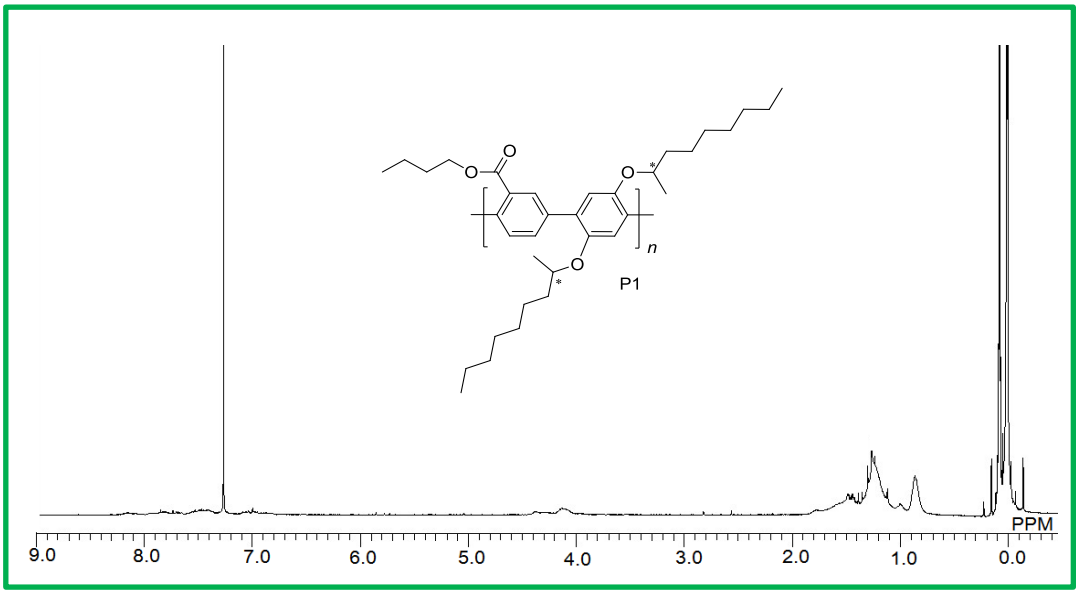
P1
n
PPM
9.0
8.0
7.0
6.0
5.0
4.0
3.0
2.0
1.0
0.0

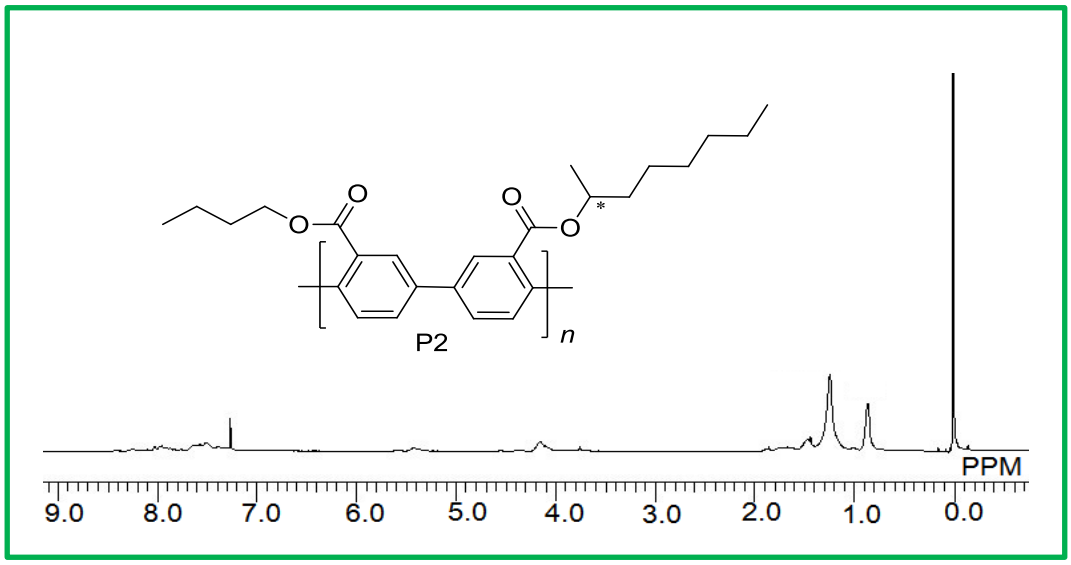
P2
n
PPM
9.0
8.0
7.0
6.0
5.0
4.0
3.0
2.0
1.0
0.0

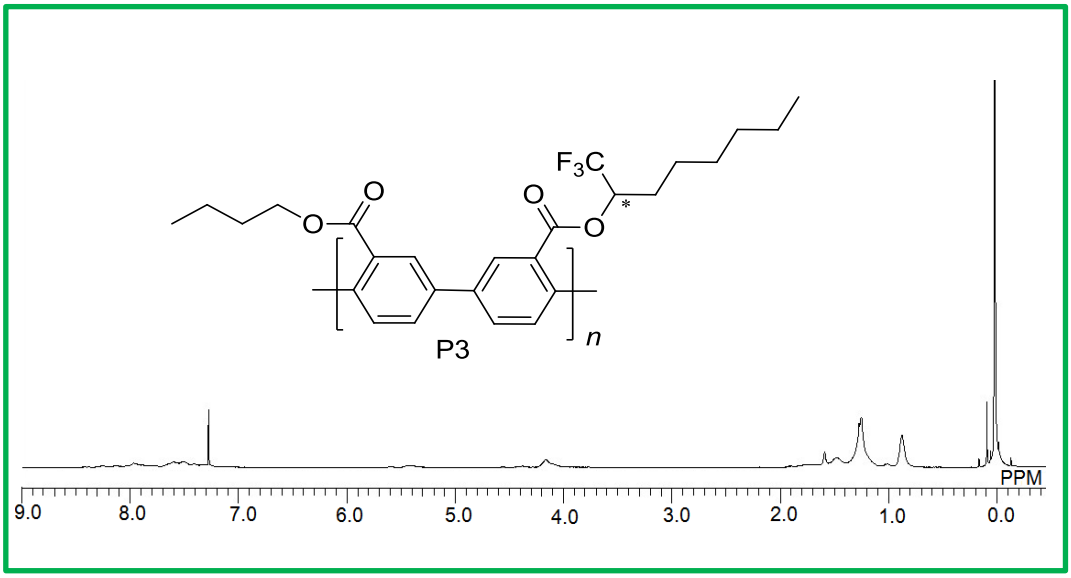
F3C
P3
n
PPM
9.0
8.0
7.0
6.0
5.0
4.0
3.0
2.0
1.0
0.0

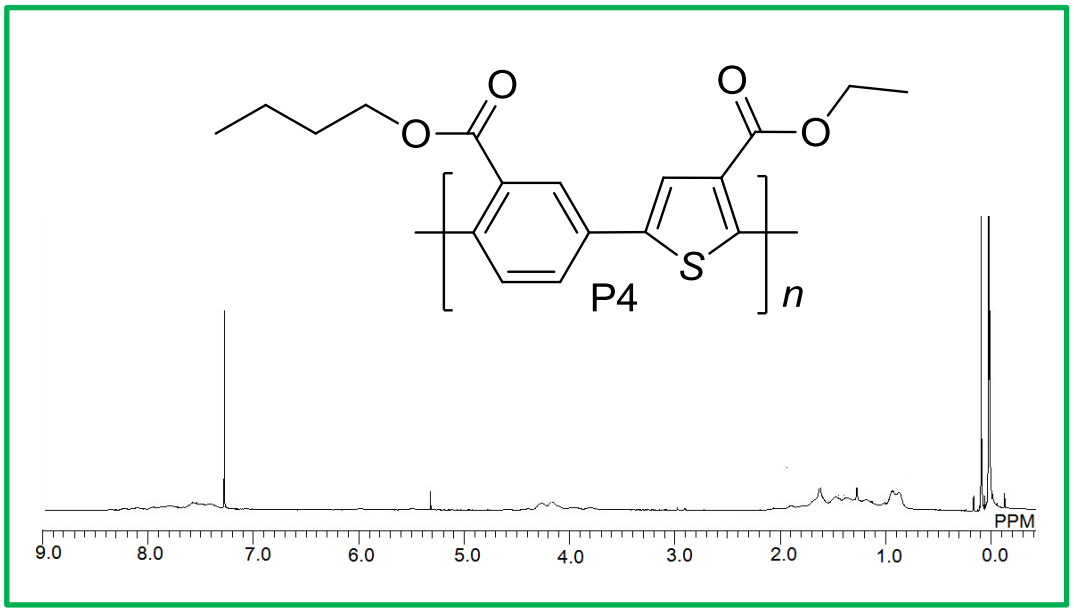
O
O
O
O
S
P4
n
PPM
9.0
8.0
7.0
6.0
5.0
4.0
3.0
2.0
1.0
0.0

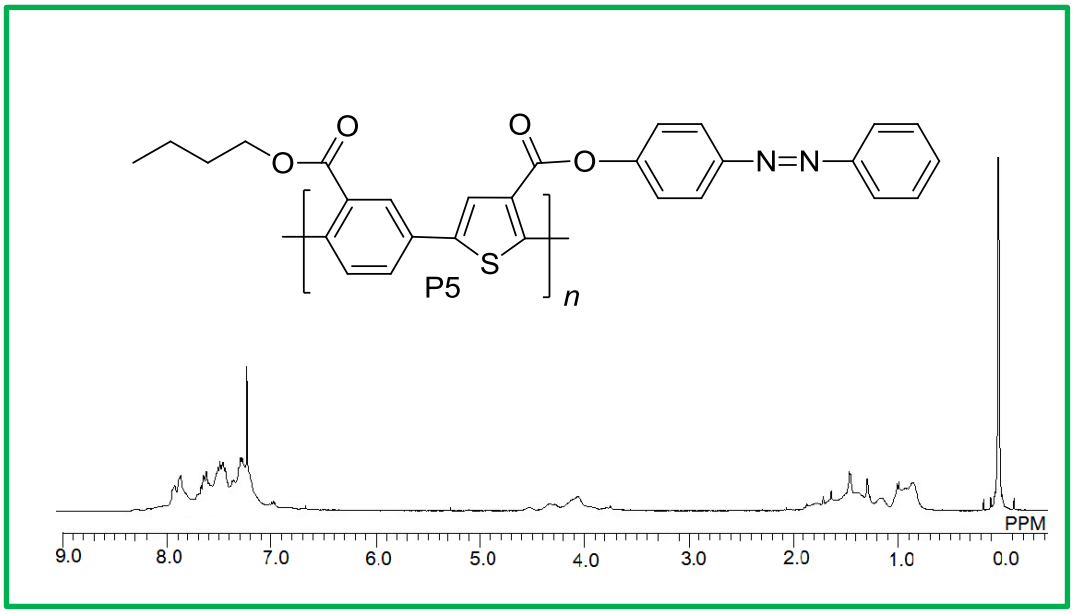
O
O
O
O
N=N
S
P5
n
PPM
9.0
8.0
7.0
6.0
5.0
4.0
3.0
2.0
1.0
0.0

Chapter 3

Synthesis and properties of functional novel paramagnetic polymers having 2,6-di-*tert*-butylphenoxyl radicals in side chains

3.1 Introduction

Conjugated polymers have garnered increasing attention in fields ranging from organic electronics to biotechnology [1] because of the ability of these materials to improve upon existing technologies by combining the unique properties of small functional molecules (e.g., optical, electronic and magnetic functional groups) in applications where flexible, mechanically robust devices are desired. [2-5] In particular, functional polymers based on π-conjugated, which have emerged for a number of device types including organic light emitting diodes (OLEDs), [6,7] biological sensors, [8,9] photovoltaic cells (PVCs), [10] bio-electrochromic devices [11] and organic thin film transistors (OTFTs). [12] An interesting subclass of functional polymers that has emerged in the last three decades contain stable organic radicals in the repeating unit pendant to their backbones. [13-16] Many research groups have continuously expended in the synthesis of organic polyradicals as potential candidates of molecular-based magnetic materials. [17-21] Nishide et al. synthesized π-conjugated polymers bearing side-chain of pendant radical groups, which also are π-conjugated with the polymer backbone. It could improve both the spin quantum number S and the stability of the polyradical [22]. Recently, the chemistry of polyradicals has taken on new aspects in the fields of organic electronic devices and industrial applications. Boudouris et al. synthesized purely organic nonconjugated polyradicals and made conductivity devices to establish the transport charge ability of a specific radical polymer. [23]

To understand the contribution of organic radicals and functional molecules to π-conjugation polymers, the characteristics of the conjugated polymers containing the functional groups and 2,6-di-tert-butylphenoxyl radicals were investigated. 2,6-Di-tert-butylphenoxyl group was introduced for generation of stable radicals by oxidation. [24, 25] The pendant radical groups are π-conjugated with the polymers backbone, and the molecular connectivity can lead to the expectation of high-spin magnetic properties or as electron-transporting blocks. [26] On the other hand, the functional groups be introduced into the electronic structure and can be fixed the conjugated main chain which form the low bandgap, optical, electrical and magnetic π-conjugated polymers. [27-36] The polymerization was executed with Suzuki-Miyaura coupling reactions and Migita-Kosugi-Stille reactions. The characterization and the determination of the structures of the products were performed with IR spectrometry and NMR spectrometry. The optical and electrochemical properties were examined by UV-vis absorption spectroscopy, photoluminescence spectroscopy, circular dichroism spectrum, electron paramagnetic resonance spectra and cyclic voltammetry.

3.2 Experimental

3.2.1 Materials

Commercially available reagents were received from Nacalai Tesque (Japan), Sigma-Aldrich (Japan), Kanto Chemical (Japan) and Tokyo Chemical Industry (Japan) unless otherwise notedand used without further purification. Common organic solvents such as dichloromethane and tetrahydrofuran (THF) were distilled and handled in a moisture-free atmosphere. The purification of the newly synthesized compounds was performed by column chromatography on silica gel (Silica gel 60 N).

3.2.2 General methods

^{1}H NMR spectra of the compounds were recorded using JNM ECS 400 spectrometer (JEOL, Japan) with $CDCl_3$ as the deuterated solvent and tetramethylsilane (TMS) as the internal standard. Chemical shifts were given in parts permillion and coupling constant (*J*) in Hz. FTIR absorption spectra were obtained with an FT/IR-300 spectrometer (Jasco) using a KBr method. UV-vis absorption spectra were recorded on a JASCO V-630 UV-vis optical absorption spectrometer. Circular dichroism (CD) spectra were measured with a J-720 (JASCO, Tokyo, Japan). Photoluminescence (PL) spectra of the polymers in chloroform were measured with F-4500 fluorescence spectrophotometer (HITACHI, Japan). Molecular weights of the polymers were determined by gel permeation chromatography (GPC) with MIXED-D HPLC column (Polymer Laboratories), PU-980 HPLC pump (Jasco) and MD-915 multiwavelength detector (Jasco), with tetrahydrofuran (THF) used as the solvent, with the instruments calibrated by polystyrene standard. ESR measurements of the samples in powder were carried out using a JEOL JES TE-200 spectrometer with 100 kHz modulation. The spin concentration was determined using $CuSO_4 \cdot 5H_2O$ as standard. The sample was packed into a 5 mm quartz tube. Cyclic voltammetry (CV) measurements were carried out with a μAUTOLAB TYPE III (ECO Chemie). Electrolyte solutions contained 0.1 M of TBAP in acetonitrile.

3.2.3 Monomer synthesis

(2,6-Di-tert-butyl-4-bromophenoxy)trimethylsilane (1)

The compound of 2,6-di-*tert*-butyl-4-bromophenol (11.4 g, 40.0 mmol) was added into tetrahydrofuran (THF, 150 mL). The *n*-BuLi (1.6 M in hexanes) (37.5 mL, 60.0 mmol) was added dropwise into the mixture under an argon stream and stirred for 2 h at -78 °C. Then a solution of chlorotrimethylsilane (7.4 g, 64.0 mmol) in THF (50 mL) was added dropwise through syringe at -78 °C. The mixture was slowly warmed up to room temperature and stirred for 3 h and was poured into water. The product was extracted with hexane twice, and the organic layers were washed with water twice. The organic layer was dried over $MgSO_4$ and filtered, and the solvent was removed from the filtrate under reduced pressure. The product was purified by column chromatography (silica gel, hexane as eluent) to provide 13.7 g of product (96%). ^{1}H NMR (400 MHz; $CDCl_3$; δ): 7.33 (s, 2H, Ar*H*), 1.39 (s, 18H, C-CH_3), 0.39 (s, 9H, Si-CH_3).

3-(3,5-Di-tert-butyl-4-trimethylsiloxyphenyl)thiophene (2).

This compound was synthesized according to the literature procedure.[37] Under Ar, to a suspension (2,6-Di-*tert*-butyl-4-bromophenoxy)trimethylsilane (9.16 g, 25.6 mmol) in 60 mL THF, Mg (0.7 g, 28.6 mmol) was added, and the reaction mixture was stirred under reflux. After disappearance of Mg, this suspension was added to a mixture of [1,3-bis(diphenylphosphino)propane]nickel(II) chloride ($NiCl_2$(dppp), 88 mg) and 3-

bromothiophene (5.0 g, 30.6 mmol) in THF (40 mL) solution under an argon stream. After stirring under reflux for 24 h, the reaction mixture poured into a mixture of crushed ice and diluted hydrochloric acid and extracted with ether. The ether layer was washed with $NaHCO_3$ (aq), water and brine and dried over $MgSO_4$. The crude product was purified by column chromatography on silica gel using hexane as eluent to afford 6.2 g product (67%). ^{1}H NMR (400 MHz; $CDCl_3$; δ): 7.47 (s, 2H, Ar*H*), 7.32 (s, 3H, Ar*H*), 1.43 (s, 18H, C-C*H*$_3$), 0.41 (s, 9H, Si-C*H*$_3$).

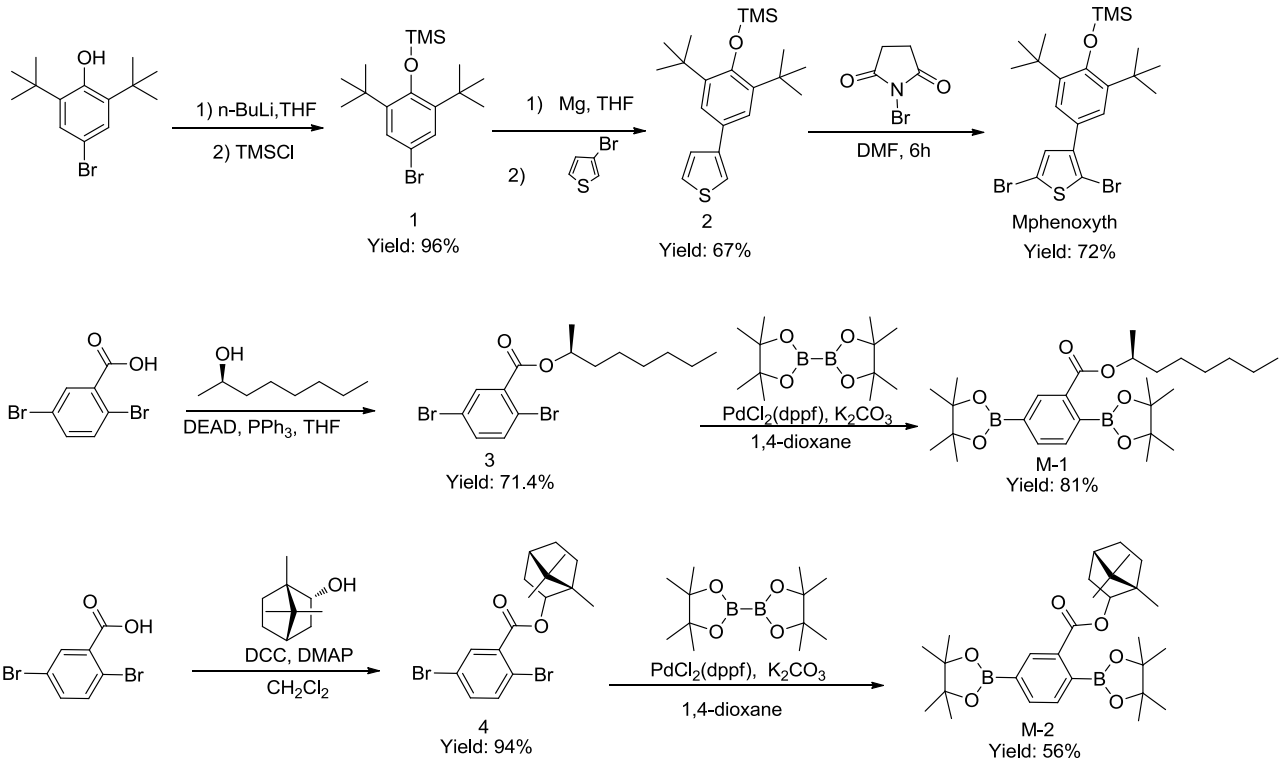

Scheme 3. 1. Synthesis of monomers of Mphenoxyth, M-1 and M-2. PPh_3 = triphenylphosphine, DEAD = diethyl azodicarboxylate, dppf = bis(diphenylphosphino)ferrocene, DCC = N,N'-dicyclohexylcarbodiimide, DMAP = 4-dimethylaminopyridine, TMS = tetramethylsilane.

2,5-Dibromo-3-(3,5-di-tert-butyl-4-trimethylsiloxyphenyl)thiophene (Mphenoxyth).

The mixture of NBS (2.17 g, 12.21 mL) in anhydrous dimethylformamide and DMF (10 mL) were slowly added dropwise to a solution of 3-(3,5-di-t-butyl-4-trimethylsiloxyphenyl)thiophene (2.1 g, 5.82 mmol) in anhydrous DMF (10 mL) at 0 °C under an argon stream. Then cooling was removed and the mixture was stirred for 6 h at room temperature. When completion of the reaction, the mixture was poured into ice water and extracted with dichloromethane twice. The organic layer was separated, washed several times with water to a neutral pH, and dried over $MgSO_4$. The solvent was evaporated to give 2.1 g product (72%). ^{1}H NMR (400 MHz; $CDCl_3$; δ): 7.41 (s, 2H, Ar*H*), 7.03 (s, 1H, Ar*H*), 1.44 (s, 18H, C-C*H*$_3$), 0.447 (s, 9H, Si-C*H*$_3$).

(S)-2,5-Dibromobenzoic acid 1-methyl-heptyl ester (3).

To a solution of 2,5-dibromobenzoic acid (10 g, 35.7 mmol) and triphenylphosphine (PPh_3, 9.63 g, 35.7mmol)

in 200 mL THF. A mixture consisting of diethylazodicarboxylate (DEAD, 15.5 g, 35.7mmol, 40 wt % in toluene) and (*R*)-(-)-2-octanol (4.64 g, 35.7 mmol) in THF (30 mL) was very slowly added dropwise into the solution under an argon stream. The reaction was stirred at room temperature overnight under an argon atmosphere. TLC indicated completion of the reaction. The solution was extracted with dichloromethane, washed with water thoroughly, and dried over anhydrous $MgSO_4$. The dichloromethane layer was removed by evaporation and was purified by column chromatography (silica gel, hexane/ethylacetate = 10:1). The solvent was removed in vacuum and the residue was further purified through vacuum distillation to give a 10 g colorless liquid (71.4 %). ^{1}H NMR (400 MHz; $CDCl_3$; δ): 7.85 (s, 1H, Ar*H*), 7.51-7.49 (d, 1H, *J* = 8 Hz, Ar*H*), 7.44-7.41 (d, 1H, *J* = 12 Hz, Ar*H*), 5.20-5.15 (sextet, 1H, proton at chiral carbon), 1.76-1.57 (m, 2H, CH-CH_2), 1.38-1.30 (m, 11H, CH_2-CH_3 and CH-CH_3), 0.89-0.87 (t, 3H, CH_2-CH_3).

M-1.

Into a 25 mL, three-necked, round-bottom flask containing (S)-2,5-Dibromobenzoic acid 1-methyl-heptyl ester (5.0 g, 12.7 mmol), $KAcO_2$ (7.5 g, 76.5 mmol), [1,1′-bis(diphenylphosphino)ferrocene] dichloropalladium(II) complex with dichloromethane ($PdCl_2$(dppf)CH_2Cl_2, 0.5 g, 0.638 mmol) and bis(4,4,5, 5-tetramethyl-[1,3]dioxolan-2-yl)borane (7.1 g, 28.0 mmol) were added into 50 mL 1,4-dioxane under an argon stream. The mixture was heated to reflux with stirring for about overnight under an argon atmosphere. After the reaction was finished and cooled to room temperature, the reaction mixture was extracted twice with CH_2Cl_2 (150 mL). The organic layer was washed with water and dried with over anhydrous $MgSO_4$. After the evaporation of the solvents, the crude products were purified by column chromatography (silica gel, ethyl acetate/hexane =1:10). The product is yellow solid 5 g. Yield: 81%. ^{1}H NMR (400 MHz; $CDCl_3$; δ): 8.25 (s, 1H, Ar*H*), 7.90-7.88 (d, 1H, *J* = 8 Hz, Ar*H*), 7.47-7.45 (d, 1H, *J* = 8 Hz, Ar*H*), 5.14-5.13 (sextet, 1H, proton at chiral carbon), 1.76-1.57 (m, 2H, CH-CH_2), 1.42-1.47 (m, 24H, C-CH_3), 1.41-1.23 (m, 11H, CH_2-CH_3 and CH-CH_3), 0.89-0.87 (t, 3H, CH_2-CH_3).

1,7,7-Trimethylbicyclo[2.2.1]hept-2-ol2,5-dibromobenzoate (4).

2,5-Dibromobenzoicacid (2.0 g, 7.14 mmol), N,N'-dicyclohexylcarbodiimide (DCC, 1.62 g, 7.85 mmol), L-borneol (2.05 g, 13.3 mmol), 4-dimethylaminopyridine (DMAP, 0.174 g, 1.42 mmol) were added in dichloromethane (25 mL) and stirred at room temperature for 16 h at 25 °C. After the reaction was finished and cooled to room temperature, the reaction mixture was extracted twice with dichloromethane (100 mL) and dried with over magnesium sulfate, then purified by silica gel column chromatography (ethyl acetate/hexane = 1:5) to afford a pale yellow solid 2.80 g (94%). ^{1}H NMR (400 MHz; $CDCl_3$; δ): 7.86 (s, 1H, Ar*H*), 7.51-7.53 (d, 1H, J = 8 Hz, Ar*H*), 7.43-7.45 (d, 1H, J = 8 Hz, Ar*H*), 5.11-5.15 (m, 1H, O-C*H*), 2.49-2.50 (m, 1H, CH-CH_2), 2.05-2.07 (m, 1H, CH-CH_2), 1.74-1.80 (m, 2H, C-CH_2), 1.29-1.39 (m, 2H, CH_2-CH_2), 1.16-1.20 (d, 1H, J = 16.8 Hz, CH_2-C*H*), 0.938-0.993 (m, 9H, CH_3).

Butyl 2,5-bis(4,4,5,5-tetramethyl-1,3,2-dioxaborolan-2-yl)benzoate (M-2).

1,7,7-Trimethylbicyclo[2.2.1]hept-2-ol2,5-dibromobenzoate (0.5 g, 1.20 mmol), $KAcO_2$ (0.7 g, 7.21 mmol), $PdCl_2$(dppf)CH_2Cl_2 (0.0489 g, 0.06 mmol) and Bis(4,4,5,5-tetramethyl-[1,3]ioxolan-2-yl)borane (0.733 g,

2.88mmol) were added into 1,4-dioxane (10 mL) under an argon stream. The mixture was heated to reflux with stirring overnight under an argon atmosphere. After the reaction was finished and cooled to room temperature, the reaction mixture was extracted with CH_2Cl_2 (25 mL). The organic layer was washed with water and dried with over anhydrous $MgSO_4$. After the evaporation of the solvents, the crude products were purified by column chromatography (ethyl acetate/hexane =1:10). The product is 0.35 g yellow solid (56 %). ^{1}H NMR (400 MHz; $CDCl_3$; δ): 8.26 (s, 1H, Ar*H*), 7.90-7.92 (d, 1H, J = 8 Hz, Ar*H*), 7.47-7.49 (d, 1H, J = 12 Hz, Ar*H*), 5.19-5.21 (m, 1H, O-C*H*), 2.47-2.48 (m, 1H, CH-CH_2), 2.15-2.17 (m, 1H, CH-CH_2), 1.84-1.88 (m, 2H, C-CH_2), 1.71-1.74 (m, 2H, CH_2-CH_2), 1.34-1.38 (m, 24H, CH_3), 1.17-1.21 (d, 1H, J = 16 Hz, CH_2-C*H*), 0.935-0.971 (m, 9H, CH_3).

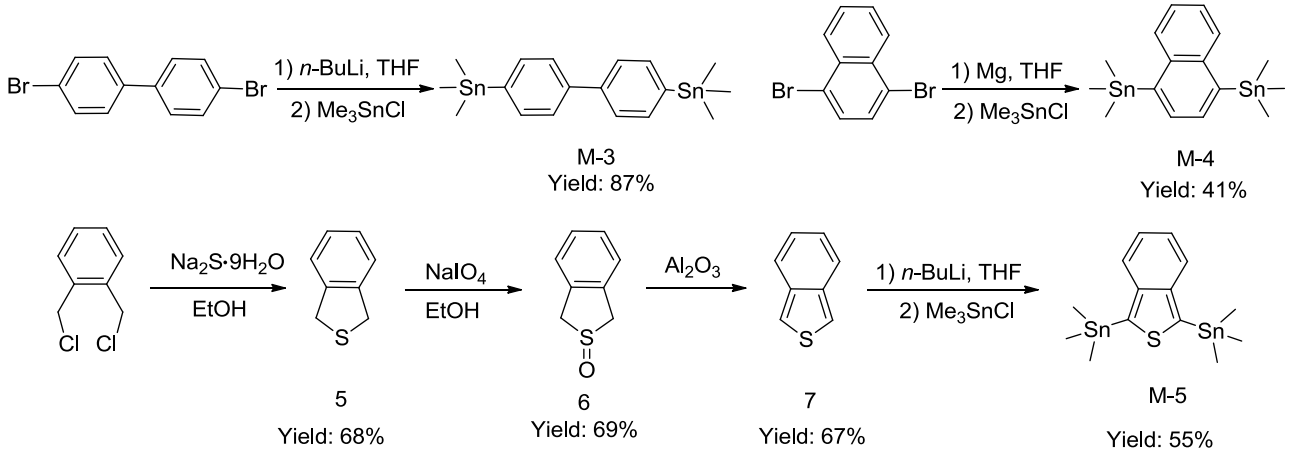

Scheme 3. 2. Synthesis of monomers of M-3, M-4 and M-5.

4,4-Bis(trimethylstannyl)-p-biphenyl (M-3).

The compound of 4,4-Dibromo-p-biphenyl (1.0 g, 6.47 mmol) was added into tetrahydrofuran (THF, 20 mL). The *n*-BuLi (1.6 M in hexanes) (5.2 mL, 16.1 mmol) was added dropwise into the mixture under an argon stream and stirred for 2 h at -78 °C. Then a solution of Me_3SnCl (2.0 g, 19.4 mmol in THF 10 mL) was added dropwise through syringe at -78 °C. The mixture was slowly warmed up to room temperature and stirred for 4 h and was poured into water, and organic residues were extracted with diethyl ether. The ether extract was washed with water and dried over $MgSO_4$. The product was purified by silica gel chromatography using dichloromethane/hexane mixtures (1/9) as an eluent to afford 2.8 g product as a white solid (87%). ^{1}H NMR (400 MHz; $CDCl_3$; δ): 7.59 (s, 8 H, Ar*H*), 0.33 (s, 18 H, Sn-CH_3).

1,4-Bis(tri-n-butylstannyl)naphthalene (M-4).

Under an argon stream, 1,4-dibromonaphthalene (0.2 g, 0.699 mmol), a mixture of magnesium turnings (0.05 g, 2.09 mmol), a small piece of diiodine in 3 mL of THF was added and the reaction mixture was sonicated under reflux for 2 h. Me_3SnCl (0.306 g, 1.53 mmol) in THF 2 mL was added with stirring under room temperature. The progress of reaction was monitored by TLC. After the reaction finished, aqueous saturated NH_4Cl solution (40 mL) was added and extracted with ethyl acetate. The combined extracts were washed with

brine (60 mL) and dried over anhydrous magnesium sulfate to afford 0.13 g white solid (41%). ^{1}H NMR (400 MHz; $CDCl_3$; δ): 7.80-7.85 (m, 2H, Ar*H*), 7.63 (s, 2H, Ar*H*), 7.26-7.55 (m, 2H, Ar*H*), 0.437 (s, 18H).

1,3-Dihydro-benzo[c]thiophene (5).

The solution of sodium sulfide nonahydride (49.3 g, 205.7 mmol) in ethanol/water (500 mL/100 mL) was added into a round-bottom flask. 1,2-bischloromethylbenzene (24.0 g, 137.1 mmol) was added into a soxhlet extractor and added dropwise into the solution and refluxed for 2 h. After the solvent was removed, the mixture was cooled to room temperature and extracted twice with dichloromethane, washed with water, and dried with anhydrous $MgSO_4$. A dichloromethane solution was filtered off and the solvent was evaporated obtained a brown solid. Yield 12.7g (68%). ^{1}H NMR (400 MHz; $CDCl_3$; δ): 7.19-7.28 (m, 4H, Ar*H*), 4.28 (s, 4H, CH_2).

1,3-Dihydro-benzo[c]thiophene 2-oxide (6)

The solution of 1,3-Dihydro-benzo[c]thiophene (5.60 g, 41.1 mmol) in ethanol (140 mL) was added into a round-bottom flask. The mixture of sodium periodate (8.77 g, 41.1 mmol) in water (115 ml) was dropwise added into the solution at 0 °C. After another 3 h stirring the reaction mixture was filtered and evaporated of the solvent evaporation of the solvent followed by washing with diethyl ether gave 1,3-Dihydro-benzo[c]thiophene 2-oxide 4.32 g (69%) as a white solid. ^{1}H NMR (400 MHz; $CDCl_3$; δ): 7.28-7.40 (m, 4H, Ar*H*), 4.25-4.28 (d, 2H, J=13.6 Hz, CH_2), 4.14-4.18 (d, 2H, J=16.0 Hz, CH_2).

Isothianaphthene (7).

The compounds of aluminum oxide powder (2.03 g, 19.8 mmol) and 1,3-Dihydro-benzo[c]thiophene 2-oxide (1.51 g, 9.9 mmol) were mixed and finely crushed in a mortar. Sublimation of the mixture was heated under reduced pressure at 25 mmHg with slowly increasing temperature from 80 °C-150 °C in a sublimer, almost pure isothianaphthene 0.9 g condensed on the cold finger in yield (67%) as a white crystalline crust. ^{1}H NMR (400 MHz; $CDCl_3$; δ): 7.58-7.65 (m, 2H, Ar*H*), 7.01-7.07 (m, 4H, Ar*H*).

1,3-Di(trimethylstannyl)isothianaphthene (M-5).

Freshly prepared isothianaphthene (0.90 g, 6.71 mmol) and tetramethliethylethylenediamine (TMEDA, 1.95 g, 16.8 mmol) were added into tetrahydrofuran (THF, 20 mL). The *n*-BuLi (1.6 M in hexanes) (10.07 mL, 16.1 mmol) was added dropwise into the mixture under an argon stream at 0 °C and stirred for 2 h at room temperature. Then a solution of chlorotrimethyltin (3.38 g, 16.99 mmol) in THF (15 mL) was added dropwise through syringe at -78 °C. The mixture was slowly warmed up to room temperature and stirred overnight. The solution was poured into 50 mL of saturated NH_4HCO_3 and separated. The aqueous phase was extracted with ether twice, and the combined organic phase was washed with water three times and dried over $MgSO_4$. After removal of solvents under reduced pressure, the product was isolated by recrystallization from petroleum ether as a pale yellow solid 2.1 g (55%). ^{1}H NMR (400 MHz; $CDCl_3$; δ): 7.65-7.67 (d, 2H, J = 8.8 Hz, Ar*H*), 7.05-7.08 (d, 2H, J = 11.6 Hz, Ar*H*), 0.489 (s, 18H, Sn-CH_3).

(S)-3,7-Dimethyloctan-1-ol (8)

A solution of (S)-3,7-dimethyloct-6-en-1-ol (10 g, 64.2 mmol) in EtOH/EtOAc (1:8, 90 mL) was treated with Pd/C (3.4 mg) under H_2 atmosphere for one day. The mixture was then filtered through a short silica pipet and concentrated to provide 9.6 g product as a colorless oil (95%). ^{1}H NMR (400 MHz; $CDCl_3$; δ): 3.61-3.71 (m, 2H, O-C*H*$_2$), 1.51-1.58 (m, 3H, CH_3-C*H* and CH_2-C*H*$_2$), 1.37-1.47 (m, 1H, CH_2-C*H*$_2$), 1.17-1.39 (m, 3H, CH_2-C*H*$_2$), 1.05-1.15 (m, 3H, CH_2-C*H*$_2$), 0.825-0.889 (m, 9H, -C*H*$_3$).

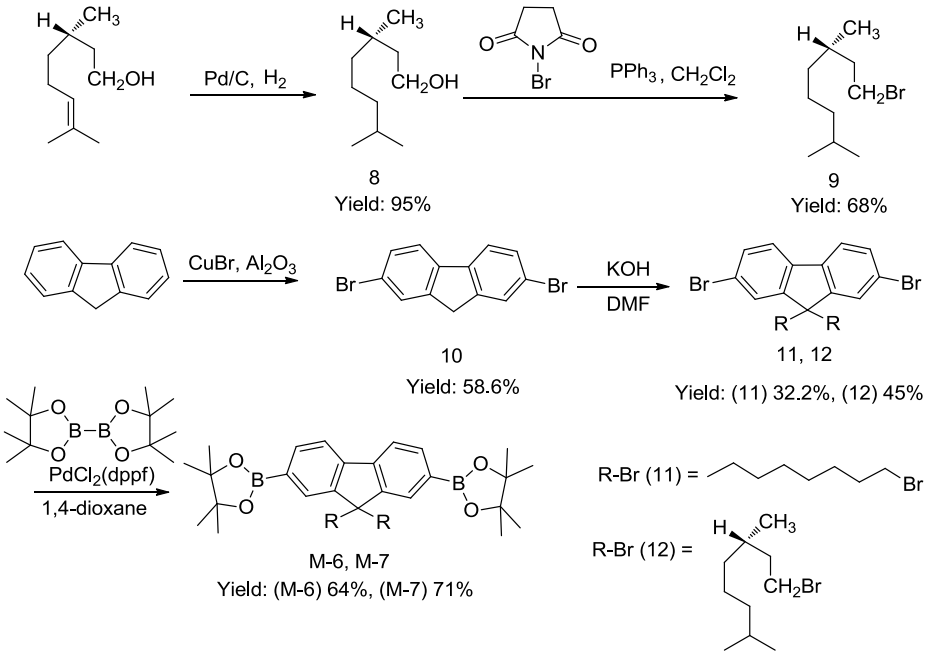

Scheme 3. 3. Synthesis of monomers of M-6 and M-7. PPh_3 = triphenylphosphine, dppf = bis(diphenylphosphino)ferrocene.

(*S*)-1-Bromo-3,7-dimethyloctane (9)

A solution of (S)-3,7-Dimethyloctan-1-ol (6.0 g, 38.4 mmol) and triphenylphosphine (15.1 g, 57.7 mmol) in dichloromethane (100 mL) was added into round-bottom flask at 0 °C, and the mixture was stirred until it became a homogeneous solution. N-Bromosuccinimide (10.3 g, 57.7 mmol) was added in portions over 15 min at 0 °C. The reaction mixture was allowed to warm to room temperature overnight. The dark reaction mixture was concentrated in vacuum, purified by filtration through a pad of silica gel (ethyl acetate/hexane = 1/20) to afford 8.6 g product as a colorless liquid (68%). ^{1}H NMR (400 MHz; $CDCl_3$; δ): 3.38-3.46 (m, 2H, O-C*H*$_2$), 1.86-1.88 (m, 1H, CH_3-C*H*), 1.62-1.68 (m, 2H, CH_2-C*H*$_2$), 1.49-1.53 (m, 1H, CH_3-C*H*), 1.24-1.30 (m, 3H, CH_2-C*H*$_2$), 1.10-1.16 (m, 3H, CH_2-C*H*$_2$), 0.858-0.892 (m, 9H, -C*H*$_3$).

2,7-Dibromofluorene (10)

The copper(II) bromide (20 g) and neutral alumina (40 g) distilled in water (50 mL) at room temperature. The water was evaporated at 80 °C under reduced pressure. The resulting reagent was then dried at 100 °C for overnight to obtain the alumina-supported copper(II) bromide 60 g as light blue solid. Then the fluorene (3.0 g, 18 mmol) and alumina-supported copper(II) bromide were added in CCl_4 (150 mL) and was stirred at reflux

for 6 h. The solution was cooled to room temperature, and the solid material was filtered and washed with CCl_4 (80 mL). The organic solution was dried over magnesium sulfate. Removal of solvent gave 3.4 g (58.6 %) of the product as yellow crystals. ^{1}H NMR (400 MHz; $CDCl_3$; δ): 7.66 (s, 2H, Ar*H*), 7.61-7.63 (d, 2H, J = 8 Hz, Ar*H*), 7.49-7.51 (d, 2H, J = 8 Hz, Ar*H*), 3.94 (s, 2H, CH_2).

2,7-Dibromo-9,9-dioctylfluorene (11).
2,7-Dibromofluorene (0.4 g, 1.23 mmol), 1-bromooctane (0.476 g, 2.45 mmol) and KOH (0.8 g, 14.2 mmol) were added to 5 mL DMF under a nitrogen atmosphere and added and stirred. After the reaction was finshed. The mixture poured into the water and added with some HCl to neutralise the solution. The organic layer was extracted by water and ethyl acetate and dried over anhydrous $MgSO_4$ and removed the solvent to afford 0.24 g product as a white solid (32.2 %). ^{1}H NMR (400 MHz; $CDCl_3$; δ): 7.49-7.51 (d, 2H, *J* = 8 Hz, Ar*H*), 7.44-7.46 (m, 4H, Ar*H*), 1.84-1.93 (m, 4H, C-CH_2), 1.05-1.25 (m, 20H, CH_2), 0.807-0.840 (m, 6H, CH_2-CH_3), 0.580 (m, 4H, CH_2).

2,7-Dibromo-9,9-di((S)-3,7-dimethyloctyl)fluorene (12).
The compound was synthesized using the same method as synthesis of 2,7-Dibromo-9,9-dioctylfluorene (11). Yield = 45%. ^{1}H NMR (400 MHz; $CDCl_3$; δ): 7.51-7.53 (d, 2H, J = 8 Hz, Ar*H*), 7.43-7.46 (m, 4H, Ar*H*), 1.86-2.00 (m, 4H, C-CH_2), 1.40-1.48 (m, 2H, C*H*), 1.00-1.15 (m, 12H, CH_2), 0.878-0.910 (m, 2H, C*H*), 0.805-0.837 (m, 12H, CH_3), 0.690-0.712 (m, 6H, CH-CH_3), 0.517-0.597 (m, 2H, CH_2), 0.387-466 (m, 2H, CH_2).

2,7-Bis(4,4,5,5-tetramethyl-1,3,2-dioxaborolan-2-yl)-9,9-dioctylfluorene (M-6).
2,7-Dibromo-9,9-dioctylfluorene (0.2 g, 0.33 mmol), $PdCl_2$(dppf)CH_2Cl_2 (0.0134 g, 0.0165 mmol), bis(pinacolato)diboron (0.163 g, 0.789 mmol) and potassium acetate (0.194 g, 1.98 mmol) in 1,4-dioxane (5 mL) were added to a flask under nitrogen stream. The reaction was stirred at 90 °C for overnight. The mixture was extracted with ethyl acetate (100 mL) twice, and the combined organic phase was washed with water three times and dried over $MgSO_4$. After removal of solvents under reduced pressure, the obtained residue was purified by silica gel chromatography (ethyl acetate/hexane = 1:10) to afford 0.150 g product as a white solid (64%). ^{1}H NMR (400 MHz; $CDCl_3$; δ): 7.79-7.81 (d, 2H, *J* = 8 Hz, Ar*H*), 7.69-7.78 (m, 4H, Ar*H*), 1.98-2.02 (m, 4H, C-CH_2), 1.38-1.47 (m, 24H, C-CH_3), 1.01-1.27 (m, 20H, CH_2), 0.781-0.834 (m, 6H, CH_2-CH_3), 0.555 (m, 4H, CH_2).

2,7-Bis(4,4,5,5-tetramethyl-1,3,2-dioxaborolan-2-yl)-9,9-di((S)-3,7-dimethyloctyl)fluorene (M-7).
The compound was synthesized using the same method as synthesis of 2,7-Bis(4,4,5,5-tetramethyl-1,3,2-dioxaborolan-2-yl)-9,9-dioctylfluorene (M-6). Yield = 71%. ^{1}H NMR (400 MHz; $CDCl_3$; δ): 7.79-7.81 (d, 2H, *J* = 8 Hz, Ar*H*), 7.70-7.75 (m, 4H, Ar*H*), 1.95-2.07 (m, 4H, C-CH_2), 1.35-1.45 (m, 26H, C*H* and C-CH_3), 1.00-1.05 (m, 12H, CH_2), 0.791-0.896 (m, 14H, C*H* and CH-CH_3), 0.648-0.664 (m, 6H, CH-CH_3), 0.508-0.537 (m, 2H, CH_2), 0.396-0.443 (m, 2H, CH_2).

3.2.4. Polymers synthesis

Polymerization by Miyaura-Suzuki polycondensation reaction (P(1)-1, P(2)-1, P(6)-1, P(7)-1) 2,5-Dibromo-3-(3,5-di-t-butyl-4-trimethylsiloxyphenyl)thiophene (Mphenoxyth) (1 equiv), monomers (1.1 equiv), K_2CO_3 (3 equiv), $Pd(PPh_3)_4$ (0.05 equiv) in water (0.5 mL) and DMF (2 mL) were added under an argon stream. The mixture was heated to reflux with stirring for about three days under an argon atmosphere. Upon cooling to room temperature, the reaction mixture was extracted with CH_2Cl_2 (150 mL). The organic layer was washed with water and dried with over anhydrous $MgSO_4$. After the evaporation of the solvents, diluted with 3 mL of chloroform, and added dropwise to 100 mL of methanol under stirring. The precipitate was allowed to stand overnight and centrifugal separation to products.

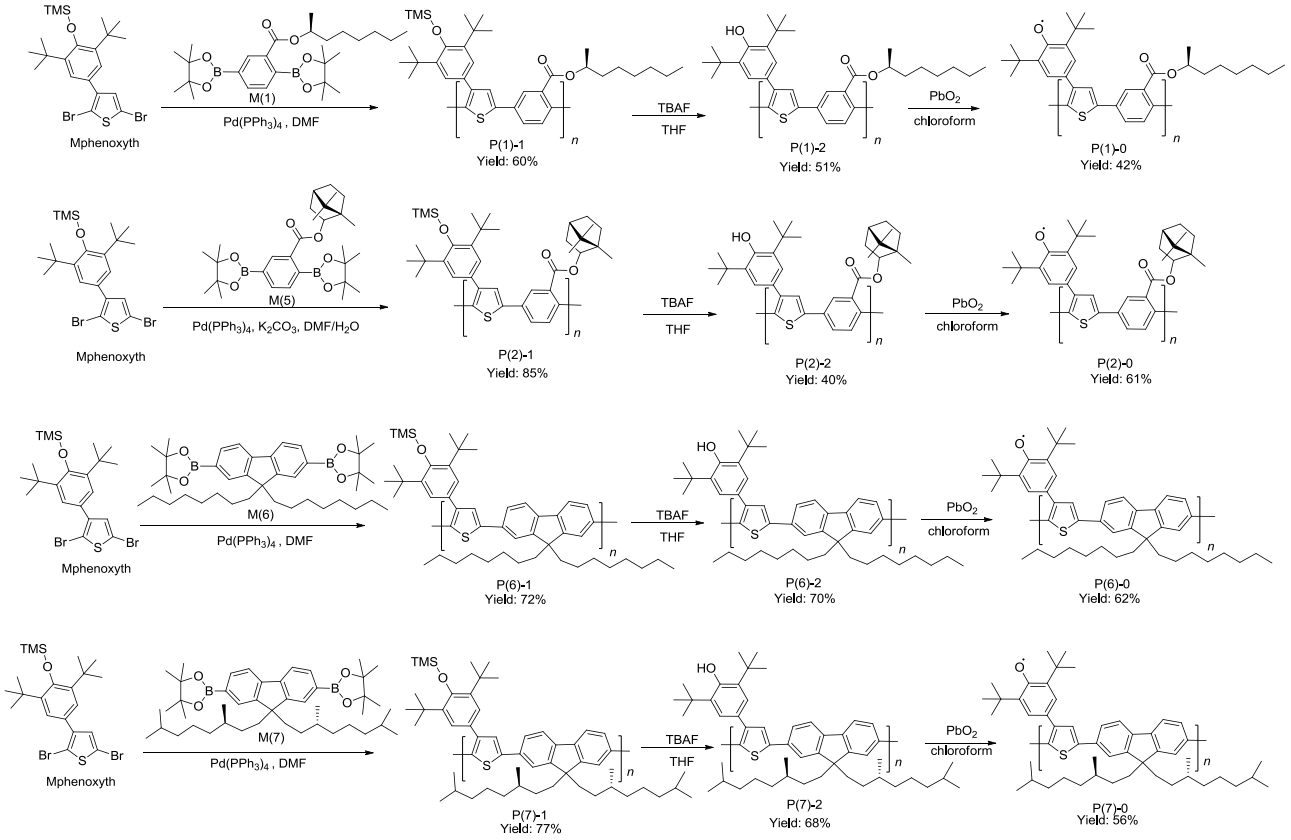

Scheme 3. 4. Synthesis of polymers. DMF = dimethylformamide, PPh_3 = triphenylphosphine, TBAF = tetrabutylammonium fluoride, TMS = tetramethylsilane.

P(1)-1

P(1)-1 is deep green solid. Yield: 60%. ^{1}H NMR (400 MHz; $CDCl_3$; δ): 7.71-8.01 (m, 1H, Ar*H*), 7.40-7.48 (m, 2H, Ar*H*), 7.01-7.13 (m, 3H, Ar*H*), 5.02-5.21 (m, 1H, O-C*H*), 1.22-1.56 (m, 31H, CH-CH_2,C-CH_3, CH_2-CH$_3$ and CH-CH_3), 0.807-0.831 (m, 3H, CH_2-CH_3), 0.442-0.501 (m, 9H, CH_2-CH_3).

P(2)-1

P(2)-1 is brown solid. Yield: 85%. ^{1}H NMR (400 MHz; $CDCl_3$; δ): 7.29-7.98 (m, 4H, Ar*H*), 6.96-7.09 (m, 2H, Ar*H*), 4.95-4.97 (m, 1H, O-C*H*), 2.15-2.30 (m, 2H, CH-CH_2), 1.19-1.56 (m, 23H, C-CH_2, CH_2-CH_2, CH_2-C*H*

and C-C*H*$_3$), 0.442-0.998 (m, 18H, C*H*$_3$ and Si-C*H*$_3$).

P(6)-1

P(6)-1 is yellow solid. Yield: 72%. ^{1}H NMR (400 MHz; $CDCl_3$; δ): 7.69-7.82 (m, 4H, Ar*H*), 7.43-7.62 (m, 3H, Ar*H*), 7.18-7.19 (m, 2H, Ar*H*), 1.99-2.03 (m, 4H, C-C*H*$_2$), 1.10-1.57 (m, 38H, C*H*$_2$ and C-C*H*$_3$), 0.42-0.81 (m, 19H, C*H*$_2$, CH_2-C*H*$_3$ and Si-C*H*$_3$).

P(7)-1

P(7)-1 is brown solid. Yield: 77%. ^{1}H NMR (400 MHz; $CDCl_3$; δ): 7.56-7.84 (m, 5H, Ar*H*), 7.38-7.41 (m, 2H, Ar*H*), 7.01-7.15 (m, 2H, Ar*H*), 1.95 (m, 4H, C-C*H*$_2$), 1.24-1.31 (m, 20H, C*H* and C-C*H*$_3$), 0.910-1.14 (m, 12H, C*H*$_2$), 0.351-0.856 (m, 33H, C*H*, C*H*$_2$, CH-C*H*$_3$ and Si-C*H*$_3$).

Polymerization by Stille coupling reaction (P(3)-1, P(4)-1, P(5)-1).

2,5-Dibromo-3-(3,5-di-t-butyl-4-trimethylsiloxyphenyl)thiophene (Mphenoxyth) (1 equiv), monomers (1 equiv), $Pd(PPh_3)_4$ (0.07 equiv) in DMF (4 mL) were added under an argon stream. The mixture was heated to 95 °C with stirring for about 3 days under an argon atmosphere. Upon cooling to room temperature, the reaction mixture was extracted with CH_2Cl_2 (150 mL). The organic layer was combined and dried over anhydrous Na_2SO_4. After the evaporation of the solvents, diluted with 3 mL of chloroform, and added dropwise to 100 mL of methanol under stirring. The precipitate was allowed to stand overnight and centrifugal separation to solid.

P(3)-1

P(3)-1 is brown solid. Yield: 79%. ^{1}H NMR (400 MHz; $CDCl_3$; δ): 7.13-7.73 (m, 11H, Ar*H*), 1.29-1.46 (m, 18H, C-C*H*$_3$), 0.436-0.459 (m, 9H, Si-C*H*$_3$).

P(4)-1

P(3)-1 is brown solid. Yield: 60%. ^{1}H NMR (400 MHz; $CDCl_3$; δ): 7.15-7.74 (m, 9H, Ar*H*), 1.37-1.45 (m, 18H, C-C*H*$_3$), 0.373-0.447 (m, 9H, Si-C*H*$_3$).

P(5)-1

P(5)-1 is purple solid. Yield: 45%. ^{1}H NMR (400 MHz; $CDCl_3$; δ): 7.18-8.11 (m, 7H, Ar*H*), 1.21-1.46 (m, 18H, C-C*H*$_3$), 0.336-0.427 (m, 9H, Si-C*H*$_3$).

Deprotection of the side chain

Polymer-1 (1 equiv) and tetrabutylammonium fluoride (TBAF, 1.5 equiv) were added in THF at 0 °C, and the mixture was stirred for 3 h at room temperature. Water was added, and the resulting mixture was extracted with CH_2Cl_2. The combined extracts were washed with solutions of NH_4Cl and brine, then dried ($MgSO_4$) and solvent was removed under reduced pressure and diluted with 3 mL of chloroform, and added dropwise to 100 mL of methanol under stirring. The precipitate was allowed to stand overnight and centrifugal separation to

solid.

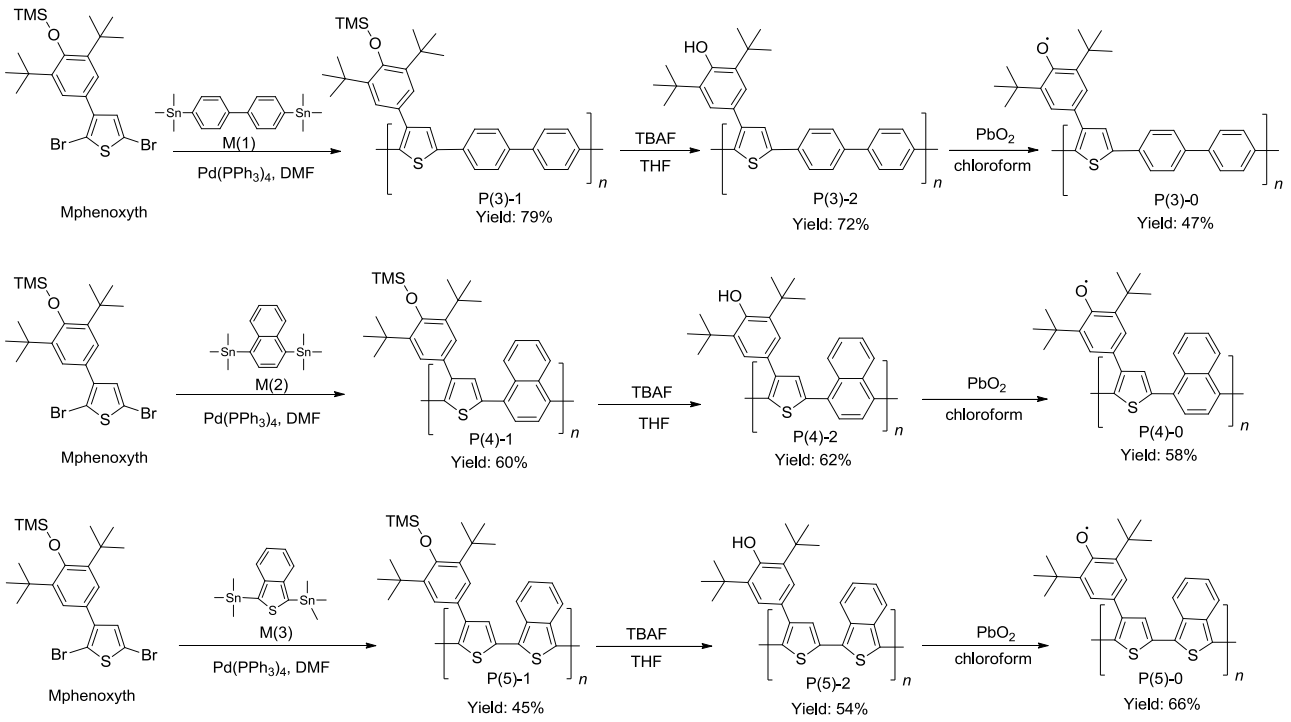

Scheme 3. 5. Synthesis of polymers. DMF = dimethylformamide, PPh_3 = triphenylphosphine, TBAF = tetrabutylammonium fluoride, TMS = tetramethylsilane.

P(1)-2.

P(1)-2 is deep green solid. Yield: 51%. ^{1}H NMR (400 MHz; $CDCl_3$; δ): 7.74-8.06 (m, 1H, Ar*H*), 7.41-7.50 (m, 2H, Ar*H*), 7.02-7.131 (m, 3H, Ar*H*), 5.21 (m, 1H, O*H*), 5.02-5.10 (m, 1H, O-C*H*), 1.22-1.57(m, 31H, CH-CH_2, C-CH_3, CH_2-CH_3 and CH-CH_3), 0.807-0.833 (m, 3H, CH_2-CH_3).

P(2)-2.

P(2)-2 is brown solid. Yield: 40%. ^{1}H NMR (400 MHz; $CDCl_3$; δ): 7.35-8.06 (m, 4H, Ar*H*), 7.02-7.16 (m, 2H, Ar*H*), 5.19 (m, 1H, O*H*), 4.95-4.98 (m, 1H, O-C*H*), 2.12-2.38 (m, 2H, CH-CH_2), 1.08-1.60 (m, 23H, C-CH_2, CH_2-CH_2, CH_2-C*H* and C-CH_3), 0.651 -0.998 (m, 9H, CH_3).

P(3)-2.

P(3)-2 is brown solid. Yield: 72%. ^{1}H NMR (400 MHz; $CDCl_3$; δ): 7.20-7.73 (m, 11H, Ar*H*), 5.21 (m, 1H, O*H*), 1.26-1.55 (m, 18H, C-CH_3).

P(4)-2.

P(4)-2 is brown solid. Yield: 62%. ^{1}H NMR (400 MHz; $CDCl_3$; δ): 7.08-7.77 (m, 9H, Ar*H*), 5.27 (m, 1H, O*H*), 1.15-1.56 (m, 18H, C-CH_3).

P(5)-2.

P(5)-2 is purple solid. Yield: 54%. ^{1}H NMR (400 MHz; $CDCl_3$; δ): 6.87-8.13 (m, 7H, Ar*H*), 5.14 (m, 1H, O*H*), 1.26-1.52 (m, 18H, C-C*H*$_3$).

P(6)-2.

P(6)-2 is brown solid. Yield: 70%. ^{1}H NMR (400 MHz; $CDCl_3$; δ): 7.62-7.82 (m, 4H, Ar*H*), 7.45-7.53 (m, 3H, Ar*H*), 7.18-7.19 (m, 2H, Ar*H*), 5.19 (m, 1H, O*H*), 1.98-2.03 (m, 4H, C-C*H*$_2$), 1.10-1.52 (m, 38H, C*H*$_2$ and C-C*H*$_3$), 0.718-0.812 (m, 10H, C*H*$_2$, CH_2-C*H*$_3$).

P(7)-2.

P(7)-2 is brown solid. Yield: 68%. ^{1}H NMR (400 MHz; $CDCl_3$; δ): 7.63-7.84(m, 5H, Ar*H*), 7.46-7.51 (m, 2H, Ar*H*), 7.02-7.22 (m, 2H, Ar*H*), 5.21 (m, 1H, O*H*), 2.05 (m, 4H, C-C*H*$_2$), 1.27-1.37 (m, 20H, C*H* and C-C*H*$_3$), 1.05-1.18 (m, 12H, C*H*$_2$), 0.599-0.917 (m, 24H, C*H*, C*H*$_2$, CH-C*H*$_3$).

Polymers of oxidation.

Under N_2, a solution of polymer-2 (1 equiv) and PbO_2 (13 equiv) in chloroform was stirred for 4 h at room temperature. After filtration, the solvent was removed by evaporation from the filtrate. The obtained powder was dried under vacuum.

P(1)-0.

P(1)-0 is black solid. Yield: 42%. ^{1}H NMR (400 MHz; $CDCl_3$; δ): 7.69-8.00 (m, 1H, Ar*H*), 7.39-7.46 (m, 2H, Ar*H*), 7.06-7.12 (m, 3H, Ar*H*), 5.00-5.10 (m, 1H, O-C*H*), 1.21-1.55 (m, 31H, CH-C*H*$_2$, C-C*H*$_3$, C*H*$_2$-CH_3 and CH-C*H*$_3$), 0.821-0.877 (m, 3H, CH_2-C*H*$_3$).

P(2)-0.

P(2)-0 is black solid. Yield: 61%. ^{1}H NMR (400 MHz; $CDCl_3$; δ): 7.36-8.05 (m, 4H, Ar*H*), 7.07-7.17 (m, 2H, Ar*H*), 4.96-4.98 (m, 1H, O-C*H*), 2.36-2.40 (m, 2H, CH-C*H*$_2$), 1.19-1.64 (m, 23H, C-C*H*$_2$, CH_2-C*H*$_2$, CH_2-C*H* and C-C*H*$_3$), 0.731-0.895 (m, 9H, C*H*$_3$).

P(3)-0

P(3)-0 is black solid. Yield: 47%. ^{1}H NMR (400 MHz; $CDCl_3$; δ): 7.17-7.73 (m, 11H, Ar*H*), 1.23-1.54 (m, 18H, C-C*H*$_3$).

P(4)-0.

P(4)-0 is black solid. Yield: 58%. ^{1}H NMR (400 MHz; $CDCl_3$; δ): 7.11-7.77 (m, 9H, Ar*H*), 1.13-1.56 (m, 18H, C-C*H*$_3$).

P(5)-0.

P(5)-0 is black solid. Yield: 66%. ^{1}H NMR (400 MHz; $CDCl_3$; δ): 6.80-8.06 (m, 7H, Ar*H*), 1.19-1.49 (m, 18H,

C-CH_3).

P(6)-0.

P(6)-0 is black solid. Yield: 62%. ^{1}H NMR (400 MHz; $CDCl_3$; δ): 7.64-7.84 (m, 4H, Ar*H*), 7.44-7.48 (m, 3H, Ar*H*), 7.17-7.19 (m, 2H, Ar*H*), 2.01 (m, 4H, C-CH_2), 1.03-1.58 (m, 38H, CH_2 and C-CH_3), 0.653-0.811 (m, 10H, CH_2, CH_2-CH_3).

P(7)-0

P(7)-0 is black solid. Yield: 56%. ^{1}H NMR (400 MHz; $CDCl_3$; δ): 7.62-7.84 (m, 5H, Ar*H*), 7.35-7.52 (m, 2H, Ar*H*), 7.02-7.22 (m, 2H, Ar*H*), 2.05 (m, 4H, C-CH_2), 1.28-1.38 (m, 20H, C*H* and C-CH_3), 1.08 (m, 12H, CH_2), 0.696-0.797 (m, 24H, C*H*, CH_2, CH-CH_3).

3.3. Results and discussion

3.3.1. Synthesis of monomers

A series of synthetic route, as shown in Scheme 3.1., Scheme 3. 2. and Scheme 3. 3., was designed to prepare the monomers of Mphenoxyth, M-1, M-2, M-3, M-4, M-5, M-6 and M-7. The monomer of Mphenoxyth (Scheme 3. 1.) has been prepared by three reactions including hydroxyl protection by trimethylsilyl, Grignard coupling and disubstitution using NBS in DMF. The reactions of synthesizing monomers diborate (M-1 and M-2 in Scheme 3. 1.) were carried out by the treatment of dibromo aromatic compounds with bis(pinacolato)diboron catalyzed by $Pd(PPh_3)_4$ in 1,4-dioxane under argon. The bistrialkylstannylated monomers (M-3 and M-5 in Scheme3. 2.) were prepared via double-lithiation of corresponding aromatic derivatives at -78 °C followed by quenching with trialkylstannyl chloride. The monomer, 1,4-Bis(tri-n-butylstannyl)naphthalene (M-4 in Scheme3. 2.), was prepared from 1,4-dibromonaphthalene and Me_3SnCl via sonicated reaction. The compound borate of fluorene derivatives (M-6 and M-7 in Scheme3. 3.) were synthesized follow as: i) fluorene is functionalized ii) hydrogen of fluorene is substituted by bromine iii) debrominated and borated.

3.3.2. Synthesis of polymers

The polymerizations were carried out by the Migita-Kosugi-Stille (P(3)-1, P(4)-1, and P(5)-1 in Scheme 3. 5.) and Miyaura-Suzuki (P(1)-1, P(2)-1, P(6)-1, and P(7)-1 in Scheme 3. 4.) polycondensation reaction using $Pd(PPh_3)_4$(0) as a catalyst. The deprotection of 2,6-di-tert-butylphenoxytrimethylsilane groups are carried out with tetrabutylammonium fluoride in THF. Then the polymers is oxidized by active PbO_2 to give corresponding polyradicals. All the polymers are soluble in common organic solvents such as *N*-methylpyrrolidone, DMF, THF, chloroform, toluene, benzene. They are perfectly soluble in common organic solvents due to the bulky aromatic rings substituents. The alkyl side chain can reduce the intermolecular packing and increase the solubility of the copolymers. The results of the molecular weights of polymers were determined by GPC in THF using polystyrene as a standard and show in Table 3. 1. Number-average molecular weights of the polymers were ranged from 2920 to 8850 g/mol, and the molecular weight distributions were 1.13-1.89.

Table 3. 1. Gel permeation chromatography (GPC) results of radical polymers from P(1)-0 to P(7)-0

Polymers-0	M_n[a][g/mol]	M_w[a][g/mol]	M_w/M_n	DP[b]
P(1)-0	4660	6020	1.2	9
P(2)-0	8840	16770	1.8	16
P(3)-0	2920	5360	1.8	7
P(4)-0	3030	4080	1.3	8
P(5)-0	4090	6590	1.6	10
P(6)-0	4160	4720	1.1	7
P(7)-0	8140	14690	1.8	11

a: Estimated by GPC using THF as the eluent on the basis of a polystyrene calibration. b: Degree of polymerization (calculated by M_n/M, M: molecular weight of monomer repeat unit).

3.3.3. Structural characterization

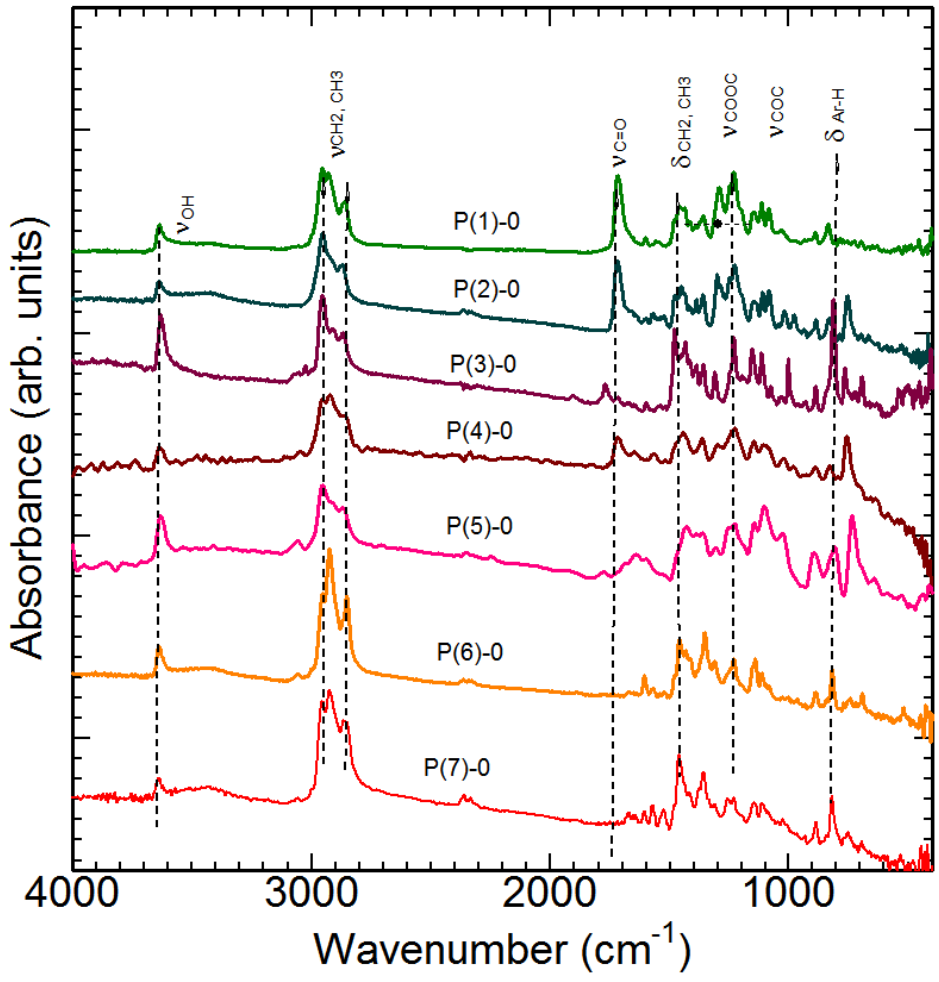

Figure 3. 1. FT-IR (Fourier transform infrared) spectra of radical polymers (solid lines).

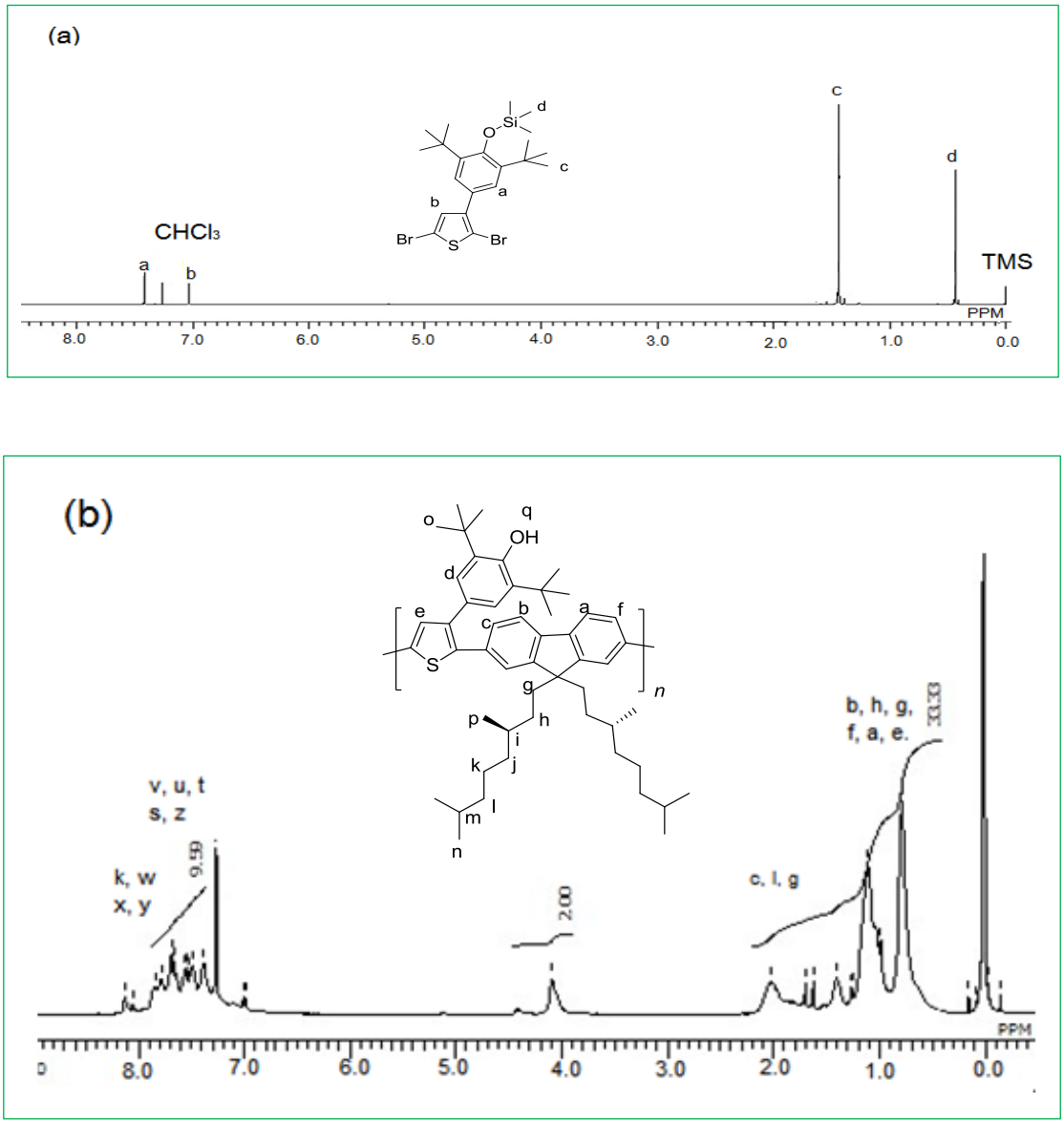

Figure 3. 2. ^{1}H NMR spectra of (a) Mphenoxyth and (b) P(7)-2 with deuterated chloroform as solvent. TMS = trimethylsilyl

IR spectra of the radical polymers were shown in the Figure 3. 1. The absorption bands at 752-809 cm^{-1} are due to C-H bending vibration at β-positions of the aromatic units, which clearly shows the effect of aromatic rings corresponding to the shift of the C-H stretching mode to a lower frequency. [38, 39] The radical polymers as the oxidation proceeded, an absorption peak at 1577 cm^{-1} of the oxy-radical in the pheonxy units were appeared. This result is consistent with the report by Kaneko et al. [40] The P(1)-0 and P(2)-0 show absorption bands at 1732 cm^{-1} and, which are attributed to C=O stretching. These sbsorption bands of CO-O-C (ester) vibrations in the side chain units were observed at 1221 cm^{-1}. The polymers show relatively intense absorptions at 2925 cm^{-1} and 2856 cm^{-1} are attributed to C-H stretching of the side chain functional units and alkyl chain attached to 2,6-di-*tert*-butylphenoxyl radical units. Particularly, the P(6)-0 and P(7)-0 show a relatively strong

absorption band at that wavenumber because of the longer branched alkyl groups of the fluorene units. In addition, the absorption bands at 3630 cm^{-1} (O-H) of the sterically hindered pheoxy group were still found after polymerization. The result is indicated that the 2,6-di-tert-butylphenoxylstructures of the side chains was incomplete oxidation by PbO_2 due to inhomogeneous reaction.

The polymeric products were characterized by ^1H NMR analyses. These results clearly indicate that well-defined these polymers have been indeed obtained and all the polymers gave satisfactory data corresponding to their expected molecular structures (Supporting Information). As an example and because of its simple repeating unit, we show here the ^1H NMR spectra of P(7)-2 in Figure3. 2. The chemical shifts from 0.599 ppm to 2.05 ppm are attributed to the longer branched alkyl groups of the fluorene units and the alkyl chain protons of 2,6-di-*tert*-butylphenoxyl units. The spectrum recorded for P(7)-2 shows no signal in the 0.447 ppm region (trimethylsilyl of Mphenoxyth), which indicates that the 2,6-di-*tert*-butylphenoxylside chains are removed the trimethylsilyl end group. The chemical shift at 5.21 ppm ascribed to the protons of hydroxyl group (O-H) is also clearly observed. A similar analysis had been previously reported by Yamamotoet al. [37] The aromatic region intense signals in the 7.02-7.84 ppm ppm region corresponding to the chemical shift of fluorene (δ: 7.70-7.81 ppm) and thiophene (δ: 7.03-7.41 ppm) protons. These results that indicating the successful polymerization of chiral fluorene derivative and Mphenoxyth.

3.3.4. Optical properties

CD and UV-vis absorption spectra were employed to investigate optical properties and conformation of the polymers in benzene solution and film state (Figures 3. 3. and Figures 3. 4.). The P(1)-2 and P(1)-0 in benzene show a clear couplet at long wavelengths with a positive cotton effect at 418 nm and a negative cotton effect at 361 nm. The result corresponds to a intense optical absorption band at around 378 nm in Uv-vis. In addition, the P(1)-2 and P(1)-0 in film state are observed negative CD signals and UV-vis absorption bands from 319 nm to 388 nm (Figures 3. 3 (a). and Figures 3. 4 (a).). These results indicate that the copolymer backbones adopted helical conformations of predominantly one-handed screw sense with optical activity (atropisomerism) [41, 42]. P(2)-2 and P(2)-0 showed negative CD signal and intense UV-vis absorption bands from 289 nm to 364 nm in the benzene solution (Figures 3. 3 (b). and Figures 3. 4 (b).). Intermolecular π-π interaction of P(2)-2 and P(2)-0 is prevented the large steric hindrance of bornyl groups in the film state. The polymers can not form chiral aggregation in the film state.[43] In addition, the CD spectrum of P(7)-2 and P(7)-0 taken clear negative CD signal at 374 nm, 380 nm and 430 nm were observed in film state in the absorption region of the backbone (Figures 3. 3 (c).). It indicates the polymers form helical arrangement of intermolecular.

The CD signals at the main chain absorption wavelength suggest that the polyradicals form second-order chiral structure such as helical structure. However, no appearance of the CD signal at the optical absorptions of radicals indicates that the phenoxy radicals form no helical structure. This may be due to the fact that effect of incomplete tiansformation of radicals reduced the radical concentration by PbO_2 oxidation.

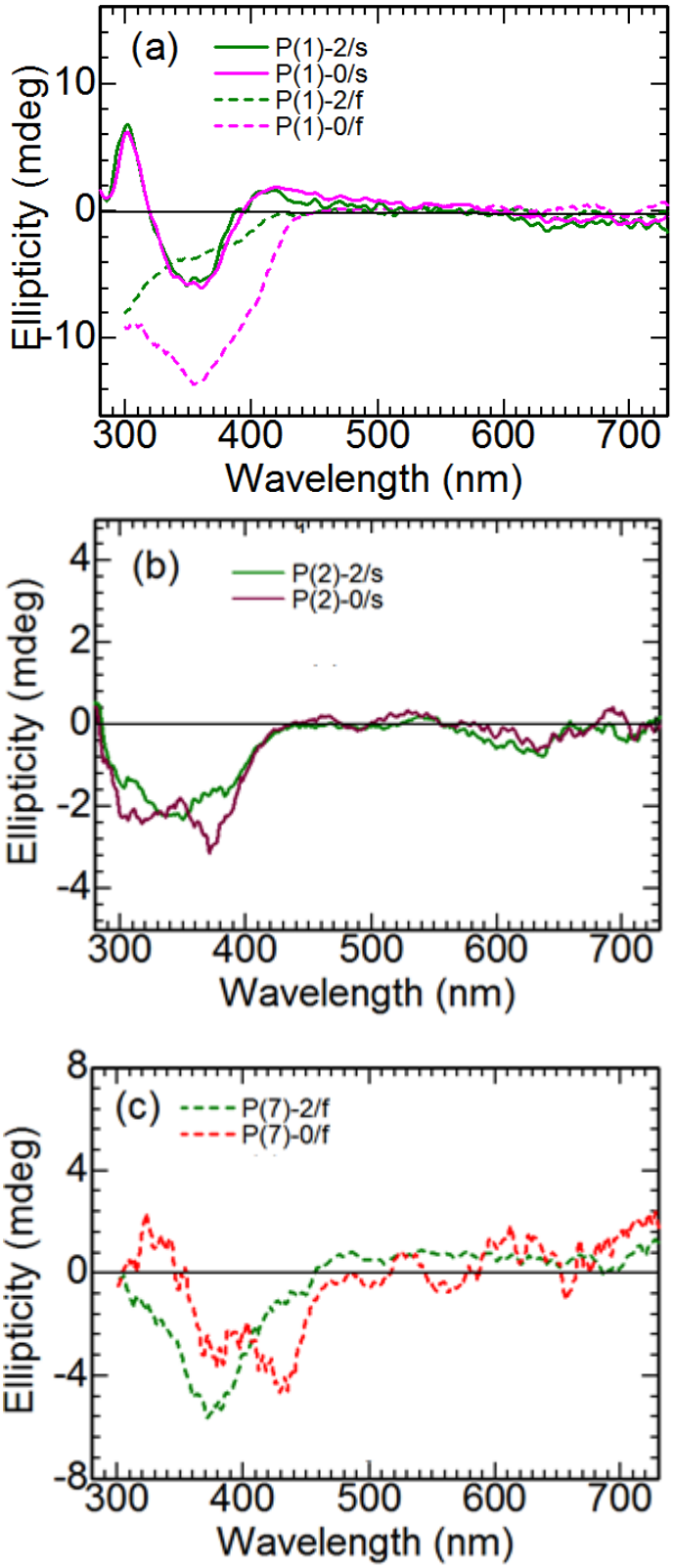

Figure 3. 3. Circular dichroism absorption of polymer-2 ((a): P(1)-2, (b): P(2)-2, (c): P(7)-2) before the oxidation and radical polymers polymer-0 ((a): P(1)-0, (b): P(2)-0, (c): P(7)-0) as the oxidation proceeded in benzene (solid lines), as thin films from benzene solution (ca. 2 mg/mL) onto ITO-coated glass substrates and dried in air at room temperature. (dashed lines). S: solution state, F: film state.

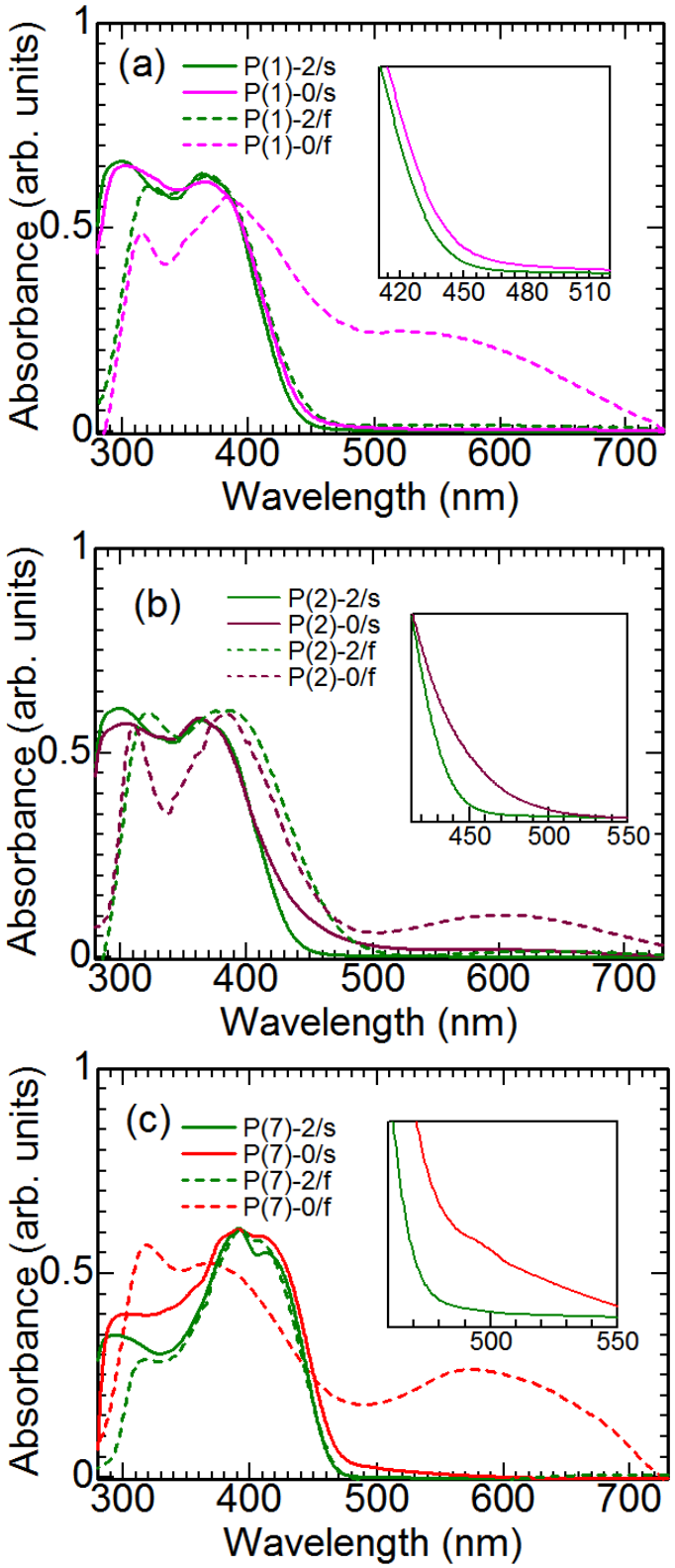

Figure 3. 4. Ultraviolet–visible absorption of polymer-2 ((a): P(1)-2, (b): P(2)-2, (c): P(7)-2) before the oxidation and radical polymers polymer-0 ((a): P(1)-0, (b): P(2)-0, (c): P(7)-0) as the oxidation proceeded in benzene (solid lines), as thin films from benzene solution (ca. 2 mg/mL) onto ITO-coated glass substrates and dried in air at room temperature. (dashed lines). S: solution state, F: film state.

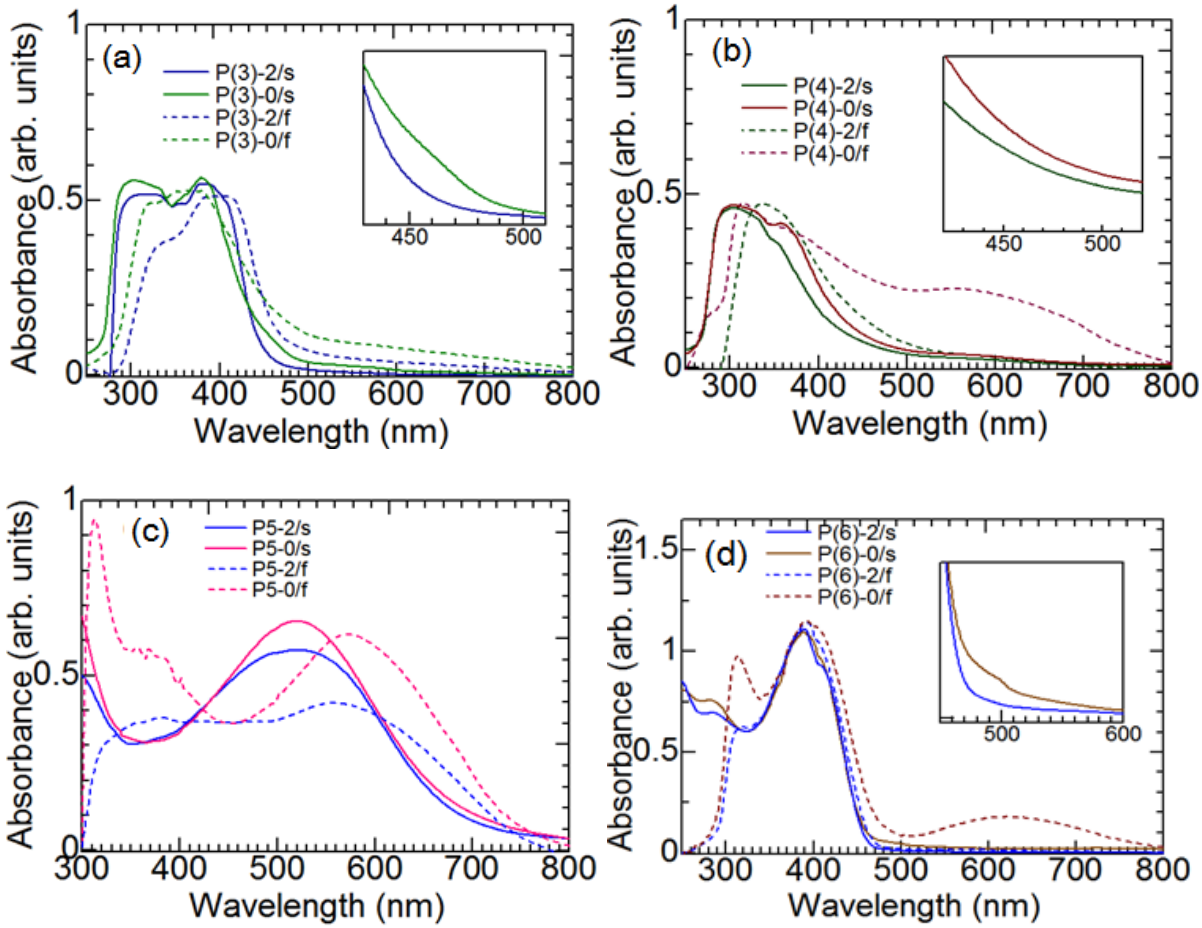

Figure 3. 5. Ultraviolet–visible absorption of polymer-2 ((a): P(3)-2, (b): P(4)-2, (c): P(5)-2, (d): P(6)-2) before the oxidation and radical polymers polymer-0 ((a): P(3)-0, (b): P(4)-0, (c): P(5)-0, (d): P(6)-0) as the oxidation proceeded in benzene (solid lines), as thin films from benzene solution (ca. 2 mg/mL) onto ITO-coated glass substrates and dried in air at room temperature. (dashed lines). S: solution state, F: film state.

Oxidation of polymers with fresh PbO_2 gives deeper color than before the oxidation than that of before oxidation. P(6)-0 and P(7) appear a new absorption band in the optical absorption spectroscopy in the benzene solution at around 497 nm ascribed to absorption of phenoxy radical (Figure 3. 4 (c). and Figure 3. 5 (d).). This result is corresponding to the previous report by Nishide et al. [45] P(5)-0 showed a broad absorption band centered around 504 nm (Figure 3. 5 (c).). The phenoxy radical and the backbone of polymer are overlapped in the absorption region. This absorption tail extends to longer wavelengths due to well develope π-conjugation of main chain of the polyradical even after the oxidation for generation of radicals. P(3)-0 exhibits a characteristic peak of phenoxy radicals near 466 nm in the benzene solution (Figure 3. 5 (a).), corresponding to the 2,6-di-tert-butyl-4-phenoxy radicals [46, 47] reported by Kaneko et al. In contrast, the UV-vis spectra of P(1)-0, P(2)-0 and P(4)-0 are monotonous and show no clear absorption peaks derived from phenoxy radical at 460 nm or the 495 nm in the solution (Figure 3. 4 (a), (b). and Figure 3. 5 (b).). However, a weak broad shoulder found in the visible region 420-520 nm is attributable to the phenoxy radicals. All the radical polymers give a new broad absorption from 540 nm to 620 nm of the phenoxy radical in the film state.

Among the series of the polymers, P(5)-2 and P(5)-0 show relatively lower energy feature changes in absorption spectra in both solution and film states (Figure 3. 5 (c).). These indicate that the main chains are introduced isothianaphthene groups and have increase interchromophoric interactions. However, P(4)-2 and P(4)-0 show opposite character in absoption spectra (Figure 3. 5 (b).). These results indicate the main chains are introduced naphthalene groups and have decrease interchromophoric interactions. The red shift of absorption bands of P(5)-2 and P(5)-0 clearly observed in the film state compare with their solution state, indicates interchain interactions in the solid state, possibly assisted by planarization and an increase of conjugation length [48]. P(6)-2 and P(6)-0 shows absorption bands at 282 nm and 390 nm (Figure 3. 5 (d).), while P(7)-2 and P(7)-0 show absorption bands at 290 nm, 391 nm and 412 nm in the solution (Figure 3. 4 (c).). P(7)-2 and P(7)-0 has a longer effective conjugation in the main chain than P(6)-2 and P(6)-0 because of a chiral group introduced in the alkyl side chains, which is likely results from the restricted bond rotation to the alkyl side chains and increase the coplanarity of the main chain.

The PL spectra of the polymers obtained in solution and film state are shown in Figure 3. 7. and Figure 3. 8.. The decrease in intensity may be due to quenching of the PL in the form of cast film. Interchain interaction of π-conjugated main chain often results in decrease of quantum yield [49].

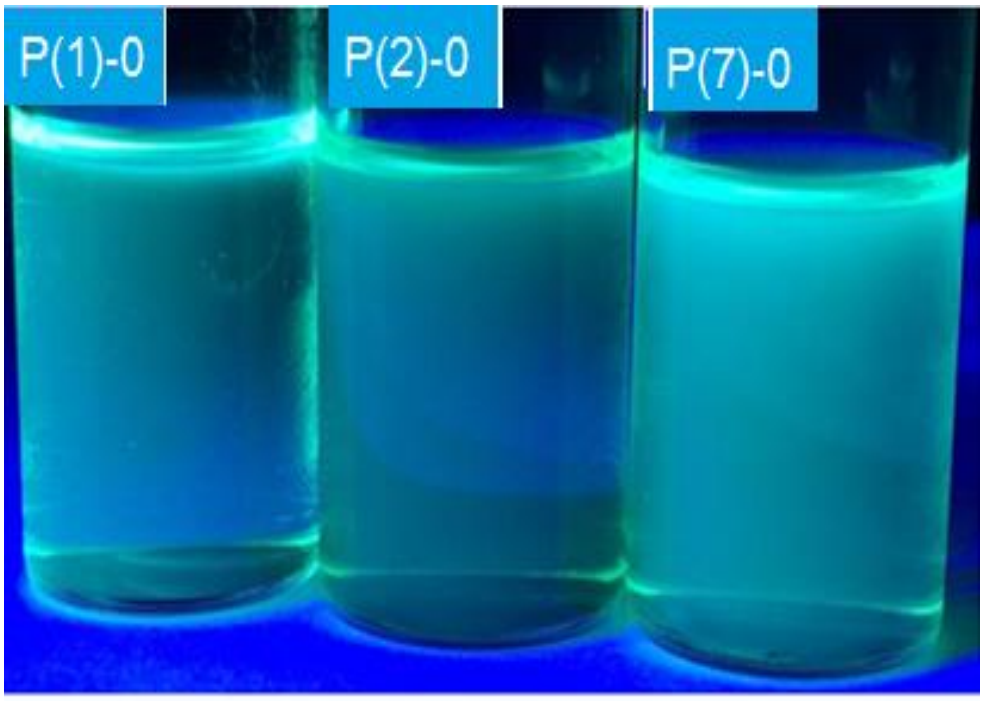

Figure 3. 6. Photos of PL emission from P(4)-0, P(5)-0, and P(7)-0 by ultraviolet excitation in chloroform.

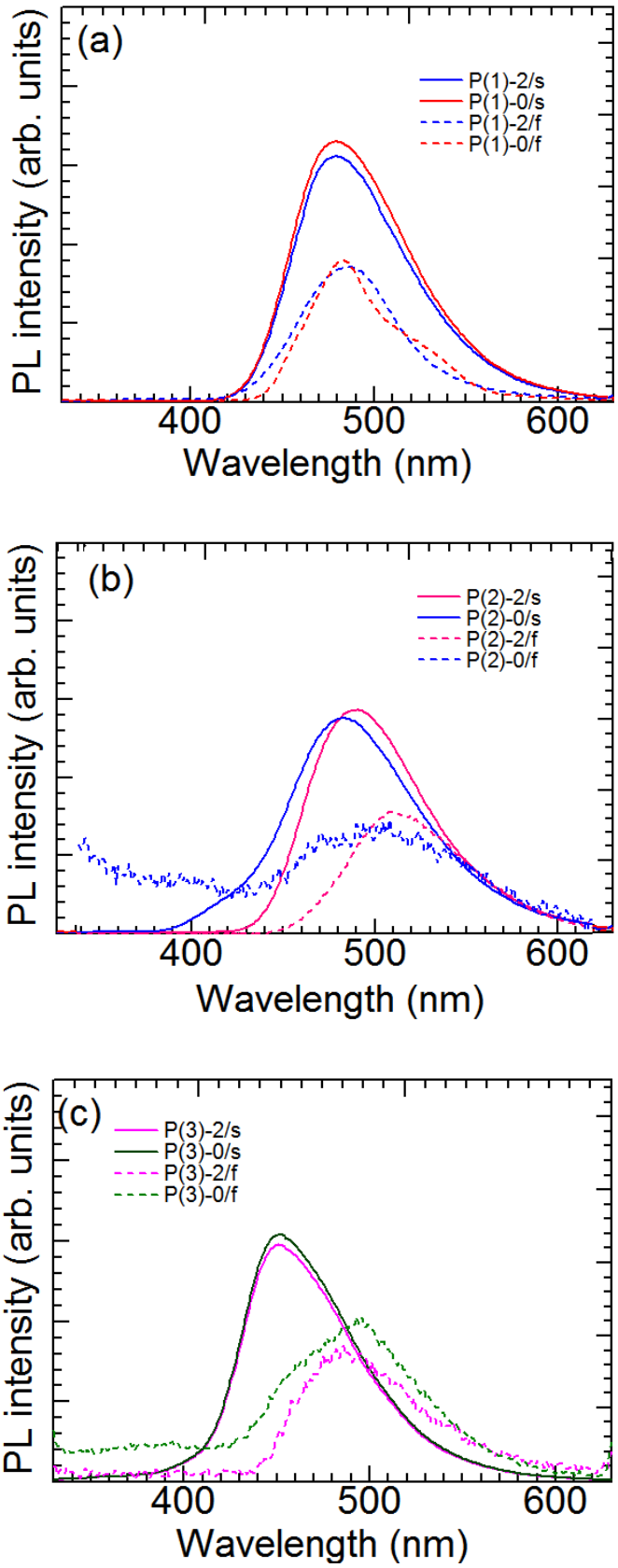

Figure 3. 7. The photoluminescence spectra of polymer-2 ((a): P(1)-2, (b): P(2)-2, (c): P(3)-2) before the oxidation and radical polymers polymer-0 ((a): P(1)-0, (b): P(2)-0, (c): P(3)-0) as the oxidation proceeded in chloroform (solid lines) and thin films (dashed lines). S: solution state, F: film state.

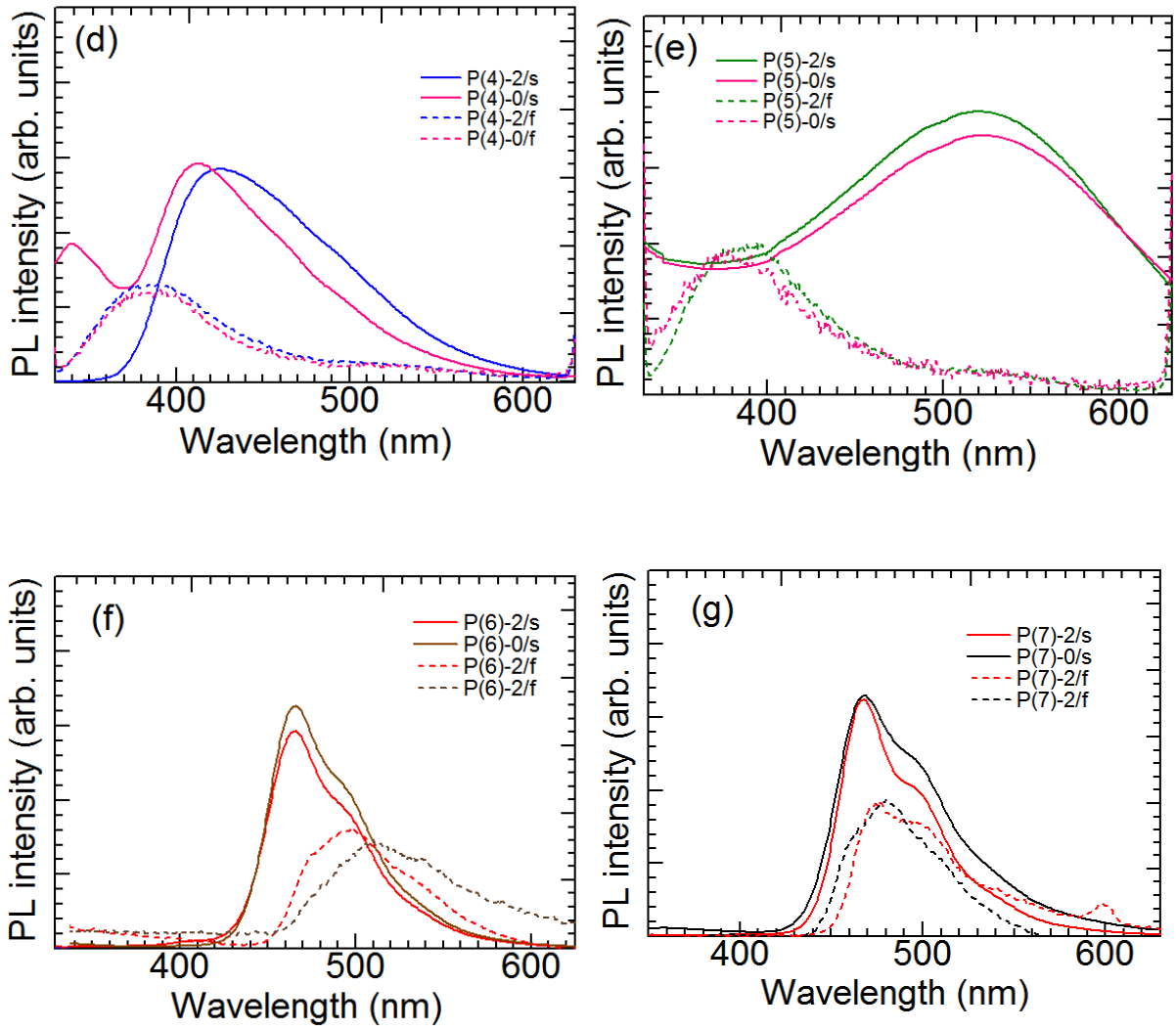

Figure 3. 8. The photoluminescence spectra of polymer-2 ((d): P(4)-2, (e): P(5)-2, (f): P(6)-2 and (g): P(7)-2) before the oxidation and radical polymers polymer-0 ((d): P(4)-0, (e): P(5)-0, (f): P(6)-0 and (g): P(7)-0) as the oxidation proceeded in chloroform (solid lines), as thin films from benzene solution (ca. 2mg/mL) onto ITO-coated glass substrates and dried in air at room temperature (dashed lines). S: solution state, F: film state.

Emission maximum wavelengths are summarized in Table 3. 2. Here, the featureless and broader emission band of P(2)-2, P(2)-0, P(3)-2, P(3)-0, P(6)-2 and P(6)-0 is actually red-shifted from solution state to film state by 28 nm, 16 nm, 32 nm, 44 nm, 31 nm and 44 nm. The red-shift values in the PL spectra are greater than that in the UV-vis absorption spectra after the film formation due to interchromophoric interaction in the film state [50]. Chiral polymers of P(1)-0, P(2)-0, and P(7)-0 show emission with excitation by ultraviolet light and show in the Figure 3. 6. Three polymers show white green light with emission bands at around 479 nm, 479 nm and 466 nm which cover the broadly visible region.

Table 3. 2. Maximum absorption wavelengths (λ_{max}), and maximum emission wavelengths (λ_{em}) of the polymers in chloroform solution and film state.

Polymer	λ_{max} (nm)	$\lambda_{max, film}$ (nm)	λ_{em} (nm)	$\lambda_{em, film}$ (nm)
P(1)-2	504	557	521	391
P(1)-0	504	576	529	377
P(2)-2	298, 371	321, 370	479	488
P(2)-0	298, 371	319, 388	479	482
P(3)-2	298, 364	321,388	490	518
P(3)-0	298, 364	309, 388	479	495
P(4)-2	380	410	450	482
P(4)-0	300, 379	379	450	494
P(5)-2	305	335	412	371
P(5)-0	305	311	424	375
P(6)-2	390	398	467	498
P(6)-0	390	398	467	511
P(7)-2	393, 412	393	466	472
P(7)-0	393, 412	321	466	480

3.3.5 Electrochemical properties

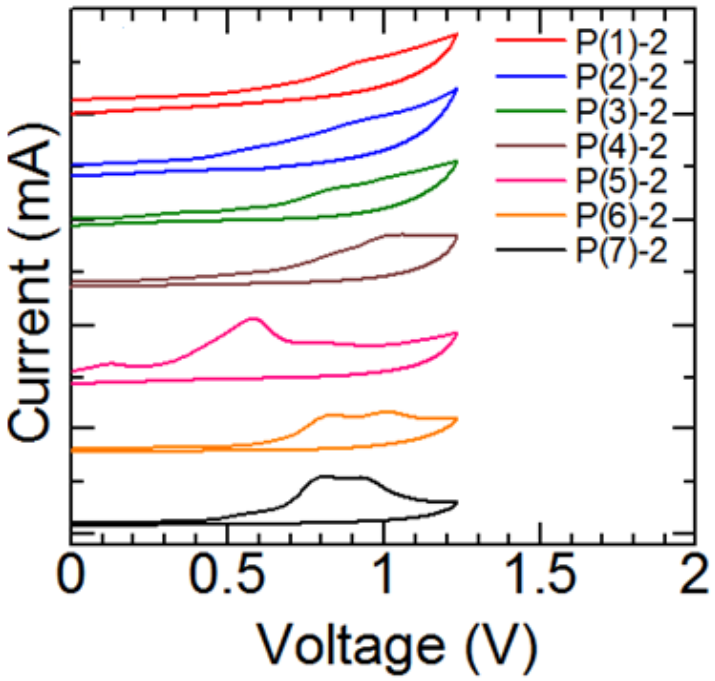

Figure 3. 9. Cyclic voltammograms of the polymers cast on platinum disc electrode (0.1 M TBAP in acetonitrile solution with a scan rate of 100 mV s^{-1}).

Table 3. 3. UV-vis absorption and cyclic voltammetry measurements for film state of polymer-2.

Polymers-2	λ_{edge} [e] (nm)	$E_{onset,ox}$ [a] (V)	E_{HOMO} [b] (eV)	E_{opt} [c] (eV)	E_{LUMO} [d] (eV)
P(1)-2	444	0.71	-5.51	2.79	-2.72
P(2)-2	475	0.52	-5.32	2.61	-2.71
P(3)-2	476	0.64	-5.44	2.60	-2.84
P(4)-2	552	0.76	-5.56	2.24	-3.32
P(5)-2	751	0.11	-4.91	1.65	-3.26
P(6)-2	462	0.65	-5.45	2.68	-2.77
P(7)-2	469	0.53	-5.33	2.64	-2.69

[a] Onset oxidation potentials of the polymers calibrated with ferrocene. [b] Calculated from the oxidation potentials. [c] Calculated from the onset wavelength of optical absorption of the polymers. [d] Calculated from optical bandgap energy and onset oxidation potential of the polymers. [e] onset absorption wavelength

Figure 3. 9. show the cyclic voltammograms of polymers (before the oxidation polymer-2) in the film state by using an Ag/Ag+ reference electrode in 0.1 M tetrabutylammonium perchlorate (TBAP) acetonitrile solution. The energy levels of the these polymers were determined by cyclic voltammetry (CV) using ferrocene as the standard that has a HOMO level of -4.8 eV [51]. The bandgap is estimated using optical energy gaps (E_{opt}) of the polymers. According to the empirical correlations suggested that the HOMO/LUMO levels of polymers were calculated by using the following equation: E_{HOMO} = (Eonset,ox + 4.8) eV and $E_{LUMO} = E_{HOMO} + E_{opt}$. [52, 53] Bandgaps are estimated to be 1.65 eV-2.79 eV and oxidation potentials of polymer-2 are in the range of 0.11-0.76 V (Table 3. 3.). Comparing with these results of redox properties in cyclic voltammograms, P(5)-2 have correspondingly lowest energy valence bands. This can be directly attributed to the resonance stabilization energy of the isothianaphthene units [54, 55].

3.3.6. ESR Spectra of the polyradicals

The polyradicals polymers were obtained by treatment of oxidizing the polymer-2 in the degassed chloroform with fresh PbO_2. The electron spin resonance (ESR) of the polymers was measured in power at room temperature (23 °C) are shown in Figure 3. 10., and the ESR data are summarized in Table 3. 4. The ESR spectrum of the radical polymers powder showed a broad signal attributed to an oxygen of the 2,6-di-*tert*-butylphenoxy moiety. The g value 2.004 of the spectra indicates the formation of an oxyen-centered radical, which produce sharp and unimodal signals suggestive of a high local concentration of the radical site along the main chain even in the solid state [56]. The spin concentration of radical polymers could be evaluated to 1.78×10^{19}-1.38×10^{20} spin/g at room temperature, showing that the radical polymers contains ca. 0.138-1.867 spins on the average as estimated from the molecular weight of the polymers. These oxidized polymers are found to be paramagnetic even in the solid state, indicating that the formed radical species are very stable, probably due to a resonance stabilization of unpaired electrons through the conjugated main chain and to a steric effect of the polymer chain.

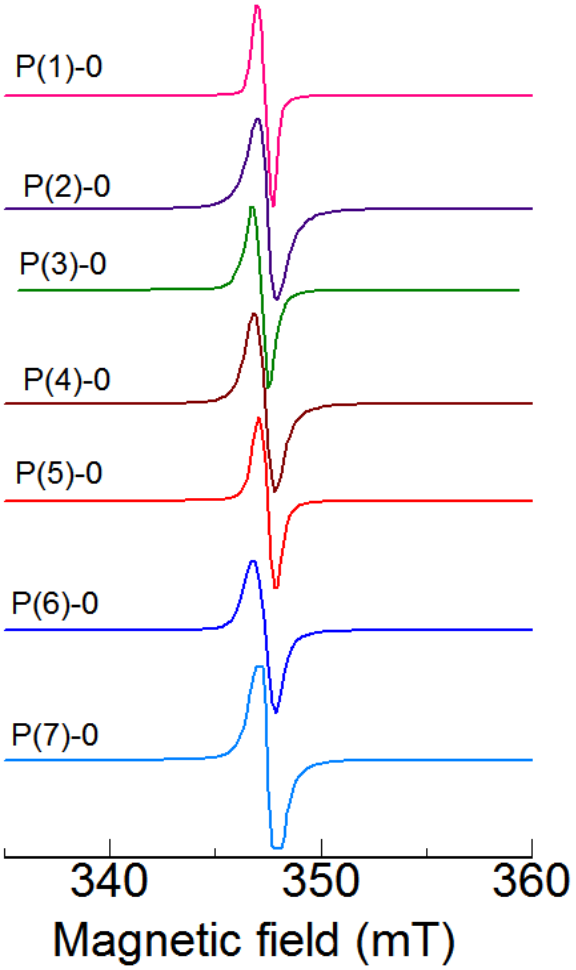

Figure 3. 10. Electron spin resonance (ESR) spectra for polymers-0 in power

Table 3. 4. Electron spin resonance (ESR) results of radical polymers

Polymers	g-value[a]	ΔHpp (mT) [a]	Spin conc (Spins/g) [a]
P(1)-0	2.00460	0.8218	1.78×10^{19}
P(2)-0	2.00461	0.8798	2.76×10^{19}
P(3)-0	2.00490	0.8211	2.99×10^{19}
P(4)-0	2.00432	1.0263	2.82×10^{19}
P(5)-0	2.00457	0.7331	2.80×10^{19}
P(6)-0	2.00490	1.1731	3.52×10^{19}
P(7)-0	2.00473	0.8798	1.38×10^{20}

[a]*g* value, the peak-to-peak line width and spin concentration were evaluated from ESR measurements.

3.4. Conclusion

This work offers a clear pathway to synthesize magnetic-opticallyactive low-bandgapπ-conjugated polymers through simple polycondansation reaction by using Pd(0) catalyst. These polymers appeared excellent

solubility, and the number average molecular weight (*M*n) of these polymers were found to be 2920-8840. Chiral polymers have good film forming property. Therefore, multi functionality of emission, magnetism, and electroactivity of the polymer can be applied for magneto-electro functional thin films.

3.5. Acknowledgments

We would like to thank Glass Work Shop of University of the Division of Materials Science (University of Tsukuba) and Chemical Analysis Division Research Facility Center for Science and Technology of University of Tsukuba for providing NMR, IR, ESR, PL measurements.

3.6. References

[1] Li H, Kim FS, Ren G, Jenekhe SA. High-mobility n-type conjugated polymers based on electron-deficient tetraazabenzodi fluoranthene diimide for organic electronics. J. Am. Chem. Soc. 2013;135:14920-14923.

[2] Boudouris BW. Engineering optoelectronically active macromolecules for polymer-based photovoltaic and thermoelectric devices. Curr. Opin. Chem. Eng. 2013;2:294-301.

[3] Sondergaard RR, Hosel M, Krebs FC. Roll-to-roll fabrication of large area functional organic materials. J. Polym. Sci. Polym. Phys. 2013;51:16-34.

[4] Sondergaard R, Hosel M, Angmo D, Larsen-Olsen TT, Krebs FC. Roll-to-roll fabrication of polymer solar cells. Mater. Today. 2012;15:36-49.

[5] Stutzmann N, Friend RH, Sirringhaus H. Self-aligned, vertical-channel, polymer field-effect transistors. Science. 2003;299:1881-1884.

[6] Friend RH, Gymer RW, Holmes AB, Burroughes JH, Marks RN, Taliani C, et al. Electroluminescence in conjugated polymers. Nature. 1999;397:121-128.

[7] Mitschke U, Bäuerle P, The electroluminescence of organic materials. J. Mater. Chem. 2000;10:1471-1507.

[8] Zhu CL, Liu LB, Yang Q, Lv FT, Wang S. Water-soluble conjugated polymers for imaging, diagnosis, and therapy. Chem. Rev. 2012;112:4687-4735.

[9] Thomas SW, Joly GD, Swager TM. Chemical sensors based on amplifying fluorescent conjugated polymers. Chem. Rev. 2007;107:1339-1386.

[10] Brabec CJ, Sariciftci NS, Hummelen JC. Plastic solar cells. Adv. Funct. Mater. 2001;11:15-26.

[11] Groenendaal L, Zotti G, Aubert PH, Waybright SM, Reynolds JR. Electrochemistry of Poly (3,4-alkylenedioxythiophene) Derivatives. Adv. Mater. 2003;15:855-879.

[12] Roberts E, Sokolov AN, Bao Z. Material and device considerations for organic thin-film transistor sensors. J. Mater. Chem. 2009;19:3351-3363.

[13] Nishide H, Kaneko T, Igarashi M, Tsuchida E, Yoshioka N, Lahti PM. Magnetic characterization and computational modeling of poly(phenylacetylenes) bearing stable radical groups. Macromolecules, 1994;27:3082-3086.

[14] Oyaizu K, Nishide H, Radical polymers for organic electronic devices: a radical departure from conjugated polymers. Adv. Mater. 2009;21: 2339-2344.

[15] Janoschka T, Hager MD, Schubert US. Powering up the future: radical polymers for battery applications. Adv. Mater. 2012;24:6397-6409.

[16] Tomlinson EP, Hay ME, Boudouris BW. Radical polymers and their application to organic electronic devices. Macromolecules. 2014;47:6145-6158.

[17] Goto H, Koyanob T, Ikedab H, Yoshizakib R, Akagia K. Synthesis and magnetic properties of polydiphenylamine derivative bearing stable radical groups. Polymer. 2004;45:4559-4564.

[18] Inoue K, Hayamizu T, Iwamura H, Hashizume D, Ohashi Y. Assemblage and alignment of the spins of the organic trinitroxide radical with a quartet ground state by means of complexation with magnetic metal ions. A molecule-based magnet with three-dimensional structure and high T_C of 46 K. J. Am. Chem. Soc. 1996;118:1803-1804.

[19] Nishide H, Takahashi M, Takashima J, Pu YJ, Tsuchida E. Acyclic and cyclic di- and tri(4-oxyphenyl-1,2-phenyleneethynylene)s: their synthesis and, ferromagnetic spin interaction. J. Org. Chem. 1999;64:7375-7380.

[20] Nishide H, Kaneko T, Nii T, Katoh K, Tsuchida E, Lahti PM. Poly(phenylenevinylene)-attached phenoxyl radicals: ferromagnetic interaction through planarized and π-conjugated skeletons. J. Am. Chem. Soc. 1996;118:9695-9704.

[21] Miurat Y, Matsumoto M, Ushitani Y. Magnetic and optical characterization of poly(ethyny1benzene) with pendant nitroxide radicals. Macromolecules. 1993;26:6673-6675.

[22] Nishide H, Kaneko T, Nii T, Katoh K, Tsuchida E, Yamaguchi K. Through-bond and long-range ferromagnetic spin alignment in a π-conjugated polyradical with a Poly(phenylenevinylene) skeleton. J. Am. Chem. Soc. 1995;117:548-549.

[23] Rostro L, Wong SH, Boudouris BW. Solid state electrical conductivity of radical polymers as a function of pendant group oxidation state. Macromolecules. 2014;47:3713-3719.

[24] Hyakutake T, Park JY, Yonekuta Y, Oyaizu K, Nishide H, Advincula R. Nanolithographic patterning via electrochemical oxidation of stablepoly(nitroxide radical)s to poly(oxoammonium salt)s. J. Mater. Chem. 2010;20:9616-9618.

[25] Wingate AJ, Boudouris BW. Recent advances in the syntheses of radical-containing macromolecules. J . Polym. Sci. Polym. Chem. 2016;54:1875-1894.

[26] Yoshioka N, Nishide H, Kaneko T, Yoshiki H, Tsuchida E. Poly[(p-ethynylphenyl)hydrogalvinoxy] and its polyradical derivative with high spin concentration. Macromolecules. 1992;25:3838-3842.

[27] Krieger PE, Landgrebe JA. Asymmetric induction in the addition of chiral carbalkoxycarbenoids to styrene. J. Org. Chem. 1978;43:4447-4452.

[28] Song J, Bi H, Xie X, Guo J, Wang X, Liu D. Natural borneol enhances geniposide ophthalmic absorption in rabbits. Int. J. Pharm. 2013;445:163-170.

[29] Al-Farhan KA, Warad I, Al-Resayes SI, Fouda MM, Ghazzali M. Synthesis, structural chemistry and antimicrobial activity of-(-)borneol derivative. Cent. Eur. J. Chem. 2010;8:1127-1133.

[30] Mohammad F, Calvert PD, Billingham NC. Thermal stability of electrochemically prepared polythiophene and polypyrrole. Bull. Mater. Sci. 1995;18:255-261.

[31] Huang X, Kim M, Suh H, Kim I. Hierarchically nanostructured carbon-supported manganese oxide for high-performance pseudo-capacitors. Korean J. Chem. Eng. 2016;33:2228-2234.

[32] Princea W, Edwards-Lajnef M, Aıtcinb PC. Interaction between ettringite and a polynaphthalene sulfonate

superplasticizer in a cementitious paste. Cement Concrete Res. 2002;32:79-85.
[33] Long G, Wan X, Zhou J, Liu Y, Li Z, He U, Zhang M, Hou Y, Chen Y. Isothianaphthene-based conjugated polymers for organic photovoltaic cells. Macromol. Chem. Phys. 2012;213:1596-1603.
[34] Hoogmartens I, Adriaensens P, Vanderzande D, Gelan J. Low-bandgap conjugated polymers. A joint experimental and theoretical study of the structure of polyisothianaphthene. Macromolecules. 1992:25:7347-7356.
[35] Oh HS, He GS, Law WC, Baev A, Jee H, Liu X, Urbas A, Lee CW, Choi BL, Swihart MT, Prasad PN. Manipulating nanoscale interactions in a polymer nanocomposite for chiral control of linear and nonlinear optical functions. Adv. Mater. 2014;26:1607-1611.
[36] Xie N, Wang J, Guo Z, Chen G, Li Q. Fluorene/carbazole alternating copolymers tethered with polyhedral oligomeric silsesquioxanes: synthesis, characterization, and electroluminescent properties. Macromol. Chem. Phys. 2013;214:1710-1723.
[37] Yamamoto T, Hayashi H. π-Conjugated soluble and fluorescent poly(thiophene-2,5-diyl)s with phenolic, hindered phenolic and *p*-$C_6H_4OCH_3$ substituents. Preparation, optical properties, and redox reaction. J . Polym. Sci. Polym. Chem.1997;35:463-474.
[38] Casado J, Hotta S, Hern V, Navarrete JTL. Vibrational spectroscopic study of a series of α, α'-diethyl end-capped oligothiophenes with different chain lengths in the neutral state. J. Phys. Chem. A. 1999;103:816-822.
[39] Casado J, Katz HE, Hern V, Navarrete JTL. Infrared spectra of two sexithiophenes in neutral and doped states: a theoretical and spectroscopic study. Vib. Spectrosc. 2002;30:175-189.
[40] Kaneko T, Tatsumi H, AokiOKI T, Oikawa E, Yoshiki H, Yoshioka N, Tsuchida E, Nishide H. Polymerization of (p-vinylphenyl)hydrogalvinoxyl and formation of a stable polyradical derivative. J . Polym. Sci. Polym. Chem. 1999;37:189-198.
[41] Langeveld-voss BMW, Janssen RAJ, Meijer EWJ. On the origin of optical activity in polythiophenes. Mol. Struct. 2000;521:285-301.
[42] Zhang HY, Yang WT, Deng JP. Optically active helical polymers with pendent thiourea groups: chiral organocatalyst for asymmetric michael addition reaction. J . Polym. Sci. Polym. Chem. 2015;53:1816-1823.
[43] Dordevic L, Marangoni T, Miletic T, Magnieto JR, Mohanraj J, Amenitsch H, Pasini D, Liaros N, Couris S, Armaroli N, Surin M, Bonifazi D. Solvent molding of organic morphologiesmade of supramolecular chiral polymers. J. Am. Chem. Soc. 2015;137:8150-8160.
[44] Kaneko T , Yoshimoto S, Hadano S,Teraguchi M, Aoki T. Synthesis of an optically active helical poly(1,3-phenyleneethynylene) bearing stable radicals and its chiroptical and magnetic properties. Polyhedron. 2007;26:1825–1829.
[45] Goto H. Magneto-optically active polythiophene derivatives bearing a stable radical group from achiral monomers by polycondensation in cholesteric liquid crystal. Polymer. 2008;49:3619-3624.
[46] Kaneko T, Abe H, Namikoshi T, Marwanta E, Teraguchi M, Aoki T. Synthesis of an optically active poly (aryleneethynylene) bearing galvinoxyl residues and its chiroptical and magnetic properties. Synth Met. 2009;159:864-867.
[47] Nishide H, Yoshioka N, Inagaki K, Tsuchida E. Poly [(3,5-di-tert-butyl-4-hydroxyphenyl)acetylene]: formation of a conjugated stable polyradical. *Macromolecules.* 1988**;***21:*3119-3120.

[48] Apperloo JJ, Janssen RAJ, Malenfant PRL, Frechet JMJ. Concentration-dependent thermochromism and supramolecular aggregation in solution of triblock copolymers based on lengthy oligothiophene cores and poly(benzyl ether) dendrons. Macromolecules. 2000;33:7038-7043.
[49] Goto H, Wang AH, Kawabata K, Yang F. Synthesis and properties of a low-bandgap liquid crystalline π-conjugated polymer. J Mater Sci. 2013;48:7523-7532.
[50] Jenekhe SA, Osaheni JA, Excimers and exciplexes of conjugated polymers. Science, 1994;265:765-768.
[51] D'Andrade BW, Datta S, Forrest SR, Djurovich P, Polikarpov E, Thompson ME. Relationship between the ionization and oxidation potentials of molecular organic semiconductors. Org. Electron. 2005;6:11-20.
[52] Brédas JL, Silbey R, Boudreaux DS, Chance RR. Chain-length dependence of electronic and electrochemical properties of conjugated systems: polyacetylene, polyphenylene, polythiophene, and polypyrrole. J. Am. Chem. Soc. 1983;105:6555-6559.
[53] Agrawal AK, Jenekhe SA. Electrochemical properties and electronic structures of conjugated polyquinolines and polyanthrazolines. Chem. Mater. 1996;8:579-589.
[54] Patil AO, Heeger AJ, Wudl F. Optical properties of conducting polymers. Chem. Rev. 1988;88:183-200.
[55] Baughman RH, Bredas JL, Chance RR, Elsenbaumer RL, Shacklette LW. Structural basis for semiconducting and metallic polymer dopant systems. Chem. Rev. 1982;82:209-222.
[56] Nishide H, Doi R, Oyaizu K, Tsuchida E. Electrochemical and ferromagnetic couplings in 4,4',4"-(1,3,5-benzenetriyl)tris(phenoxyl) radical formation. J. Org. Chem. 2001;66:1680-1685.

3.7. Supporting Information

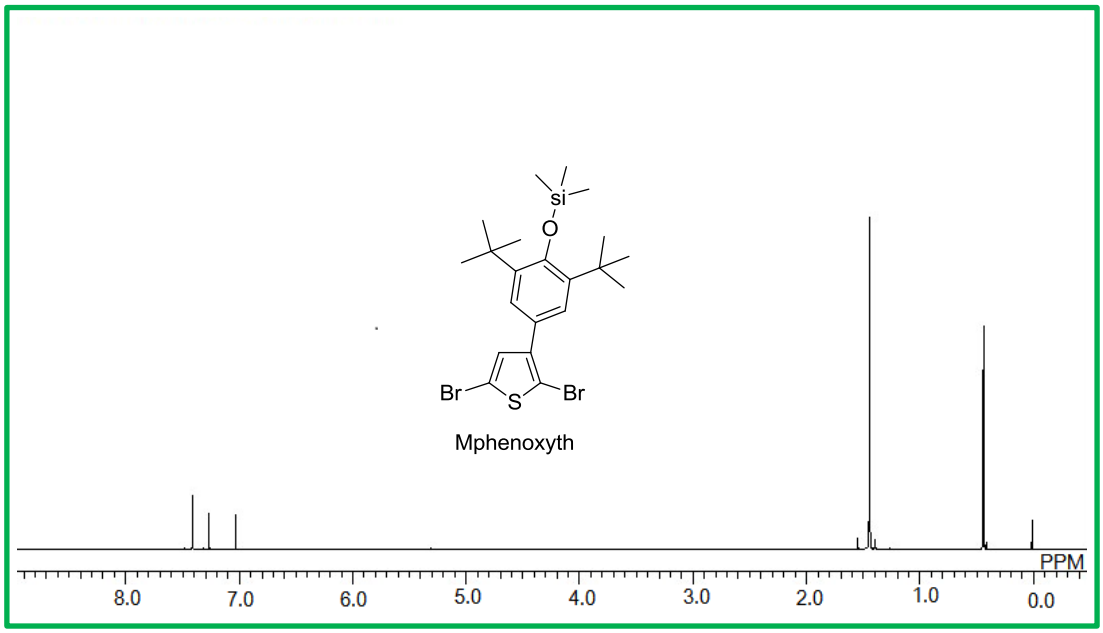

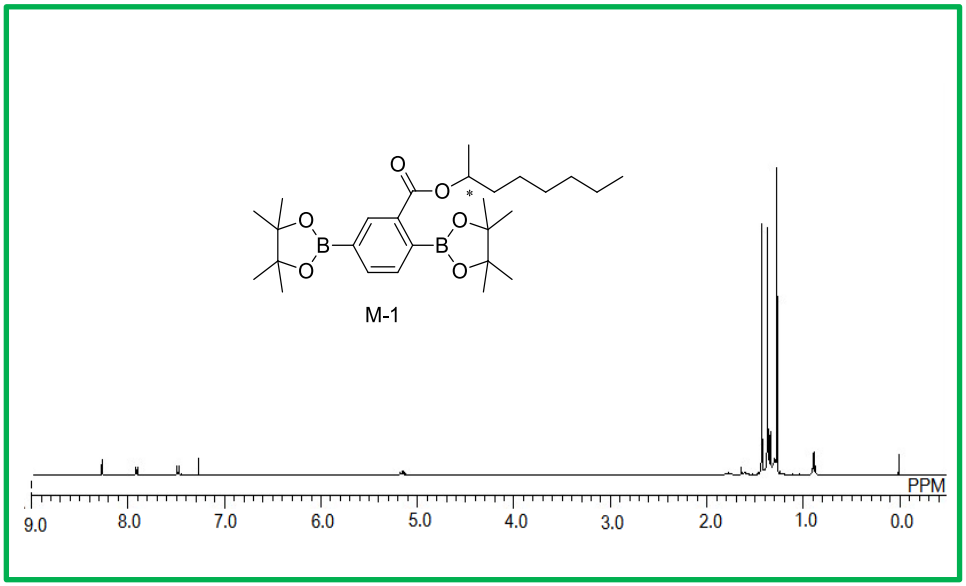
M-1
PPM
9.0
8.0
7.0
6.0
5.0
4.0
3.0
2.0
1.0
0.0

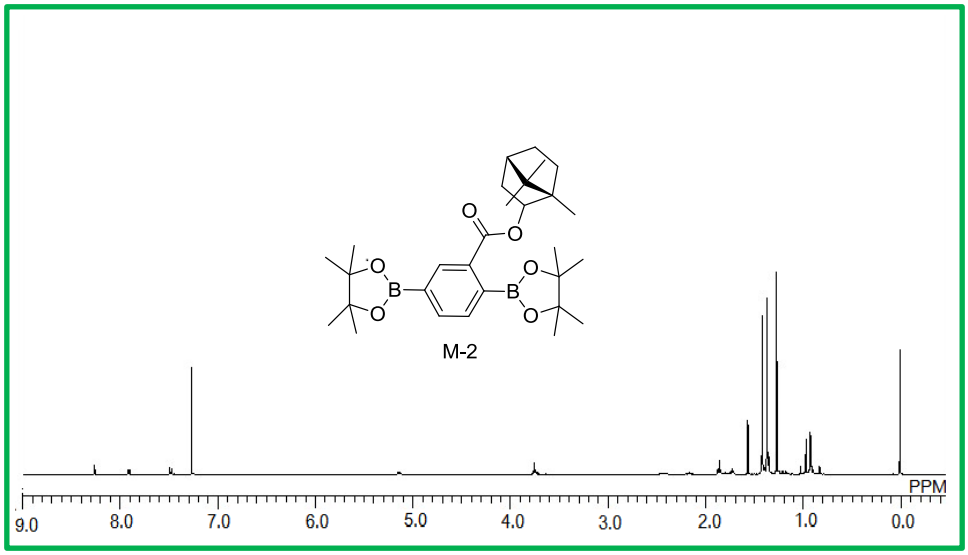
M-2
PPM
9.0
8.0
7.0
6.0
5.0
4.0
3.0
2.0
1.0
0.0

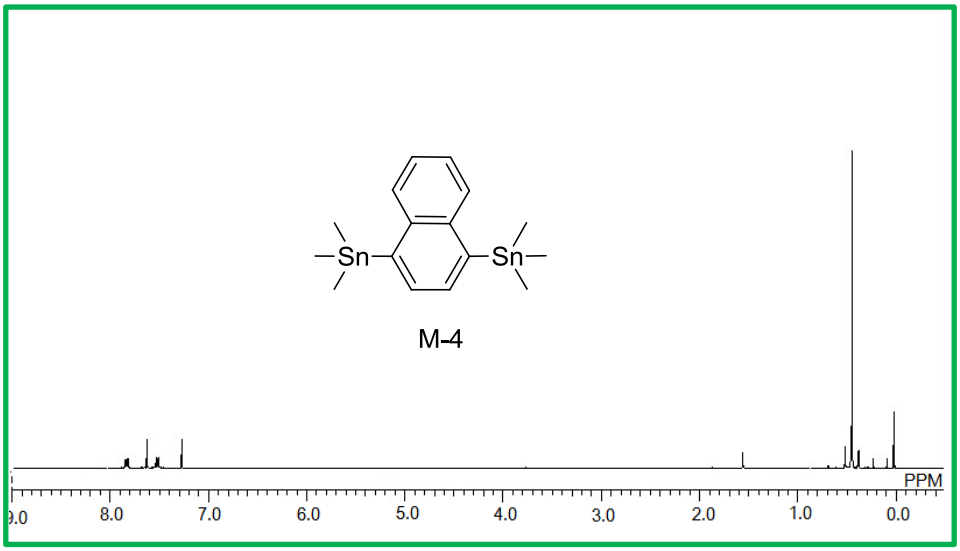
M-4
PPM
8.0
7.0
6.0
5.0
4.0
3.0
2.0
1.0
0.0

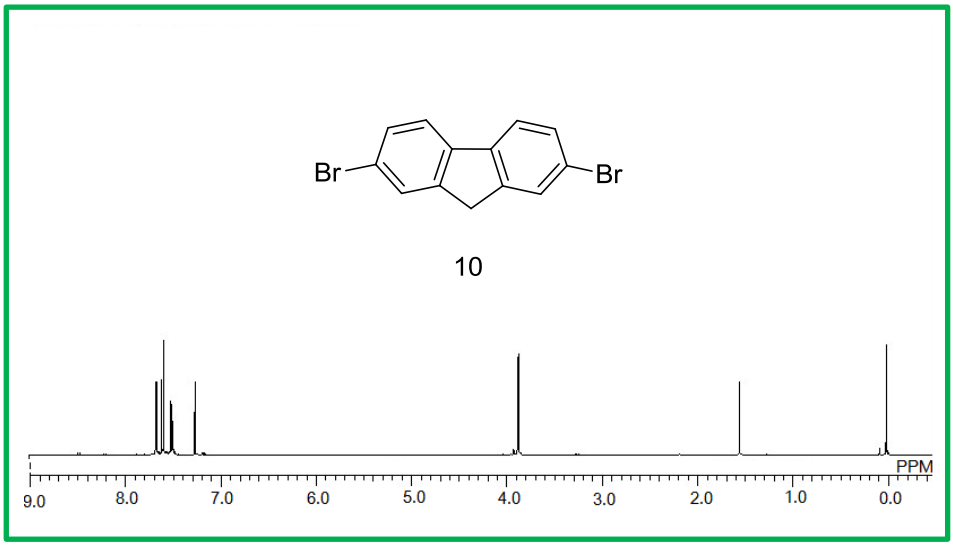
Br
Br
10
PPM
9.0
8.0
7.0
6.0
5.0
4.0
3.0
2.0
1.0
0.0

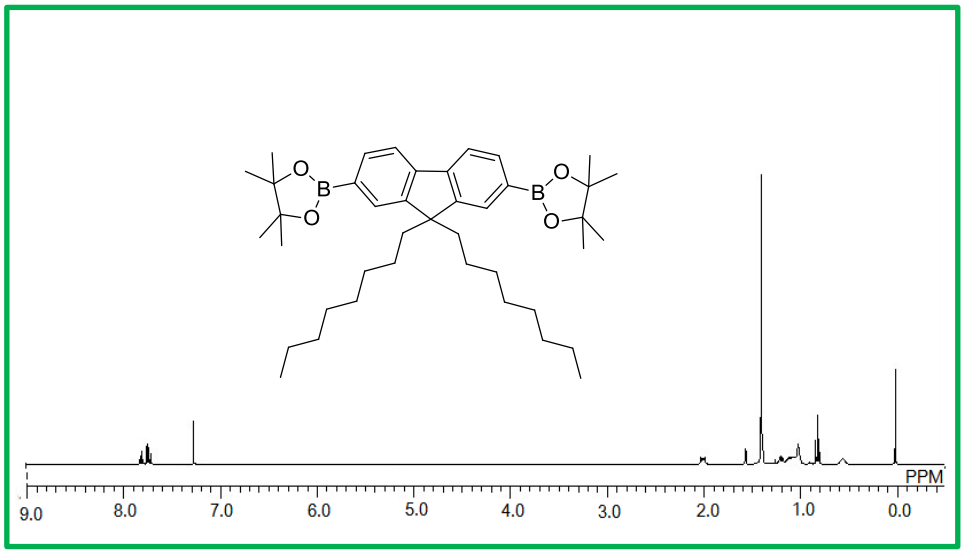
O
B
O
B
O
O
PPM
9.0
8.0
7.0
6.0
5.0
4.0
3.0
2.0
1.0
0.0

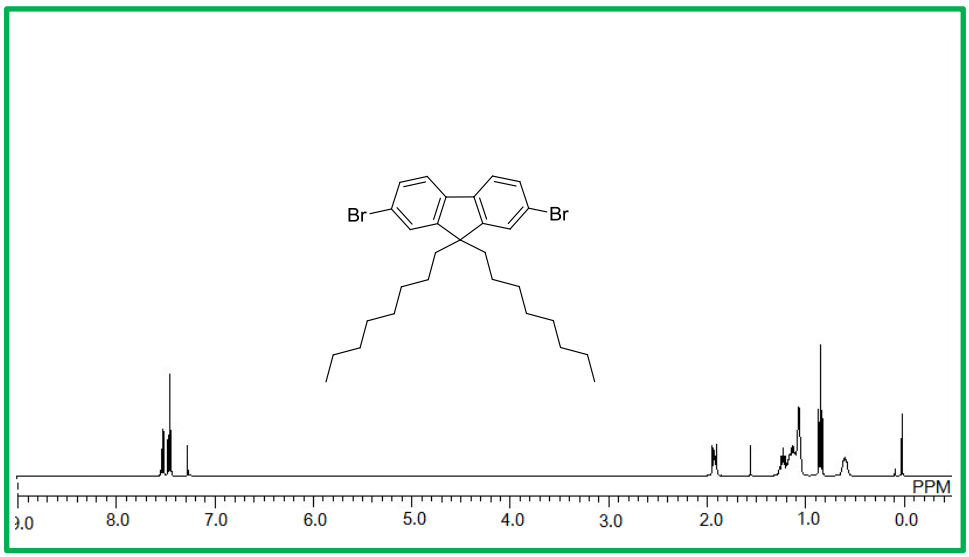
Br
Br
PPM
8.0
7.0
6.0
5.0
4.0
3.0
2.0
1.0
0.0

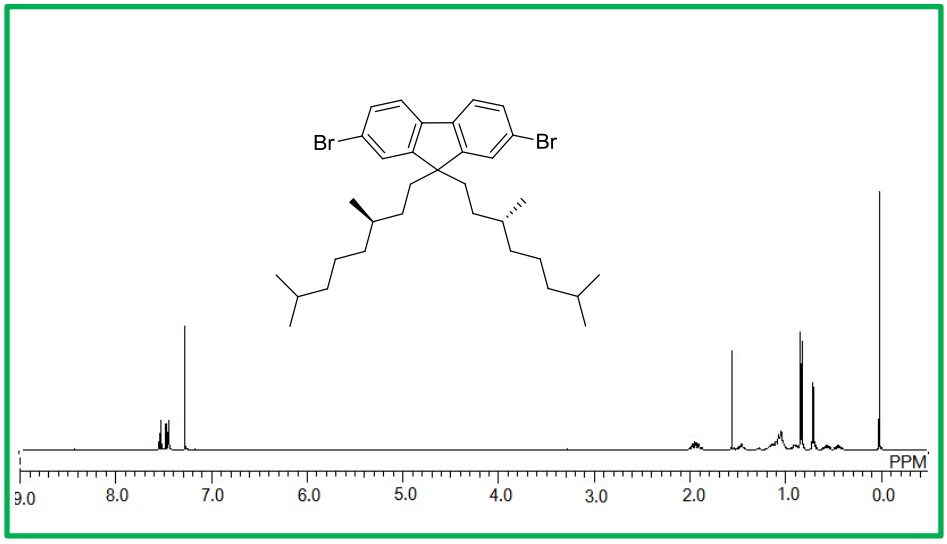
Br
Br
PPM
9.0
8.0
7.0
6.0
5.0
4.0
3.0
2.0
1.0
0.0

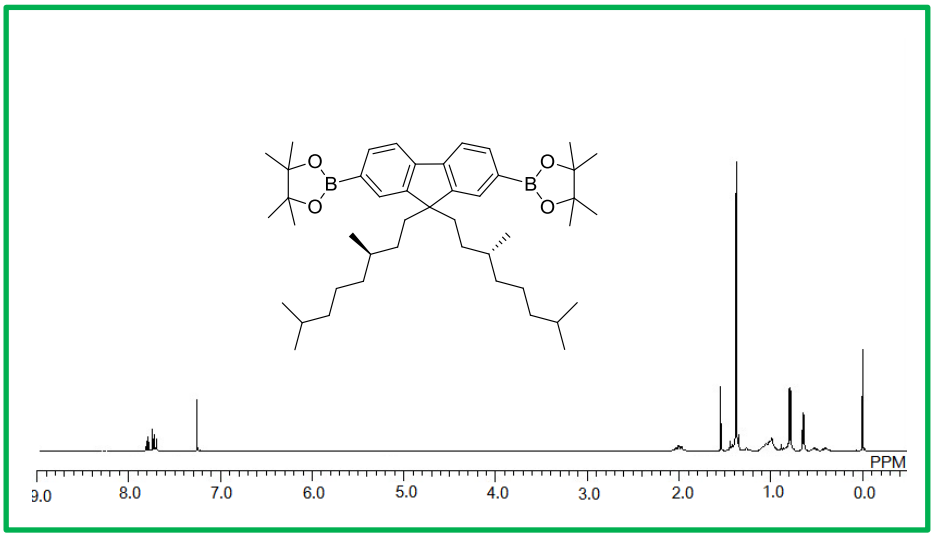
O
B
O
O
B
O
PPM
9.0
8.0
7.0
6.0
5.0
4.0
3.0
2.0
1.0
0.0

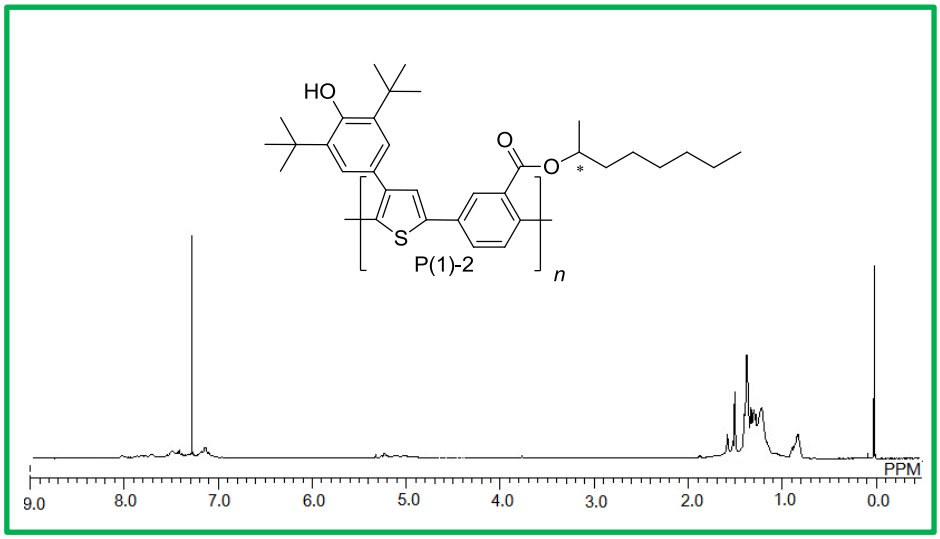
HO
O
O
*
S
P(1)-2
n
PPM
9.0
8.0
7.0
6.0
5.0
4.0
3.0
2.0
1.0
0.0

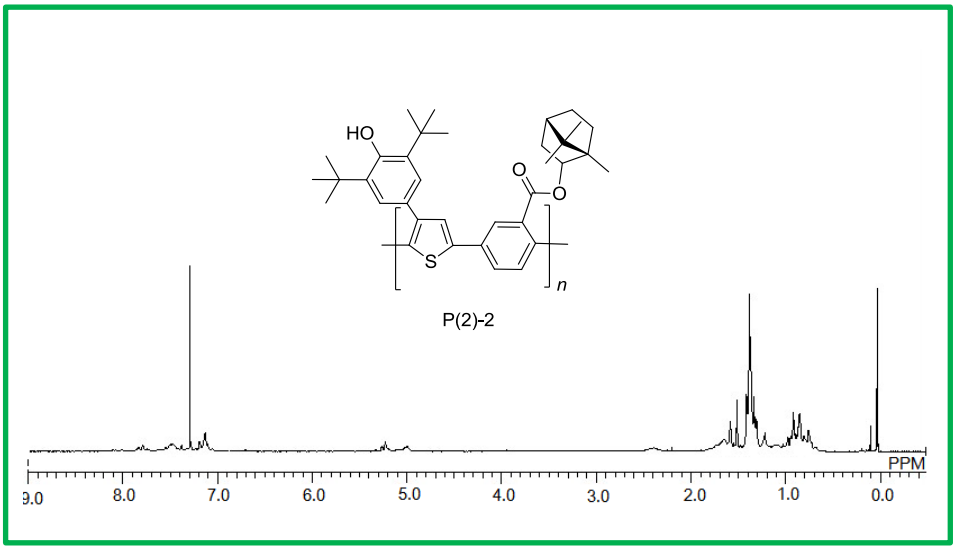
HO
O
O
S
n
P(2)-2
PPM
9.0
8.0
7.0
6.0
5.0
4.0
3.0
2.0
1.0
0.0

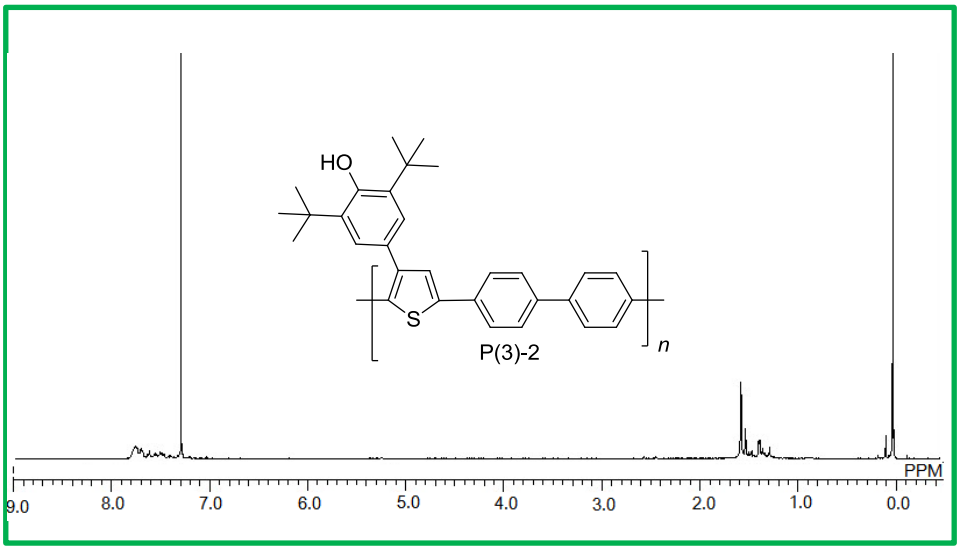
HO
S
n
P(3)-2
PPM
9.0
8.0
7.0
6.0
5.0
4.0
3.0
2.0
1.0
0.0

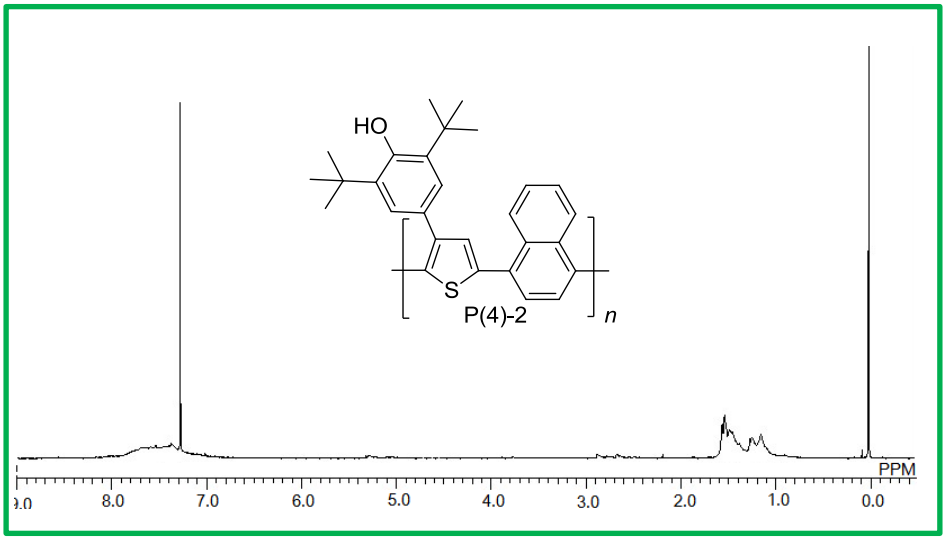
HO
S
n
P(4)-2
PPM
8.0
7.0
6.0
5.0
4.0
3.0
2.0
1.0
0.0

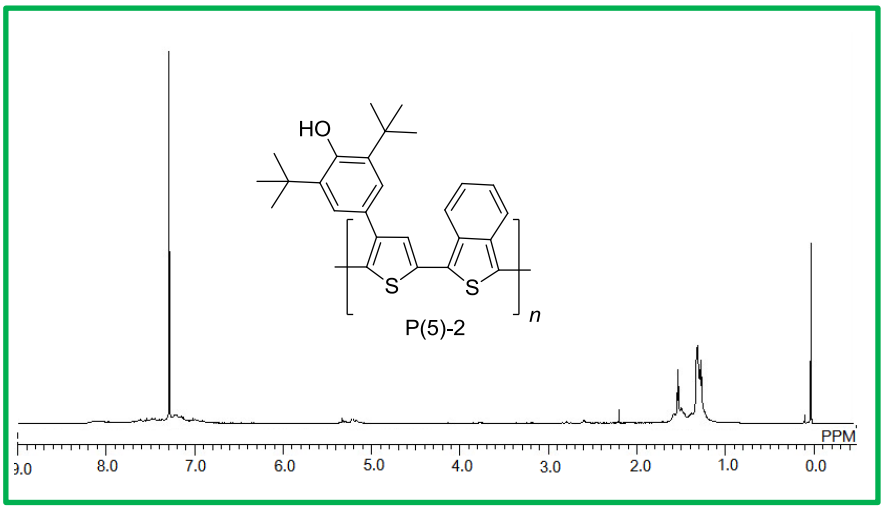
HO
S
S
n
P(5)-2
PPM
9.0
8.0
7.0
6.0
5.0
4.0
3.0
2.0
1.0
0.0

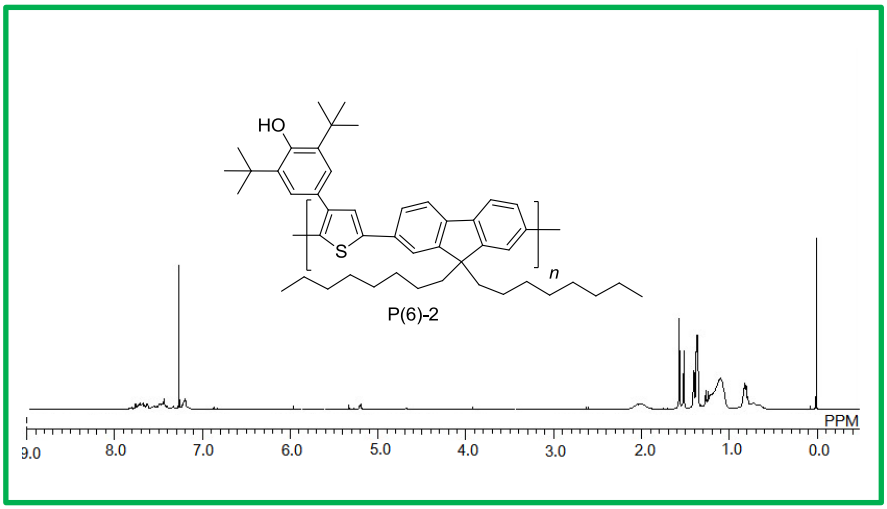
HO
S
n
P(6)-2
PPM
9.0
8.0
7.0
6.0
5.0
4.0
3.0
2.0
1.0
0.0

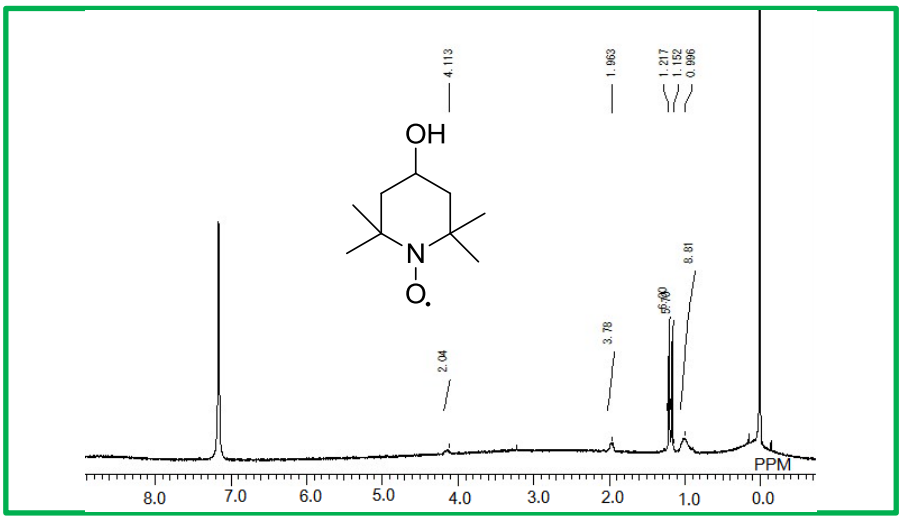
4.113
1.963
1.217
1.152
0.996
OH
N
O.
8.81
3.78
2.04
PPM
8.0
7.0
6.0
5.0
4.0
3.0
2.0
1.0
0.0

Chapter 4

Synthesis and properties of low bandgap isothianaphthene-based polymers bearing bornyl side groups

4.1. Introduction

Conjugated polymers are promising in low cost, thin film flexibility, versatility of functionalization, their electronic properties and so on. These materials have attracted to the applications in field effect transistors, organic photovoltaic (OPV) cells and light-emitting diodes. [1-6] The applications require proper organic semiconducting materials with specific properties. The lowest unoccupied molecular orbital and the highest occupied molecular orbital of polymers can be modulated to optimize the manipulation by increasing quinoid character of conjugated main chain and substituent modifications of conjugated polymers. For example: resonance energy, inter-ring torsion angle, bond length alternation, substituent effects, inter-chain effects, and so on [7, 8].

Three low band gap isothianaphthene-based (ITN) polymers with different π-conjugated backbone as main chain and chiral bornyl group as a side chain were designed, synthesized and characterized. The different π-conjugated main chain (isothianaphthene phenylene, isothianaphene thiophene and isothianaphthene methane) show different properties. Their cyclic voltammetry (CV) shows narrowed HOMO-LUMO gaps of the isothianaphthene derivatives. This indicates high efficiency of π-electron delocalization in the isothianaphthenes along the conjugated backbone. The polymer (P3) of isothianaphthene methane as conjugated backbone showed lowest band gap of 1.57 eV. In addition, the bornyl group as side chain was introduced in the conjugated polymers. We further investigated by optimizing the geometries of three polymers and optical properties by Circular dichroism (CD) spectra, Photoluminescence (PL) spectra, UV-vis absorption spectra and optical rotatory dispersion (ORD) spectra.

4.2. Experiment section

4.2.1. Materials

Commercially available reagents were received from Nacalai Tesque (Japan), Sigma-Aldrich (Japan), Kanto Chemical (Japan) and Tokyo Chemical Industry (Japan) unless otherwise noted and used without further purification. Common organic solvents such as dichloromethane and tetrahydrofuran (THF) were distilled and handled in a moisture-free atmosphere. The purification of the newly synthesized compounds was performed by column chromatography on silica gel (Silica gel 60 N).

4.2.2. General methods

Chemical shifts were given in parts permillion and coupling constant (*J*) in Hz. FTIR absorption spectra were obtained with an FT/IR-300 spectrometer (Jasco) using a KBr method. ^{1}H NMR spectra of the compounds were recorded using JNM ECS 400 spectrometer (JEOL, Japan) with $CDCl_3$ as the deuterated solvent and tetramethylsilane (TMS) as the internal standard. Circular dichroism (CD) spectra and optical rotatory dispersion (ORD) spectra were measured with a J-720 (JASCO, Tokyo, Japan). UV-vis absorption spectra were recorded on a JASCO V-630 UV-vis optical absorption spectrometer. Photoluminescence (PL) spectra of the polymers in chloroform were measured with F-4500 fluorescence spectrophotometer (HITACHI, Japan). ESR measurements of the samples in powder were carried out using a JEOL JES TE-200 spectrometer with 100 kHz modulation. The spin concentration was determined using $CuSO_4 \cdot 5H_2O$ as standard. The sample was packed into a 5 mm quartz tube. Molecular weights of the polymers were determined by gel permeation chromatography (GPC) with MIXED-D HPLC column (Polymer Laboratories), PU-980 HPLC pump (Jasco) and MD-915 multiwavelength detector (Jasco), with tetrahydrofuran (THF) used as the solvent, with the instruments calibrated by polystyrene standard. Cyclic voltammetry (CV) measurements were carried out with a μAUTOLAB TYPE III (ECO Chemie). Electrolyte solutions contained 0.1 M of TBAP in acetonitrile.

4.2.3. Monomer synthesis

1,3-Dihydro-benzo[c]thiophene (1).

The solution of sodium sulfide nonahydride (26.4 g, 109 mmol) in ethanol/water (250 mL/50 mL) was added into a round-bottom flask. 1,2-bischloromethylbenzene (12.3 g, 70.3 mmol) was added into a soxhlet extractor and added dropwise into the solution and refluxed for 2 h. After the solvent was removed, the mixture was cooled to room temperature and extracted twice with dichloromethane, washed with water, and dried with anhydrous $MgSO_4$. A dichloromethane solution was filtered off and the solvent was evaporated obtained a brown solid. Yield 7.5g (78%). ^{1}H NMR (400 MHz; $CDCl_3$; δ): 4.27 (s, 4H, CH_2), 7.18-7.28 (m, 4H, Ar*H*).

1,3-Dihydro-benzo[c]thiophene 2-oxide (2).

The solution of sodium periodate (11.7 g, 55.1 mmol) in water (115 ml) was added into a round-bottom flask. The mixture of 1,3-Dihydro-benzo[c]thiophene (7.50 g, 55.1 mmol) in ethanol (140 mL) was dropwise added into the solution at 0 °C. After another 3 h stirring the reaction mixture was filtered and evaporated of the solvent evaporation of the solvent followed by washing with diethyl ether gave 1,3-Dihydro-benzo[c]thiophene 2-oxide 6 g (72%) as a white solid. ^{1}H NMR (400 MHz; $CDCl_3$; δ): 4.15-4.19 (d, 2H, CH_2, J = 16.0 Hz), 4.26-4.29 (d, 2H, CH_2, J = 13.6 Hz), 7.27-7.40 (m, 4H, Ar*H*).

Isothianaphthene(3).

The compounds of aluminum oxide powder (1.6 g, 15.8 mmol) and 1,3-Dihydro-benzo[c]thiophene 2-oxide (1.2 g, 7.9 mmol) were mixed and finely crushed in a mortar. Sublimation of the mixture was heated under reduced pressure at 25 mmHg with slowly increasing temperature form 80°C-150°C in a sublimer, almost pure isothianaphthene 0.6 g condensed on the cold finger in yield (57%) as a white solid white. ^{1}H NMR (400 MHz; $CDCl_3$; δ): 7.00-7.08 (m, 4H, Ar*H*), 7.56-7.66 (m, 2H, Ar*H*).

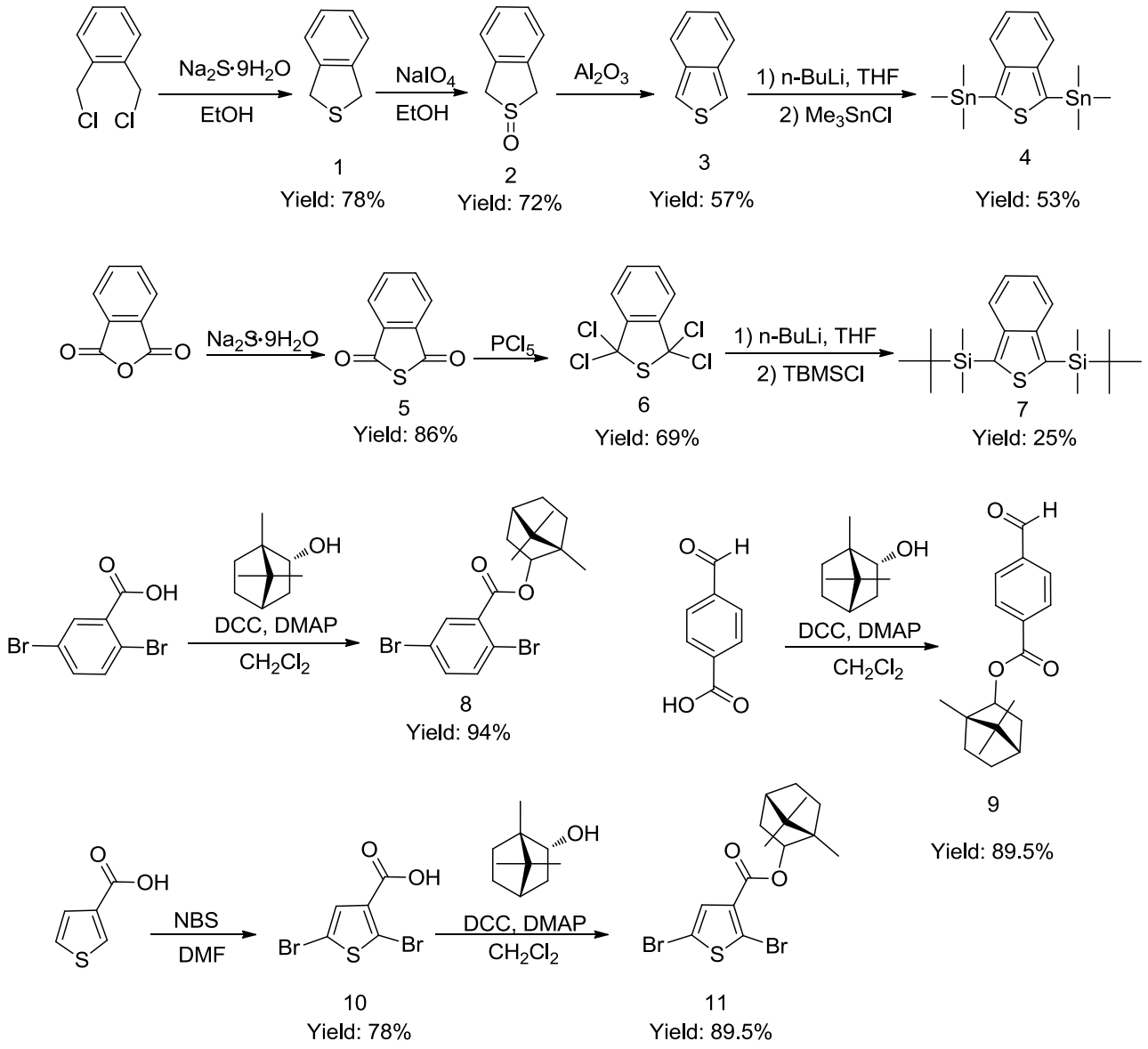

Scheme 4. 1. Synthesis of monomers. DCC: dicyclohexylcarbodiimid. DMAP: 4-dimethylaminopyridine. NBS: *N*-bromosuccinimide

1,3-Di(trimethylstannyl)isothianaphthene (4).

Freshly prepared isothianaphthene (0.60 g, 4.48 mmol) and tetramethliethylethylenediamine (TMEDA, 1.30 g, 11.12 mmol) were added into tetrahydrofuran (THF, 15 mL). The *n*-BuLi (1.6 M in hexanes) (6.7 mL) was added dropwise into the mixture under an argon stream at 0 °C and stirred for 2 h at room temperature. Then a solution of chlorotrimethyltin (2.20 g, 11.3 mmol) in THF (10 mL) was added dropwise through syringe at -78 °C. The mixture was slowly warmed up to room temperature and stirred overnight. The solution was poured into 50 mL of saturated NH_4HCO_3 and separated. The aqueous phase was extracted with ether twice, and the combined organic phase was washed with water three times and dried over $MgSO_4$. After removal of solvents under reduced pressure, the product was isolated by recrystallization from petroleum ether as a pale yellow

solid 1.1 g (53%). (400 MHz; $CDCl_3$; δ): 0.488 (s, 18H, Sn[CH_3]$_3$), 7.06-7.08 (d, 2H, J = 8.0, ArH), 7.65-7.67 (d, 2H, J = 8.8, ArH).

Benzo[c]thiophene-1,3-dione (5).

$Na_2S{\cdot}9H_2O$ (4.20 g, 18.9 mmol) and Isobenzofuran-1,3-dione (2.00 g, 13.5mmol) was added in the flask with stirring at room temperature for 5 h. The reaction was quenched with 50 mL water H_2O and the mixture was acidified with 25 mL 2 M HCl. The solid product was collected by filtration and was obtained as white powder solid, yield 1.90 g (86%).^{1}H NMR (400 MHz; $CDCl_3$; δ) 7.80-7.84 (m, 2H, ArH), 7.96-7.99 (m, 2H, ArH).

1,1,3,3-Tetrachlorothiophthalan (6).

phosphorus pentachloride (6.03 g, 28.9 mmol), phosphorus oxychloride (0.5 mL) and Benzo[c]thiophene-1,3-dione (1.90 g, 11.59 mmol) were heated at 160 °C for 15 h. Phosphorus oxychloride was removed under reduced pressure. Toluene was added to the residue and removed by distillation. The residue was dissolved in chloroform. The organic layer was washed with a 1 M sodium bicarbonate solution several times and with water twice, evaporated, and the residue was crystallized from n-hexane with decolorizing carbon to give 2.2 g (yield 69%) of the product as white crystals. ^{1}H NMR (400 MHz; $CDCl_3$; δ) 7.61-7.63 (d, 2H, J = 8, ArH), 7.64-7.66 (d, 2H, J = 8, ArH).

1,3-Bis (tert -butyldimethylsily1)isothianaphthene (7).

A solution of 1,1,3,3-Tetrachlorothiophthalan (1.0 g, 3.65mmol) in 80 mL THF was cooled to -78°C.The compound of *n*-BuLi (1.6 M, 7.98 mL, 12.77 mmol) was added dropwise into the mixture under an argon stream at -78 °C and stirred for 1 h at room temperature. Then a solution of tert-butyldimethylsilyl chloride (TBDMS-Cl (1.38 g, 9.12 mmol)) in THF (30 mL) was cooled down to -78 °C and added dropwise through syringe. The mixture was slowly warmed up to room temperature and stirred overnight 1 h. It was poured into ice-water. The aqueous phase was extracted with ether twice, and the combined organic phase was washed with water three times and dried over $MgSO_4$. After removal of solvents under reduced pressure, the product was isolated by recrystallization from petroleum ether as a pale yellow solid 320 mg (25%). (400 MHz; $CDCl_3$; δ): 0.354 (s, 12H, CH_3), 0.935 (s, 18H, CH_3), 7.08-7.09 (d, 2H, J = 2.4, ArH), 7.77-7.78 (d, 2H, J = 3.2, ArH).

1,7,7-Trimethylbicyclo[2.2.1]hept-2-ol2,5-dibromobenzoate (8).

2,5-Dibromobenzoicacid (2.0 g, 7.14 mmol), 4-dimethylaminopyridine (DMAP) (0.174 g, 1.42 mmol), dicyclohexylcarbodiimid (DCC) (1.62 g, 7.85 mmol), L-borneol (2.05 g, 13.3 mmol) were mixed in 25 mL dichloromethane at room temperature with stirring for overnight. The mixture was extracted with dichloromethane, and dried over magnesium sulfate, then purified by silica gel column chromatography (ethyl acetate/hexane = 1:5) to afford a pale yellow solid 2.80 g (94%).^{1}H NMR (400 MHz; $CDCl_3$; δ): 0.938-0.993 (m, 9H, CH_3), 1.16-1.20 (d, 1H, J = 16.8, CH_2CH), 1.29-1.39 (m, 2H, CH_2CH_2), 1.74-1.80 (m, 2H, CCH_2), 2.05-2.07 (m, 1H, CHCH_2), 2.49-2.50 (m, 1H, CHCH_2), 5.11-5.15 (m, 1H, OCH), 7.43-7.45 (d, 1H, J = 8, ArH), 7.51-7.53 (d, 1H, J = 8, ArH), 7.86 (s, 1H, ArH).

4-((1R,4R)-1,7,7-trimethylbicyclo[2.2.1]heptan-2-oxycarbonyl)benzaldehyde (9).

4-Dimethylaminopyridine (DMAP) (0.163 g, 1.33 mmol), dicyclohexylcarbodiimid (DCC) (1.5 g, 7.30 mmol), borneol (1.85 g, 11.9 mmol) and 4-formylbenzoic acid (1.0 g, 6.66 mmol) were added to 15 mL of dichloromethane and stirred at room temperature for overnight. The mixture was filtered and filtrate was extracted with dichloromethane, and dried over magnesium sulfate, then purified by silica gel column chromatography (eluent: hexane/dichloromethane = 3/2) to afford a pale yellow oily liquid (0.660g, 89.5%). (400 MHz; $CDCl_3$; δ): 0.912-0.970 (m, 9H, CH_3), 1.09-1.13 (d, 1H, J = 16, CH_2CH), 1.22-1.37 (m, 2H, CH_2CH_2), 1.72-1.74 (m, 2H, CCH_2), 2.07-2.10 (m, 1H, $CHCH_2$), 2.44-2.45 (m, 1H, $CHCH_2$), 5.13-5.16 (m, 1H, OC*H*), 7.95-7.96 (d, 2H, J = 8.4, Ar*H*), 8.20-8.22 (d, 2H, J = 8.0, Ar*H*), 10.1 (s, 1H, CO*H*).

2,5-Dibromo-3-thiophenecarboxylic Acid (10).

A solution of 3-thiophenecarboxylic acid (1.00 g, 7.81 mmol) in 10 mL of DMF was added dropwise into a mixture of *N*-bromosuccinimide (NBS) (2.78 g, 15.6 mmol) and 10 mL of DMF at room temperature with stirring. The mixture was stirred at 50 °C overnight and then poured into 200 mL of saturated aqueous solution of sodium bicarbonate. The resulting precipitate was collected by filtration and washed with ethanol. The crude product was recrystallized from ethanol and water to get 1.72 g white needle, yield (78%). (400 MHz; $CDCl_3$; δ): 7.43 (s, 1H, Th*H*).

1,7,7-Trimethylbicyclo[2.2.1]hept-2-ol2,5-dibromo-3-thenoate (11).

4-Dimethylaminopyridine (DMAP) (0.0427 g, 0.349 mmol), borneol (0.40 g, 2.60 mmol), 2,5-dibromothiophenic acid (0.50 g, 1.75 mmol) and dicyclohexylcarbodiimid (DCC) (0.396 g, 1.92 mmol) were added to 10 mL of dichloromethane and stirred at room temperature for overnight. The mixture was filtered and filtrate was extracted with dichloromethane, and dried over magnesium sulfate, then purified by silica gel column chromatography (eluent: hexane/dichloromethane = 3/2) to afford a pale yellow oily liquid (0.660 g, 89.5%). (400 MHz; $CDCl_3$; δ): 0.912-0.970 (m, 9H, CH_3), 1.09-1.13 (d, 1H, J = 13.6, CH_2CH), 1.24-1.39 (m, 2H, CH_2CH_2), 1.73-1.75 (m, 2H, CCH_2), 2.07-2.10 (m, 1H, $CHCH_2$), 2.46-2.47 (m, 1H, $CHCH_2$), 5.06-5.09 (m, 1H, OC*H*), 7.36 (s, 1H, Th*H*).

4.2.4. Polymer synthesis

P1.

1,7,7-Trimethylbicyclo[2.2.1]hept-2-ol 2,5-dibromobenzoate (100 mg, 0.217 mmol), 1,3-Di(trimethylstannyl)isothianaphthene (90.4 mg, 0.217 mmol), $Pd(PPh_3)_4$ (25 mg, 0.0217 mmol), toluene (2 mL) were added under an argon stream. The mixture was heated to reflux with stirring for three days under an argon atmosphere. The reaction was cooled to room temperature and the reaction mixture was extracted with 150mL CH_2Cl_3. The organic layer was washed with water and dried with over anhydrous $MgSO_4$. After the evaporation of the solvents, diluted with 3mL of chloroform, and added dropwise to 100mL of methanol under stirring. The precipitate was allowed to stand overnight and centrifugal separation to 60 mg black solid. Yield (71%). ^{1}H NMR (400 MHz; $CDCl_3$; δ): 0.51-0.79 (m, 9H, CH_3), 0.91-1.76 (m, 5H, CCH_2, CH_2CH_2 and CH_2CH), 2.12 (m, 2H, $CHCH_2$), 4.75-4.87 (m, 1H, OC*H*), 7.72-7.04 (m, 4H, Ar*H*), 7.90-8.10 (m, 2H, Ar*H*),

8.30 (m, 1H, Ar*H*).

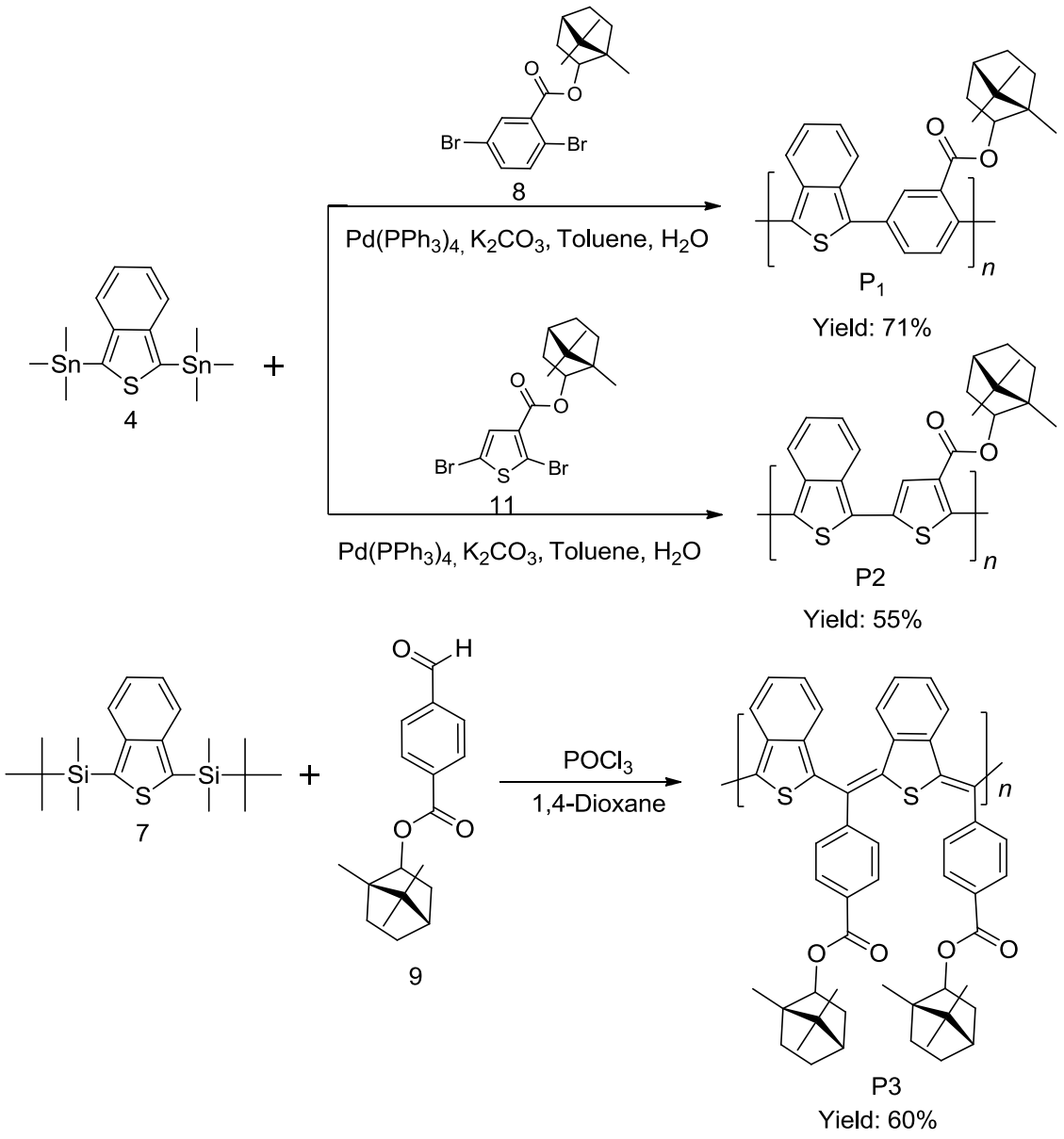

Scheme4. 2. Synthesis of polymers. PPh_3 = triphenylphosphine.

P2.

1,7,7-Trimethylbicyclo[2.2.1]hept-2-ol2,5-dibromo-3-thenoate (0.2 g, 0.474 mmol), $Pd(PPh_3)_4$ (0.011 g, 0.01 mmol), 1,3-Di(trimethylstannyl)isothianaphthene (0.218 g, 0.474 mmol), toluene (2mL) were added under an argon stream. The mixture was heated to reflux with stirring for about three days under an argon atmosphere. The reaction was cooled to room temperature and the reaction mixture was extracted with 150 mL CH_2Cl_3. The organic layer was washed with water and dried with over anhydrous $MgSO_4$. After the evaporation of the solvents, diluted with 3mL of chloroform, and added dropwise to 100 mL of methanol under

stirring. The precipitate was allowed to stand overnight and centrifugal separation to 103 mg black solid. Yield (55%). ^{1}H NMR (400 MHz; $CDCl_3$; δ): 0.60-0.76 (m, 9H, C*H*$_3$), 0.82-1.80 (m, 5H, CC*H*$_2$, CH_2C*H*$_2$ and CH_2C*H*), 2.21 (m, 2H, CHC*H*$_2$), 4.92 (m, 1H, OC*H*), 7.15-7.89 (m, 3H, Ar*H* and Th*H*), 7.92-8.01 (m, 2H, Ar*H*).

P3.

4-((1R,4R)-1,7,7-trimethylbicyclo[2.2.1]heptan-2-oxycarbonyl)benzaldehyde (0.286 g, 1.0 mmol), 1,3-bis(tert-butyldimet hylsily1)isothianaphthene (0.363 g, 1.0 mmol) and phosphoryl chloride (2 mL) were added into 1,4-dioxane (8 mL) and refluxed at 85 °C for overnight. The solution was cooled to room temperature and poured into 200 mL methanol and the precipitate was collected to obtain the crude product. Then the crude product was subsequently neutralized with an excess amount of triethylamine. The polymer was treated with excess amount of triethylamine for obtaining neutral state of the polymer followed by vacuum drying to remove residual triethylamine in the polymer and afford 0.12 g dark solid. Yield (60%). ^{1}H NMR (400 MHz; $CDCl_3$; δ): 0.87 (m, 9H, C*H*$_3$), 1.08-2.01 (m, 5H, CC*H*$_2$, CH_2C*H*$_2$ and CH_2C*H*), 2.45 (m, 2H, CHC*H*$_2$), 5.10 (m, 1H, OC*H*), 6.89-8.15 (m, 8H, Ar*H*).

4.3. Results and discussion

4.3.1. Synthesis of monomers

A series of monomers (4, 7, 8, 9 and 11) were designed and prepared and show in Scheme 4. 1. The monomers (8, 9 and 11) were obtained by esterifing with L-borneol in the presence of 4-(dimethylamino)-pyridine (DMAP) and 1,3-dicyclohexylcarbodiimine (DCC). On the other hand, the isothianaphthene monomers (4 and 7) were prepared via double-lithiation of corresponding thiophene derivatives at -78 °C followed by quenching with tert-butyldimethylsilyl chloride or trialkylstannyl chloride.

4.3.2. Synthesis of polymers

Table 4. 1. GPC results for P1, P2 and P3.

Polymer	M_n[a] [g/mol]	M_w[a] [g/mol]	M_w/M_n	DP[b]	Yield[c] [g/mol]
P1	1660	2340	1.4	5	71 %
P2	1730	1820	1.1	5	55 %
P3	1860	3140	1.7	5	62 %

[a]Estimated with GPC using THF as an eluent against polystyrene standard.

[b]Degree of polymerization (calculated by M_n/M, M: molecular weight of monomer repeat unit).

[c]Calculation by ($W_g/(W_m \times N_m)$).

W_g: Weight of the polymer sample (g).

W_m: Weight of monomer repeating units of the polymers (g mol^{-1}).

N_m: Amount of the used monomer (mol).

P1 and P2 were synthyesied with an equivalent amount of dibromo aromatic monomer and 1,3-Di(trimethylstannyl)isothianaphthene (monomer 4) by well-known catalyst of $Pd(PPh_3)_4$ for the Migita–Kosugi–Stille polycondensation reactions. P3 have been synthesized with monomer 7 and benzaldehyde in the presence of $POCl_3$ by a polycondensation reaction (Scheme 4. 2). The results of the molecular weights of polymers were determined by GPC in THF using polystyrene as a standard and show in Table 4. 1. The number-averaged molecular weight of polymers ranged from 1660 to 1860 and the molecular weight distribution were 1.1-1.6. The molecular weights seem to be somewhat low because the rigid shaped main chain reduced solubility result in low-molecular weight estimation. Because their film forming property and optical absorption at long wavelengths indicate molecular weights as polymers.

4.3.3. Structural characterization

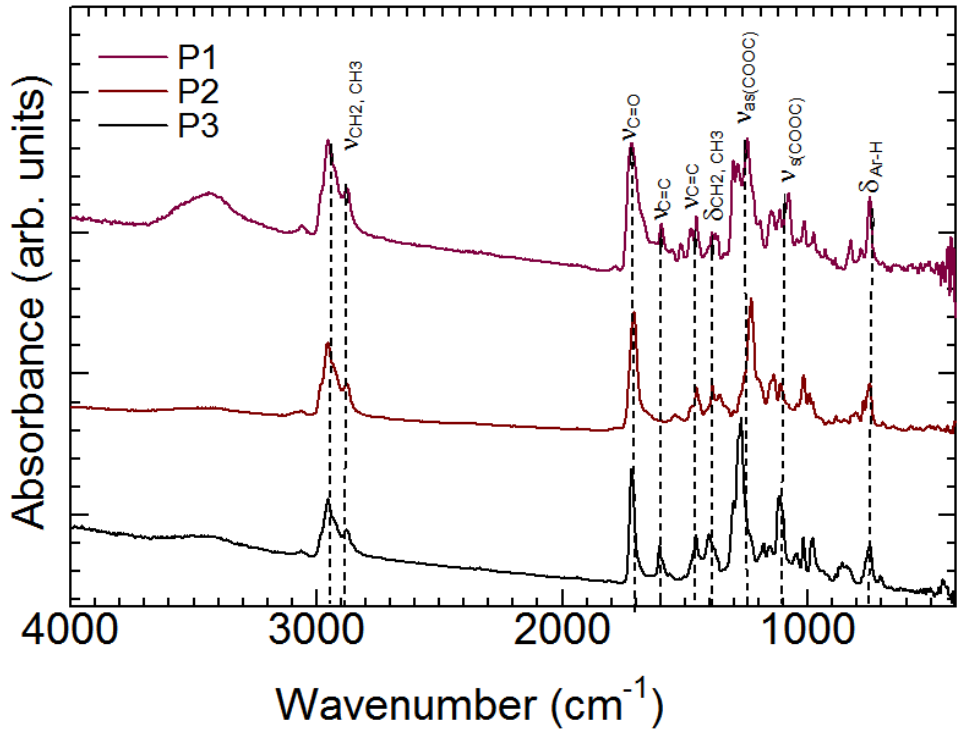

Figure 4. 1 Infrared absorption spectra of the polymers P1, P2 and P3.

Infrared (IR) absorption spectra of the polymers are shown in Figure 4. 1. The absorption bands at 750-770 cm^{-1} due to C-H bending vibration at β-positions of the aromatic units, which clearly shows the effect of aromatic rings corresponding to the shift of the C-H stretching mode to a lower frequency. [9, 10] The absorption peaks at 1600 cm^{-1} and 1468 cm^{-1} are due to C=C vibrations of quinonoid character, which results are in good agreement with previous reports on the C=C stretching vibration of quinonoid thiophene systems is found between 1665 cm^{-1} and 1645 cm^{-1} [11, 12]. The intense absorption peak at 1704 cm^{-1} due to C=O stretching band of ester groups of side chain. The polymers also show an absorption band at 1242 cm^{-1}. The

band is due to CO-O-C (ester) antisymmetric vibrations in the side chain units. On the other hand, the symmetric vibrations of CO-O-C (ester) groups shown at 1103 cm^{-1}. The polymers show absorption bands at 2950-2880 cm^{-1} attributable to ν_{CH2} and ν_{CH3} stretching band of a chiral bornyl chain and the weak absorption peaks shown at 1396 cm^{-1} due to C-H bending vibration of a chiral bornyl chain.

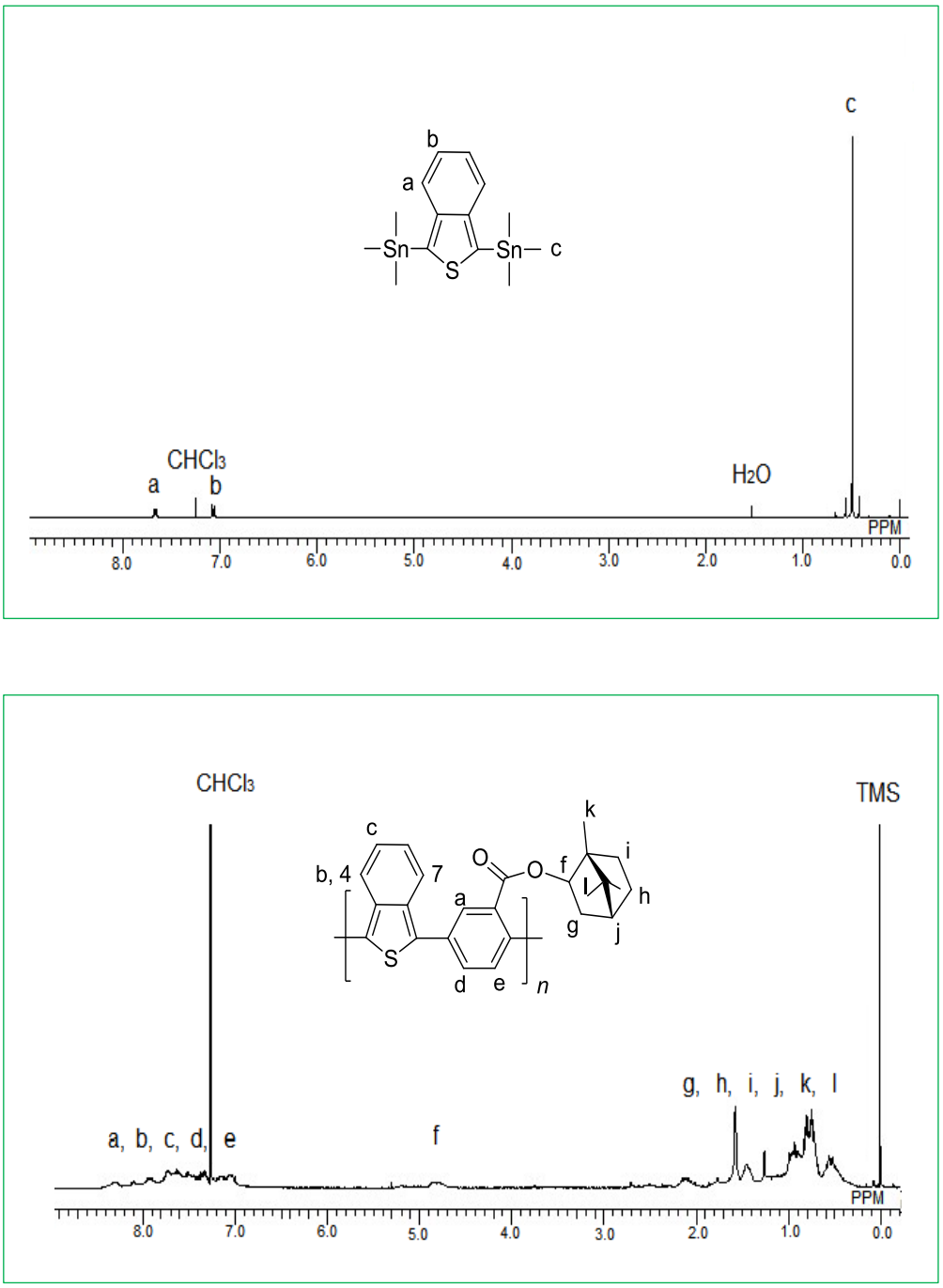

Figure 4. 2. ^{1}H NMR spectra of monomer 1,3-Di(trimethylstannyl)isothianaphthene and P1. TMS = tetramethylsilane.

The synthsitic products were characterized by ^{1}H NMR analyses indicate clearly that well-defined these lower

bandgap polymers have been indeed obtained and all the polymers gave satisfactory data corresponding to their expected molecular structures. As an example and because of its simple repeating unit, we show here the ^{1}H NMR spectra of 1,3-di(trimethylstannyl)isothianaphthene [13] and P1 are given in Figure 4. 2. The spectrum recorded for P1 shows no signal in the 0.488 ppm region. The result indicates the successful polymerization of chiral bornyl derivative and 1,3-di(trimethylstannyl)isothianaphthene. The chemical shifts at around 0.51-2.12 ppm are attributed to the protons of bornyl groups. The chemical shifts at 4.75-4.87 ppm are also clearly observed and ascribed to the protons of bornyl group (O-C*H*). The chemical shifts of the protons at around 8.3 are attributable to the aromatic protons of chiral bornyl derivative unit. It is noteworthy that the ITN protons 4 and 7 (b of P1 in Figure 4. 2.) in monomer give one signal at 7.6 ppm and the protons of monomer shift to lower magnetic field after the polymerization, which indicating the effect to the protons adjacent to the bornyl groups and the protons away from the bornyl groups [13].

4.3.4. Optical properties

The ORD, CD, UV-vis absorption spectra of the polymers in THF solution and film form are shown in the Figure 4. 3. and Figure 4. 4. The P1 in solution state demonstrated negative CD signal at 399 nm and UV-vis absorption at around 403 nm. The CD spectra of P2 in THF show a clear couplet with a negative cotton effect at 395 nm and a positive one at 461 nm. These results are indicating that the copolymer backbones of P1 and P2 forming helical conformations of predominantly one-handed screw sense. In addition, P3 has no signal of CD in the visible region, which indicating that the polymer backbone therefore seems not to form specific helical configurations [14]. In the film state, the P1, P2 and P3 show no CD signals. The reault is indicating that polymers have large steric hindrance from the bornyl group that prevents intermolecular π-π interaction of the polymers [15].

Optical rotations at visible range were observed in the ORD spectra of the polymers. In the solution state, P1, P2 and P3 gave the negative signal at around 432 nm, 436 nm and 601 nm. In the film state, P1 and P3 showed positive signal at around 470 nm and 479 nm, P2 showed a negative signal at 571 nm. These results indicate that the optical rotations of the polymers are derived from the chiral side chains, suggesting that the sign of optical rotation of the polymers depends on chirality of the side chains [16].

The emission from P1, P2 and P3 are observed at around 527 nm, 580 nm, 598 nm, 456 nm, and 478 nm in the solution state (Figure 4. 5.). However, in the film state, P1 nad P2 show some weak peaks around at 611 nm and 582 nm, P3 showed no signal of emission. The strong photoluminescence quenching in the film form was observed for polymers, which was mainly due to the enhanced quinoid character formed by introducing the isothianaphthene unit. Interchain interaction of π-conjugated main chain often results in decrease of quantum yield in the PL [17]. On the other hand, the absorption (P1, P2 and P3) and emission (P1) maximum values were significantly red-shifted compared with the film state compareing with theirs solution state. The shift toward long wavelengths in the film state indicates development of intermolecular π-stacking between main chains, leading to good main chain coplanarity.

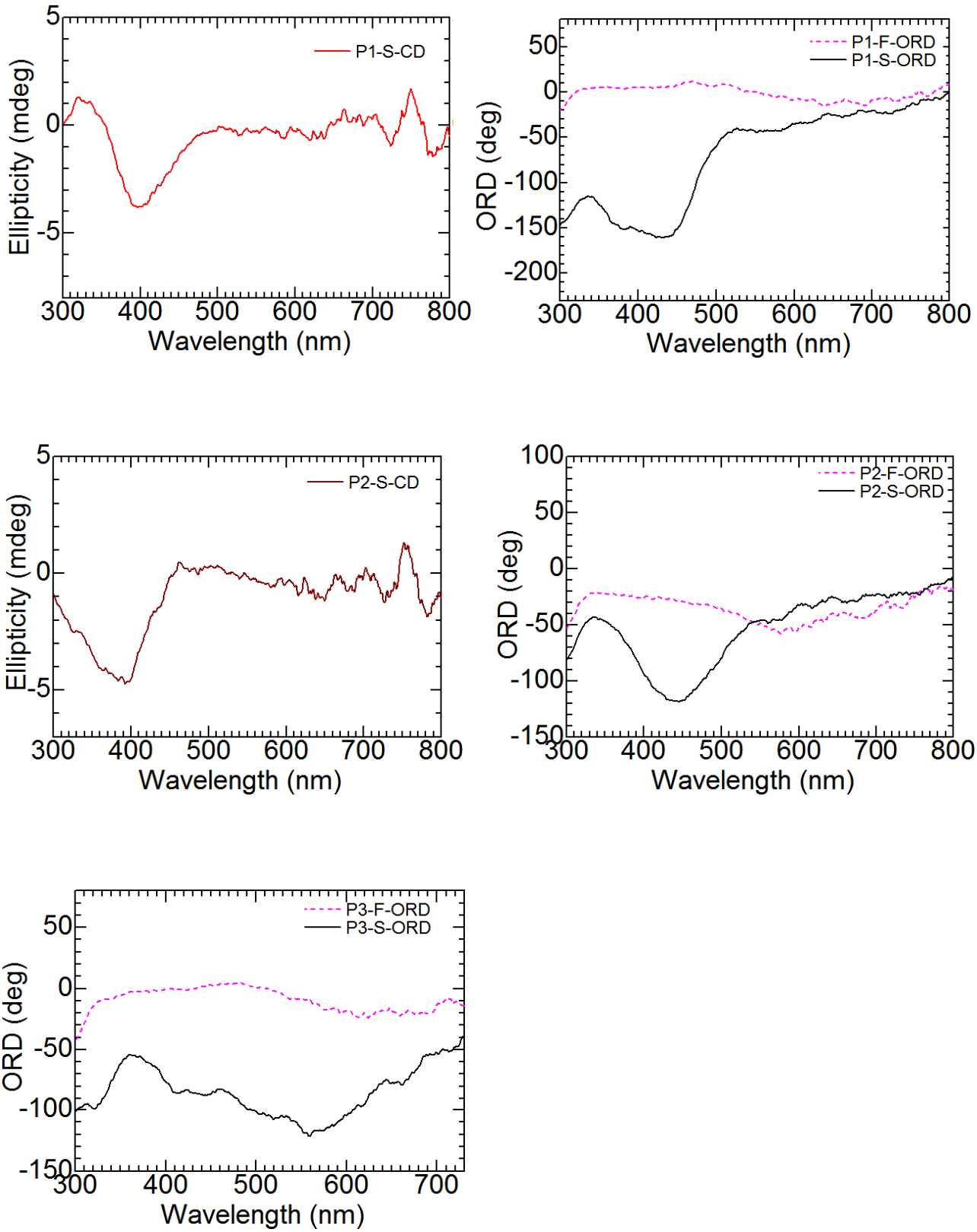

Figure 4. 3. Optical rotatory dispersion (ORD) and circular dichroism (CD) absorption of P1, P2 and P3 in THF (solid line) and thin films state (dashed lines). S: solution state, F: film state.

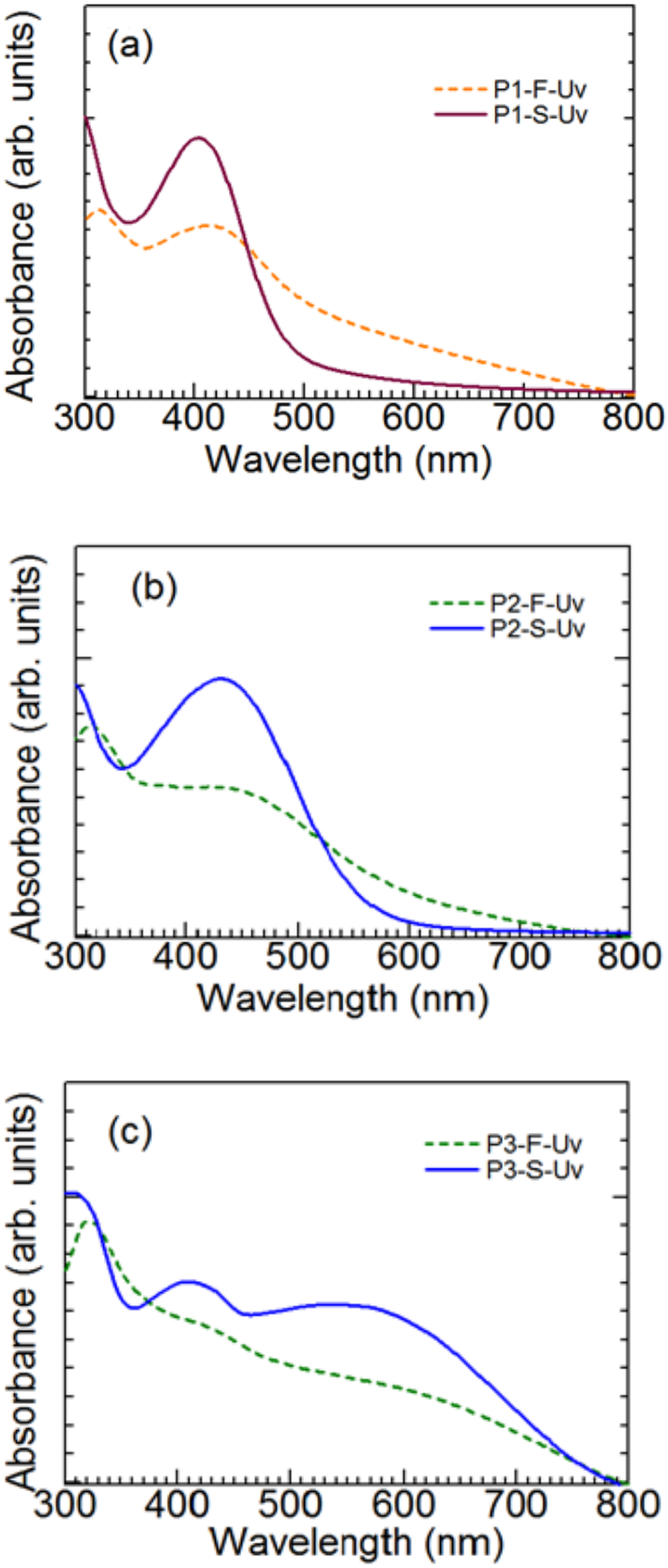

Figure 4. 4. UV-vis absorption of P1, P2 and P3 in THF (solid line) and thin films state (dashed lines). S: solution state, F: film state.

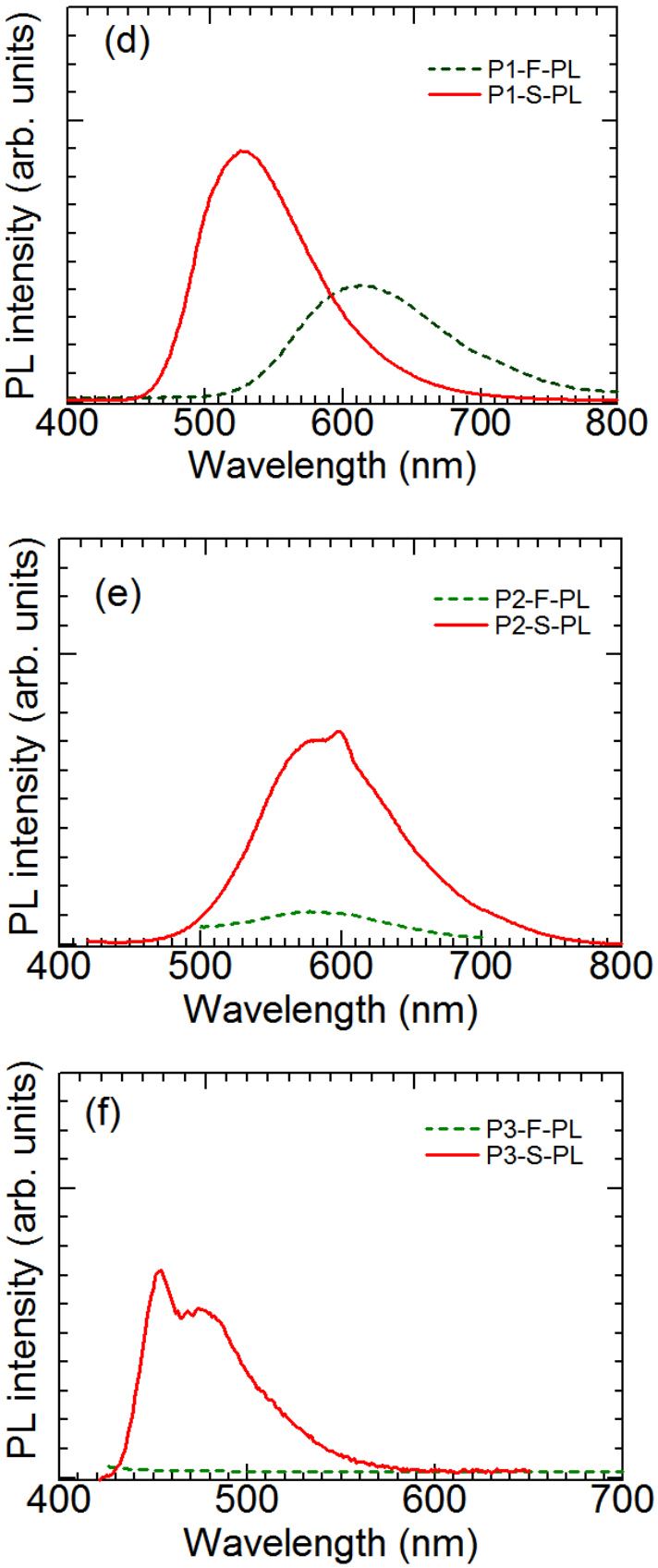

Figure 4. 5. Photoluminescence spectra (PL) of P1, P2 and P3 in THF (solid line, S: solution state), as thin films from THF solution (ca. 2mg/mL) onto glass substrates and dried in air at room temperature. (dashed lines, F: film state)

4.3.5. Electrochemical Properties

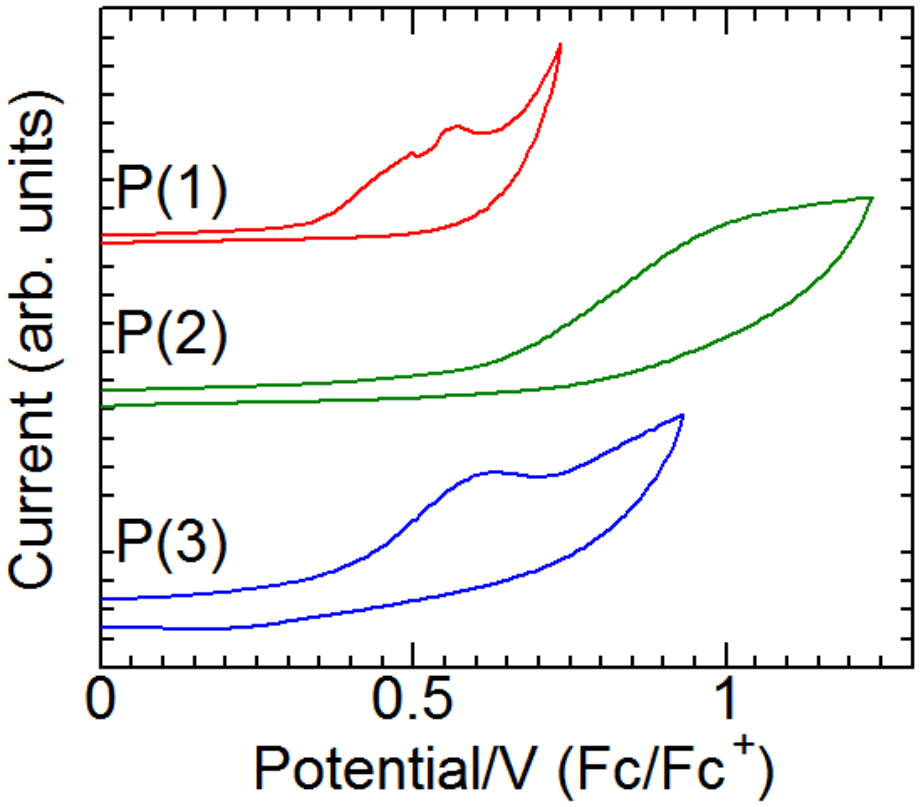

Figure 4. 6. Cyclic voltammograms of the polymers cast on platinum disc electrode (0.1 M TBAP in acetonitrile solution with a scan rate of 100 mVs^{-1}.

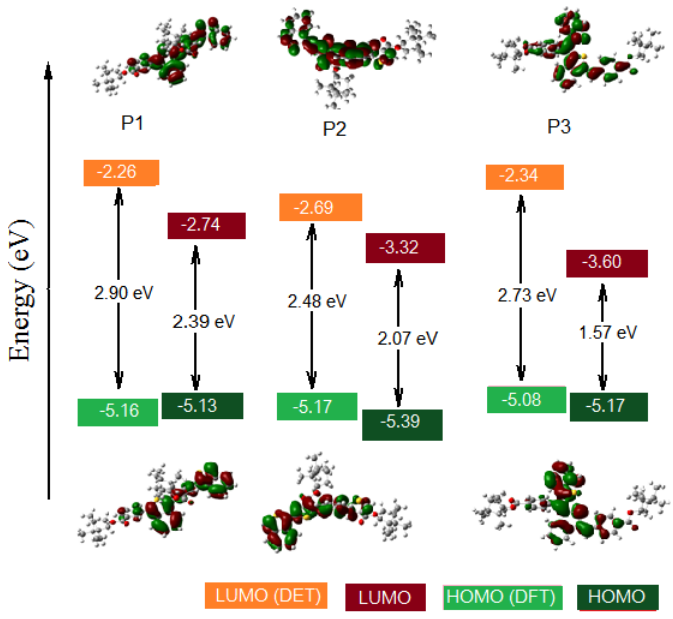

Figure 4. 7. Highest occupied molecular orbital and lowest unoccupied molecular orbital and their energy levels of model compounds calculated by the DFT (density functional theory) method and P1, P2 and P3 state estimated from observed oxidation potentials and optical band gaps in the film.

Table 4. 2. UV-vis absorption and cyclic voltammetry measurements results of polymers

Polymers	λ_{edge} [a] (nm)	E_{opt} [b] (eV)	$E_{onset,ox}$ [c] (V)	E_{LUMO} [d] (eV)	E_{HOMO} [e] (eV)
P1	519	2.39	0.33	-2.74	-5.13
P2	589	2.07	0.59	-3.32	-5.39
P3	787	1.57	0.37	-3.60	-5.17

a: Onset absorption wavelength

b: Calculated from the onset wavelength of optical absorption of the polymers.

c: Onset oxidation potentials of the polymers calibrated with ferrocene.

d: Calculated from optical bandgap energy and onset oxidation potential of the polymers.

e: Calculated from the oxidation potentials.

As shown in Figure 4. 6., electrochemical cycling of polymers in the film state by using an Ag/Ag+ reference electrode in 0.1 M tetrabutylammonium perchlorate (TBAP) acetonitrile solution. The energy levels of the these polymers were determined by cyclic voltammetry (CV) using ferrocene as the standard that has a HOMO level of -4.8 eV [18]. P1 two consecutive one-electron oxidations occur at half-wave potentials of +0.59 V and +0.67 V. P2 and P3 exhibit one one-electron redox patterns with $E_{1/2}$ = -0.59 and -0.37 V. In contrast, P1 is likely easier to lose electrrons because of the lowest oxidation potential. A pseudoreversible redox cycle with oxidation peaks were observed for polymers. The bandgap is estimated using optical energy gaps (E_{opt}) of the polymers. According to the empirical correlations suggested that the HOMO/LUMO levels of polymers were calculated by using the following equation: E_{HOMO} = (Eonset,ox + 4.8) eV and $E_{LUMO} = E_{HOMO} + E_{opt}$. [19, 20] The experimental E_{HOMO} and the E_{LUMO} energy level obtained by employing optical band gaps (E_{opt}) in the UV spectra are summarized in the Table 4. 2..

Comparison between the experimental results and energy diagram by DFT calculations is summarized in Figure 4. 7.. The effect of different main chain about these polymers was evaluated by comparing the energy levels of P1, P2 and P3. The E_{HOMO} value of P1 was observed at the lower oxidation potential compare with P2 and consistent with the results of the DFT calculation (E_{HOMO}(P1) = -5.13 eV and E_{HOMO}(P2) = -5.39 eV). The E_{HOMO} value of P3 was comparable to that of P1 contrary to the theoretical prediction (E_{HOMO}(P3) = -5.17 eV). This is probably because the structure of isothianaphthene methine as main chain induces increasing quinonoid character of P3. There compared the energy levels from experimental data and DFT calculation results of model compounds. The experimentally estimated HOMO values show good agreement with those of DFT calculation results. The experimental HOMO, LUMO and associated gap trends are all well represented at the energy level of DFT calculation. It was clearly shown that all HOMOs delocalized through the molecules involving the repeat units.

4.3.6. ESR Spectroscopy

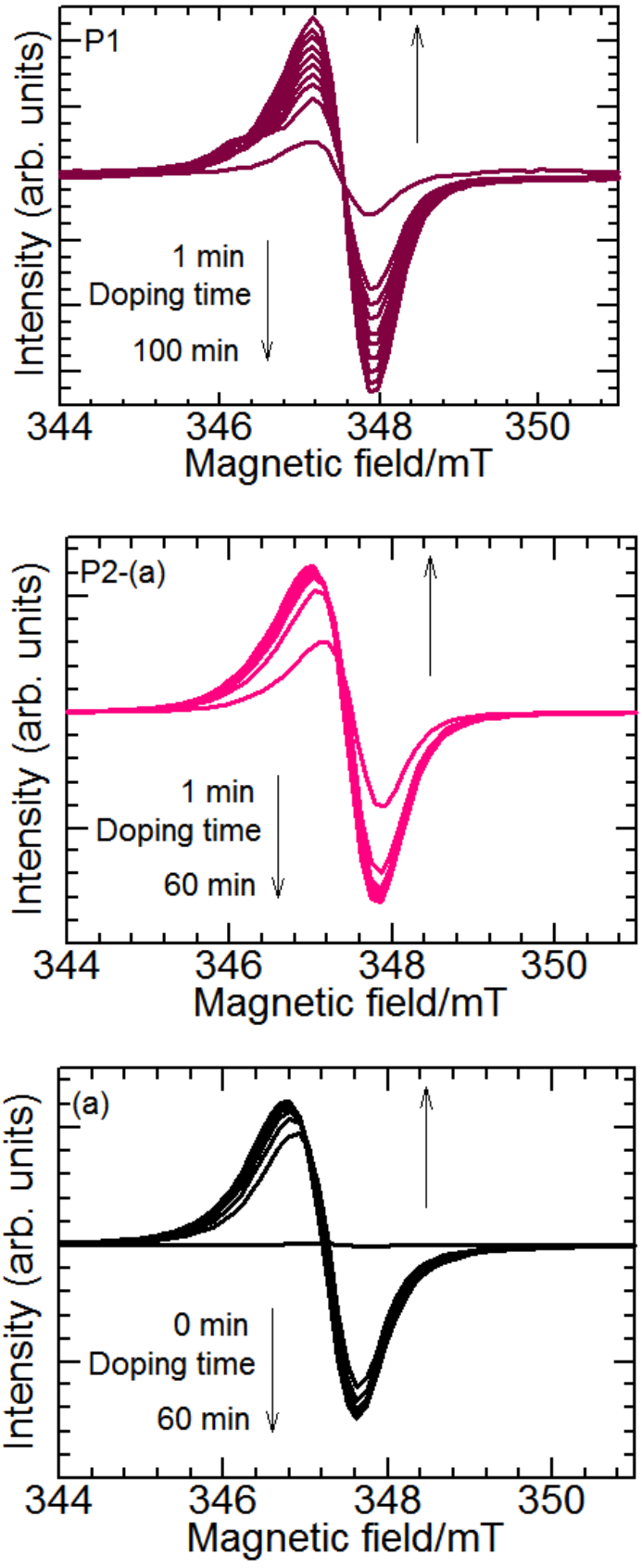

Figure 4. 8. Electron spin resonance (ESR) spectra of P1, P2 and P3 during vapor-phase doping of iodine.

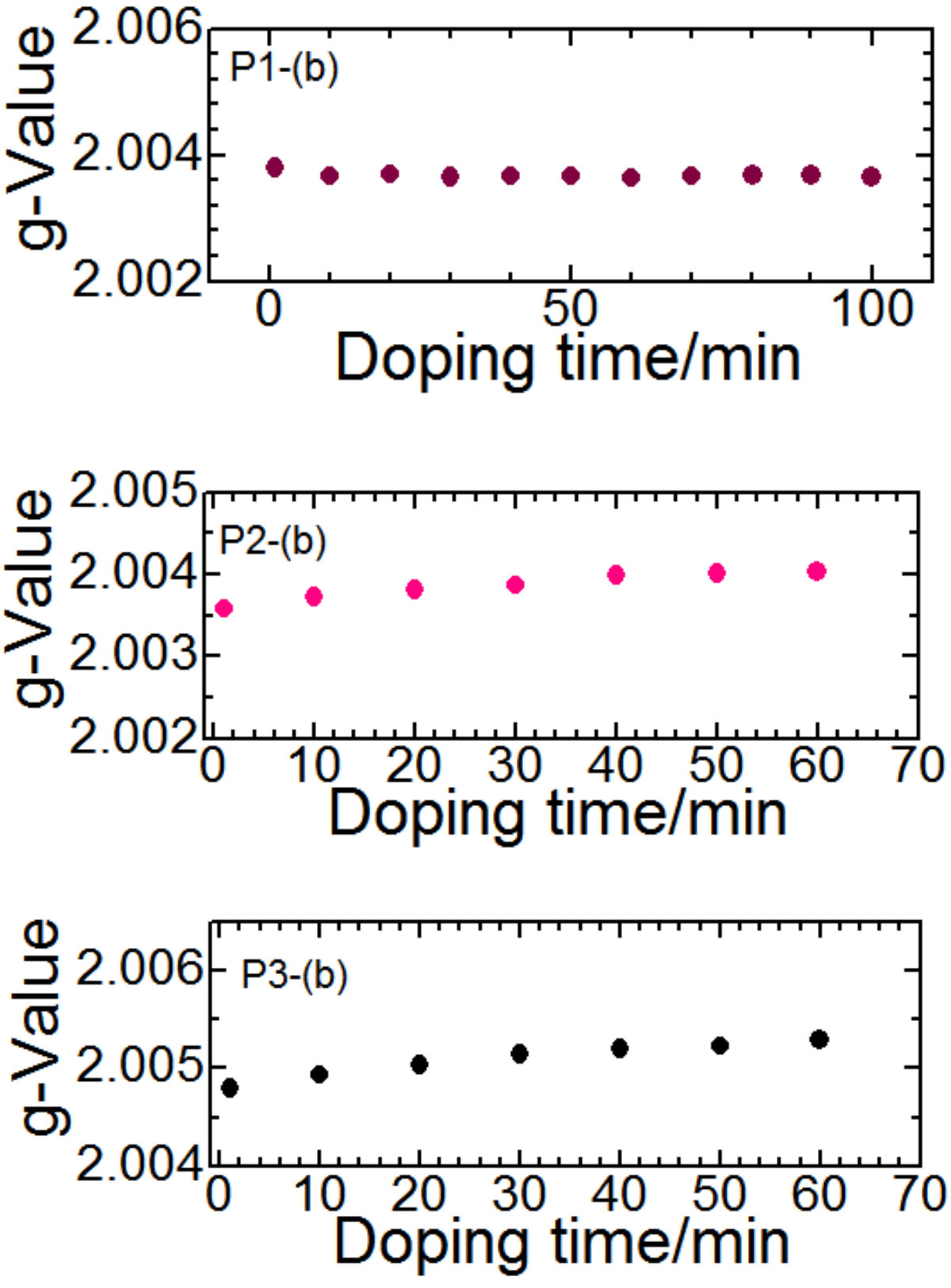

Figure 4. 9. *g*-value of P1, P2 and P3 during vapor-phase doping of iodine.

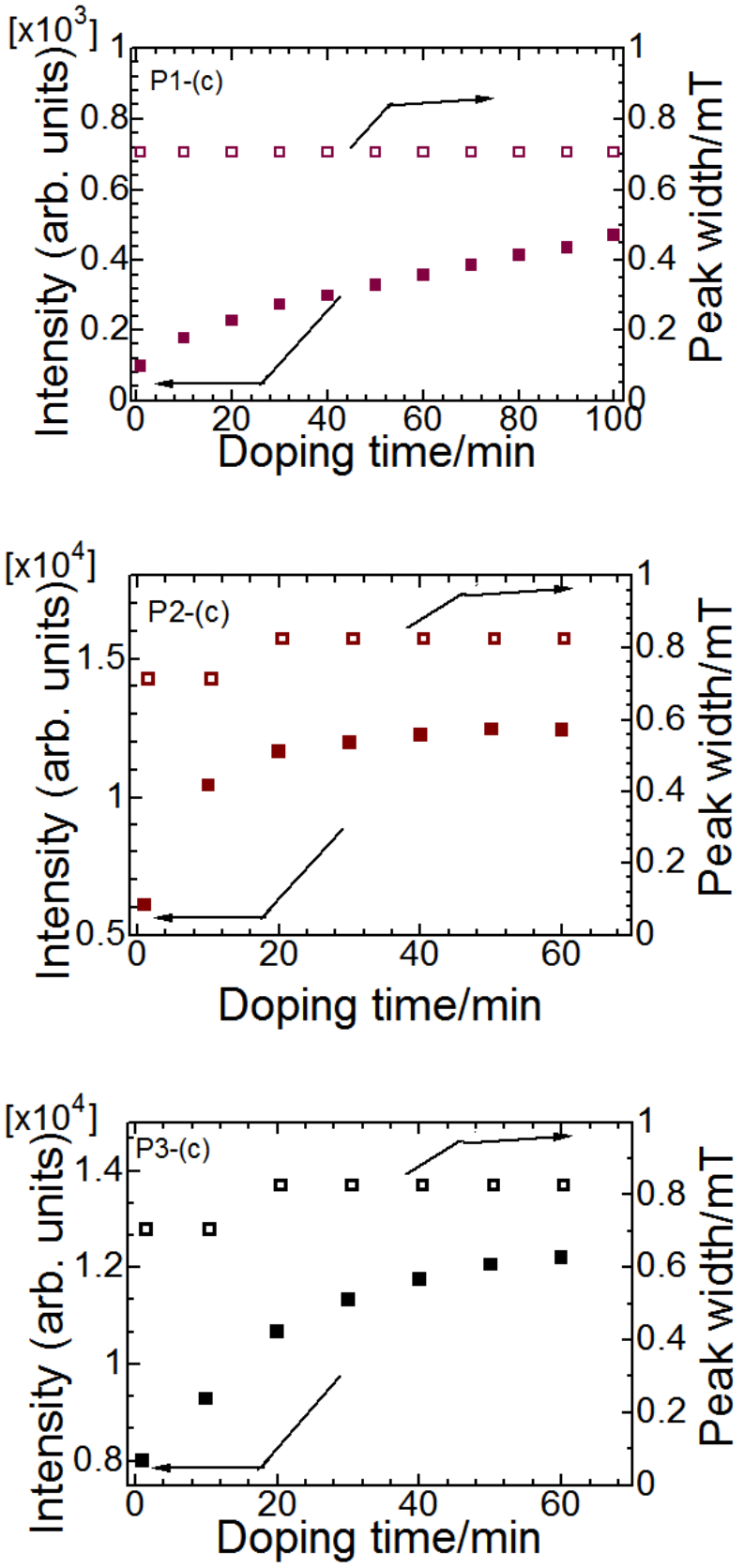

Figure 4. 10. Electron spin resonance (ESR) intensity and peak-width plots of P1, P2 and P3 during vapor-phase doping of iodine.

Table 4. 3 The maximum spin number of the polymers and monomer units after doping

Polymers	Spin concentration	
	[Spins/g][a]	[Spins/mru][b]
P1	1.574×10^{18}	8.337×10^{-4}
P2	1.107×10^{19}	6.279×10^{-3}
P3	1.155×10^{19}	7.374×10^{-3}

[a] spin concentration were evaluated from ESR measurements.

[b] The number of the spin concentration is estimated as per monomer units.

The ESR measurements were carried out on a bulk polymer sample with vapor phase iodine doping at room temperature detecting unpaired electrons and ESR spectra of the polymers are shown in Figure 4. 8. All the spectra show an asymmetric single line with no hyperfine splittings. ESR experiments in the power of the polymers and generated the polarons (radical cations) by doping iodine, which resut in signal intensity gradually increased with the doping time. The result indicates that iodine doping leads to increase of spin concentration with doping time. The *g*-value, peak width (ΔH_{pp}) and ESR intensity of polymers with doping time were shown in Figure 4. 9. and Figure 4. 10. The *g*-value and the linewidth of P1 (Figure P1-b and P1-c) are almost constant. These results indicate that the charge species did not change during the doping time. However, the *g*-value and the linewidth of P2 and P3 (Figure P2-b, c and P3-b, c) have increased with doping time. These results could be interpreted by rather short π-conjugation [21] and the localization of radical spins in the present samples. This is in good accordance with the results obtained from the IR spectra. [22, 23] The increase of the peak-to-peak linewidth in the ESR measurements indicates that charge carriers of polarons and bipolarons generated by the iodine doping may be localized. [16] The maximum spin number of the polymers after doping was summerized in the Table4. 3.. P3 has greater spin-number comare with P2 and P1, which indicates that one spin exist in 140 mru of P3 after the doping.

4.4. Conclusion

Two series of new ITN-based different π-conjugated main chain copolymers with quinoidal character and chiral bornyl substituents that function as induce main chain chirality were synthesized. The introduction of the ITN unit in the backbone lowered the bandgapowing to the stabilized quinoid resonance structure. Bandgap of the polymers is estimated to be evaluated at 1.57 eV-2.39 eV from optical absorption spectroscopy. These indicate high efficiency of π-electron delocalization in the isothianaphthenes along the conjugated backbone. The optical properties of P1 and P2 form the main chain chirality in the solution sate also are showed. P1, P2 and P3 showed signal optical rotation from 439 nm-606 nm in the solution sate and film state, suggesting that the sign of optical rotation of the polymers depends on chirality of the side chains. P1, P2 and P3 show very low PL intensities in the film state. This result was mainly due to the enhanced quinoid character lead to photoluminescence quenching. In addition, ESR study indicated that extension of effective different conjugation main chain creates a different susceptibility to the dopants.

4.5. Acknowledgements

We would like to thank Glass Work Shop of University of the Division of Materials Science (University of Tsukuba) and Technology of University of Tsukuba for providing NMR, IR, ESR, PL measurements and Chemical Analysis Division Research Facility Center for Science.

4.6. References

[1] Grimsdale AC, Chan KL, Martin RE, Jokisz PG, Holmes AB (2009) Synthesis of light-Emitting conjugated polymers for applications in electroluminescent devices. Chem. Rev 109:897-1091.

[2] Roncali J (1992) Conjugated poly(thiophenes): synthesis, functionalization, and applications. Chem. Rev 92:711-738.

[3] Wang CL, Dong HL, Hu WP, Liu YQ, Zhu DB (2012) Semiconducting π-conjugated systems in field-effect transistors: amaterial odyssey of organic electronics. Chem. Rev 112:2208-2267.

[4] Gunes S, Neugebauer H, Sariciftci NS. (2007) Conjugated polymer-based organic solar cells. Chem. Rev 107:1324-1338.

[5] Thompson BC, Frechet JMJ (2008) Polymer-fullerene composite solar cells. Angew. Chem., Int. Ed 47:58-77.

[6] Gunes S, Neugebauer H, Sariciftci NS (2007) Conjugated polymer-based organic solar cells. Chem. Rev 107:1324-1338.

[7] Jung YK, KIM H, Park JH, Lee J, Lee SK, Lee YS, Shim HK (2008) Alternating fluorene copolymers containing isothianaphthene derivatives: a Study of their aggregation properties and small band gap. J Polym Sci Pol Chem 46:3573-3590.

[8] Roncali J (1997) Synthetic principles for bandgap control in linear π-conjugated systems. Chem. Rev 97:173-206.

[9] Casado J, Hotta S, Hern V, Navarrete JTL (1999) Vibrational Spectroscopic Study of a Series of α, α'-Diethyl End-Capped Oligothiophenes with Different Chain Lengths in the Neutral State. J. Phys. Chem. A 103:816-822.

[10] Casado J, Katz HE, Hern V, Navarrete JTL (2002) Infrared spectra of two sexithiophenes in neutral and doped states: a theoretical and spectroscopic study. Vib. Spectrosc 30:175-189.

[11] Chen WC, Jenekhe SA (1995) Small-bandgap conducting polymers based on conjugated poly (heteroarylene methines). 1. Precursor poly (heteroarylene methylenes). Macromolecules 28:454-464.

[12] Chen WC, Jenekhe SA (1995) Small-bandgap conducting polymers based on conjugated poly (heteroarylene methines). 2. Synthesis, structure, and properties. Macromolecules 28:465-480.

[13] Qin Y, Kim JY, Frisbie CD, Hillmyer MA (2008) Distannylated isothianaphthene: A versatile building block for low bandgap conjugated polymers. Macromolecules 41:5563-5570.

[14] Kiebooms RHL, Goto H, Akagi K (2001) Synthesis of a new class of low-band-gap polymers with liquid crystalline substituents. Macromolecules 34:7989-7998.

[15] Langeveld-Voss BMW, Janssen RAJ, Meijer EWJ (2000) On the origin of optical activity in polythiophenes. Mol. Struct 521:285-301.

[16] Innami Y, Kawashima H, Kiebooms RHL, Aizawa H, Matsuishi K, Goto H (2012) Synthesis and

Properties of Poly(Isothianaphthene Methine)s with Chiral Alkyl Chain. Materials 5:317-326.
[17] Goto H, Wang AH, Kawabata K, Yang F (2013) Synthesis and properties of a low-bandgap liquid crystalline π-conjugated polymer. J Mater Sci 48:7523-7532.
[18] Andrade BWD, Datta S, Forrest SR, Djurovich P, Polikarpov E, Thompson ME (2005) Relationship between the ionization and oxidation potentials of molecular organic semiconductors. Org. Electron 6:11-20.
[19] Brédas JL, Silbey R, Boudreaux DS, Chance RR (1983) Chain-length dependence of electronic and electrochemical properties of conjugated systems: polyacetylene, polyphenylene, polythiophene, and polypyrrole. J. Am. Chem. Soc 105: 6555-6559.
[20] Agrawal AK, Jenekhe SA (1996) Electrochemical properties and electronic structures of conjugated polyquinolines and polyanthrazolines. Chem. Mater 8:579-589.
[21] Ohnishi S, Ikeda Y, Sugimoto S, Nitta I (1960) On the ESR singlet spectra frequently observed in irradiated polymers at a large dose. J. Polym. Sci. Pol. Chem 47, 503-507.
[22] Neugebauer H, Kvarnström C, Brabec C, Sariciftci NS, Kiebooms R, Wudl F, Luzzati S (1999) Infrared spectroelectrochemical investigations on the doping of soluble poly(isothianaphthene methine) (PIM). J. Chem. Phys 110:12108-12115.
[23] Moraes F, Davidov D, Kobayashi M, Chung TC, Chen J, Heeger AJ, Wudl F (1985) Doped poly (thiophene): electron spin resonance determination of the magnetic susceptibility. Synthetic Metals 10:169-179.

4.7. Supporting Information

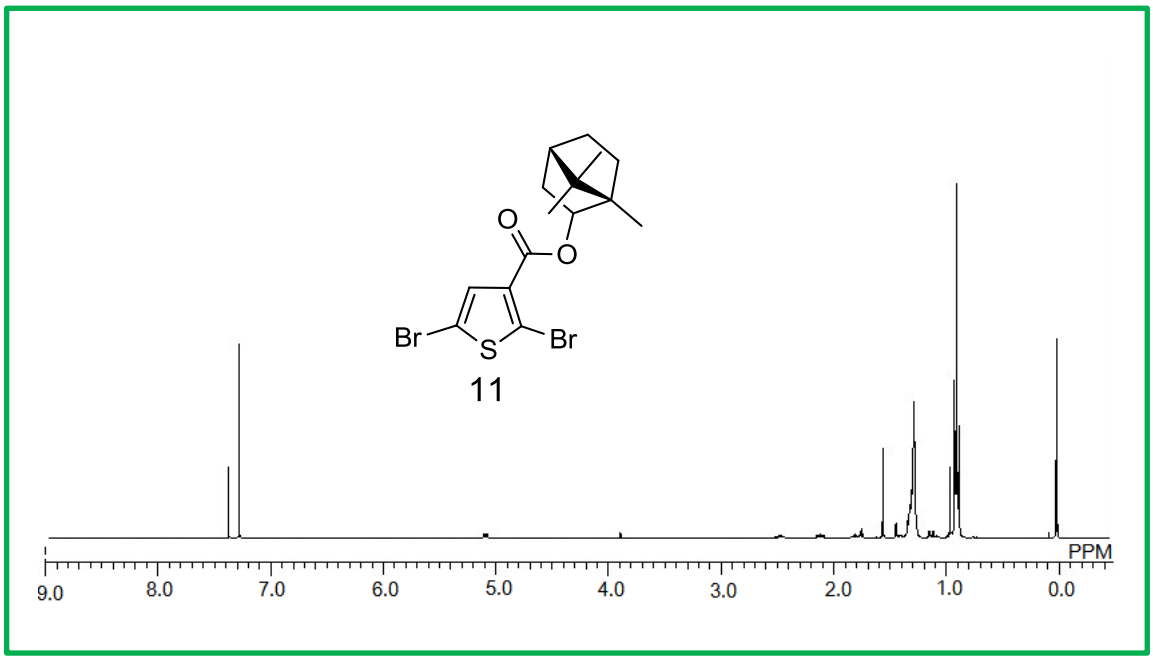

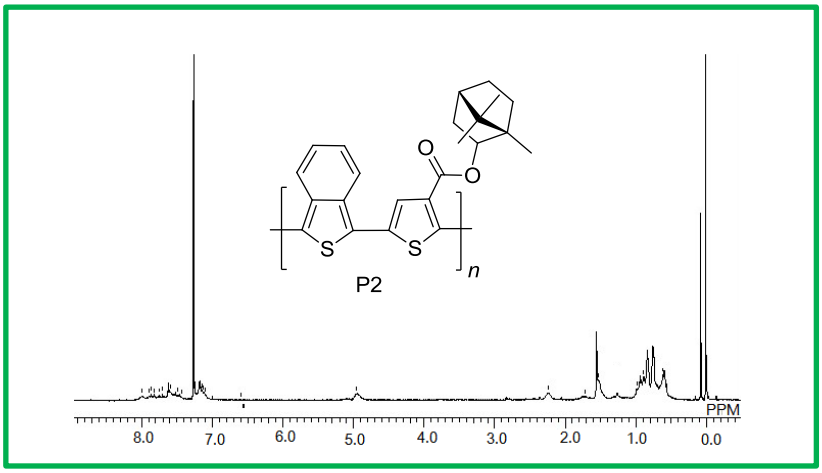
O
O
S
S
n
P2
PPM
8.0
7.0
6.0
5.0
4.0
3.0
2.0
1.0
0.0

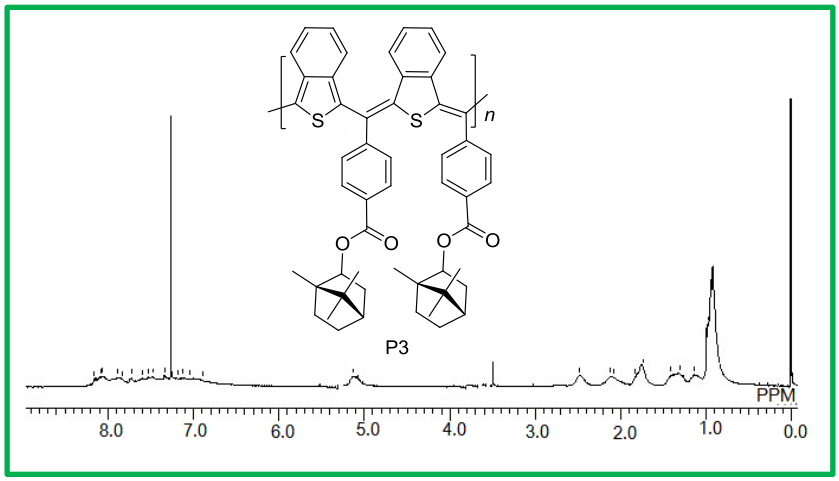
S
S
n
O
O
O
O
P3
PPM
8.0
7.0
6.0
5.0
4.0
3.0
2.0
1.0
0.0

Chapter 5

Synthesis of three-ring chiral inducers and electrochemical polymerization of carbazole in a cholesteric electrolyte solution

5.1. Introduction.

Optically active π-conjugated polymers have seen much attention due to their properties for applications, such as organic electronic devices, [1-3] organic field-effect transistors [4-6] and optoelectronic devices [7]. These applications require proper synthesis methods to prepare polymers with specific properties. Asymmetric selective polymerization, [8, 9] optically active monomers polymerization, [10, 11] and introduction of a chiral group into polymer [12] are known as useful synthesis ways of high quality conjugated polymers. Particularly, asymmetric selective polymerization of monomers in cholesteric liquid crystal by inducing that is effective method for ordered conjugated polymers [13-15].

In this study, three new chiral inducers were designed based on core of [1,1'-biphenyl]-4-yl benzoate for application in electrochemical polymerization. The liquid crystal (LC) electrolyte solution was prepared by adding the chiral inducer to LC of 4-Cyano-4'-hexylbiphenyl (6CB). Liquid crystal molecules form one-handed helical structure and induce one-handed helical aggregation of polymer backbone during the polymerization process in the LC. Therefore, a series of optically active polymer films were prepared by asymmetric electrochemical polymerization in CLC electrolyte solution with these chiral inducers and obtained forms an intermolecular twisted structure, which the orientation is transcript of the electrolyte solution texture. [16]

5.2. Experimental section

5.2.1. Materials

Commercially available reagents were received from Nacalai Tesque (Japan), Sigma-Aldrich (Japan), Kanto Chemical (Japan) and Tokyo Chemical Industry (Japan) unless otherwise noted and used without further purification. Common organic solvents such as dichloromethane and tetrahydrofuran (THF) were distilled and handled in a moisture-free atmosphere. The purification of the newly synthesized compounds was performed by column chromatography on silica gel (Silica gel 60 N). The monomer was prepared by previously reported method.[17]

5.2.2. General methods

Chemical shifts were given in parts permillion and coupling constant (*J*) in Hz. FTIR absorption spectra were obtained with an FT/IR-300 spectrometer (Jasco) using a KBr method. ^{1}H NMR spectra of the compounds were recorded using JNM ECS 400 spectrometer (JEOL, Japan) with $CDCl_3$ as the deuterated solvent and tetramethylsilane (TMS) as the internal standard. Circular dichroism (CD) spectra were measured with a J-720 (JASCO, Tokyo, Japan). UV-vis absorption spectra were recorded on a JASCO V-630 UV-vis optical absorption spectrometer. Cyclic voltammetry (CV) measurements were carried out with a μAUTOLAB TYPE III (ECO Chemie). Electrolyte solutions contained 0.1 M of TBAP in acetonitrile.

5.2.3. Synthsis of chiral inducers.

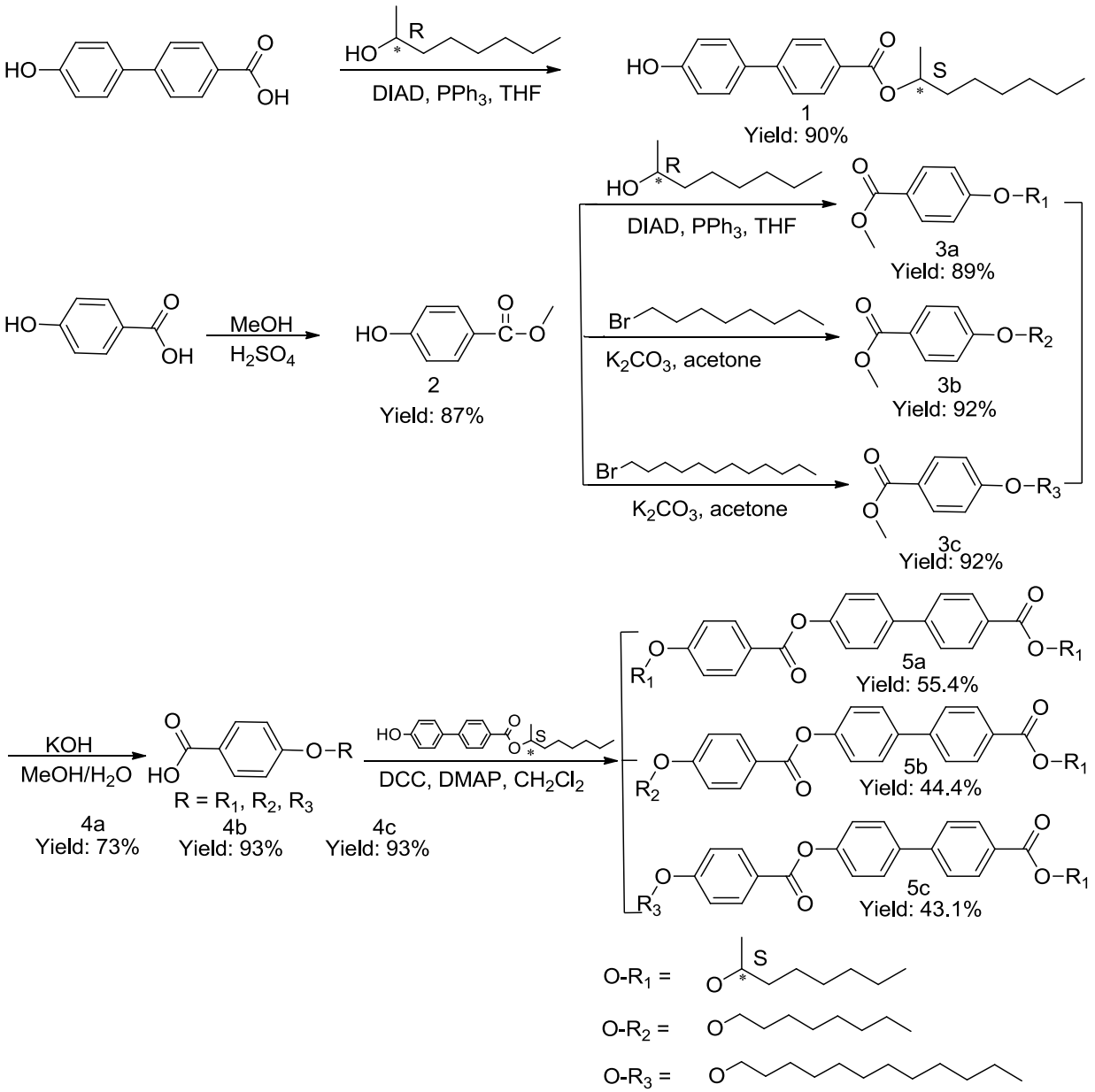

Scheme5. 1. Synthetic routes to three-ring chiral inducers. DIAD: diisopropylazodicarboxylate, PPh_3: triphenylphosphine, DCC: dicyclohexylcarbodiimid, DMAP: 4-dimethylaminopyridine.

(S)-1-methylheptyl 4'-biphenyl-4-carboxylate (1).

Triphenylphosphine (2.45 g, 9.35 mmol), 4'-hydroxybiphenyl-4-carboxylic acid (2.0 g, 9.35 mmol), (*R*)-octan-2-ol (1.20 g; 9.35 mmol) and diisopropylazodicarboxylate (DIAD) (1.89 g, 9.35 mmol) were dissolved in THF (60 mL) and added into a flask. The solution was stirred at room temperature until completion. The solvent was removed in vacuum and the crude product was purified by column chromatography over silica (ethyl acetate: haxene = 1:10). A white powder. Yield 3.70 g (90%). ^{1}H NMR (400 MHz; $CDCl_3$; δ): 0.871-0.905 (t, 3H, CH_3), 1.25-1.39 (m, 11H, CH_2 and CH_3), 1.60-1.66 (m, 1H, CH_2), 1.56- 1.69 (m, 1H, CH_2), 4.99 (s, 1H,

O*H*), 5.16-5.20 (sext, 1H, C*H*CH_2CH_3), 6.93-6.96 (d, 2H, *J* = 8.8 Hz, Ar*H*), 7.49-7.54 (d, 2H, *J* =18.8 Hz, Ar*H*), 7.58-7.61 (d, 2H, *J* = 8.4 Hz, Ar*H*), 8.05-8.09 (d, 2H, *J* = 14.8 Hz, Ar*H*).

Methyl 4-hydroxybenzoate (2).

Concentrated sulfuric acid (6 mL) was carefully added to a suspension of 4-hydroxy benzoic acid (6 g, 43.5 mmol) in methanol (40 mL) and the solution refluxed for 6 h. After cooling to room temperature, NaOH was added to neutralise the solution. The resulting mixture was allowed to stand for 30 min, before being poured into a cool beaker, and made up to 200 mL with water. The white precipitate was filtered, and dried in vacuum to afford (5.8 g) white solid (87%). ^{1}H NMR (400 MHz; $CDCl_3$; *δ*): 3.90 (s, 3H, C*H*$_3$), 5.64 (s, 1H, O*H*), 6.87-6.88 (d, 2H, *J* = 5.6 Hz, Ar*H*), 7.94-7.97 (d, 2H, *J* = 11.6 Hz, Ar*H*).

(S)-methyl 4-(octan-2-yloxy)benzoate (3a).

Into a 100 ml round double-neck flask, Methyl 4-hydroxybenzoate (5.80 g, 38.0 mmol), (*R*)-2-octanol (4.90 g, 38.0 mmol) and triphenylphosphine (PPh_3) (15.0g, 57.2 mmol) were mixed at nitrogen condition and added with anhydrous THF (200 mL). Compound of diisopropylazodicarboxylate (DIAD) (11.6 g, 57.2 mmol) was injected into the flask at ice bath condition and stirred overnight. Thin layer chromatography (TLC) plates were used to determine the reaction was complete. After removal of the solvent by evaporation under reduced pressure, the residue was extracted with water and ethyl acetate. Then, the organic layer was dried over anhydrous $MgSO_4$, the residue was purified by silica gel column chromatography (ethyl ether: hexane = 5: 95) to afford 10.0 g product as a white solid. Yield: 89%. ^{1}H NMR (400 MHz; $CDCl_3$; *δ*): 0.871-0.904 (t, 3H, C*H*$_3$), 1.26-1.44 (m, 11H, C*H*$_2$ and C*H*$_3$), 3.89 (s, 3H, C*H*$_3$), 4.42-4.46 (m, 1H, C*H*CH_2CH_3), 6.87-6.89 (d, 2H, *J* = 6.8 Hz, Ar*H*), 7.96-7.98 (d, 2H, *J* = 6.8 Hz, Ar*H*).

Methyl 4-(octyloxy)benzoate (3b).

Into a 500 ml round bottom single-neck flask, Methyl 4-hydroxybenzoate (5.5 g, 36.18 mmol), 1-bromooctane (7.2 g, 37.3 mmol) and K_2CO_3 (16.0 g, 116 mmol) were dissolved into acetone (50 mL) and then and refluxed at 48 °C overnight. Furthermore, thin layer chromatography (TLC) plates were used to determine the reaction was complete. After removal of the solvent by evaporation under reduced pressure, the residue was extracted with water and ethyl acetate. Then, the organic layer was dried over anhydrous $MgSO_4$, the residue was purified by silica gel column chromatography (ethyl acetate: hexane = 1: 20) to afford product 8.78 g as a white solid. Yield: 92%. ^{1}H NMR (400 MHz; $CDCl_3$; *δ*): 0.882-0.916 (t, 3H, C*H*$_3$), 1.28-1.50 (m, 12H, C*H*$_2$), 3.89 (s, 3H, C*H*$_3$), 4.01-4.07 (t, 2H, C*H*$_2$), 6.89-6.91 (d, 2H, *J* = 9.2 Hz, Ar*H*), 7.96-7.98 (d, 2H, *J* = 8 Hz, Ar*H*).

Methyl 4-(dodecyloxy)benzoate (3c).

The method is same with 4-(octyloxy)benzoic acid (3b). As a white solid. Yield: 92%. ^{1}H NMR (400 MHz; $CDCl_3$; δ): 0.875-0.910 (t, 3H, C*H*$_3$), 1.27-1.50 (m, 18H, CH_2), 3.88 (s, 3H, C*H*$_3$), 4.01-4.07 (t, 2H, C*H*$_2$), 6.89-6.91 (d, 2H, *J* = 8.4 Hz, Ar*H*), 7.97-7.99 (d, 2H, *J* = 8.8 Hz, Ar*H*).

4-((S)-octan-2-yloxy)-benzoic acid (4a)**.**

Into a 100 mL round single-neck flask, (*S*)-methyl 4-(octan-2-yloxy)benzoate (10.0 g, 33.9 mmol) and KOH (7.60 g, 136 mmol) were added with methanol/water (100 mL/50 mL). The mixture was heated and refluxed overnight. Thin layer chromatography (TLC) plates were used to determine the reaction was complete. The residue was dried with a rota evaporator and added with some HCl. The organic layer was extracted by water and ethyl acetate and dried over anhydrous $MgSO_4$ and recrystallized by hexane to afford 7.0 g product as a white solid (73%). ^{1}H NMR (400 MHz; $CDCl_3$; δ): 0.874-0.908 (t, 3H, CH_3), 1.25-1.44 (m, 11H, CH_2 and CH_3), 4.44-4.49 (m, 1H, CHCH_2CH_3), 6.89-6.93 (d, 2H, J = 9.6 Hz, ArH), 8.03-8.05 (d, 2H, J = 10 Hz, ArH).

4-(Octyloxy)benzoic acid (4b).

The method is same with 4-((*R*)-octan-2-yloxy)-benzoic acid (4a). As a white solid. Yield: 93%. ^{1}H NMR (400 MHz; $CDCl_3$; δ): 0.884-0.910 (t, 3H, CH_3), 1.30-1.51 (m, 12H, CH_2), 4.01-4.04 (t, 2H, CH_2), 6.92-6.94 (d, 2H, J = 8.8 Hz, ArH), 8.04-8.07 (d, 2H, J = 12 Hz, ArH).

4-(Dodecyloxy)benzoic acid (4c).

The method is same with 4-((*R*)-octan-2-yloxy)-benzoic acid (4a). As a white solid. Yield: 93%. ^{1}H NMR (400 MHz; $CDCl_3$; δ): 0.874-0.907 (t, 3H, CH_3), 1.19-1.83 (m, 20H, CH_2), 4.01-4.04 (t, 2H, CH_2), 6.92-6.94 (d, 2H, J = 8.8 Hz, ArH), 8.02-8.04 (d, 2H, J = 8.8 Hz, ArH).

4'-(Octan-2(*S*)-yloxybenzoyloxy)biphenyl-4-carboxylic acid (*S*)-1-methylheptyl ester (5a).

To a solution of 4-((*S*)-octan-2-yloxy)-benzoic acid (1.32 g, 4.76 mmol) and N,N'-dicyclohexylcarbodiimide (0.97 g, 4.67 mmol) in dichloromathane (20 mL) was added a solution of (*S*)-1-methylheptyl 4'-biphenyl-4-carboxylate (1.50 g, 4.2 mmol) and *N*,*N*-dimethyl-4-aminopyridin (0.12 g, 0.94 mmol) in dichloromathane (20 mL) was dropwise added over 1 h. After stirring for 20 h at room temperature, white precipitate was removed by filtration. The crude product was purified by silica gel column chromatography (eluent: chloroform) followed by recrystallization from hexane/ethanol to afford 1.60 g product as a white solid (55.4%). ^{1}H NMR (400 MHz; $CDCl_3$; δ): 0.876-0.919 (t, 6H, CH_3), 1.30-1.78 (m, 26H, CH_2CH$_2$ and CHCH_3), 4.49-4.50 (m, 1H, CHOAr), 5.29-5.31 (m, 1H, CHOCO), 6.95-6.97 (d, 2H, J = 8 Hz, ArH), 7.30-7.32 (d, 2H, J = 8 Hz, ArH), 7.68-7.6 (m, 4H, ArH), 8.10-8.16 (m, 4H, ArH).

4'-(4-(Octyloxy)benzoyloxy)biphenyl-4-carboxylic acid (*S*)-1-methylheptyl ester (5b)

The method is same with 5a**.** As a white solid. Yield: 44.4%. ^{1}H NMR (400 MHz; $CDCl_3$; δ): 0.875-0.926 (t, 6H, CH_3), 1.30-1.85 (m, 25H, CH_2CH$_2$ and CHCH_3), 4.04-4.07 (m, 2H, CHOAr), 5.17-5.19 (m, 1H, CHOCO), 6.97-6.99 (d, 2H, J = 8 Hz, ArH), 7.30-7.32 (d, 2H, J = 8 Hz, ArH), 7.65-7.68 (m, 4H, ArH), 8.10-8.16 (m, 4H, ArH).

4'-(4-(Dodecyloxy)benzoyloxy)biphenyl-4-carboxylic acid (S)-1-methylheptyl ester (5c)

The method is same with 5a**.** As a white solid. Yield: 43.1%. ^{1}H NMR (400 MHz; $CDCl_3$; δ): 0.885-0.937 (t, 6H, CH_3), 1.29-1.88 (m, 33H, CH_2CH$_2$ and CHCH_3), 4.06-4.08 (m, 2H, CHOAr), 5.18-5.20 (m, 1H, CHOCO), 6.96-6.98 (d, 2H, J = 8 Hz, ArH), 7.28-7.30 (d, 2H, J = 8 Hz, ArH), 7.64-7.67 (m, 4H, ArH), 8.11-8.17 (m, 4H,

Ar*H*).

5.2.4. Polymerztion.

Cholesteric LC electrolyte was prepared by addition of the chiral inducer (5 wt%), the monomer (1 wt%) in 6CB (LC solvent, 93 wt%), and TBAP (supporting electrolyte salt 1 wt%) (Table 5.1.). The cholesteric LC electrolyte solution was injected between two indium-tin-oxide (ITO) glass electrodes separated by a Teflon sheet (thickness = 0.2 mm) as a spacer. Electrochemical polymerization was performed with application of constant 4.0 V direct-current at room temperature (20 °C). After 5 min, a thin polymer film deposited on the anode side of ITO glass electrode. The residual cholesteric LC solution was washed off with hexane, dried at room temperature and obtained a polymer film.

Table 5. 1. Constituents of liquid crystal electrolyte solution.

Reagent	Chemical structure	Wt%
4-Cyano-4′-n-hexylbiphenyl (6CB)	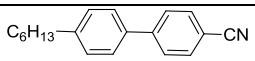	93
Chiral inducer	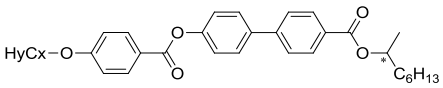	5
Tetrabutylammonium perchlorate (supporting electrolyte salt)	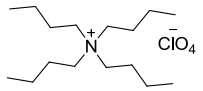	1
Monomer	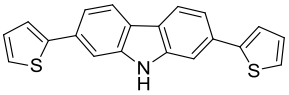	1

5.3. Results and discussions

5.3.1. Helical sense and helical twisting power.

Table 5. 2. Helical twisting power and helical sense of chiral inducers.

Chiral inducer	LC solvent	THP[b] (μm^{-1})	MTHP[c] $(\mu m^{-1})mol^{-1}$ kg	β_M[d] (μm^{-1})	Helical sense
5a	6CB[a]	6.40	3.77	13.4	Left-hand
5b	6CB	4.51	2.52	9.55	Right-hand
5c	6CB	3.83	2.34	8.92	Right-hand

a: 6CB: (4-cyano-4′-n-hexyl biphenyl)

b: HTP (helical twisting power) = $(p \times c)^{-1}$, p: helical pitch; c: weight conc. of the chiral inducer.

c: MHTP (molar helical twisting power) = HTP$\times M_d \times 10^{-3}$

d: $\beta_M = (p \times c \times M_h/M_d)^{-1}$. M_d and M_h are the molecular weight of the chiral inducer and the solvent

In order to determinate the helical sense of inducers (5a, 5b and 5c), miscibility testing was performed. Cholesteryl oleyl carbonate was employed as a standard cholesteric LC (left-hand helical sense). If the standard material has the differene helical sense with test sample, schlieren texture of the nematic phase would be

observed at the boundary of the two compounds. Here, miscibility testing of 5a is showed in the figure 5. 1. Helicity texture is clearly observed at the boundary. Therefore, the testing sample has left-hand helical sense. Compounds of 5b and 5c were tested by the same method and show right-hand helical sense in the miscibility test.

Helical twisting powers of the chiral inducers were measured by the Grandjean-Cano wedge method. [18] The macroscopic helical twisting power (β_M), helical twisting power (HTP) and molar helical twisting power (MHTP) are estimated by the following formulas:

$$\beta_M = (p \times c \times M_h/M_d)^{-1} \quad (1)$$

$$HTP = (p \times c)^{-1} \quad (2)$$

$$MHTP = HTP \times M_d \times 10^{-3} \quad (3)$$

Here, p is the helical pitch of the cholesteric LC, c is the weight concentration of the chiral inducer, M_d and M_h are the molecular weight of the chiral inducer and the solvent. Calculation results are summarized in the Table 5. 2..

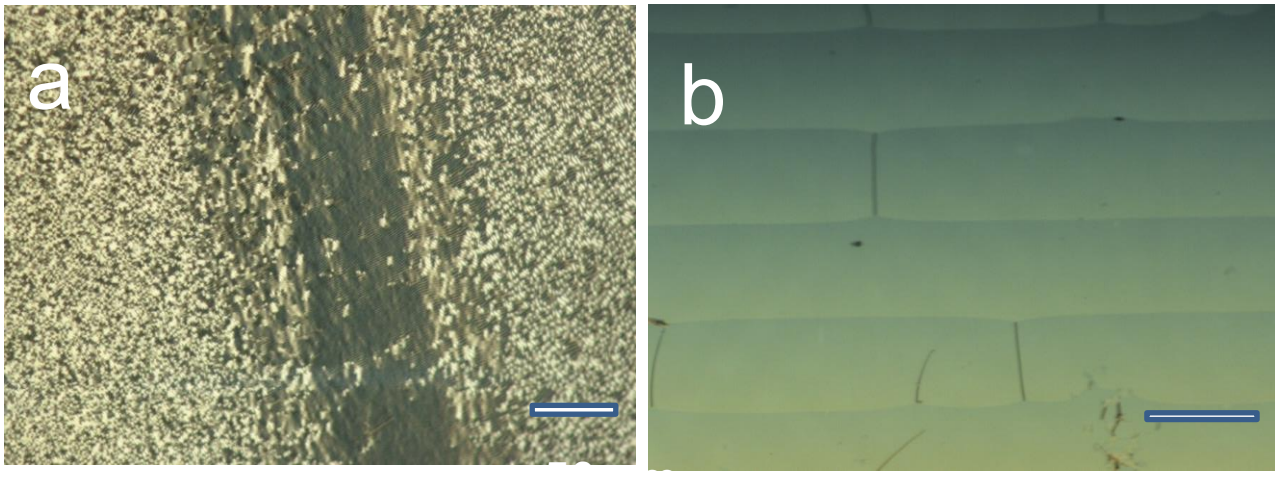

Figure 5. 1. (a) Polarizing optical microscopy (POM) images of miscibility test. (b) An example of Cano-wedge cell (5a in 6CB).

5.3.2. POM observation.

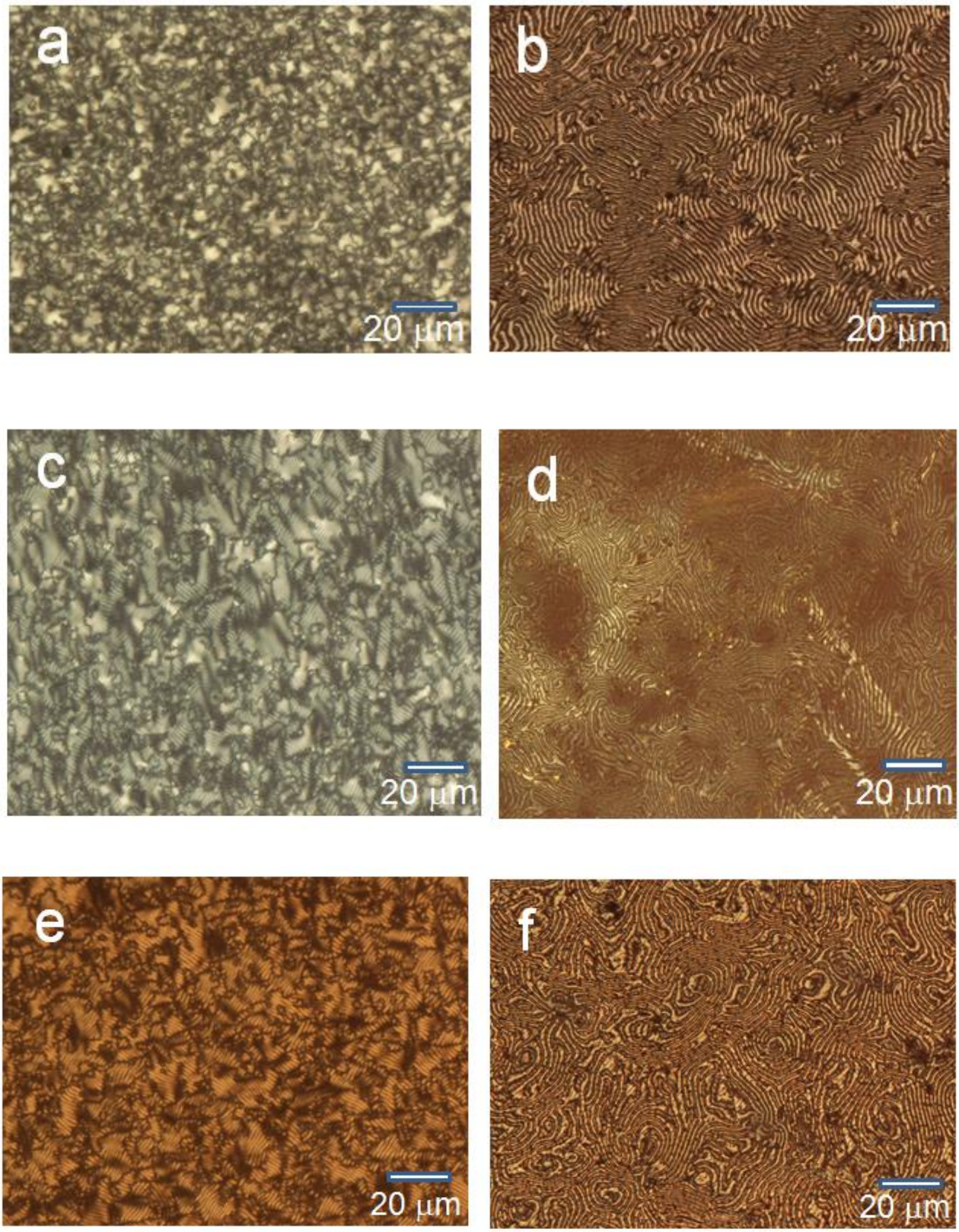

Figure 5. 2. (a), (c) and (e) Polarizing optical microscopy (POM) image of cholesteric liquid crystal electrolyte solution containing monomers at room temperature. (b), (d) and (f) POM image of the polymer film prepared in a cholesteric liquid crystal electrolyte induced by chiral inducer. (a: 5a, c: 5b, e: 5c, b: PCB5a, d: PCB5b, f: PCB5c)

The Polarizing optical microscopy (POM) images of the polymer film prepared by electrochemical polymerization in cholesteric LC electrolyte were showed in the Figure 5. 2. The Figure 5. 2 (a), (c) and (e) were showed the POM image of cholesteric liquid crystal electrolyte solution containing monomers and inducers (a: 5a, c: 5b, e: 5c) at room temperature. The Figure 5. 2 (b), (d) and (f) were show POM images of the polymer films (b: PCB5a, d: PCB5b, f: PCB5c) prepared in a cholesteric liquid crystal electrolyte induced by chiral inducer. Fingerprint textures of polymer films were observed. These textures are similar to typical fingerprint texture of cholesteric phase, indicates transcription of the CLC texture to the polymer film.

5.3.3. Structural characterization

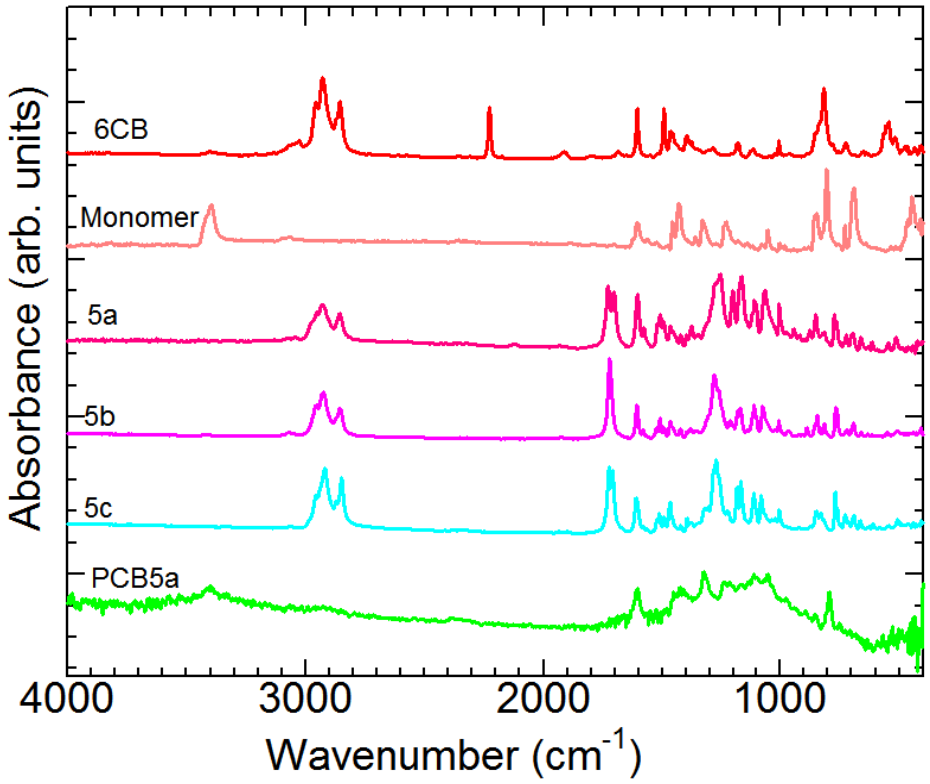

Figure 5. 3. FT-IR (Fourier transform infrared) absorption spectra of PCB5a, monomer, 6CB, 5a, 5b, and 5c.

The polymeric products were characterized spectroscopically. All the polymers give satisfactory analysis data corresponding to their expected molecular structures. The monomer, 6CB, inducers of 5a, 5b, and 5c, and polymer of PCB5a are shown in Figure 5. 3.. These inducers of 5a, 5b, and 5c show absorption bands at 2881-2952 cm^{-1} attributable to ν_{CH2} and ν_{CH3} stretching band of alkyl chains and the intense absorption peak at 1721 cm-1 due to C=O stretching band of ester groups of side chain. These results indicate the successful synthesis of inducers. On the other hand, the absorption peaks at 2200 cm^{-1} is due to CN triple bond vibrations of 6CB liquid crystal. The polymer of PCB5a has no peaks at around 2200 cm^{-1}, 1721 cm-1 and 2881-2952 cm^{-1} in the spectrum, indicates that neither 6CB nor inducer remain in the PCB5a film.

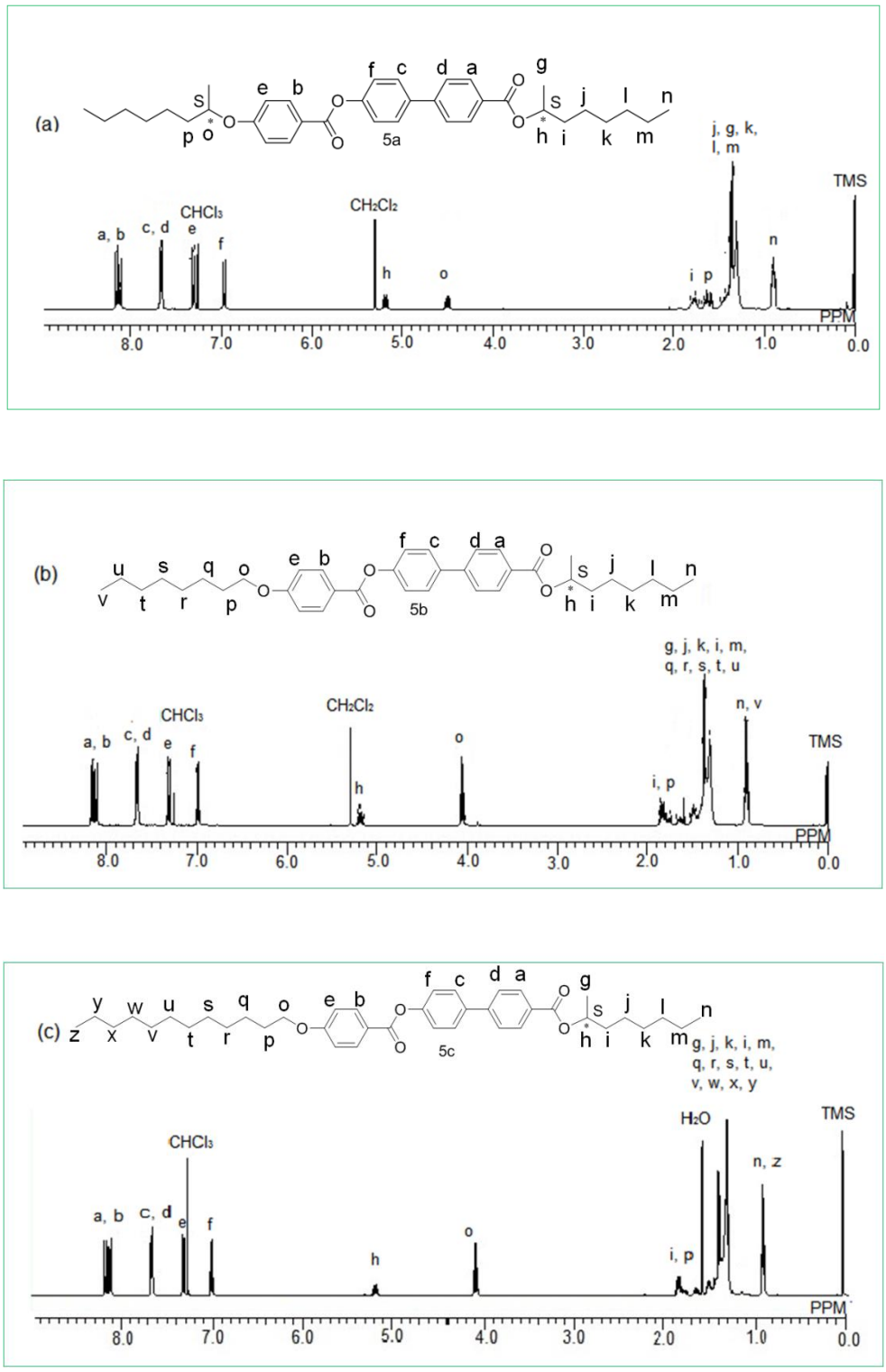

Figure 5. 4. ^{1}H NMR spectra of three-ring chiral inducers. TMS: tetramethylsilane.

The inducers were characterized by ^{1}H NMR analyses. The results were shown in the Figure5. 4. All the inducers gave satisfactory data corresponding to their expected molecular structures. The chemical shifts of three inducers at around 4.04-4.50 ppm are attributed to the protons of C*H*OAr groups. The chemical shifts of three inducers at 5.17-5.31 ppm are also clearly observed and ascribed to the protons of C*H*OCO groups. The

result indicates that we successfully synthesized the desired compound.

5.3.4. Optical activity.

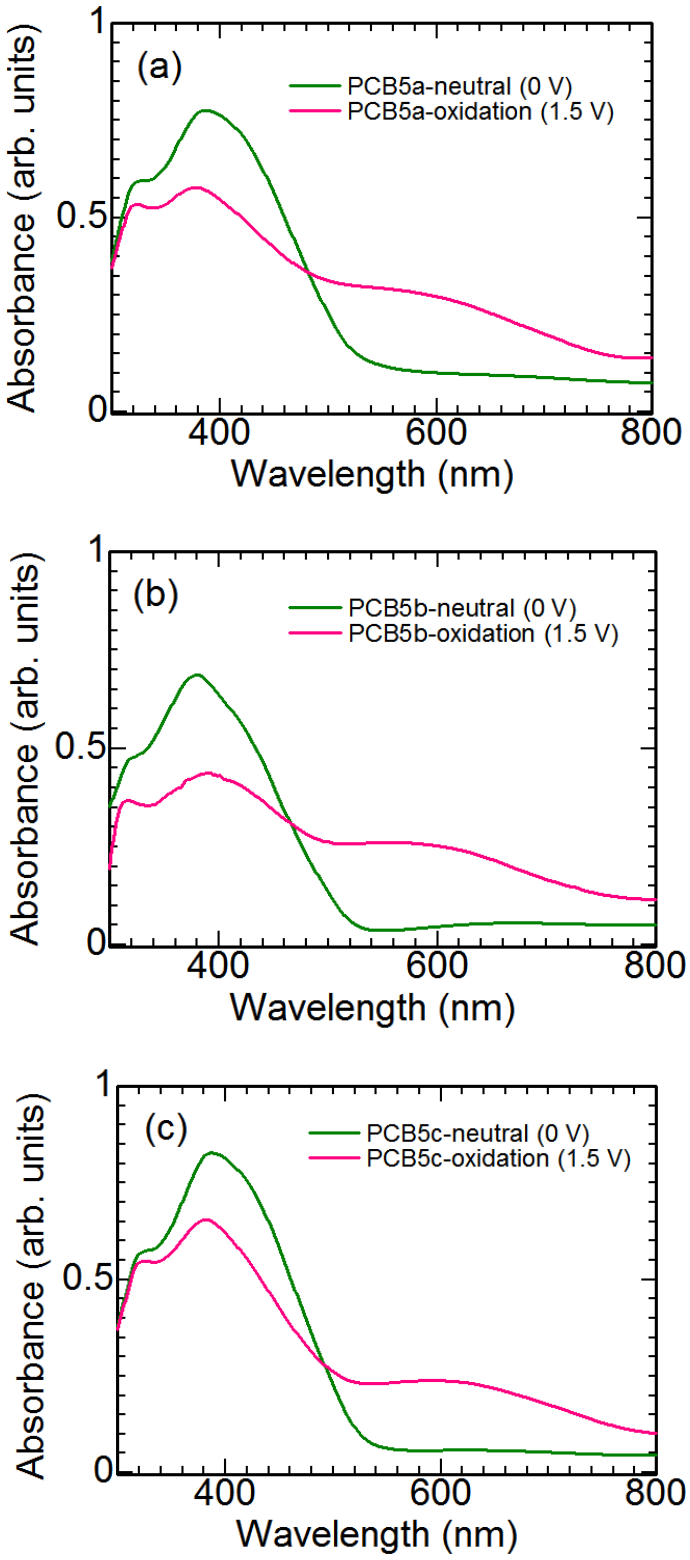

Figure 5. 5. CD absorption (a, b and c) of the films prepared from the cholesteric LC electrolyte induced by the series of the three-ring type chiral compounds.

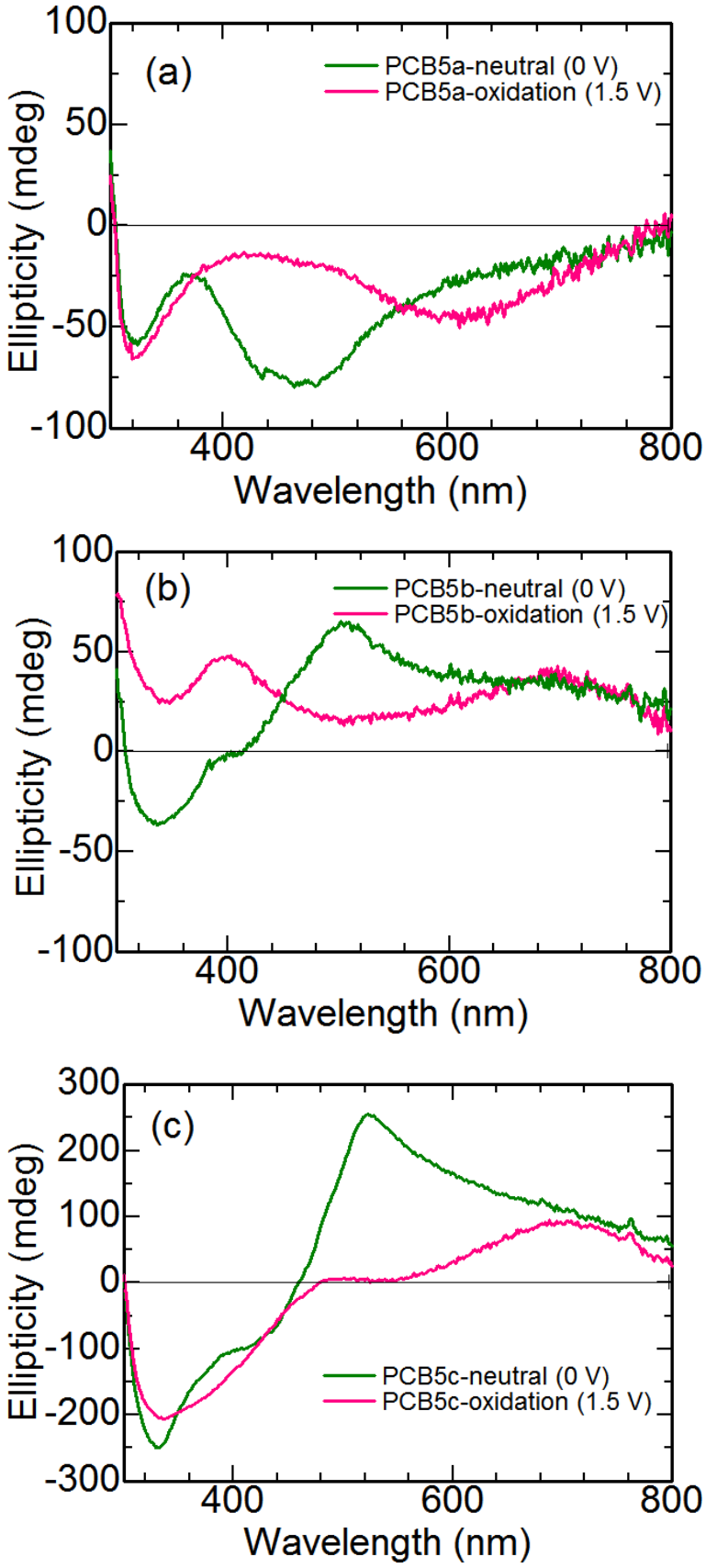

Figure 5. 6. UV-vis absorption (a, b and c) of the films prepared from the cholesteric LC electrolyte induced by the series of the three-ring type chiral compounds.

All the polymer films in oxidation and neutral states show absorption bands at 300–500 nm (Figure 5. 5.), which are due to π–π* transitions of the conjugated backbone. The films in oxidation states show another absorption band at 520-800 nm, indicates that the polarons were generated by electrochemical doping. In the CD spectra (Figure 5. 6 (a).), PCB5a in oxidation and neutral states shows negative signals at long wavelength, indicates that the polymer backbones form left-handed helical aggregation. The result is consistent with the left-handed order of 5a electrolyte solution. PCB5b in neutral state and PCB5c in oxidation and neutral state are observed cotton effect at their absorption maximum wavelengths (Figure 5. 6 (b), (c).) and formed cotton effect at long wavelength can be due to Davydov splitting. [19] These results suggest that the polymers backbones form right-handed helical aggregation. The result is consistent with the right-handed order of 5b and 5c electrolyte solution.

5.3.5. Electrochemical Properties

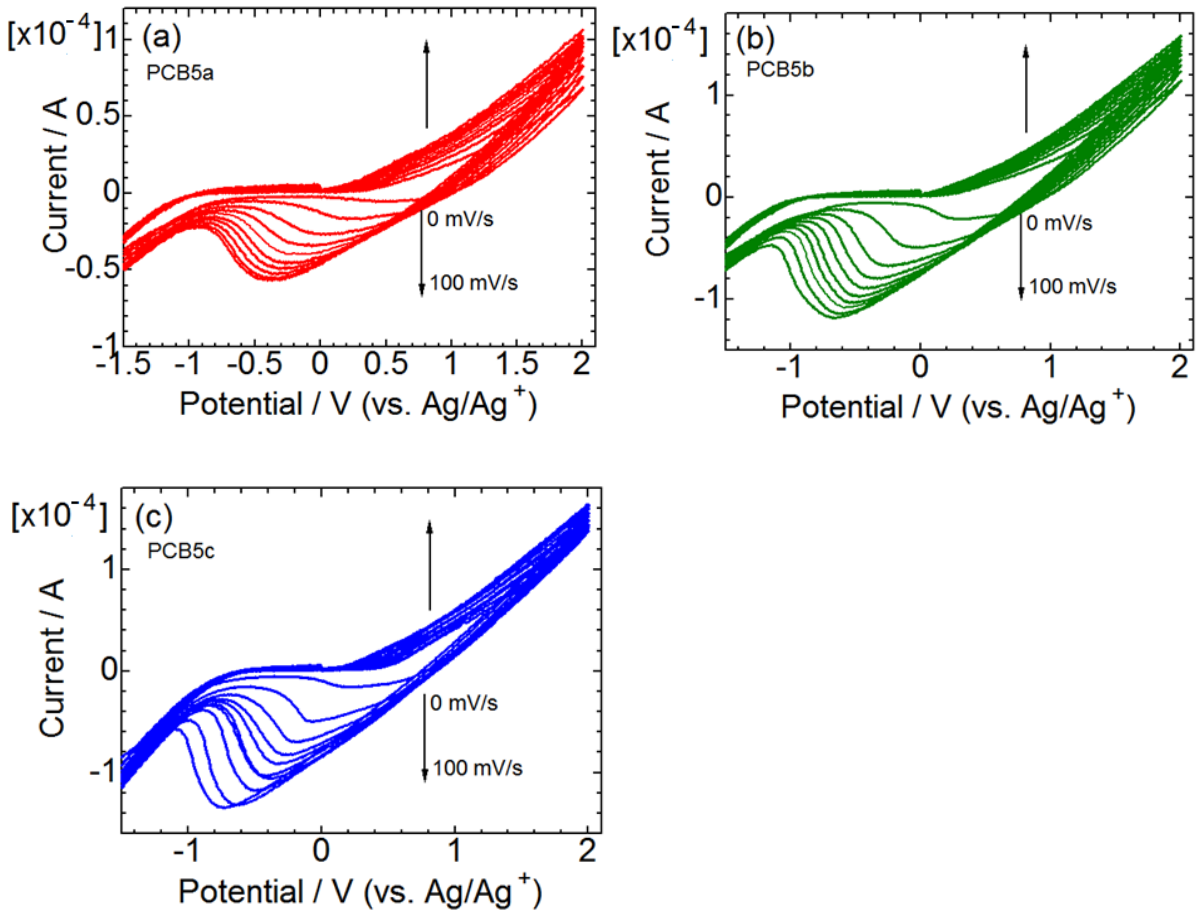

Figure 5. 7. Cyclic voltammograms of polymers observed the polymer film. (a) PCB5a (b) PCB5b (c) PCB5c.

Electrochemical properties of the films prepared in the cholesteric electrolyte solution induced by 5a, 5b and

5c were examined with cyclic voltammetry (CV) at scan rates of at scan rates of 10 to 100 mV s^{-1} in acetonitrile containing 0.1 M TBAP and show in the Figure 5. 7.. The potentials are estimated relative to a silver–silver ion (Ag/Ag+) reference electrode. The current value increased gradually with the increase of scan rates, indicate that the electron transfer can be accessed applied voltage. [20] Cyclic voltammograms of PCB5a, PCB5b and PCB5c show oxidation and reduction signals at the same position and electrochemical response, indicates that the redox properties depend on the primary structure of the polymers.

3.4. Acknowledgments

We would like to thank Glass Work Shop of University of the Division of Materials Science (University of Tsukuba) and Chemical Analysis Division Research Facility Center for Science and Technology of University of Tsukuba for providing NMR, IR, ESR, PL measurements.

3.5. References

[1] Burroughes JH, Bradley DDC, Brown AR, Marks RN, Mackay K, Friend RH, Burns PL, Holmes AB. Light-emitting diodes based on conjugated polymers. Nature. 1990;347:539-541.

[2] Bao Z, Dodabalapur A, Lovinger A. Soluble and processable regioregular poly (3−hexylthiophene) for thin film field‐effect transistor applications with high mobility. J. Appl. Phys. Lett. 1996;69:4108-4110.

[3] Yu G, Gao J, Hummelen JC, Wudl F, Heeger AJ. Polymer photovoltaic cells: enhanced efficiencies via a network of internal donor-acceptor heterojunctions. Science 1995;270:1789-1791.

[4] Horie M, Majewski LA, Fearn MJ, Yu CY, Luo Y, Song A, Saunders BR, Turner ML. Cyclopentadithiophene based polymers; a comparison of optical, electrochemical and organic field-effect transistor characteristics. J. Mater. Chem. 2010;20:4347-4355.

[5] Tanaka H, Watanabe S, Ito H, Marumoto K, Kuroda S. Direct observation of the charge carrier concentration in organic field-effect transistors by electron spin resonance. Appl. Phys. Lett., 2009, 94, 103308-1-103308-3.

[6] Ding X, Guo J, Feng X, Honsho Y, Guo J, Seki S, Maitarad P, Saeki A, Nagase S, Jiang D. Synthesis of metallophthalocyanine covalent organic frameworks that exhibit high carrier mobility and photoconductivity. Angew. Chem. Int. Ed. 2011;50:1289-1293.

[7] Resta C, Pietro S, Majerić Elenkov M, Hamersak Z, Pescitelli G, Bari L. Consequences of chirality on the aggregation behavior of poly[2-methoxy-5-(2'-ethylhexyloxy)-p-phenylenevinylene] (MEH-PPV). Macromolecules. 2014;47:4847–4850.

[8] Tsuruta T, Inoue S, Furukawa J. Synthesis of optically active polymers by asymmetric catalysts. V. Resolution of poly‐DL‐propylene oxide. Macromol. Chem. 1965;84:298-299.

[9] Ebert PE, Price C. Polyethers. VI. Aluminum alkyls as catalysts for polymerization of propylene oxide. J. Polym. Sci. 1959;34:157-160.

[10] Tang H, Fujiki M, Sato T. Thermodriven conformational transition of optically active poly [2, 7-{9, 9-bis [(S)-2-methyloctyl]} fluorene] in solution. Macromolecules 2002, 35, 6439-6445.

[11] Nakao H, Mayahara Y, Nomura R, Tabata M, Masuda T. Effect of chiral substituents on the helical conformation of poly (propiolic esters). Macromolecules. 2000;33:3978-3982.

[12]Yashima E, Maeda K, Okamoto Y, Memory of macromolecular helicity assisted by interaction with achiral small molecules. Nature. 1999;399:449-451.
[13] Khiew PS, Radiman S, Huang NM, Kan CS, Ahmad MS. In situ polymerization of conducting polyaniline in bicontinuous cubic phase of lyotropic liquid crystal. Colloids Surf. A Physicochem. Eng. Asp. 2004;247:35–40.
[14] Yang J, Kimb DH, Hendricksb JL, Leachb M, Northeya R, Martin DC. Ordered surfactant-templated poly(3,4-ethylenedioxythiophene) (PEDOT) conducting polymer on microfabricated neural probes. Acta Biomater. 2005;1:125–136.
[15] Matsushita S, Jeong YS, Akagi K. Electrochromism-driven linearly and circularly polarized dichroism of poly(3,4-ethylenedioxythiophene) derivatives with chirality and liquid crystallinity. Chem. Commun. 2013;49:1883–1890.
[16] Kihara H, Miura T. Morphology of a hydrogen-bonded LC polymer prepared by photopolymerization-induced phase separation under an isotropic phase. Polymer, 2005;46: 10378-10382.
[17] Miura M, Izawa T, Morihara Y, Sugioka T, Fujita A. Manufacture and use of polymer having π-skeleton plane with good absorption for visible to near IR wave region. Jpn. Kokai Tokkyo Koho. *2013;* 2013234265:29
[18] Wilson M, Earl DJ. Calculating the helical twisting power of chiral dopants. J. Mater. Chem. 2001;11:2672-2677.
[19] Matsumura A, Yang F, Goto H. Synthesis of a terpene-based new chiral inducer and preparation of an asymmetric polymer. Polymers. 2015;7:147-155
[20] Dong J, Kawabata K, Goto H. Synthesis and characterization of a novel donor–acceptor–donor chiral inducer and its application in electrochemical polymerization. J. Mater. Chem. C. 2015;3:2024–2032.

Acknowledgements

First of all, I would like to express my sincere gratitude to my supervisor, Hiromasa Goto, for providing me opportunity to do my PH.D. research in Goto laboratory and his instructive advice and his constant encouragement and guidance through my doctoral course. I am deeply grateful of his help in the completion of the academic studies

I am also deeply indebted to Prof. Dr. Kihara Hideyuki in National Institute of Advanced Industrial Science and Technology. He offered me valuable suggestions in the academic studies and language learning. I have benefited a lot and academically prepared for the thesis.

I am also grateful to Miss Aohan Wang and Mr Jiuchao Dong, who kindly gave me a hand when I was making the question in study and life.

Finally, I am special thanks should go to Goto laboratory numbers: Miss Kudou Yuki, Mr Hayashi Hiroki, Mr Shen Haoyue, Mr Eguchi Naoto, Mr Kikuchi Ryosuke, Mr Yamabe Kohei, Mr Otaki Masashi, Mr Hirokawa Shota. For their patient assistance and friendly encouragement in my academic research and life, it would be possible for me to complete this thesis in three years. Their willingness to give me his time so generously has been much appreciated. Truly, without their painstaking efforts in paper correction and language learning the present thesis would not have been possible.

Appebdix

光学和磁性功能的π-共轭聚合物的设计合成及性能

在半世纪以前，通过掺杂等手段，使共轭聚合物电导率有了很大程度的提高。[1-3] 在它们的主链上含有交替的单键和双键，从而形成了大的共轭 π 体系，π 电子的流动产生了导电性。这使共轭聚合物在有机半导体材料和光电器件上得到广泛的应用。近年来，更多研究团队专注于探索合成功能化的共轭聚合物，这类聚合物具有易成膜，加工性好，成本低的特点。因此，功能基团引进聚合物，获得功能共轭聚合，变得越来越重要。

根据主链结构的不同，共轭聚合物可以分为三类。第一类，共轭的芳香环作为主链的共轭聚合物，这类共轭聚合物包括聚对苯，聚芴，聚噻吩，聚吡咯等。第二类，双键作为主链的共轭聚合物，这类聚合物包括聚乙炔。第三类，芳香环和双键作为聚合物主链的共轭聚合物，这类聚合物包括聚对苯撑乙炔，聚苯胺等。

所有的这些类别的共轭聚合物做成器件应用到我们的生活，离不开这些共轭聚合物的合成，然而合成工作开始于对这些单体和共轭聚合物的设计。所以设计合成这些共轭聚合物，进而得到想要的功能物质，越来越吸引人们的兴趣。在我的论文中，我探讨了得到功能共轭聚合物的合成策略，进而设计了一些功能性共轭聚合物，然后讨论了功能共轭聚合物的性质。另外还设计了电解聚合合成光学的共轭聚合物。下面分别叙述。

一．多功能共轭聚合物的合成策略以及实例探讨。

功能性共轭聚合物包括主链功能性的聚合物和侧链功能性的共轭聚合物。主链功能性聚合物是在主链引入功能性基团或者通过外力诱发主链形成功能性的共轭主链（例如,引入醌式结构的功能团形成低能系的共轭聚合物或者通过诱导剂诱发主链手性的排列，形成螺旋排列的共轭聚合物）。侧链功能性聚合物是功能基团引入芳环，形成功能性的单体，这些功能单体经由聚合反应产生功能化的共轭聚合物。[4,5] 在这里我们首先探讨功能性共轭聚合物的合成方法。

1）合成理念

在化学合成中，有许多功能基团影响了单体和聚合物的合成。例如，带有酯基或者氨基的化合物很难用锂化反应得到聚合的单体，因为正丁基锂的活性很高，他会和侧链的这些基团发生反应，影响单体的生成。Suzuki 偶联反应条件相对温和，对侧链功能团的包容性强，易得到想要的单体。在这里我们用二溴芳环羧酸链接功能基团，形成侧链酯基功能化合物，然后这个二溴功能化合物通过钯催化和硼酸酯取代，形成功能化的单体。 这个二硼酸酯可以通过偶联反应形成共轭主链，从而得到多功能的共轭聚合物（图 1）

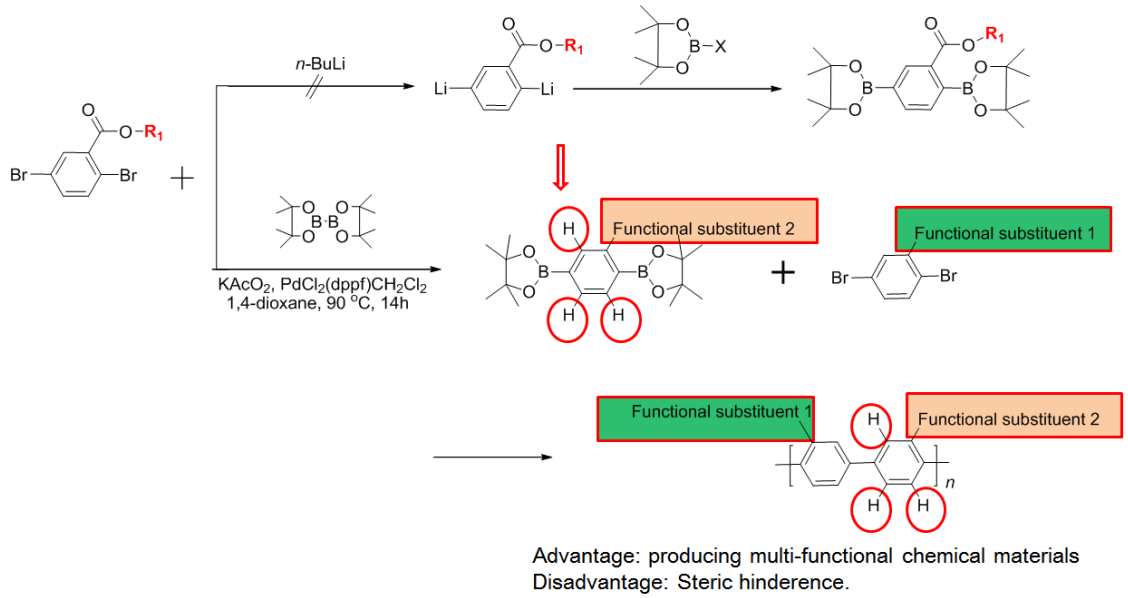

图 1. 多功能共轭聚合物的合成策略

这种合成方法可以在芳环引入不同的功能基团，产生多功能的共轭聚合物。鉴于这个合成理念，我们合成了六个共轭聚合物（图式 1），来验证这个设计理念的可行性，进而探索了这些功能基团对共轭高分子的影响。

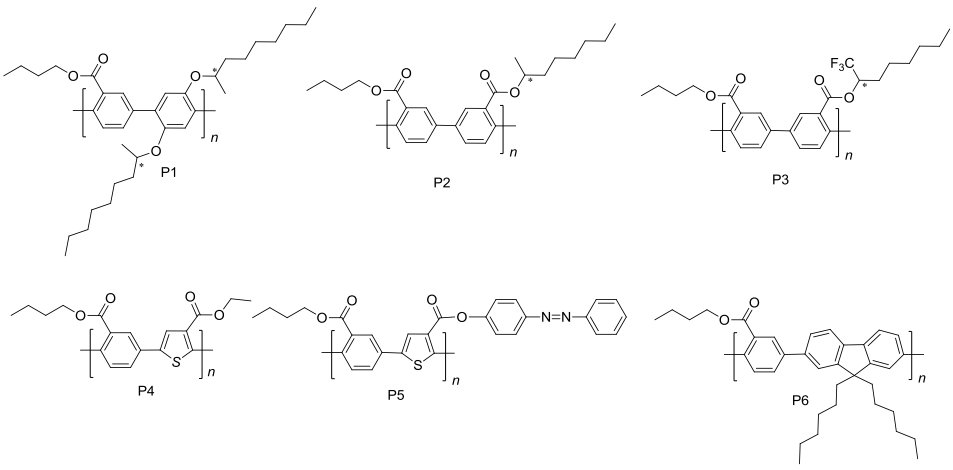

图式 1 合成的六个带有不同功能团的共轭聚合物

2）功能基团赋予共轭高分子的功能性实例探讨。

在这六个共轭聚合物的实例中，我们选择烷基链和具有光学活性的功能团引入主链，想得到溶解性能完好具有光学性能的共轭聚合物。首先，我们对这些功能共轭聚合物做了溶解性实验，由于烷基的引入，这些聚合物都具有很好的溶解性能，能溶于常见有机溶剂，例如，四氢呋喃，三氯甲烷，二氯甲烷，DMF 中。

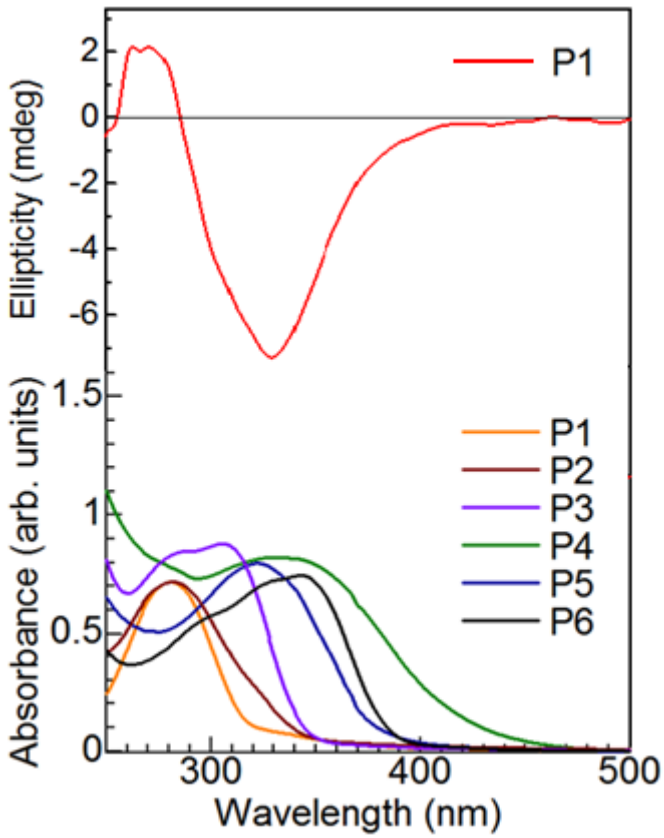

图 2. 共轭聚合物的 CD 光谱和紫外光谱。

另一方面，我们也调查了功能基团赋予共轭高分子的性能。手性基团和偶氮本基团被引入共轭主链（P1,P2 和 P3 被引入手性的功能团，P5 被引入偶氮本功能团）。在 CD 光谱中，P1 展示了明显的对联峰，负峰出现在 324 纳米，正峰出现在 271 纳米，对应 P1 在 280 纳米的紫外吸收峰,这一结果表明受侧链手性功能团的影响,P1 在溶液里形成了主链螺旋排列(图 2)。具有手性功能基团的 P2 和 P3 没有显示这一性能。这可能是因为它们的手性功能基在溶液里没有形成有序的排列，没有显示出 CD 信号。

功能基团导入芳香环，然后聚合形成共轭聚合物，这个功能基团能赋予共轭聚合物新的性能，

形成功能化的共轭聚合物，这一策略是可行的。但是功能基团具有比较大的空间位阻效应，影响这个反应的进程，往往得到低分子量的聚合物产品。

二.功能化的磁性共轭聚合物和低能隙共轭聚合物的合成及性质

在探索了功能化的共轭聚合物的合成方法之后，合成了一系列的功能化的共轭聚合物，希望能得到性能优良的功能材料，进而实现应用。在这里，侧重介绍两种共轭聚合物的合成和性能，一个是给共轭聚合物引入磁性和一些功能基团的，另外一个是把能产生低能隙的基团和光学活性的基团引入共轭聚合物。希望得到这些性质的共轭聚合物。在下面我们分别介绍。

1. 功能化的磁性共轭聚合物的合成及性能研究。

1）设计理念。

在共轭聚合物的合成设计以及性能研究中，有关磁性共轭聚合物的研究很多，比如西出，做了大量的研究，发现共轭聚合物带有自由基苯氧自由基侧链，这个侧链可以影响共轭主链，从而使共轭聚合物呈现顺磁性。[6-7] 但是，在一个聚合物分子里，具有自由基又带有别的功能基团（如，手性基团，低能隙的结构），成功得到功能化的磁性共轭聚合物研究鲜有报道。在这里设计的这类共轭聚合物，（图 3）一部分带了叔丁基苯氧自由基，这个基团相对稳定，溶解性好，是氧化活性物质。它有可能使聚合物表现较好的电子特性，溶解性能和磁性，并且这个聚自由基有可能在螺旋结构里表现二维手性特征。另一部分是功能基团单体，例如，带手性基团的单体，能形成低能隙聚合物的单体和能形成具有光发射性能的聚合物单体。这些单体有可能形成新的特性共轭聚合物，比如，主链螺旋的共轭聚合物，低能隙的共轭聚合物，具有光发射性能的共轭聚合物等等。

在这里，我设计了 7 个功能化的磁性共轭聚合物。（图式 2.）它们都带有苯氧自由基的同时，还各自带有不同的功能团。P1-0，P2-0 和 P7-0 带有不同的手性功能团，这三个共轭聚合物有可能出现手性的螺旋排列，在螺旋排列的结构中，苯氧自由基有可能出现二维的手性结构，这一现象的原因到现在还不是很明确，希望进一步探索。P3-0，P4-0 和 P5-0 有不同的主链结构，合成三个共轭聚合物观察他们的能级的变化。P6-0 和 P7-0 包含着芴结构，芴是一个可以发射蓝光的基团，引入芴做共轭主链的一部分，想观察这两个聚合物在光学的电子的性能变化。为了对比共轭聚合物氧化前（羟基聚合物）和氧化后（自由基聚合物）的性能变化，在这里也列举出氧化前结构式。（图式 3）

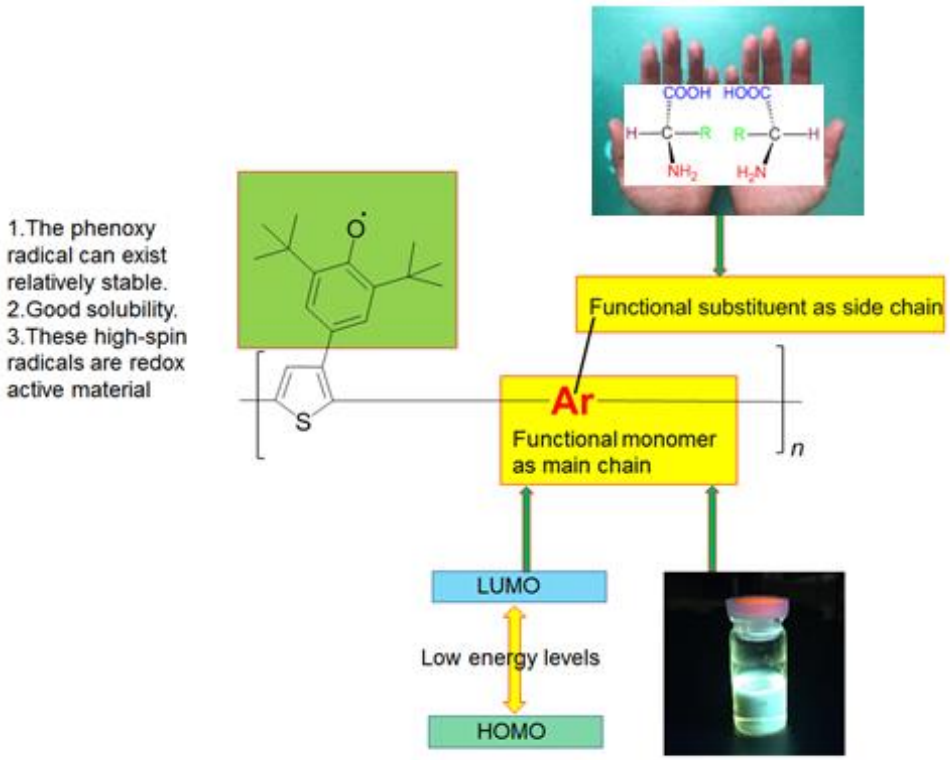

图 3. 功能化的磁性共轭聚合物的设计

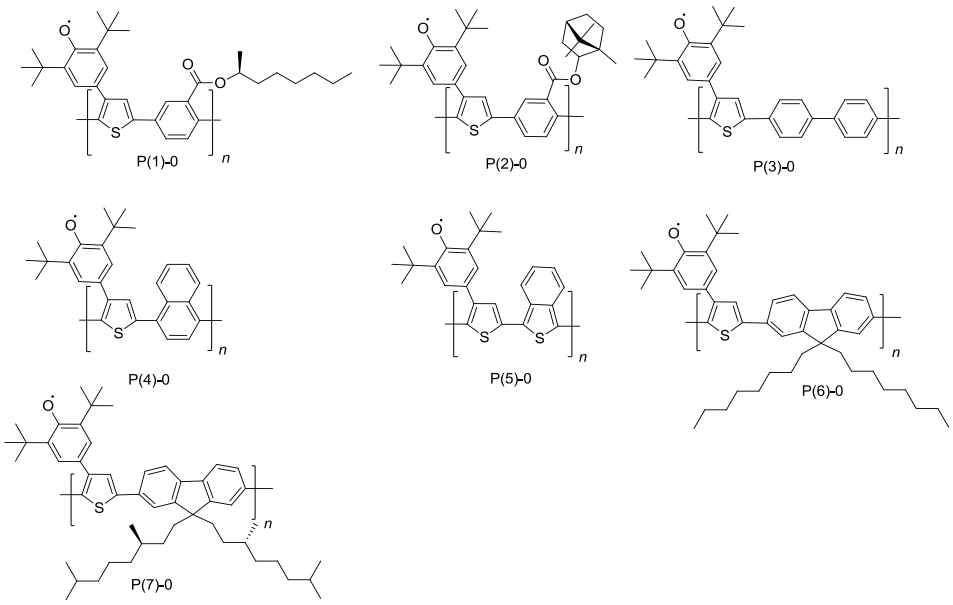

图式 2. 功能化的磁性共轭聚合物

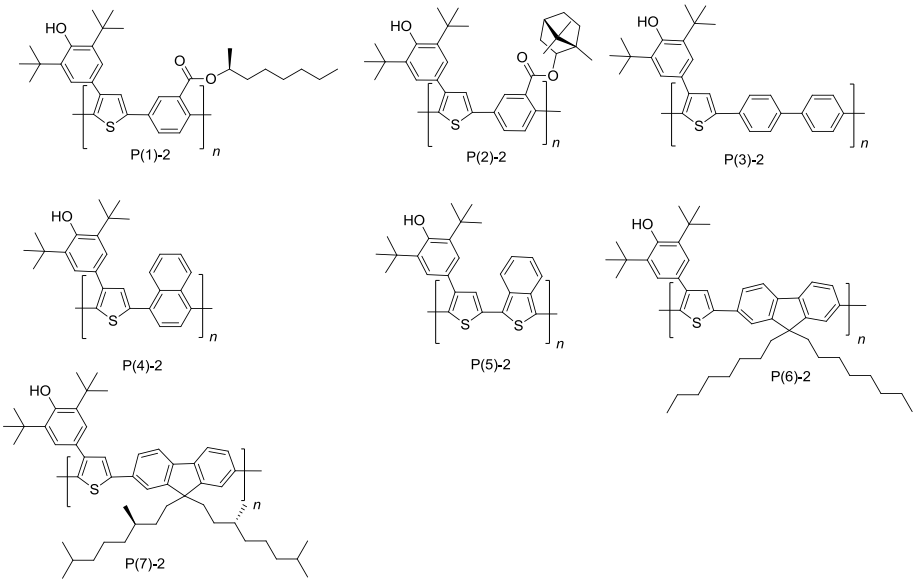

图式 3. 功能化的羟基共轭聚合物

2）共轭聚合物的性能。

（1）光学性能。

功能性聚合物的光学性能在溶液或者膜的状态用紫外光谱，CD 光谱，荧光光谱来表征。在 CD 光谱中，（图 5）苯溶液里 P(1)-2 和 P(1)-0 显示了明显的对联峰，正的 CD 信号出现在长波长 418 纳米，负的 CD 信号出现在 361 纳米，对应 378 纳米处的紫外吸收峰（图 6）。在薄膜状态，P(1)-2 和 P(1)-0 显示了负的 CD 信号。这些结果表明共轭骨架或者共轭分子间形成了螺旋的排列,具有了光学活性。P(2)-2 和 P(2)-0 在苯溶液里显示了 CD 信号和强烈的吸收峰，在薄膜态没有显示 CD 信号，这是应为龙脑基有比较大的空间位阻，在膜的状态，龙脑基团阻止了分子间的π-π相互作用，聚合物不能形成手性的排列。P(7)-2 和 P(7)-0 显示了 CD 信号在薄膜态，这表明这两个聚合物形成了分子间的螺旋排列。

一般情况下，在螺旋的结构里，聚自由基会显示二维的手性结构。可是在这里，并没有观察到聚自由基的 CD 信号，这个原因有可能是在合成的这些共轭聚合物时，氧化剂 PbO_2 并没有把羟基聚合物全部转化自由基聚合物，这个不完全氧化反应，降低了聚合物中自由基的浓度，低浓度的自由基没有显示出 CD 信号。到目前为止，出现这种信号的机制还不太明确，以后的研究会继续探讨。

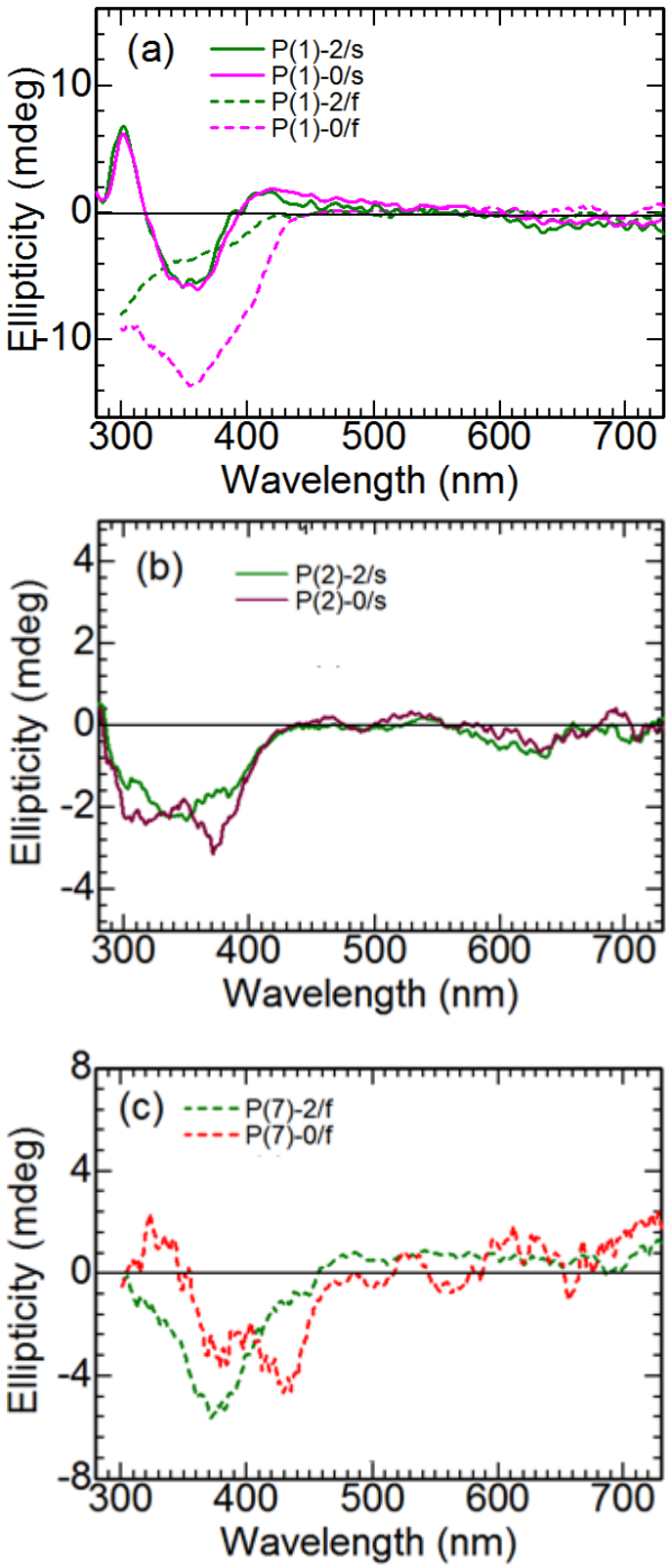

图 5.Polymer-2 ((a): P(1)-2, (b): P(2)-2, (c): P(7)-2 氧化前的聚合物)和polymer-0 ((a): P(1)-0, (b): P(2)-0, (c): P(7)-0氧化后的聚合物)的CD光谱。实线代表溶液状态的测量曲线，虚线代表膜的状态的测量曲线

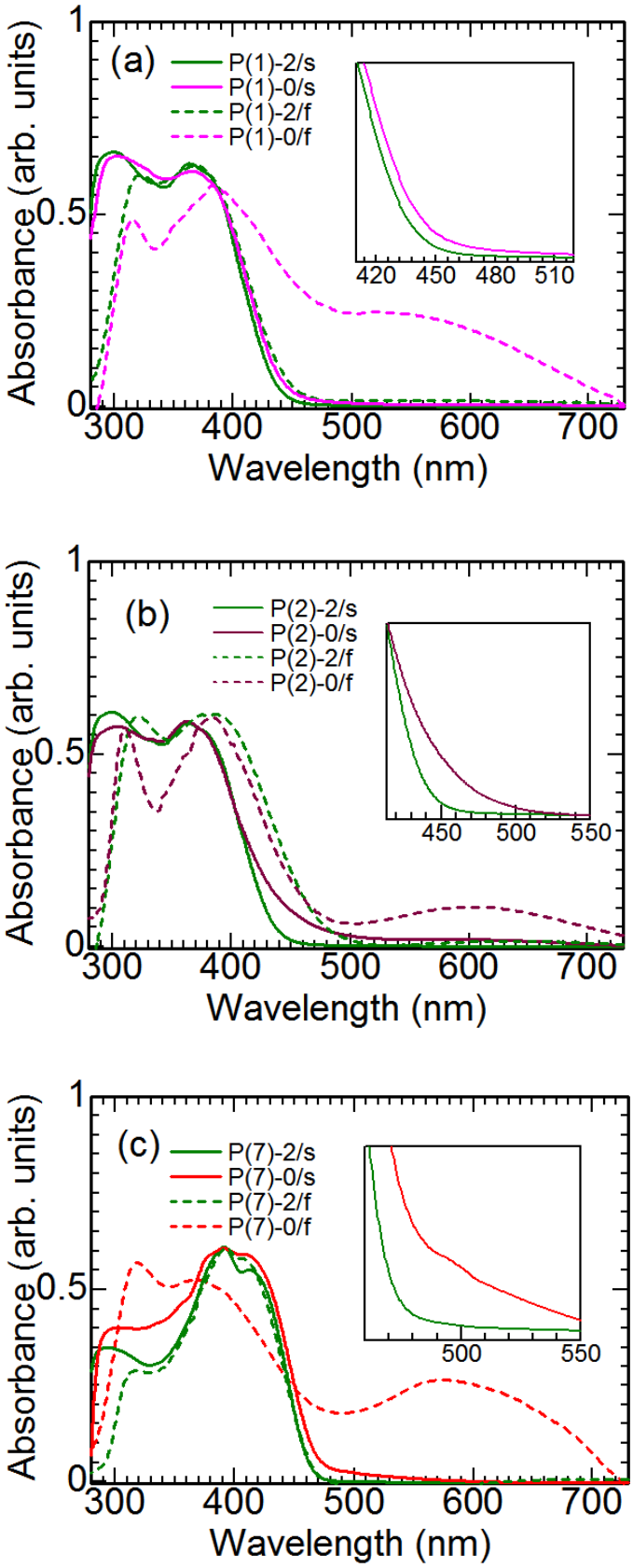

图 6.Polymer-2 ((a): P(1)-2, (b): P(2)-2, (c): P(7)-2 氧化前的聚合物)和polymer-0 ((a): P(1)-0, (b): P(2)-0, (c): P(7)-0氧化后的聚合物)的紫外光谱。实线代表溶液状态的测量曲线，虚线代表膜的状态的测量曲线。

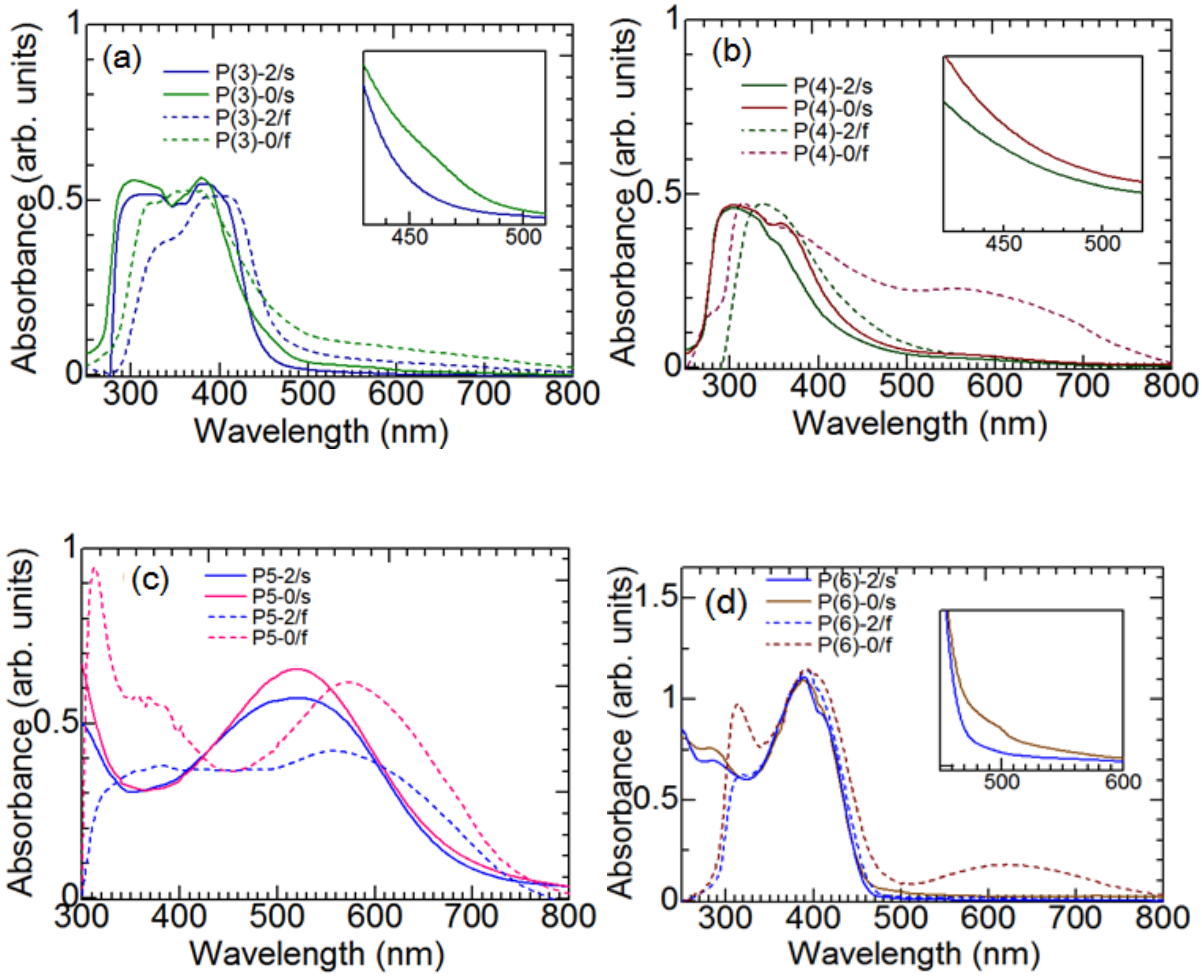

图 7.Polymer-2 ((a): P(3)-2, (b): P(4)-2, (c): P(5)-2, (d): P(6)-2 氧化前的聚合物)和polymer-0 ((a): P(3)-0, (b): P(4)-0, (c): P(5)-0, (d): P(6)-0 氧化后的聚合物)的紫外光谱。实线代表溶液状态的测量曲线，虚线代表膜的状态的测量曲线。

氧化后得到的自由基聚合物比氧化之前出现了更深的颜色。在苯溶液里，P(6)-0 和 P(7)-0 出现新峰在 497 纳米，P(3)-0 新的吸收峰在 466 纳米，（图 7）归属于氧自由基的吸收峰。[8-10] 这一结果也类似以前的研究人员的报道，例如西出和 Kaneko 报道的苯氧自由基的吸收峰的位置也是出现在这一区域。P(5)-0 在 504 纳米的吸收峰比 P(5)-2 明显的增强，这说明苯氧基的吸收峰和共轭主链的吸收峰出现了叠加。P(1)-0, P(2)-0 和 P(4)-0 比较 P(1)-2, P(2)-2 和 P(4)-2 没有明显的吸收峰，（图 6 和图 7）只是表现了一个吸收带从 420 纳米到 520 纳米，这个吸收带是来自于苯氧基自由基的吸收。另外，在薄膜态，所有的自由基聚合物比羟聚合物多了一个新的吸收从 540 纳米到 620 纳米，这是自由基吸收。

在这些聚合物中，P(5)-2 和 P(5)-0 显示了较低的能量特征，这说明在共轭主链引入 ITN

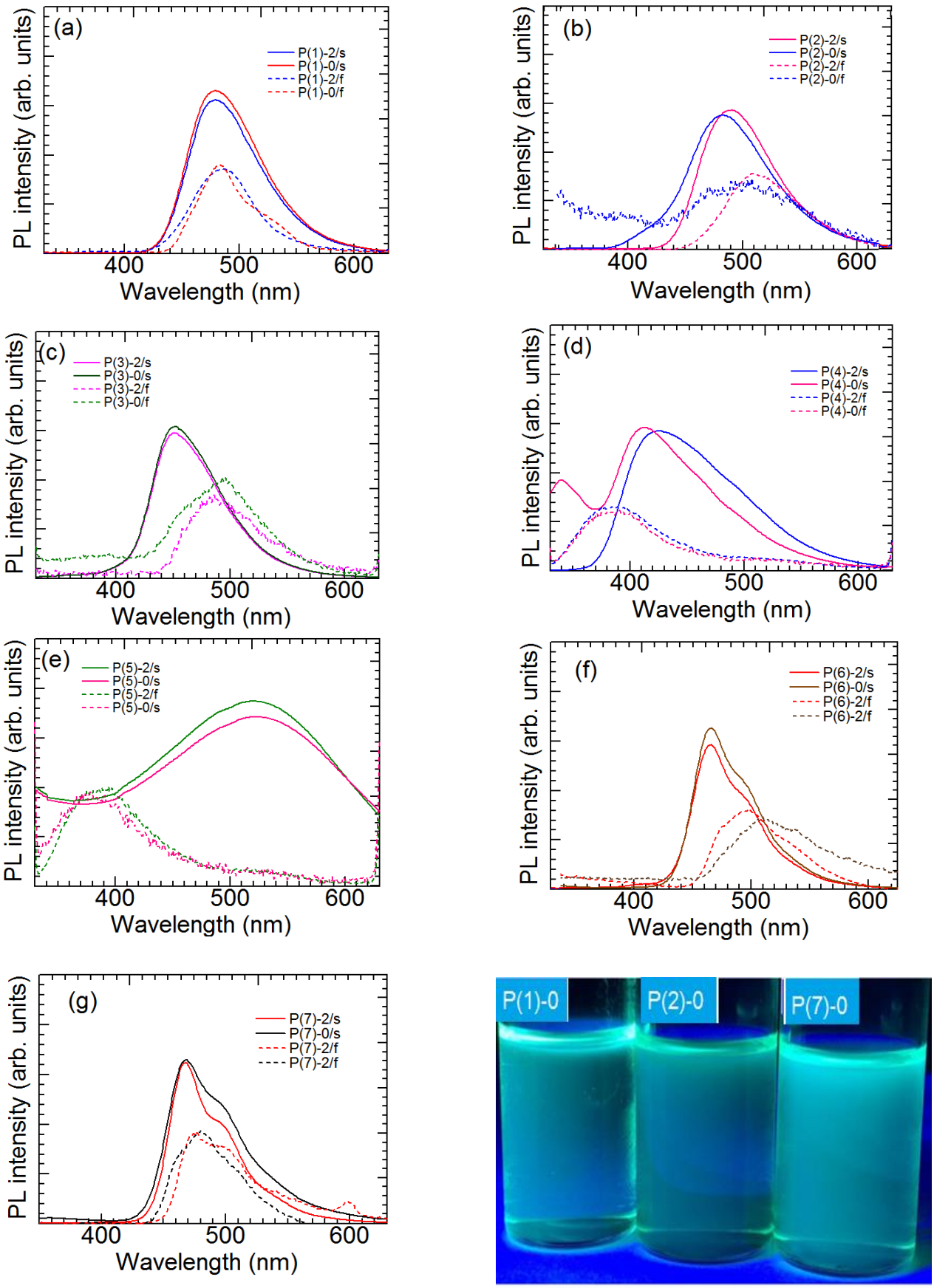

图 8. Polymer-2和polymer-0的紫外光谱以及P(4)-0， P(5)-0， 和P(7)-0在紫外灯下的照片 实线代表溶液状态的测量曲线，虚线代表膜的状态的测量曲线。

（isothianaphthene）后，降低了能隙，形成了低能隙的共轭聚合物。而 P(4)-2 和 P(4)-0 显示了最高的能量水平。另外，聚合物 P(6)-2 和 P(6)-0 出现最大吸收峰在 282 纳米和 390 纳米，P(7)-2 和 P(7)-0 的最大吸收峰是在 290 纳米，391 纳米和 412 纳米. P(7)-2 和 P(7)-0 比 P(6)-2 和 P(6)-0 有更长的共轭主链，这是应为手性的基团引入 P(7)的烷基侧链，这个手性官能团可能限制了烷基侧链的旋转，增加了主链的共平面性，使聚合物出现了更长的有效共轭。

荧光光谱展示在图 8 里。所有的共轭聚合物在溶液里显示了荧光发射从 412 纳米到 521 纳米。但是，在膜的状态，所有的聚合物显示了很弱的发射信号，这个信号强度的降低可能是因为共轭主链之间的相互作用降低了量子效应，在膜的状态发生了荧光淬灭。[11] 在 400 纳米的紫外灯照射，下 P(4)-0, P(5)-0, 和 P(7)-0 发射白绿光。

（2）电子性能。

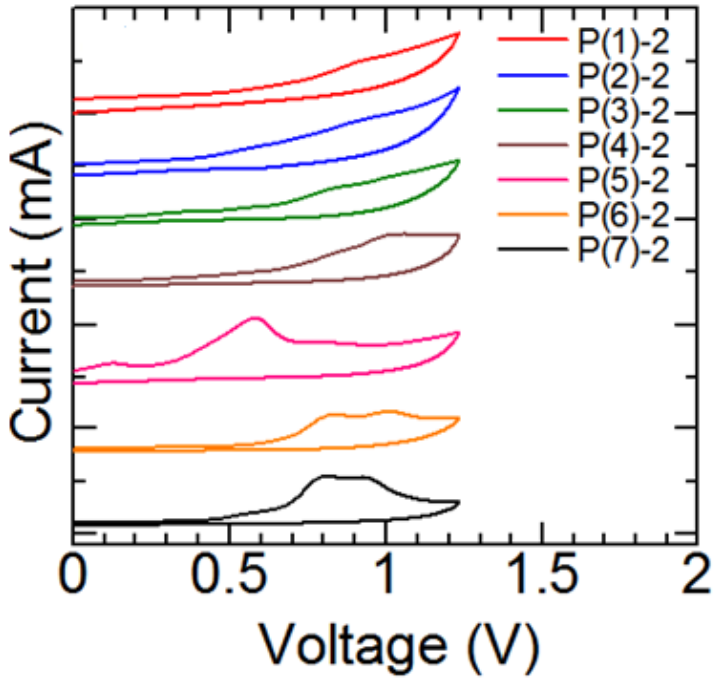

图 9. 共轭聚合物的循环伏安曲线(电解液用0.1摩尔TBAP乙氰溶液，扫描速率是100 mV s^{-1}).

氧化前的聚合物膜的循环伏安曲线通过一个Ag/Ag+参考电极在0.1摩尔每升的四丁基溴化铵的乙腈溶液测定。能带隙是通过吸收光谱计算，羟基共轭聚合物能带隙的值是在1.65 电子伏 - 2.79电子伏范围。氧化电势在0.11伏-0.76伏的范围。最高占有分子轨道和最低占有分子轨道是根据经验公式: $E_{HOMO} = -(E_{onset,ox} + 4.8)$ eV和 $E_{LUMO} = E_{HOMO} + E_{opt}$计算得到。[12, 13] 在循

环伏安的测量结果中，比较这些氧化电势，P(5)-2拥有最低的氧化电势值，这可能是由于INT（isothianaphthene）单元的作用，降低了能量值。

表格 1. polymer-2在薄膜状态的紫外吸收和循环伏安测定结果。

Polymers-2	λ_{edge} [e] (nm)	$E_{onset,ox}$ [a] (V)	E_{HOMO} [b] (eV)	E_{opt} [c] (eV)	E_{LUMO} [d] (eV)
P(1)-2	444	0.71	-5.51	2.79	-2.72
P(2)-2	475	0.52	-5.32	2.61	-2.71
P(3)-2	476	0.64	-5.44	2.60	-2.84
P(4)-2	552	0.76	-5.56	2.24	-3.32
P(5)-2	751	0.11	-4.91	1.65	-3.26
P(6)-2	462	0.65	-5.45	2.68	-2.77
P(7)-2	469	0.53	-5.33	2.64	-2.69

[a] Onset oxidation potentials of the polymers calibrated with ferrocene. [b] Calculated from the oxidation potentials. [c] Calculated from the onset wavelength of optical absorption of the polymers. [d] Calculated from optical bandgap energy and onset oxidation potential of the polymers. [e] onset absorption wavelength

用PbO_2氧化羟基聚合物得到自由基聚合物。聚合物的电子自旋共振光谱是在粉末状态室温环境里测得（图 10）。所有的电子自旋共振光谱都显示了单峰信号，这个强的单峰信号表明自由基沿着共轭主链有一个最大局部浓度。g-值，线宽和自旋浓度通过电子自旋共振计算并总结于图表2。g-值是2.004表明共轭聚合物形成了氧中心自由基，这是2,6-二-叔丁基苯氧基自由基的片段信号。自由基聚合物的自旋浓度在1.78×10^{19}-1.38×10^{20} spins/g, 表明一个聚合物分子里包含0.138-1.867spin。

表格 2. 功能化的磁性共轭聚合物的电子自旋光谱的结果。

Polymers	g-value[a]	ΔHpp (mT) [a]	Spin conc (Spins/g) [a]
P(1)-0	2.00460	0.8218	1.78×10^{19}
P(2)-0	2.00461	0.8798	2.76×10^{19}
P(3)-0	2.00490	0.8211	2.99×10^{19}
P(4)-0	2.00432	1.0263	2.82×10^{19}
P(5)-0	2.00457	0.7331	2.80×10^{19}
P(6)-0	2.00490	1.1731	3.52×10^{19}
P(7)-0	2.00473	0.8798	1.38×10^{20}

[a] *g* value, the peak-to-peak line width and spin concentration were evaluated from ESR measurements.

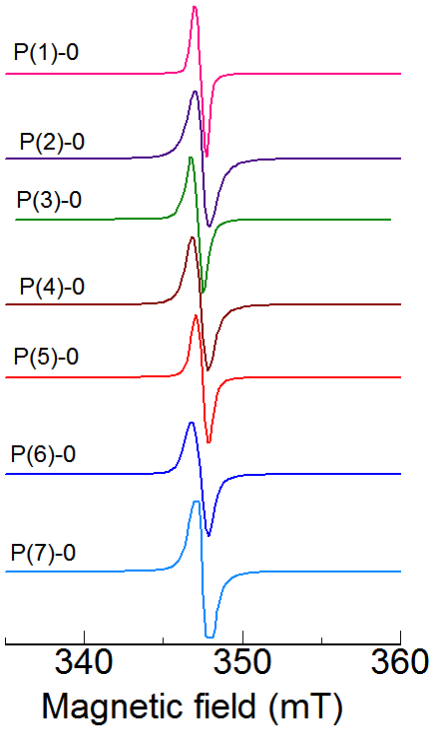

图 10. 功能化的磁性共轭聚合物的电子自旋光谱。

2. 功能化的低能系共轭聚合物的合成及性能研究。

1）设计理念。

在这个功能化低能隙共轭聚合物的设计里，首先考虑了对主链的设计，ITN (Isothianaphthene)被选择作为聚合物的主链的一部分，ITN可以增强共轭聚合物的醌式结构，醌式结构有利于电子的特性，例如，减少键长的交替，增强电子在共轭主链的离域等，这样的性质可以降低能隙，产生低能隙的共轭聚合物。主链的另一部分是噻吩，苯和次甲基。这些基团和ITN合成不同主链的聚合物，进而调查比较不同基团和ITN基团产生不同低能隙共轭聚合物的电子性质。其次是对侧链的设计，在这里我们选择了龙脑基作为侧链，龙脑的价格便宜，在医学上具有散郁火，治惊痫，亦能生肌止疼的作用。在物质材料的合成上，我们更侧重其光学性能，龙脑基是一个好的光学活性功能团，它可能诱导主链带有光学性能。另外，这个光学侧链的引入增加聚合物的溶解性和影响主链的共平面性。在此设计中，我们想得到低能隙的有光学活性的共轭高分子，进而探索它的性质。

在这个设计里，我们设计了三个聚合物，P1是以ITN和苯为主链龙脑基作为侧链的共轭聚合物，P2是以ITN和噻吩作为主链龙脑基作为侧链的共轭聚合物。P3是以ITN和亚甲基作为主链龙脑作为侧链的共轭聚合物。（图式 4）

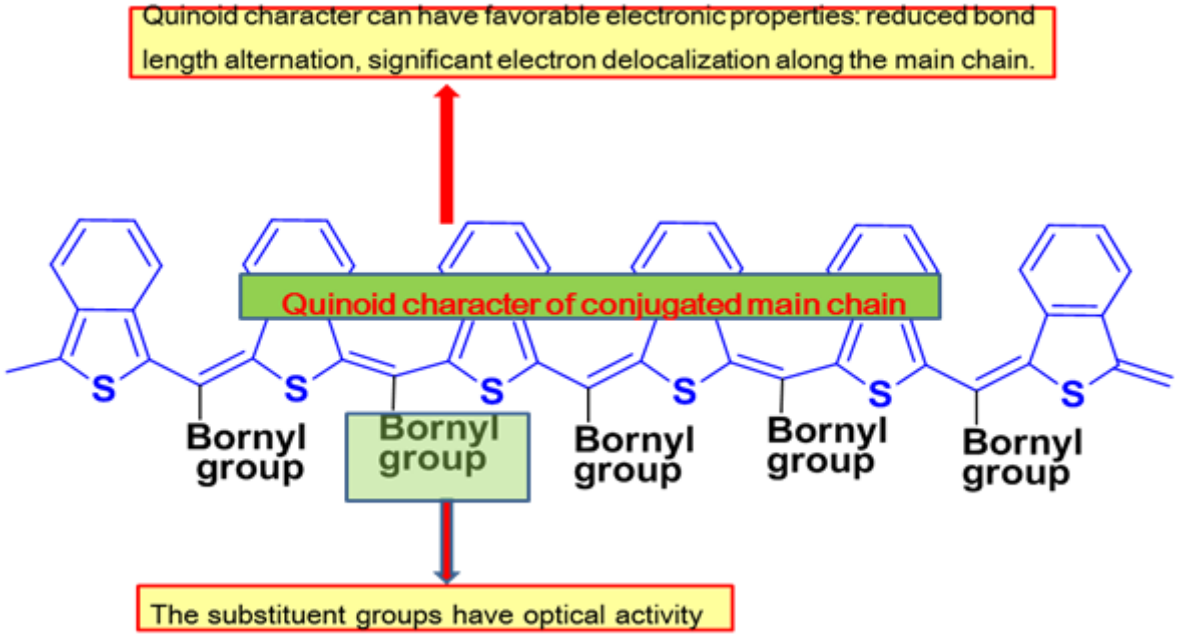

图 11. 功能化低能隙的共轭聚合物设计示意图。

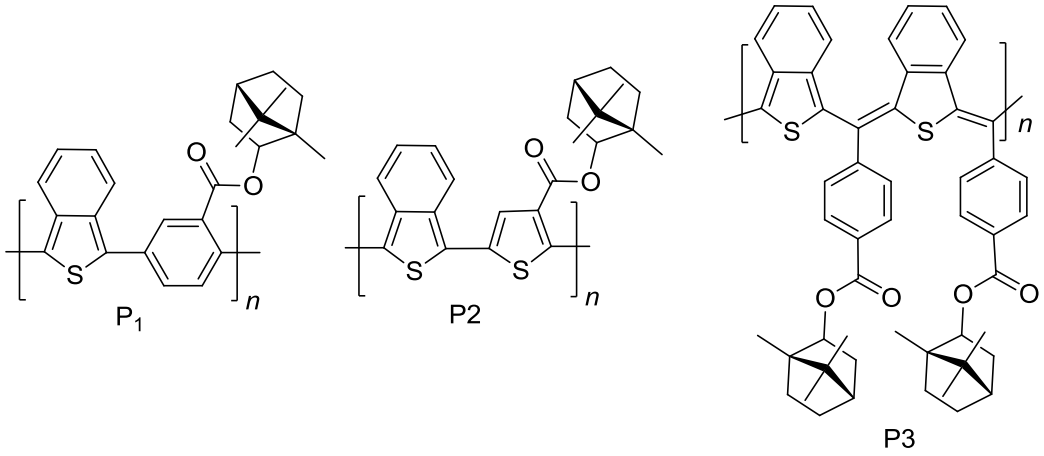

图式 4。 功能化低能隙共轭聚合物的结构式。

2）共轭聚合物的性能。

(1)光学性能。

在四氢呋喃溶液的 CD 和紫外光谱里（图 12），P1 在 312 纳米，399 纳米处显示了明显的 CD 信号，吸收信号出现在 403 纳米。P2 也显示了明显的对联峰，正的 CD 信号出现在 461 纳米，负的 C D 信号出现在 395 纳米吸收信号出现在 438 纳米。这些结果表明，在四氢呋喃溶液里，

聚合物形成了分子内的螺旋结构。P3 在溶液里没有显示 CD 信号。在膜的状态，所有的聚合物并没有形成分子间的螺旋排列，那是应为龙脑基是个球形的形状，这个形状有比较大的空间位阻，从而影响聚合物分子间的π–π相互作用，不能形成分子间的手性排列。

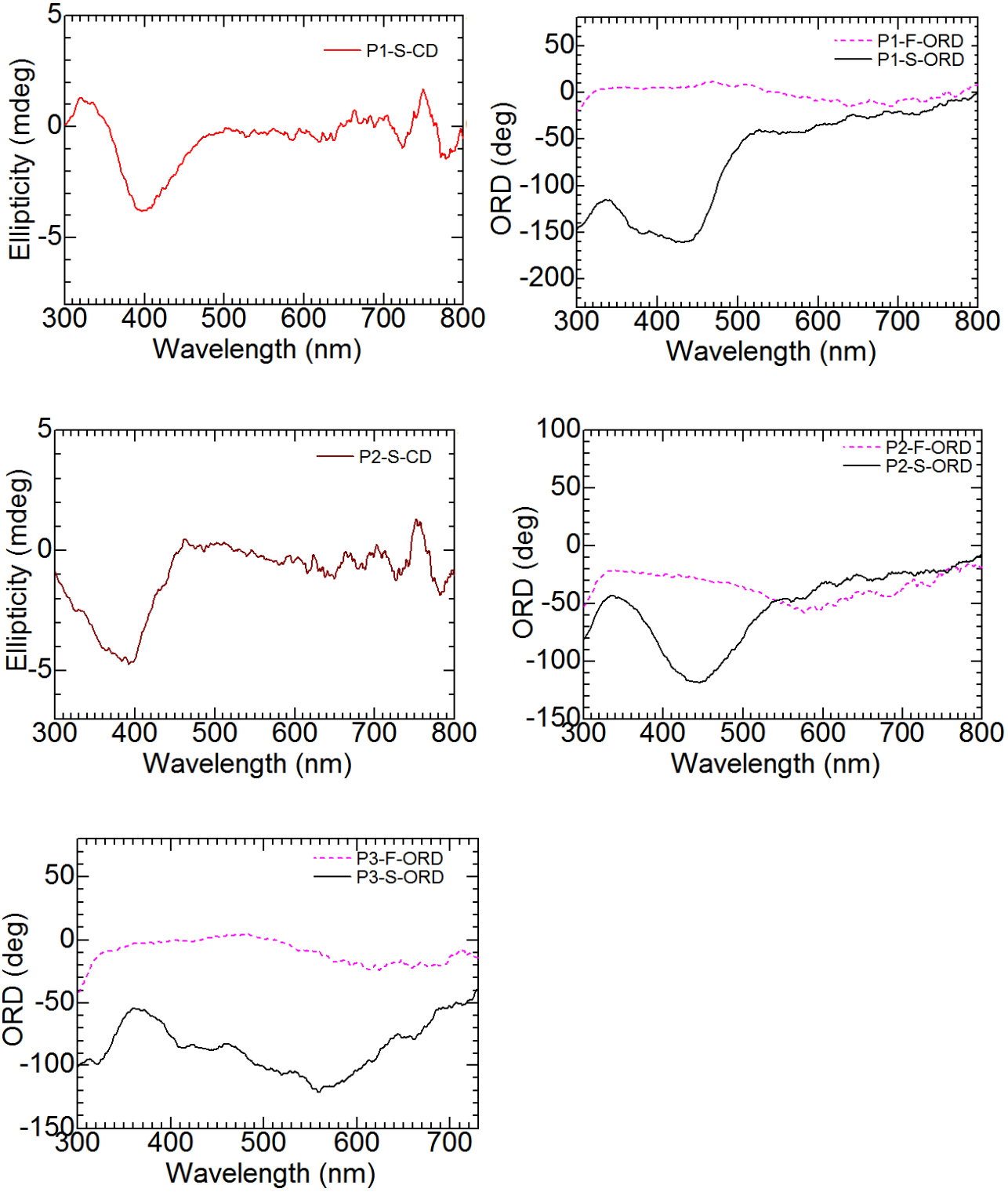

图 12. 在四氢呋喃溶液（实线）和膜的状态下（虚线）的聚合物的圆二色(CD)光谱（，旋光色散光谱。

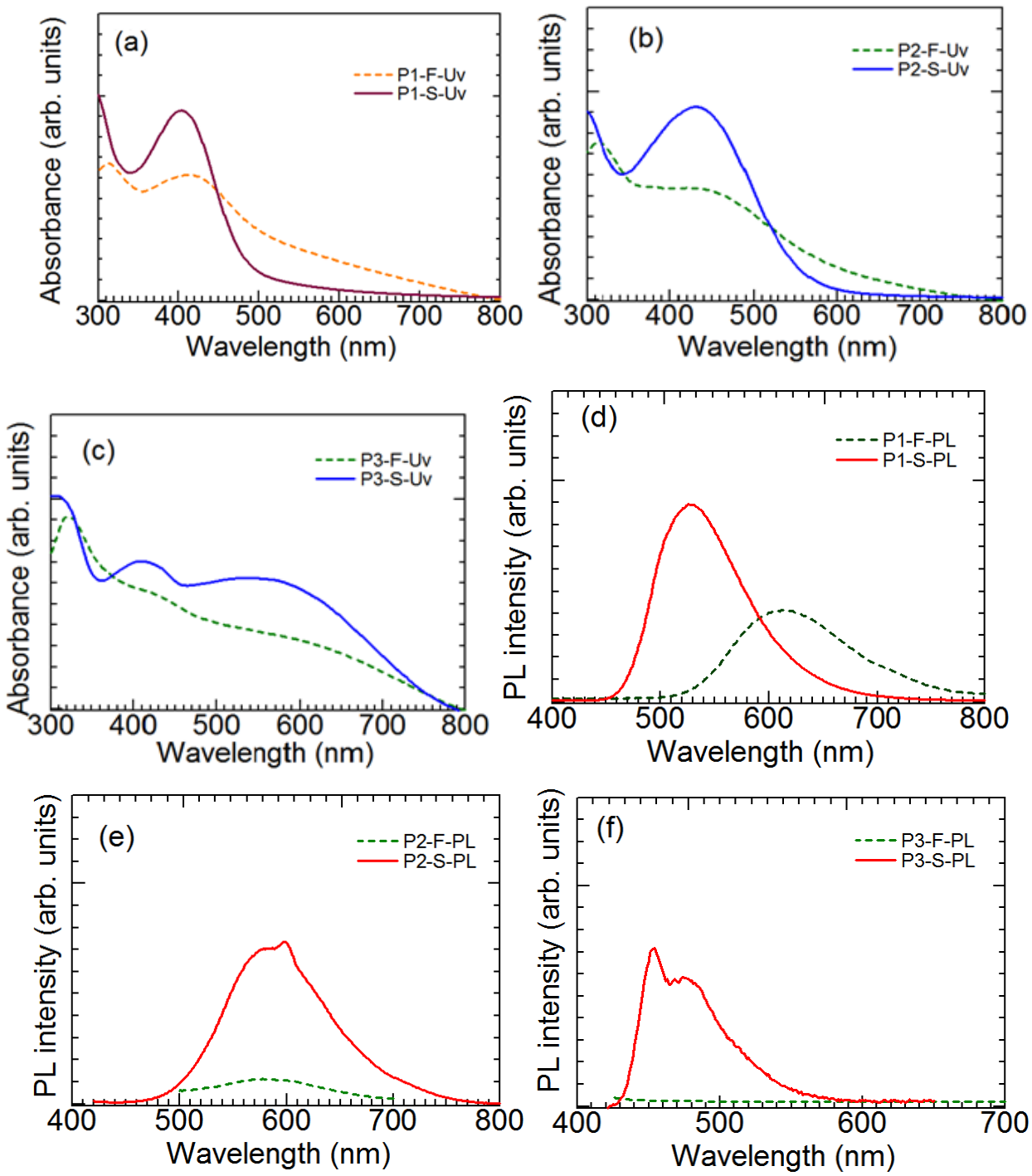

图 13. 在四氢呋喃溶液（实线）和膜的状态下（虚线）的聚合物紫外光谱和荧光光谱。

聚合物的光学性能用圆二色(CD)光谱，紫外光谱，旋光色散光谱和荧光光谱来表征。

在可视区，观察到所有的聚合物的旋光色散光谱（图 12)。四氢呋喃溶液里，P1，P2 和 P3 显示了负的信号，分别在 432 纳米，436 纳米和 601 纳米。膜的状态，P2 在 571 纳米显示了负

的信号，P1 和 P3 分别在 470 纳米和 479 纳米显示了正的信号。膜的状态和溶液态比较，P1 和 P3 出现了不一样的旋光色散信号，其原因有可能是在溶液态它们较大的侧链位阻，降低了共轭主链的共平面性，所以表现了较强的旋光色散。而在膜的状态，由于分子间的π-π键之间的相互作用，增加了它们的醌式结构，从而出现了不一样的信号。在这里，所有的聚合物在溶液状态和膜的状态都在可视区显示了明显的旋光色散信号，这一结果表明，聚合物的旋光性来自于手性侧链。

P1，P2 和 P3 的发射信号显示在图 13。在四氢呋喃溶液里，P1，P2 和 P3 的发射峰分别在 527 纳米，580 纳米，598 纳米，456 纳米和 478 纳米。但是在膜的状态，P1 和 P2 分别在 611 纳米，582 纳米显示了弱的发射峰，P3 没有发射峰。在膜的状态下这种共轭聚合物强的荧光淬灭主要是因为 ITN 单元的引入到主链，增强了醌式结构，共轭主链之间的相互作用会降低荧光的量子效率。另外，共轭聚合物膜的状态和溶液态比较所有聚合物的最大吸收信号和 P1 的最大发射信号出现了红移，这种红移现象说明，在膜的状态共轭主链之间的π键的堆积，导致了好的主链共平面性。

（2）电子的性质。

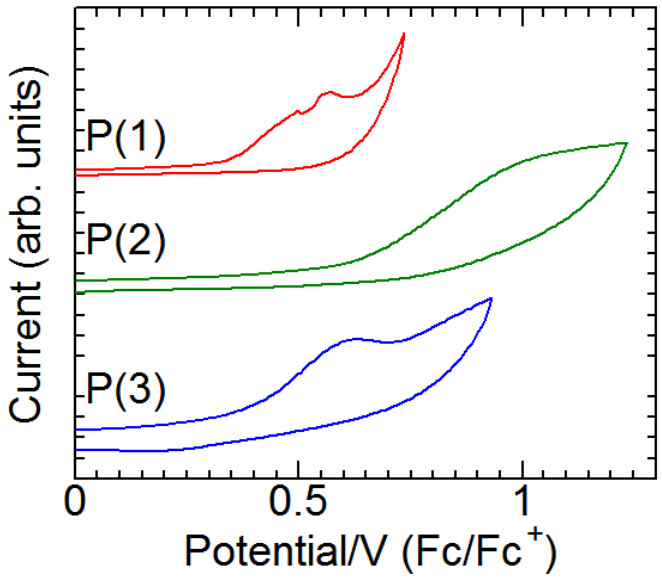

图 14. 功能化的低能系共轭聚合物的循环伏安曲线(电解液用 0.1 摩尔 TBAP 乙氰溶液，扫描速率是 100 mV s^{-1})。

聚合物的循环伏安测定是在 0.1 摩尔每升的四丁基溴化铵电解液里用 Ag/Ag+作为参考电极完成（图 14）。P1 在+0.59V，+0.67V 显示了两个连续的单电子氧化。P2 和 P3 显示了一个单

电子氧化模式，这些结果可以看出，P1 有较低的氧化电势可能更容易丢掉电子。这些聚合物

表格 3. 功能化的低能系共轭聚合物在薄膜状态的紫外吸收和循环伏安测定结果。

Polymers	λ_{edge}[a] (nm)	E_{opt}[b] (eV)	$E_{onset,ox}$[c] (V)	E_{LUMO}[d] (eV)	E_{HOMO}[e] (eV)
P1	519	2.39	0.33	-2.74	-5.13
P2	589	2.07	0.59	-3.32	-5.39
P3	787	1.57	0.37	-3.60	-5.17

a: Onset absorption wavelength. **b**: Calculated from the onset wavelength of optical absorption of the polymers. **c**: Onset oxidation potentials of the polymers calibrated with ferrocene. **d**: Calculated from optical bandgap energy and onset oxidation potential of the polymers. **e**: Calculated from the oxidation potentials.

的能带隙由吸收光谱计算得出，总结在表格 3 里。这三个聚合物中，P3 有最窄的能带隙，这可能是次甲基引入到共轭主链，有利于增长共轭主链的醌式结构，从而降低了 P3 的能带隙。

电子自旋共振光谱测定是在聚合物的粉末态室温下经由碘掺杂获得。所有的聚合物显示了无超精细分裂的不对称单线，信号的强度随着掺杂时间的延长在逐渐的增加，这意味着随着时间的增长，碘的掺杂导致了自旋浓度的增加。电子自旋共振谱的强度，g-值，线宽展示在图 15 和图 16 中。随着掺杂时间的延长，P1 的 g-值和线宽并没有随掺杂时间而变化，这说明掺杂时间的增长不会变聚合物的电荷。而 P2 和 P3 的 g-值和线宽随着掺杂时间的增长而增加，这个现象可能被认为短的共轭和自旋定域存在于样品。比较 P1 和 P2，P3 有比较大的自旋浓度 1.155×10^{19}Spins/g，一个自旋存在于 140 个单体的结构单元。

三． 电解聚合法合成光学性能的共轭聚合物。

1) 设计理念。

在这个研究里，我们设计了三个三元环的手性化合物应用到电解聚合中作为诱导剂，另外选择 6CB (4'-己基-(1,1'-联苯基)-4-腈)做为液晶溶剂， 四丁基高氯酸铵作为支持电解质盐，通过诱导剂诱导，电解质溶液形成单手螺旋的结构。在这样的环境中聚合，聚合物骨架也会形成单手螺旋的排列。这样的结构赋予共轭聚合物光学的性能。(图 15) 在这些不同诱导剂的液晶电解质（5a, 5b, 5c）溶液里，(图式 5) 通过不对称电化学聚合的方法，制备一系列具有光学活性的聚合物膜。这些聚合物可能形成分子间的旋钮构造，聚合物的分子取向将转录电解液的构造。

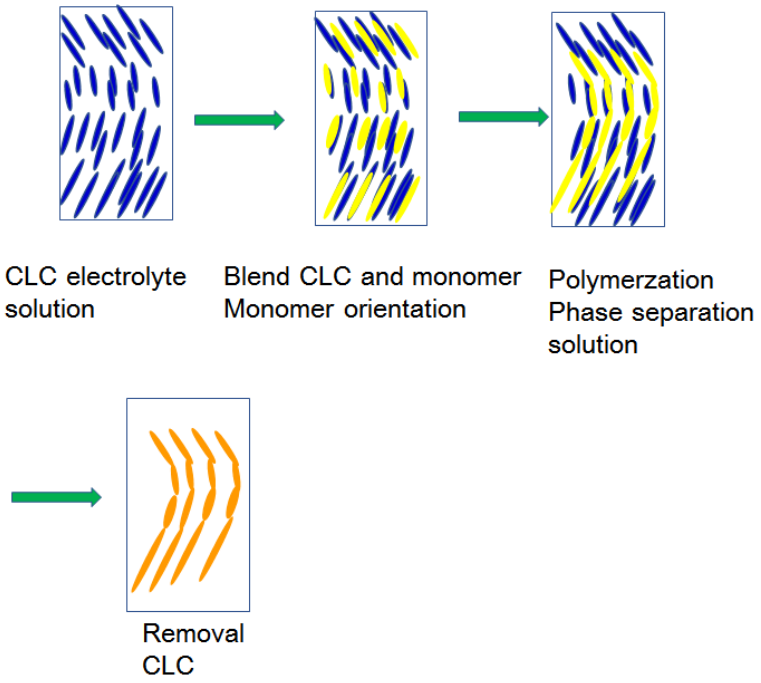

图 15. 光学活性的聚合物膜形成过程。

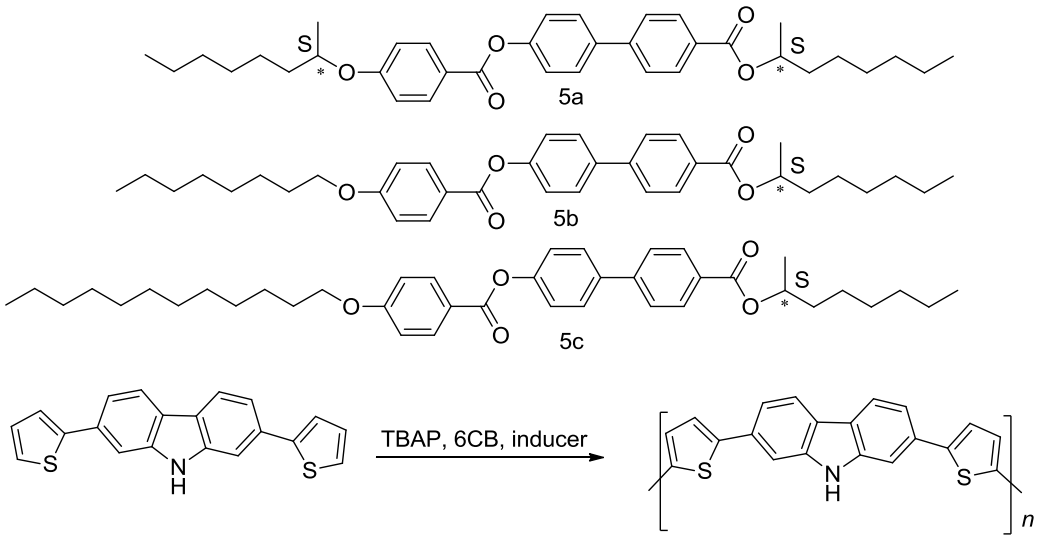

图式 5. 诱导剂和聚合物的结构式

2）光学性质。

在氧化态和自然态的紫外光谱中，所有的聚合物膜在 300-500 纳米显示了吸收带，这是共轭骨架π-π*传递的信号。在氧化态，聚合物膜在 520 纳米到 800 纳米显示了另外一个吸收带，

这是由于电化学的掺杂产生了极子的信号。在膜的 CD 光谱中，在长波长 PCB5a 显示了负的信号，这表明聚合物 PCB5a 形成了左手螺旋排列，这一结果一致于 5a 电解液的左手螺旋秩序。而 PCB5b 和 PCB5c 在长波长显示了正的 CD 信号，PCB5b 和 PCB5c 形成了右手螺旋排列，一致于它们的电解液的排列顺序。这些结果表明聚合物的分子取向转录了电解液的构造，形成了分子间的旋钮构造。PCB5b，PCB5c 在自然状态和 PCB5c 在氧化态出现了科顿效应，这是由于分子内的电荷传递或者π-π*传递引起的。而 PCB5b 在氧化态没有出现此类的信号，只是显示了正的 CD 信号，而可能是由于在氧化态下极子的影响所致。

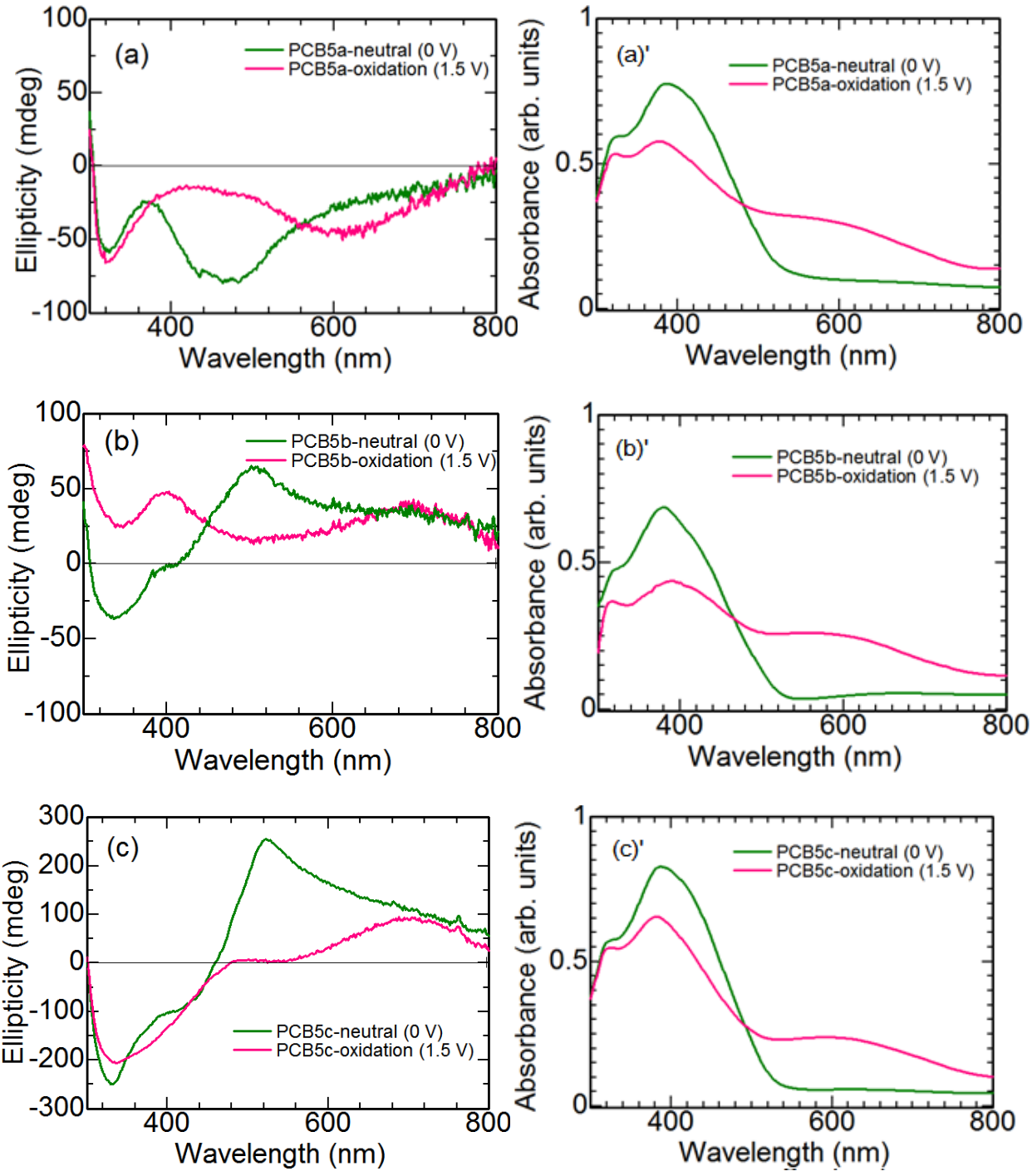

图 16. 光学活性的共轭聚合物的 CD 光谱((a),(b),(c))和紫外光谱光谱((a’),(b’),(c’))。

四． 參考文獻。

[1] Bredas JL, Chance RR, Silbey R. Comparative theoretical study of the doping conjugated polymers; Polarons in polyacetylene and polyparaphenylene. Physical Review B. 1982;26:5843-5854.

[2] Shirakawa H, Louis EJ, MacDiarmid AG, Chiang CK, Heeger AJ. Synthesis of electrically conducting organic polymers: halogen derivatives of polyacetylene, (CH)x. Journal of Chemical Society of Chemical Communication. 1977;474:578-580.

[3] Dou L, Liu YS, Hong ZR, Li G, Yang Y. Low-bandgap near-IR conjugated polymers/molecules for organic electronics. Chem. Rev. 2015;115:12633-12665.

[4] Miyaura N, Suzuki A. Palladium-catalyzed cross-coupling reactions of organoboron compounds. Chem. Rev. 1995;95:2457-2483.

[5] He G, Kang L, Torres DW, Shynkaruk O, Ferguson M, McDonald R, Rivard E. The marriage of metallacycle transfer chemistry with suzuki-miyaura cross-coupling to give main group element-containing conjugated polymers, J. Am. Chem. Soc. 2013;135:5360-5363.

[6] Nishide H, Takahashi M, Takashima J, Pu YJ, Tsuchida E. Acyclic and cyclic di- and tri(4-oxyphenyl-1,2-phenyleneethynylene)s: their synthesis and, ferromagnetic spin interaction. J. Org. Chem. 1999;64:7375-7380.

[7] Nishide H, Kaneko T, Nii T, Katoh K, Tsuchida E, Yamaguchi K. Through-bond and long-range ferromagnetic spin alignment in a π-conjugated polyradical with a Poly(phenylenevinylene) skeleton. J. Am. Chem. Soc. 1995;117:548-549.

[8] Nishide H, Yoshioka N, Inagaki K, Tsuchida E. Poly [(3,5-di-tert-butyl-4-hydroxyphenyl)acetylene]: formation of a conjugated stable polyradical. Macromolecules. 1988;*21*:3119-3120.

[9] Goto H. Magneto-optically active polythiophene derivatives bearing a stable radical group from achiral monomers by polycondensation in cholesteric liquid crystal. Polymer. 2008;49:3619-3624.

[10] Kaneko T, Abe H, Namikoshi T, Marwanta E, Teraguchi M, Aoki T. Synthesis of an optically active poly (aryleneethynylene) bearing galvinoxyl residues and its chiroptical and magnetic properties. Synth Met. 2009;159:864-867.

[11] Goto H, Wang AH, Kawabata K, Yang F. Synthesis and properties of a low-bandgap liquid crystalline π-conjugated polymer. J Mater Sci. 2013;48:7523-7532.

[12] Brédas JL, Silbey R, Boudreaux DS, Chance RR. Chain-length dependence of electronic and electrochemical properties of conjugated systems: polyacetylene, polyphenylene, polythiophene, and

polypyrrole. J. Am. Chem. Soc. 1983;105:6555-6559.
[13] Agrawal AK, Jenekhe SA. Electrochemical properties and electronic structures of conjugated polyquinolines and polyanthrazolines. Chem. Mater. 1996;8:579-589.